Sedimentological, geomorphological and geochronological studies on Holocene tsunamis in the Lefkada – Preveza area (NW Greece) and their implications for coastal evolution

Inaugural-Dissertation
zur
Erlangung des Doktorgrades
der Mathematisch-Naturwissenschaftlichen Fakultät
der Universität zu Köln

vorgelegt von

Simon Matthias May

aus Düsseldorf

Köln 2010

Berichterstatter: Prof. Dr. Andreas Vött
Prof. Dr. Helmut Brückner

Termin der mündlichen Prüfung: 29.04.2010

To determine what's right, you must first have doubted in the right way

(Aristoteles, 384-322 v. Chr.)

Preface – acknowledgements

This dissertation is the result of four years of intense scientific research in Marburg and Cologne, of enjoyment and trouble, and of countless memorable hours in Greece. My sincerest thanks are directed to my supervisor Prof. Dr. Andreas Vött for having supported me throughout the last years and for having introduced me to geo-scientific working. He enabled this study and the related academic step and was responsible for numerous enjoyable days, weeks and months (years?) in the Greek field (and fields). Special thanks are also dedicated to Prof. Dr. Helmut Brückner, who inspired and initiated my attention to geomorphology and coastal research and who always was present during the time of work.

For the fruitful time of collaboration in the "Bunsenzimmer" particular thanks are directed to Max Engel and Daniel Kelterbaum, who provided immense scientific and private support and help during the last four years and who "considerably correlated" to my interests, not only in terms of geo-scientific research. Dr. Nicole Klasen is being thanked not only but also for the realization of the OSL datings. To Marita Budde, Christine Günther and Dr. Walter-Wilhelm Jungmann dearest thanks are addressed for steady support and for a good time in the laboratory. Dr. Volker Wennrich is being thanked for the implementation of XRF measurements in Cologne. Matthias Handl and Alessandra Smedile are gratefully acknowledged for macro- and microfaunal investigations. Ralf Grapmayer and Ule Ewelt are sincerely thanked for the underwater investigations and their overall effort during their "holidays". For the (immediate) composition and correction of the Greek summary thanks go to Kostas Panagiotopoulos and Nikolaos Tougiannidis. Last but not least, special thanks are dedicated to Prof. Dr. Franziska Lang and Claudia Melisch, who were a great help in Greece (and Greek) and who contributed to the special time in Greece.

During the time in Marburg, in Cologne and in the field, I explicitely have enjoyed the friendship and support of Svenja Brockmüller, Dr. Peter Fischer, Hanna Hadler, Kosta Ntageretzis, Dr. Armin Schriever and Timo Willershäuser. Sincerest thanks also go to "Saschko" Oleksander Balyk, Lena Behrendes, "Jonny" Bremer, Constance Curdt, Uli Floth, Jens Hahn, Prof. Dr. Rainer Herd, Dirk Hoffmeister, Isa Kaya, Sabine Klaffke, Odette Kretschmer, Lukas Lehnert, Stefan Lindauer, Milica Markovic, Florian Melles, Lukas Müller, Johanna Pfeiffer, Melanie Scholz, Friederike Stock, Johann Friedrich Tolksdorf and many others who helped and participated during the last four years. Lisa Döring is thanked for her patience and lenience especially during the last months.

In Greece, special thanks are dedicated to Thanassi Kirkos and several other people from Palairos who all contributed to the exclusively memorable spent time. Moreover, I have to thank Kalliope Gaki-Papanastassiou, Hampik Maroukian and Dimitri Papanastassiou for overall support and for providing maps and materials. Dr. Dimitris Sakellariou and his "crew" are being thanked for the offshore geophysical investigations and the related interpretation.

Last but not least, my dearest thanks are dedicated to my parents Friedhelm and Ingrid, and to my brother Hendrik. Their unconditional, comprehensive and undemanding support, friendship and interest are part of this dissertation and one of the most important things in my life.

Table of Contents

Preface – acknowledgements I

List of Figures V

List of Tables VI

Index of Appendices (CD enclosure) VI

1 Introduction and background ... 1

1.1 INTRODUCTION ... 2

1.2 STUDY AREA ... 3

1.2.1 TECTONIC SETTING ... 3

1.2.2 GEOGRAPHICAL CONTEXT ... 5

1.3 STUDY AIMS ... 7

1.4 PALAEO-EVENT RESEARCH ... 7

1.4.1 TSUNAMI DEPOSITS IN THE GEOLOGICAL RECORD ... 7

1.4.2 SEDIMENTARY EVIDENCE FOR TSUNAMIS WORLDWIDE AND IN THE EASTERN MEDITERRANEAN ... 10

1.4.3 HISTORICAL REPORTS ON TSUNAMIS IN THE EASTERN MEDITERRANEAN ... 11

1.5 STUDY OUTLINE ... 12

1.6 REFERENCES ... 13

2 Geomorphology and geomorphodynamics in the Lefkada – Preveza coastal zone ... 25

2.1 STUDY BACKGROUND ... 26

2.2 STUDY AREA ... 27

2.3 METHODS ... 28

2.4 RESULTS ... 29

2.4.1 GEOMORPHOLOGY ... 29

The Lefkada barrier beach ... 29

Washover structures along the Lefkada barrier beach ... 32

The Plaka beachrock system ... 34

The Phoukias sand spit in southern Aktium Headland ... 36

The Bay of Aghios Nikolaos - offshore geophysical studies ... 37

2.4.2 GEOMORPHODYNAMICS ... 39

The Lefkada barrier beach ... 39

Southern Aktium Headland ... 42

2.5 INTERPRETATION AND DISCUSSION ... 43

2.5.1 GRADUAL COASTAL PROCESSES ... 43

2.5.2 TECTONICS ... 45

2.5.3 EXTREME WAVE EVENTS - TSUNAMIS ... 46

2.6 CONCLUSIONS ... 47

2.7 REFERENCES ... 48

3 Tsunami-induced coastal changes at Aktium Headland, NW-Greece 53

3.1 STUDY BACKGROUND 54
3.2 STUDY AREA 55
3.3 METHODS 56
3.4 RESULTS 57
3.4.1 STRATIGRAPHY OF VIBRACORES AKT 35 AND ANI 2 59
Vibracore AKT 35 59
Vibracore ANI 2 60
3.4.2 GENERALIZATION AND INTERPRETATION OF SEDIMENTARY UNITS 62
3.4.3 DETAILED INVESTIGATIONS ON EVENT UNIT E 64
Macro- and microfaunal investigations on vibracore AKT 35 64
Grain size distribution of unit E in vibracore AKT 35 66
Taphonomic investigations on shells of vibracore AKT 35 66
Characteristics of event unit E in sediment profile AKT S2 68
3.4.4 VIBRACORE TRANSECTS AND CHRONOSTRATIGRAPHICAL INTERPRETATION 70
Vibracore transect A 70
Vibracore transect B 72
Vibracore transect C 74
Vibracore transect D 76
3.5 INTERPRETATION AND DISCUSSION 76
3.5.1 EVENT-INDUCED COASTAL CHANGES – EVIDENCE FOR TSUNAMI OR STORM? 76
3.5.2 THE EVOLUTION OF THE PHOUKIAS SAND SPIT – EVIDENCE FOR TSUNAMI-INDUCED COASTAL CHANGES 80
Tsunami induced coastal changes at ~1000 cal BC 81
Tsunami induced coastal changes at around or after 300 cal BC 83
Evidence for a tsunami event from the central part of the Phoukias sand spit 84
3.6 CONCLUSIONS 86
3.7 REFERENCES 87

4 Washover fans in the northern Lagoon of Lefkada 94

4.1 STUDY BACKGROUND 95
4.2 STUDY AREA 95
4.3 METHODS 96
4.4 RESULTS 97
4.4.1 THE LEFKADA WASHOVER SYSTEM 97
4.4.2 THE GYRA FAN 99
Stratigraphy of vibracore profile LEF 44 99
Macro- and microfaunal investigations on vibracore LEF 44 100
Stratigraphy of the Gyra washover structure 102
4.4.3 THE TEKI FAN 106
Stratigraphy of vibracore profile LEF 21 106
Microfaunal investigations on vibracore LEF 21 107
Stratigraphy of the Teki washover system 109
4.4.4 THE CANALI STRETTI FAN 111
4.5 INTERPRETATION AND DISCUSSION 114
4.5.1 THE WESTERN PART OF THE LEFKADA LAGOON 115
4.5.2 THE EASTERN PART OF THE LEFKADA LAGOON 118
Washover generation I 119
Washover generation II 121
4.6 CONCLUSIONS 123
4.7 REFERENCES 124

5 Block and boulder dislocation in the Lefkada coastal zone 131

5.1 STUDY BACKGROUND 132
5.2 STUDY AREA 132
5.3 METHODS 134
5.4 RESULTS 134
5.4.1 BLOCK TRANSPORT ALONG THE LEFKADA BARRIER BEACH 134
5.4.2 BOULDER TRANSPORT ALONG THE PLAKA SURFACE 136
5.4.3 UNDERWATER SURVEYS ALONG THE PLAKA 138
Transect A *138*
Transect B *139*
Further underwater block deposits *140*
5.4.4 UNDERWATER CORES FROM THE BAY OF AGHIOS NIKOLAOS 141
5.5 INTERPRETATION AND DISCUSSION 142
5.5.1 THE ORIGIN OF BLOCK AND BOULDER FIELDS IN THE STUDY AREA 142
5.5.2 CHRONOLOGICAL IMPLICATIONS 145
5.6 CONCLUSIONS 146
5.7 REFERENCES 147

6 Synthesis 151

6.1 MIDDLE HOLOCENE TO RECENT EVOLUTION OF THE LEFKADA – PREVEZA COASTAL ZONE 152
6.2 SIGNIFICANCE OF EVENT DEPOSITS 154
6.3 BROADER IMPLICATIONS FOR COASTAL EVOLUTIONARY CONCEPTS 155
6.4 PERSPECTIVES 156
6.5 REFERENCES 158

7 Summary 160

8 Zusammenfassung 162

9 Περίληψη 164

Curriculum Vitae 167

List of Figures

Fig. 1-1: Tectonic overview of the eastern Mediterranean. 4
Fig. 1-2: Topographical overview of the Lefkada – Preveza coastal zone 6
Fig. 1-3: Topographical overview of the central and eastern Mediterranean with geo-scientific findings of tsunami deposits 10
Fig. 1-4: Historical tsunami events reported for the Ionian Sea and the study area. 12

Fig. 2-1: Overview of the study area 27
Fig. 2-2: Elevation profiles along the Lefkada barrier beach. 30
Fig. 2-3: The Lefkada barrier beach 31
Fig. 2-4: Sediment supply of the Lefkada barrier beach system. 32
Fig. 2-5: Location of washover- and/or scour fan structures along the Lefkada barrier beach system 33
Fig. 2-6: The Canali Stretti fan as seen from the Lamia Mountain 33
Fig. 2-7: Characteristics and occurrence of the extensive beachrock sequence 36
Fig. 2-8: DGPS transects carried out across the Phoukias sand spit 37
Fig. 2-9: Selected "boomer" profiles carried out in the Bay of Aghios Nikolaos. 38
Fig. 2-10: Historical maps showing the eastern part of the Lefkada barrier beach system. 40
Fig. 2-11: Overview of the study area and areas of sediment accumulation and erosion during different time periods along the Aghia Mavra barrier beach and the Phoukias sand spit 41
Fig. 2-12: The western shore of Aktium Headland 42

Fig. 3-1: Overview of the study area with coring sites and main geomorphological features 55
Fig. 3-2: Sedimentary sequence and geochemical characteristics of vibracore profile AKT 35 59
Fig. 3-3: Results of grain size analysis carried out for samples of vibracore profile AKT 35. 59
Fig. 3-4: Sedimentary sequence and geochemical characteristics of vibracore profile ANI 2 62
Fig. 3-5: Summarized characteristics of each sedimentary unit found in the study area. 63
Fig. 3-6: Results of microfaunal investigations carried out for vibracore AKT 35b. 65
Fig. 3-7: Photography of the core section between 3.00 – 3.90 m b.s.l. of core AKT 35c 67
Fig. 3-8: Photographs of selected mollusc fragments with taphonomic characteristics 67
Fig. 3-9: Taphonomic characteristics of samples AKT 35c/1-AKT 35c/5 and reference sample AKT 35/11 68
Fig. 3-10: Results of grain size analysis carried out for sediment profile AKT S2. 69
Fig. 3-11: Photographs of sediment profile AKT S2. 70
Fig. 3-12: Schematic illustration of vibracore transects A and B. 73
Fig. 3-13: Schematic illustration of vibracore transects C and D. 75

Fig. 4-1: Overview of the study area. 96
Fig. 4-2: Selected washover fan structures in the study area 98
Fig. 4-3: Core section between 0.14 m and 1.32 m b.s.l. of vibracore LEF 44. 99
Fig. 4-4: Stratigraphy and results of microfaunal investigations carried out for cores LEF 44A and 44B 101
Fig. 4-5: Sediment cores carried out on top of the Gyra washover with selected geochemical proxis 105
Fig. 4-6: Vibracore LEF 45, core section between 0.10 m a.s.l. and 1.27 m b.s.l. 105
Fig. 4-7: Sedimentary and geochemical characteristics of vibracore profile LEF 21 and results of microfaunal investigations 109
Fig. 4-8: Vibracore transect A across the Teki washover structure and transect B across the Canali Stretti fan structure 111
Fig. 4-9: The Canali Stretti fan structure with coring sites and locations of DGPS transects 112
Fig. 4-10: Upper section of cores LEF 42 and LEF 40 and sediment core LEF 40 with selected high-resolution proxies 113

Fig. 5-1: Overview of the study area 133
Fig. 5-2: Photo comparison of a block field at the Aghia Mavra barrier beach. 135
Fig. 5-3: Dislocated boulders on top of the platform-like Plaka surface 138
Fig. 5-4: Relation of block size and distance from the provenance area, found for the dislocated blocks and boulders along the Plaka surface and the underwater transects 138
Fig. 5-5: Schematic profile of underwater transect A carried out east of Skoupeloi Achilleos. 139
Fig. 5-6: Schematic profile of underwater transect B carried out east of the in-situ Plaka 140

Fig. 5-7: Schematic transect between the entrance of the Bay of Aghios Nikolaos and the depression in the center of the bay and underwater core ANI 12 with selected geochemical parameters. 141

Fig. 6-1: Schematic illustration of the evolution of main coastal features in the Lefkada – Preveza area based on the findings presented in this study. 152
Fig. 6-2: Summary of main characteristics commonly used for the detection of event deposits in fine-grained near-coast geological archives, found for the event deposits at different locations in this study. 154

List of Tables

Tab. 3-1: ^{14}C-AMS dating results used for the chronological interpretation of the stratigraphy in chapter 3. 71
Tab. 3-2: OSL datings of parallel cores AKT 3b, AKT 36b and sediment profile AKT 35D. 72

Tab. 4-1: ^{14}C-AMS dating results used for the chronological interpretation of the stratigraphy in chapter 4. .. 106

Tab. 5-1: ^{14}C-AMS dating results used for the chronological interpretation in this study in chapter 5 134

Index of Appendices (CD enclosure)

Appendix A – Photos of cores and sediment profiles [2]

Appendix B – Grain size data [13]

Appendix C – Geochemical dataset of cores and sediment profiles [15]

Appendix D – OSL data [25]

Appendix E – Field record of cores and sediment profiles [27]

Chapter I

Introduction and background

1.1 INTRODUCTION

Coastlines constitute the interface of marine and terrestrial environments. About 50 % of the human population lives within a distance of < 60 km to the coast (WOODROFFE 2003, BIRD 2008). Low-lying coastal regions below the 10 m contour line represent the living space for 10% of the human population (MCGRANAHAN et al. 2007, FITZGERALD et al. 2008). Within the context of the ongoing debate of global climate change, a minimum of 634 million people are therefore directly affected by the related coastal changes. Recently, the manifold effects of marine and coastal processes on human population have dramatically been demonstrated by devastating extreme wave events, such as the December 26th, 2004 Indian Ocean Tsunami (IOT) or hurricane Katrina in 2005.

Since 1972, the UNESCO and the International Union of Geological Sciences (IUGS) operate and support numerous geo-scientific projects within the International Geological Correlation Programme (IGCP). According to the Homepage of the IGCP 495 Project “Quaternary Land-Ocean Interactions: Driving Mechanisms and Coastal Responses” (*http://www.geography.dur.ac.uk/projects/igcp495/AbouttheProject/NewChallenges/tabid/1775/Default.aspx*), *“Coastal change in the future will be driven by a combination of local, regional and global processes.* [It is therefore important]…*to better understand these processes, including defining the potential driving mechanisms behind future sea-level change and shoreline evolution […] at regional to local scales. This will include a focus on palaeo-extreme events, such as storm surges, tidal surges and tsunamis*.” Therefore, in addition to the interaction of gradual sea level change and the related coastal response, one of the main objectives in coastal research is to decipher the contribution of extreme wave events to coastal change throughout time.

The devastating effects of tsunami events on coastal configuration particularly are documented by the IOT (DAS GUPTA 2006, MAMO et al. 2009, PARIS et al. 2009, LIEW et al. 2010), which dramatically changed public awareness of tsunami hazards all over the world. However, the event not only showed the catastrophic wave-induced energy of tsunamis and its potential for destruction. In particular, it demonstrated the need for intensified geo-scientific research on tsunami events and on extreme wave events (MAMO et al. 2009). Comprehensive knowledge about comparable tsunami events in the past is necessary for the estimation of tsunami hazard in a distinct area and for effective coastal protection measures. Obviously, reliable information on frequency and magnitude of tsunamis are inevitable for an appropriate hazard assessment (BONDEVIK 2008). Besides the analysis of historical accounts, geo-scientific investigations on the imprint of extreme wave events on near-coast geological archives are considered as one of the most promising approaches in palaeo-tsunami and palaeo-event research, since they are capable of extending length and chronological resolution of the record well beyond that of the historical period (CISTERNAS et al. 2005, DOMINEY-HOWES et al. 2006, BAHLBURG & WEISS 2007, DONNELLY & WOODRUFF 2007, SATAKE & ATWATER 2007, MAMO et al. 2009). For the IOT, this fact has recently been demonstrated by MONECKE et al. (2008) and JANKAEW et al. (2008). In this context, the differentiation of different extreme wave events – usually storm and tsunami – still represents one of the main problems in palaeo-event research. Hence, geo-scientific investigations on event deposits promise to improve the available research toolkit (MAMO et al. 2009).

From a geomorphological point of view, coastlines are considered to be considerably young morphological features since they formed due to the global eustatic sea level rise after the last glacial maximum. Moreover, they are subject to continuous morphological changes depending on the interacting effects of their controlling mechanisms, such as sediment supply, sea level fluctuations and tectonic movements (WOODROFFE 2003, MORTON 2009). In addition, the occurrence of extreme wave events, such as winter storm surges, tropical cyclones and tsunamis, have induced considerable changes in coastal configuration, although affecting the coastline no longer than a few days or hours (e.g. ANDRADE 1992, COCH 1994, DAWSON 1994, MORTON & SALLENGER 2003, WOODROFFE 2003, WANG & HORWITZ 2007, CHOOWONG et al. 2009, LIEW et al. 2010). For instance, several devastating storm surges, such as the 2nd "Marcellusflut" in 1362 and the "Burchardiflut" in 1634, considerably changed coastal configuration (for instance the evolution of the *Jadebusen*) in northern Germany (BEHRE 2004, BIRD 2008). However, only exceptional storm surges are reported to involve the deposition of washover sediments in backbeach areas and/or the breakdown or movement of entire barrier beaches. From a geomorphological point of view, palaeo-tsunami and palaeo-event research is thus crucial not only in terms of hazard estimation – it is also important (i) to document event related changes in shoreline evolution, (ii) to understand coastal responses on extreme wave events, and (iii) to decipher the influence and morphodynamic effects of such events on coastal systems throughout time (GOFF et al. 2009, MAMO et al. 2009, PARIS et al. 2009, WONG 2009).

During the last 8 years, comprehensive geo-scientific investigations on the evolution of coastal Akarnania (NW Greece) have been carried out, dealing with its palaeogeographical evolution and its geoarchaeological background (MAY 2006, VÖTT et al. 2006a, 2006b, 2006c, 2007b, 2007c, BROCKMÜLLER et al. 2007, MAY et al. 2008a, SCHRIEVER 2007). Within the course of these studies, investigations have been carried out in the Lefkada – Preveza coastal zone as well. Here, as also documented for numerous coastal areas in the Aegean (e.g. KRAFT et al. 1980, BRÜCKNER et al. 2005, VOUVALIDIS et al. 2005) and western Greece (e.g. KRAFT et al. 1977, BESONEN 1997, MAY 2006, VÖTT 2006, 2007, VÖTT et al. 2007b, 2007c, ENGEL et al. 2009b), coastal morphology implies widespread palaeogeographical changes throughout time. However, the investigations revealed several anomalies in the sedimentary record which were related to the effects of extreme wave events. According to the investigations of VÖTT et al. (2006d, 2007a, 2008, 2009a, 2009b) and MAY et al. (2007, 2008b), the study area thus was also affected by extreme wave events which have contributed to the evolution of the present coastline. The interaction of long-term, gradual coastal processes and sudden, impulsive coastal changes during the coastal evolution, the latter representing singularities in the geomorphic system (SCHEIDEGGER 1994), and in particular the contribution of tsunami events to coastal changes in the study area is thus evident and worth analyzing.

1.2 STUDY AREA

1.2.1 TECTONIC SETTING

The area between Lefkada Island and Preveza at the entrance to the Ambrakian Gulf (NW Greece) is exposed to the northern part of the Hellenic Arc (Fig. 1-1 a). Here, the Adriatic

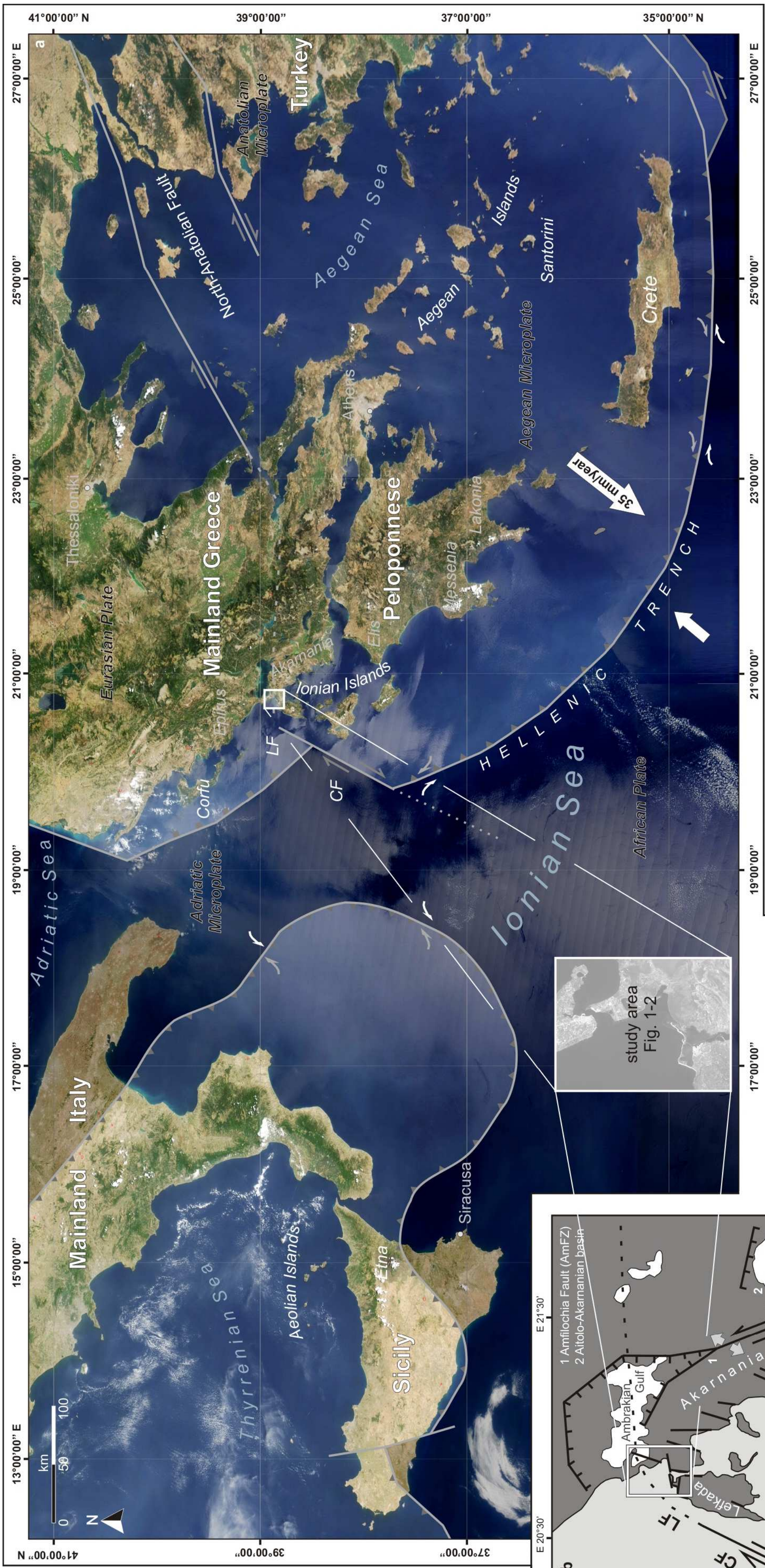

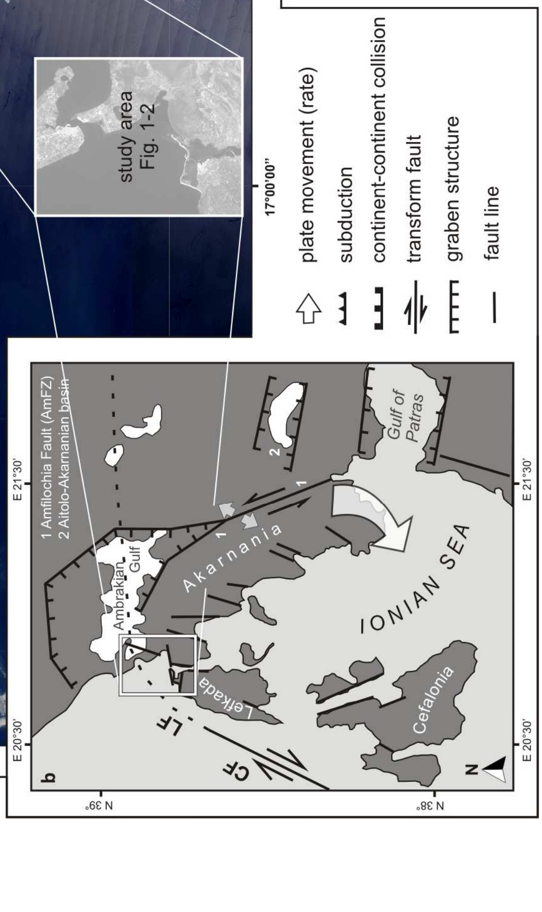

Fig. 1-1: Tectonic overview of the eastern Mediterranean (a) and north-western Greece (b) with main tectonical features [maps based on Modis Satellite Image (NASA), Clews 1989, Haslinger et al. 1999, McClusky et al. 2000, Wortel & Spakman 2000, Doutsos & Kokkalas 2001, Facenna et al. 2001].

microplate is subducted by the Aegean microplate, resulting in the formation of the accompanying Hellenic Trench and a typical volcanic arc in the Aegean Sea to the north. According to COCARD et al. (1999), the overriding Aegean microplate is moving south-westwards by 35 mm/yr. This motion is accompanied by a 30° clockwise rotation and a separation of the Akarnanian block from the Greek mainland (Fig. 1-1 b). In the study area, numerous fault lines result from the related high crustal stress and are responsible for the given topographical preconditions (Fig. 1-1 b).

The Cefalonia transform fault (CF) and the Lefkada transform fault (LF), situated west of the Ionian Islands Cefalonia and Lefkada, connect this zone of subduction with an area of continent-continent collision beginning off the southern epirotic coast (Fig. 1-1 a). The CF and the LF, as its northern prolongation, show a remarkably high seismic activity and have been responsible for numerous strong earthquakes during history (COCARD et al. 1999, LOUVARI et al. 1999, SACHPAZI et al. 2000, PAPADOPOULOS et al. 2003, KARAKOSTAS et al. 2004, BENETATOS et al. 2005, KOKINOU et al. 2006). Therefore, the study area belongs to the seismically most active regions of the Mediterranean. According to SOLOVIEV (1990) and PAPAZACHOS & DIMITRIU (1991), it owns a high tsunamigenic potential.

1.2.2 GEOGRAPHICAL CONTEXT

From a topographical point of view, the study area comprises the coastal area between the northern point of Lefkada Island and the southern part of Aktium Headland (Fig. 1-2), situated in NW Greece. Lefkada Island is separated from the Greek mainland of Akarnania by the shallow lagoonal environment of the Lefkada Lagoon and the Sound of Lefkada. This shallow lagoonal environment is sealed off from the open Ionian Sea by an extended barrier beach system the base of which is made up of beachrock down to approximately 12 m below present mean sea level (b.s.l). To the north-east, the barrier beach forms a spit, extending into the southern part of the Bay of Aghios Nikolaos. Here, the recent beach ridge is shifted eastwards and thus separated from its beachrock base. This beachrock base – the so-called Plaka – is partly submerged and represents a reef-like palaeo-coastline (Fig. 1-2). To the north, the beachrock sequence is fragmented. However, it protects the Bay of Aghios Nikolaos from the open sea and considerably reduces wave energy.

To the east, the Bay of Aghios Nikolaos is characterized by a funnel-like topography and a remarkable depression in its central part. The northern part of the Bay of Aghios Nikolaos is bordered by the south-western coast of Aktium Headland, which is surrounded by the Strait of Preveza to the north and the Ambrakian Gulf to the east. The Phoukias spit, an accretional sand spit, is situated in the south-western part of Aktium Headland (NW Greece). To the south, the spit extends several hundred meters into the Bay of Aghios Nikolaos.

The Lefkada Lagoon is crossed by a narrow artificial channel of ~ 5 m water depth from north to south, which was excavated in the 19th and 20th centuries. Outside the channel, the lagoon is characterized by a water depth between 0.1 m and 0.7 m. Here, the depositional environment is quiescent and characterized by partly anoxic conditions and clayey to silty sediments. Shallow areas periodically fall dry related to wind and tidal conditions and represent mud flats exposed to subaerial conditions. The lagoon is sheltered from wave activity by the extensive barrier beach of the Lefkada barrier beach system, which can be divided into a western (Gyrapetra barrier beach) and an eastern part (Aghia Mavra barrier beach, see Fig. 1-2).

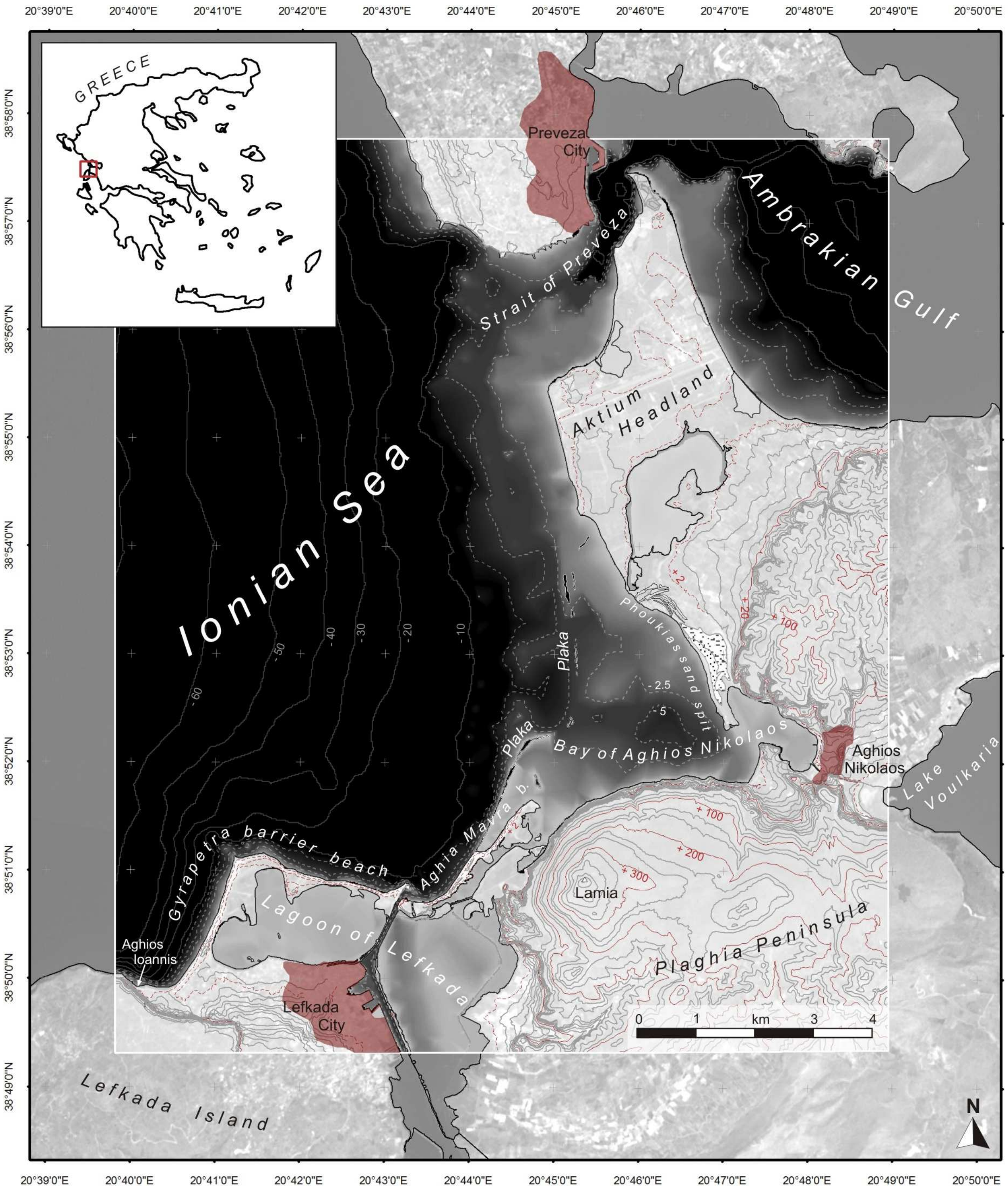

Fig. 1-2: Topographical overview of the Lefkada – Preveza coastal zone. The study area comprises the northern part of the Lagoon of Lefkada, the Bay of Aghios Nikolaos and the southern part of Aktium Headland [map based on Aster satellite image 2003 (USGS), TM 1:50.000 sheets Vonitsa & Lefkada (HMGS), bathymetrical chart Amvrakikos Gulf (HNHS) and SRTM elevation data (NASA)].

For the study area the occurrence of tropical cyclones can be excluded, although initial tropical cyclone-like generation of storm areas is theoretically possible (EMANUEL 2005). However, strong winds and storms are well known in the Mediterranean, but most storm surges apparently are triggered by the polar jet stream, periodically affecting the area during winter (see e.g. LIONELLO et al. 2006). For this reason, wave intensity, if at all, comparable to tsunamis may only be attained by exceptionally large winter storms.

1.3 STUDY AIMS

For the eastern Mediterranean and, in particular, for the Ionian Sea and the study area, a high seismic activity and a resulting tsunamigenic potential is evident. For the study area, sedimentary imprints in near-coast geological archives must be expected and have already been documented by previous investigations. Tsunamis are thus assumed to have contributed to the coastal evolution. In the context of the main objectives of extreme wave event research, the distinguishability of event deposits in the geological record and the evaluation of event recurrence rates, the present dissertation aims

(i) to document coastal changes and the palaeogeographical context in the Lefkada – Preveza coastal zone,
(ii) to detect possible event layers in the sedimentary record,
(iii) to determine the related hydrodynamic process (tsunami/storm) which induced the event deposits, and
(iv) to date the encountered event deposits and main changes in the study area's coastal configuration.

Thereby, it attempts

(v) to verify and to decipher the influence of extreme wave events on the coastal evolution, and
(vi) to determine the main reasons for the coastal changes in the study area.

In conclusion, this study thus contributes to the detection of extreme event deposits in near-coast geological archives and their influence on coastal change. Moreover, it provides further geo-scientific evidence of extreme wave event deposits and may enhance the data pool of palaeo-tsunami deposits.

1.4 PALAEO-EVENT RESEARCH

1.4.1 TSUNAMI DEPOSITS IN THE GEOLOGICAL RECORD

Tsunami and storm waves are characterized by different hydrodynamic regimes (WEISS et al. 2008). The term „Tsunami“ is derived from the Japanese word for harbor wave and is equally used for seismic sea waves since 1963. Tsunamis are "water waves with long wavelengths…[that]…can travel for thousands of kilometers from the disturbance area where they have been created with a minimum loss of energy" (HELENE & YAMASHITA 2006: 855). They are generated by a sudden vertical movement of the whole water column or the quick replacement of large amounts of water (BRYANT 2001). In contrast to wind generated waves, tsunamis have wavelengths of up to several hundred kilometers and are characterized by periods – the time between the passing of two wave crests – of 1.6 to 30 minutes (BRYANT 2001) or 10 to 120 minutes (DAS GUPTA 2006), respectively. Highest velocities can reach 160 to 250 m/s in the open sea, but speed of wave propagation is reduced to 85 m/s in shelf regions and ca. 10 m/s onshore due to the increasing ground friction of the rising subaqueous topography. Here, the resultant deceleration and the accompanied orbital flattening of the wave results in diminished wavelengths and increasing wave heights, whereas the periodicity is not affected. In contrast, storms typically comprise a storm surge with superimposed wind waves (WEISS et al. 2008). Storms are indicated by smaller wave heights, shorter periods, higher frequency of inundation pulses and overall lower energy (SWITZER & JONES 2008a). The differences in the hydrodynamic characteristics of storm and tsunami are assumed to involve differences in the sedimentary record (BAHLBURG & WEISS 2007).

First sedimentary studies about tsunami imprints in geological archives were carried out in the late 1980s (ATWATER 1987, DAWSON et al. 1988). Since then, two main types of extreme wave event deposits have been described: (i) fine grained allochthonous marine sediments found in near-coast geological archives, such as lagoons or coastal swamps (e.g. DAWSON et al. 1988, CLAGUE & BOBROWSKI 1994, BONDEVIK et al. 2005, ENGEL et al. 2009a, VÖTT et al. 2009a, 2009b), and (ii) wave-emplaced block deposits along rocky shorelines (e.g. NOTT 1997, 2003, MASTRONUZZI & SANSO 2000, SCHEFFERS & KELLETAT 2005, GOTO et al. 2007, 2009, SCHEFFERS & SCHEFFERS 2007, MAOUCHE et al. 2009). Submarine tsunami deposits have been described for instance by REINHARDT et al. (2006) and GOODMAN-TCHERNOV et al. (2009) from the coasts of Israel. The IOT considerably increased research on extreme wave events and numerous studies on both storm and tsunami events have been published (MAMO et al. 2009). However, in many cases the interpretation of palaeo-event deposits and the determination of the event source remains problematic, and only the marine origin and the high-energy nature of the deposit can be proved. Therefore, a vivid discussion on the distinguishability between tsunami and storm deposits in the geological record has evolved (e.g. NOTT 1997, 2003, NANAYAMA et al. 2000, SCHEFFERS & KELLETAT 2001, KORTEKAAS 2002, GOFF et al. 2004, WILLIAMS & HALL 2004, SCHEFFERS 2005, ROBINSON et al. 2006, KORTEKAAS & DAWSON 2007, MORTON et al. 2007, 2008a, NANAYAMA 2008, SPISKE et al. 2008, SWITZER & JONES 2008a, 2008b, SWITZER & BURSTON 2010) and several authors summarized sedimentary characteristics of both storm and tsunami deposits existing to date (e.g. DOMINEY-HOWES et al. 2006, DAWSON & STEWART 2007, KORTEKAAS & DAWSON 2007, MORTON et al. 2007, SUGAWARA et al. 2008, SWITZER & JONES 2008a, MAMO et al. 2009).

Most depositional signatures in extreme wave event deposits have been found for both tsunami and storm deposits. Thus, if encountered in a potential event deposit, many sedimentary features are not capable to appropriately distinguish between tsunami and storm and do not represent independent, diagnostic criteria for the determination of the related hydrodynamic process (SWITZER & JONES 2008a). Nevertheless, according to MORTON et al. (2007) and KORTEKAAS & DAWSON (2007), rip-up clasts and/or mud clasts from the eroded underlying strata occur in tsunami deposits but have not been detected in most storm sediments. This is also true for mud drapes separating individual layers within an event deposit, which are interpreted to form due to decreasing flow velocities subsequent to a major inundation impulse during a tsunami event (MORTON et al. 2007, KORTEKAS & DAWSON 2007). Additionally, most storm deposits are reported to be characterized by a sequence of numerous thin layers or laminae, typically more than 15, consisting of sandy material and showing fining upward (normal grading) or coarsening upward (inverse grading) sequences. In contrast, considerably fewer subunits are reported from most tsunami deposits (MORTON et al. 2007, SWITZER & JONES 2008a, WILLIAMS 2009, NICHOL et al. 2007, TUTTLE et al. 2004). More subunits and/or lamination within tsunami sediments for instance have been described by PARIS et al. (2007), who examined sediments of the IOT and attribute these findings to the effects of backwash and/or waning phases during the event. Recently, promising results also have been presented by REINHARDT et al. (2006) and DONATO et al. (2008), the latter investigating known tsunami and storm deposits from Oman and focusing on the macrofaunal and taphonomic characteristics of the sediments. According to these authors tsunami deposits considerably differ from storm deposits in (i) the percentage of mollusc fragments showing angular breaks, (ii) the percentage of rounded and/or reworked mollusc fragments and (iii) the percentage of articulated bivalves within the event deposit. DONATO et al. (2008, p. 209) states that "it is the collection of these characters, however, that is diagnostic of a tsunami deposit rather than any one of these variables alone".

In contrast, further depositional characteristics, such as sharp erosional contacts at the base of an event deposit, poor and/or well sorting, normal and inverse graded sequences, a thinning and fining landward of event deposits as well as ostracod, diatom and foraminifera assemblages are considered to only prove the event-induced origin of the sediment (KORTEKAAS & DAWSON 2007, MORTON et al. 2007, SWITZER & JONES 2008a), due to the fact that these characteristics are all a product of the marine source or the high energy nature of the sediment. However, according to SWITZER & JONES (2008a), storm related sandy washover deposits in backbarrier environments are often characterized by better sorting since the material is assumed to be solely of littoral origin. In contrast, tsunamigenic sediments appear mixed and poorly sorted in most cases, since tsunami also incorporate material from both the sublittoral and littoral zone.

Distinguishing storm generated from tsunami generated sediments, particularly documented by recent investigations on sandy deposits accumulated during the IOT, is still problematic and "remains a serious challenge" (BRIDGE 2008: 94). A number of difficulties in the interpretation of event deposits remain (MORTON et al. 2007, SWITZER & JONES 2008a), since the characteristics of each tsunami and therefore its sedimentary imprint in the geological archive and/or its effects on coastal morphology depend on the regional setting, comprising bathymetry, shelf- and coastal topography or the amount and type of available sediment. These circumstances can vary considerably between each affected area. Therefore, a general comparison of tsunami deposits from different locations and their depositional characteristics has to be carefully implemented. Where possible, investigations on local modern analogues, such as the sedimentary traces of either storm or tsunami, may be carried out (ENGEL et al. in review). Moreover, a combination of different characteristics and "diagnostic" criteria for tsunami may allow to "positively attributing a sedimentary sequence to deposition by a tsunami" (MAMO et al. 2009: 268). However, (i) detailed sedimentary analysis of event deposits, comprising the implementation of as many empirical sedimentary signatures as possible, as well as their chronological interpretation, and (ii) comprehensive investigations on coastal geographies and the related geomorphologic and geomorphodynamic characteristics of the area of interest may help to better understand the main characteristics of extreme wave events and their imprints in geological archives and may improve their interpretation (SATAKE & ATWATER 2007, MAMO et al. 2009).

1.4.2 Sedimentary evidence for tsunamis worldwide and in the eastern Mediterranean

Apart from the ongoing debate about the distinguishability of event deposits in near-coast geological archives, several authors presented indication for tsunami and palaeo-tsunami events in numerous coastal areas of the world by the detection of related sediments in geological archives within the last decades (Dawson & Shi 2000, Kelletat & Scheffers 2003), for instance along the circum-pacific coasts (e.g. Nott 1997, Clague et al. 2000, Fujiwara et al. 2000, Goff et al. 2001, Pinegina & Bourgeois 2001, Davies et al. 2003, Gelfenbaum & Jaffe 2003, Keating et al. 2005, Switzer et al. 2005, Wallner 2008), the Caribbean (e.g. Hearty 1997, Scheffers 2003, Scheffers et al. 2005, Engel et al. 2009a, in review), or the Atlantic ocean and the western Mediterranean (Dawson et al. 1995, Hindson & Andrade 1999, Luque et al. 2002, Scheffers & Kelletat 2005, Kortekaas & Dawson 2007, Reicherter & Becker-Heidmann 2009), and especially the IOT involved a large number of publications on the characteristics of tsunami deposits (e.g. Bishop et al. 2005, Szczucinski et al 2005, Bahlburg & Weiss 2007, Choowong et al. 2007, Goto et al. 2007, Narayana et al. 2007, Hawkes et al. 2007, Paris et al. 2007, Srinivasalu et al. 2007, Morton et al. 2008b, Fujino et al. 2009, Jagodzinski et al 2009, Paris et al. 2009).

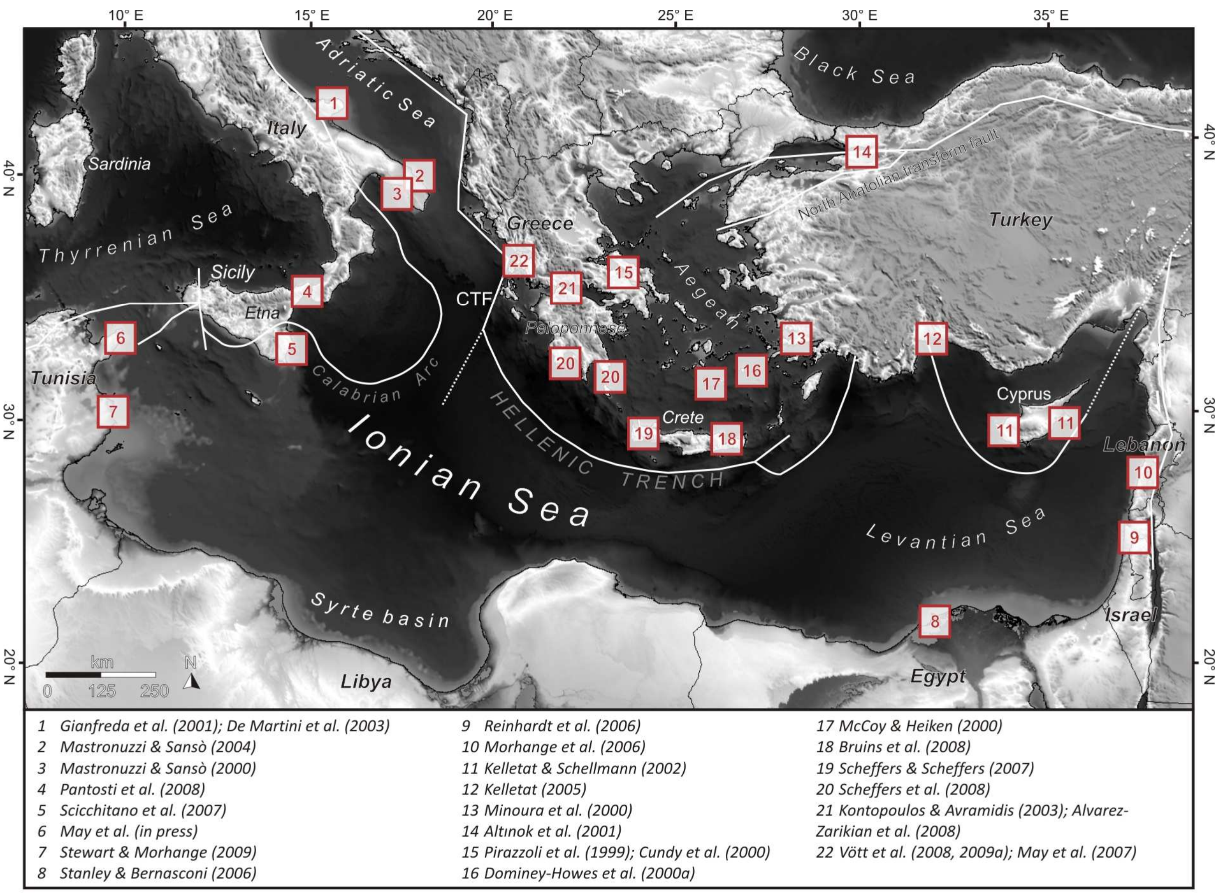

Fig. 1-3: Topographical overview of the central and eastern Mediterranean with geo-scientific findings of tsunami deposits [map based on SRTM elevation data (NASA), Wortel & Spakman 2000, Facenna et al. 2001].

For the eastern Mediterranean, Vött & May (2009) summarized geo-scientific evidence for tsunamis in the recent past (see Fig. 1-3). In Greece, sedimentary evidence for palaeo-tsunami events first was reported from the Aegean Sea and adjacent Islands. Especially the Santorini-eruption, dated to ~1600 BC, was subject to geological investigations and probable related tsunami deposits are reported from Crete (MINOURA et al. 2000, DOMINEY-HOWES et al. 2000b, MCCOY & HEIKEN 2000, SCHEFFERS & SCHEFFERS 2007, BRUINS et al. 2008) and the western coast of Turkey (MINOURA et al. 2000), partly associated to archaeological excavation sites and investigations. For the Santorini tsunami, evidence is brought also by REINHARDT et al. (2006) and GOODMAN-TCHERNOV et al. (2009) from the Levante. According to DOMINEY-HOWES et al. (2000a), the 1956 tsunami in the southern Aegean Sea deposited imbricated pebbles on the island of Astypalaea.

Recently, KORTEKAAS (2002) and KONTOPOULOS & AVRAMIDIS (2003) gave evidence for tsunamigenic sediments in the Corinthian Gulf, and SCHEFFERS et al. (2008) could provide findings for palaeo-tsunami imprints from the southern and south-western Peloponnese. For the study area, VÖTT et al. (2006d, 2007a, 2008, 2009a, 2009b) and MAY et al. (2007, 2008b) presented manifold sedimentary evidence for tsunami influence. Several studies about tsunami induced changes of coastal morphology, such as boulder and block accumulations along rocky shorelines (MASTRONUZZI & SANSO 2000, 2004, SCICCHITANO et al. 2007), washover fans (GIANFREDA et al. 2001), and anomalies in near-coast geological archives (DE MARTINI et al. 2003, PANTOSTI et al. 2008) also exist for southern and south-eastern Italy. Nevertheless, the event source of these deposits is a matter of discussion.

1.4.3 HISTORICAL REPORTS ON TSUNAMIS IN THE EASTERN MEDITERRANEAN

Besides the detection of event deposits in the geological record, information about palaeo-events is brought by historical reports. Ancient historians like Strabo and Tukydides report on natural hazards, such as earthquakes, floods or landslides, that occurred during or before their lifetimes and which had catastrophic effects on ancient population and settlements. Some of these events can be ascribed to tsunamis or at least point to related tsunami generation. The destruction of the famous ancient city of Helike (Gulf of Corinth), 373 BC, for example is attributed to a strong earthquake and an accompanying major tsunami event, and several further tsunami events, such as the earthquake-induced tsunami 365 AD southwest of Crete, are reported to have catastrophically affected the eastern Mediterranean coasts (STEFANAKIS 2006, SHAW et al. 2008, VÖTT & MAY 2009).

Comparable historical sources and anthropogenic records provide information about palaeo-tsunami events since 2500 or so years (PAPAZACHOS & DIMITRIU 1991). These records have been summarized in tsunami catalogues, which now represent a comprehensive tsunami database for the last 2.5 millennia and provide information about ca. 4000 tsunami events within the last 2000 years (SCHEFFERS & KELLETAT 2003).

For the study area, VÖTT et al. (2006d) and FLOTH (2008) summarized available palaeo-tsunami data by investigating global and regional tsunami catalogues of the National and Atmospheric Administration (NOAA, http://www.ngdc.noaa.gov/hazard/tsu_db.shtml), the National Observatory of Athens (NOA, http://www.gein.noa.gr/services/tsunami.htm), the Tsunami Laboratory Novosibirsk (TLN, http://tsun.sscc.ru/On_line_Cat.htm), PAPAZACHOS & PAPAZACHOU (1997) and SOLOVIEV et al. (2000). TINTI et al. (2001, 2004) compiled the historical tsunami data for the entire European area and for the Italian coasts. Disregarding their intensities and the given differences in their reliability, tsunami reoccurrence rates of 8-11 years can be assumed for western Greece according to VÖTT et al. (2006d), SOLOVIEV et al. (2000) and SCHIELEIN et al. (2007). For the Ionian Sea and therefore also for the broader study area, the latter authors document the highest frequency of historical tsunami reports within the last 2500 years (Fig. 1-4).

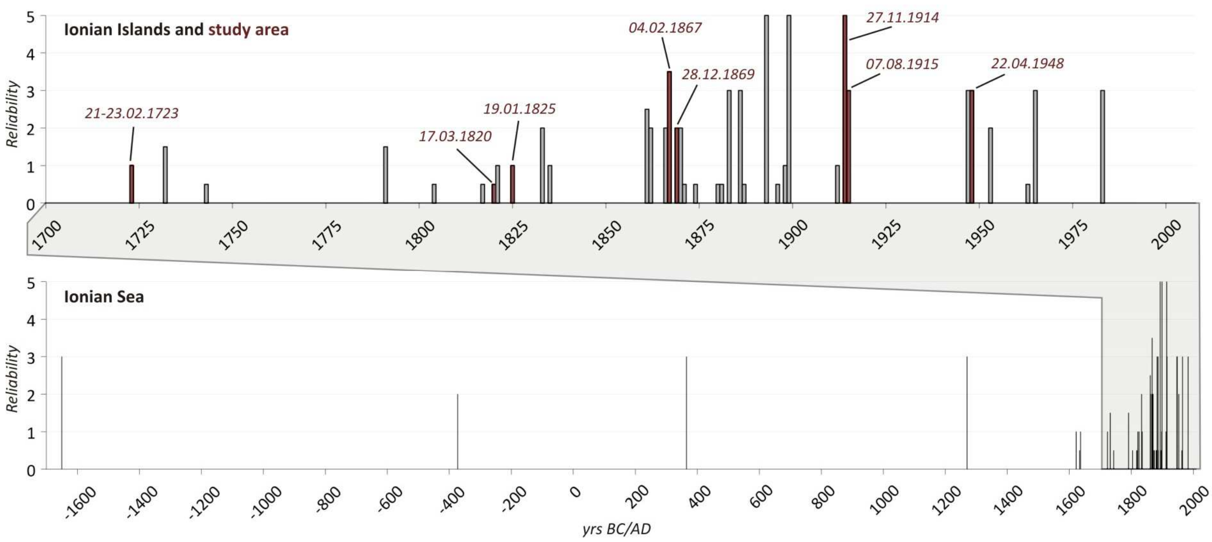

Fig. 1-4: Historical tsunami events reported for the Ionian Sea and the study area (red label). Reliability of the tsunami event based on SOLOVIEV et al. (2000): 1 - questionable, 2 - possible, 3 - probable, 4 - reliable, 5 - definite. Depicted data is based on global and regional tsunami catalogues (NOAA, NOA, TLN, PAPAZACHOS & PAPAZACHOU 1997, SOLOVIEV et al. 2000) and compilations carried out by VÖTT et al. (2006d) and FLOTH (2008). The increase in quality and quantity of the tradition of events during the last 200 – 300 years is due to a more accurate recording.

1.5 STUDY OUTLINE

For the study area, the interaction of long-term, gradual and episodic, impulsive coastal processes is evident. The contribution of extreme wave events to coastal change throughout time is not yet well understood and may also be underestimated. Consequently, geo-scientific research on the evolution of coastal areas has to consider both gradual and sudden processes. *Chapter 1* introduces the scientific background of the study and serves to clarify the relevance of research on extreme wave events, in particular on tsunami, within the context of coastal change. Without knowledge about the continuous gradual coastal processes and related coastline changes, the detection and the interpretation of event deposits is difficult. In turn, when implementing geo-scientific studies on palaeo-event deposits, the interpretation of the sedimentary record demands a comprehensive understanding of its (palaeo-) geographical context. Since the geomorphological pattern of coastal areas stores comprehensive information about its geodynamic evolution and the contributing morphodynamic processes, the geomorphological inventory of the investigated area is introduced in *Chapter 2*. The related geomorphodynamic processes, their controlling mechanisms and their interacting effects on coastal evolution are discussed, and coastal changes are documented in order to decipher the palaeogeographical context of the study area. It thereby focuses on the main geological archives and serves as a precondition for the following chapters by establishing the geomorphological framework. In *Chapter 3* and *Chapter 4*, detailed sedimentary and geomorphological investigations on fine grained sediments found in coastal geo-archives in the study area are presented. The investigations intend to detect possible event layers and to verify and to decipher a possible influence of extreme wave events on the coastal evolution. A determination of the main reasons for the coastal changes is attempted. Moreover, the contribution and the interaction of gradual and sudden geomorphodynamic changes are discussed. Thereby, the study aims to determine the related hydrodynamic process (tsunami/storm) which induced the event deposits and the related coastal changes. Where possible, dating of the main coastal changes, the related morphodynamic processes and possible major extreme wave events is presented. In *Chapter 5* block deposits found in the study area, representing the second category of extreme wave event deposits, are described and their high energy wave origin is discussed. Finally, the obtained results are combined in *Chapter 6*, providing a synthesis.

1.6 REFERENCES

Altinok, Y., Tinti, S., Alpar, B., Yalçiner, A.C., Ersoy, S., Bortolucci, E., Armigliato, A., (2001). The Tsunami of August 17, 1999 in Izmit Bay, Turkey. *Natural Hazards*, 24, 133–146.

Alvarez-Zarikian, C.A., Soter, S. & Katsonopoulou, D. (2008). Recurrent Submergence and Uplift in the Area of Ancient Helike, Gulf of Corinth, Greece: Microfaunal and Archaeological Evidence. *Journal of Coastal Research,* 24(SI1), 110-125.

Andrade, C. (1992). Tsunami Generated Forms in the Algarve Barrier Islands (South Portugal). *Science of Tsunami Hazards*, 10(1), 21-34.

Atwater, B. F. (1987). Evidence for Great Holocene Earthquakes along the Outer Coast of Washington State. *Science,* 236, 942-944.

Bahlburg, H. & Weiss, R. (2007). Sedimentology of the December 26, 2004, Sumatra tsunami deposits in eastern India (Tamil Nadu) and Kenya. *International Journal of Earth Sciences*, 96(6), 1195-1209.

Behre, K.-E. (2004). Coastal development, sea-level change and settlement history during the later Holocene in the Clay District of Lower Saxony (Niedersachsen), northern Germany. *Quaternary International*, 112(1), 37-53.

Benetatos, C., Kiratzi, A., Roumelioti, Z., Stavrakakis, G., Drakatos, G. & Latoussakis, I. (2005). The 14 August 2003 Lefkada Island (Greece) earthquake: Focal mechanisms of the mainshock and of the aftershock sequence. *Journal of Seismology,* 9, 171–190.

Bernasconi, M.P., Melis, R. & Stanley, J.-D. (2006). Benthic biofacies to interpret Holocene environmental changes and human impact in Alexandria's Eastern Harbour, Egypt. *The Holocene*, 16, 1163-1176.

Besonen, M.R. (1997). *The Middle and Late Holocene Geology and Landscape Evolution of the Lower Acheron River Valley, Epirus, Greece*. Unpublished M.Sc. thesis, University of Minnesota.

Bird, E. (2008). *Coastal Geomorphology – An Introduction*. New York, 411 pp.

Bishop, P., Sanderson, D.C.W., Hansom, J.D. & Chaimanee, N. (2005). Age-dating of tsunami deposits: lessons from the 26 December 2004 tsunami in Thailand. *Geographical Journal*, 171, 379-384.

Bondevik, S. (2008). The sands of tsunami time. *Nature*, 455, 1183-1184.

Bondevik, S., Mangerud, J., Dawson, S., Dawson, A. & Lohne, Ø. (2005). Evidence for three North Sea tsunamis at the Shetland Islands between 8000 and 1500 years ago. *Quaternary Science Reviews*, 24, 1757–1775.

Bridge, J.S. (2008): Discussion of articles in “Sedimentary features of tsunami deposits”. *Sedimentary Geology*, 211, 94.

Brockmüller, S., Vött, A., May, S.M. & Brückner, H. (2007). Palaeoenvironmental changes of the Lefkada Sound (NW Greece) and their archaeological relevance. *Coastline Reports*, 9, 127-138.

Brückner, H., Vött, A., Schriever, A. & Handl, M. (2005). Holocene delta progradation in the eastern Mediterranenan – case studies in their historical context. *Mediterranée*, 1(2), 95-106.

Bruins, H.J., MacGillivray, J.A., Synolakis, C.E., Benjamini, C., Keller, J., Kisch, H.J., Klügel, A. & van der Plicht, J. (2008). Geoarchaeological tsunami deposits at Palaikastro (Crete) and the Late Minoan IA eruption of Santorini. *Journal of Archaeological Science*, 35, 191-212.

Bryant, E. (2001). Tsunami: The Underrated Hazard. Berlin, 342 pp.

Choowong, M., Murakoshi, N., Hisada, K., Charusiri, P., Daorerk, V., Charoentitirat, T., Chutakositkanon, V., Jankaew, K. & Kanjanapayont, P. (2007). Erosion and Deposition by the 2004 Indian Ocean Tsunami in Phuket and Phang-nga Provinces, Thailand. *Journal of Coastal Research*, 23(5), 1270-1276.

Choowong, M., Phantuwongraj, S., Charoentitirat, T., Chutakositkanon, V., Yumuang, S. & Charusiri, P. (2009). Beach recovery after 2004 Indian Ocean tsunami from Phang-nga, Thailand. *Geomorphology*, 104(3-4), 134-142.

Cisternas, M., Atwater, B.F., Torrejon, F., Sawai, Y., Machuca, G., Lagos, M., Eipert, A., Youlton, C., Salgado, I., Kamataki, T., Shishikura, M., Rajendran, C.P., Malik, J.K., Rizal, Y. & Husni, M. (2005). Predecessors of the giant 1960 Chile earthquake. *Nature,* 437, 404-407.

Clague, J.J. & Bobrowsky, P.T. (1994). Evidence for a Large Earthquake and Tsunami 100-400 Years Ago on Western Vancouver Island, British Columbia. *Quaternary Research,* 41(2), 176-184.

Clague, J.J., Bobrowsky, P.T. & Hutchinson, I. (2000). A review of geological records of large tsunamis at Vancouver Island, British Columbia, and implications for hazard. *Quaternary Science Reviews*, 19, 849-863.

Clews, J.E. (1989). Structural controls on basin evolution: Neogene to Quaternary of the Ionian zone, Western Greece. *Journal of the Geological Society*, 146, 447-457.

Cocard, M., Kahle, H.-G., Peter, Y., Geiger, A., Veis, G., Felekis, S., Paradissis, D. & Billiris, H. (1999). New constraints on the rapid crustal motion of the Aegean region: recent results inferred from GPS measurements (1993–1998) across the West Hellenic Arc, Greece. *Earth and Planetary Science Letters,* 172, 39–47.

Coch, N.K. (1994). Geologic effects of hurricanes. *Geomorphology*, 10(1-4), 37-63.

Cundy, A.B., Kortekaas, S., Dewez, T., Stewart, I.S., Collins, P.E.F., Croudace, I.W., Maroukian, H., Papanastassiou, D., Gaki-Papanastassiou, P., Pavlopoulos, K. & Dawson, A. (2000). Coastal wetlands as recorders of earthquake subsidence in the Aegean: a case study of the 1894 Gulf of Atalanti earthquakes, central Greece. *Marine Geology,* 170(1-2), 3-26.

Das Gupta, S.P. (2006). The Indian Ocean Mega-Tsunami of 2004. *Geographical Review of India*, 68(2), 113-160.

Davies, H.L., Davies, J.M., Perembo, R.C.B. & Lus, W.Y. (2003). The Aitape 1998 Tsunami: Reconstructing the Event from Interviews and Field Mapping. *Pure and Applied Geophysics*, 160, 1895–1922.

Dawson, A.G. (1994). Geomorphological effects of tsunami run-up and backwash. *Geomorphology*, 10, 83-94.

Dawson, A.G. & Shi, S. (2000). Tsunami Deposits. *Pure and Applied Geophysics*, 157*,* 875-897.

Dawson, A.G. & Stewart, I. (2007). Tsunami deposits in the geological record. *Sedimentary Geology*, 200(3-4), 166-183.

Dawson, A.G., Long, D. & Smith, D.E. (1988). The Storegga Slides: Evidence from eastern Scotland for a possible tsunami. *Marine Geology,* 82(3-4), 271-276.

Dawson, A.G., Hindson, R., Andrade, C., Freitas, C., Parish, R. & Bateman, M. (1995). Tsunami sedimentation associated with the Lisbon earthquake of 1 November AD 1755: Boca do Rio, Algarve, Portugal. *The Holocene*, 5(2), 209-215.

Dawson, S., Smith, D.E., Ruffmann, A. & Shi, S. (1996). The Diatom Biostratigraphy of Tsunami Sediments: Examples from Recent and Middle Holocene Events. *Physics and Chemistry of the Earth,* 21(1-2), 87-92.

De Martini, P.M., Burrato, P., Pantosti, D., Maramai, A., Graziani, L. & Abramson, H. (2003). Identification of liquefaction features and tsunami deposits in the Gargano area (Italy): paleoseismological implication. *Annals of Geophysics*, 46(5), 883-902.

Dominey-Howes, D., Cundy, A. & Croudace, I. (2000a). High energy marine flood deposits on Astypalaea Island, Greece: possible evidence for the AD 1956 southern Aegean tsunami. *Marine Geology*, 163, 303–315.

Dominey-Howes, D.T.M., Papadopoulos, G.A. & Dawson, A.G. (2000b). Geological and Historical Investigation of the 1650 Mt. Columbo (Thera Island) Eruption and Tsunami, Aegean Sea, Greece. *Natural Hazards*, 21, 83–96.

Dominey-Howes, D.T.M., Humphreys, G.S. & Hesse, P.P. (2006). Tsunami and palaeotsunami depositional signatures and their potential value in understanding the late-Holocene tsunami record. *The Holocene*, 16(8), 1095-1107.

Donato, S.V., Reinhardt, E.G., Boyce, J.I., Rothaus, R. & Vosmer, T. (2008). Identifying tsunami deposits using bivalve shell taphonomy. *Geology*, 36(3), 199-202.

Donnelly, J.P. & Woodruff, J.D. (2007). Intense hurricane activity over the past 5,000 years controlled by El Nino and the West African monsoon. *Nature*, 447, 465-468.

Doutsos, T. & Kokkalas, S. (2001). Stress and deformation patterns in the Aegean region. *Journal of Structural Geology*, 23, 455-472.

Emanuel, K. (2005). Genesis and maintenance of "Mediterranean hurricanes", *Advances in Geosciences*, 2, 217-220.

Engel, M., Bolten, A., Brückner, H., Daut, G., Kelletat, D., Schäbitz, F., Scheffers, A., Scheffers, S.R., Vött, A., Wille, M. & Willershäuser, T. (2009a). Reading the chapter of extreme wave events in nearshore geo-bio-archives of Bonaire (Netherlands Antilles) - initial results from Lagun and Boka Bartol. *Marburger Geographische Schriften*, 145, 157-178.

Engel, M., Knipping, M., Brückner, H., Kiderlen, M. & Kraft, J.C. (2009b). Reconstructing middle to late Holocene palaeogeographies of the lower Messenian plain (southwestern Peloponnese, Greece): Coastline migration, vegetation history and sea level change. *Palaeogeography, Palaeoclimatology, Palaeoecology*, 284(3-4), 257-270.

Engel, M., Brückner, H., Wennrich, V., Scheffers, A., Kelletat, D., Vött, A., Schäbitz, F., Daut, G., Willershäuser, T. & May, S.M. (in review). The back-barrier record of eastern Bonaire (Netherlands Antilles): new insights into the palaeo-tsunami history of the southern Caribbean.

Faccenna, C., Becker, T.W., Lucente, F.P., Jolivet, L. & Rossetti, F. (2001). History of subduction and back-arc extension in the Central Mediterranean. *Geophysical Journal International*, 145, 809–820.

FitzGerald, D.M., Fenster, M.S., Argow, B.A., & Buynevich, I.V. (2008). Coastal Impacts Due to Sea-Level Rise. *Annual Review of Earth and Planetary Sciences*, 36(1), 601-647.

Floth, U. (2008). *The tsunami hazard between Lefkada and Preveza, NW Greece, based on computer models as well as field and laboratory evidence*. Unpublished diploma thesis, Philipps-Universität Marburg.

Fujino, S., Naruse, H., Matsumoto, D., Jarupongsakul, T., Sphawajruksakul, A. & Sakakura, N. (2009). Stratigraphic evidence for pre-2004 tsunamis in southwestern Thailand. *Marine Geology*, 262, 25–28.

Fujiwara, O., Masuda, F., Sakai, T., Irizuki, T. & Fuse, K. (2000). Tsunami deposits in Holocene bay mud in southern Kanto region, Pacific coast of central Japan. *Sedimentary Geology*, 135(1-4), 219-230.

Gelfenbaum, G. & Jaffe, B. (2003). Erosion and Sedimentation from the 17 July, 1998 Papua New Guinea Tsunami. *Pure and Applied Geophysics*, 160, 1969–1999.

Gianfreda, F., Mastronuzzi, G. & Sanso, P. (2001). Impact of historical tsunamis on a sandy coastal barrier: an example from the northern Gargano coast, southern Italy. *Natural Hazards and Earth System Sciences*, 1, 213–219.

Goff, J., Chagué-Goff, C. & Nichol, S. (2001). Palaeotsunami deposits: a New Zealand perspective. *Sedimentary Geology*, 143, 1-6.

Goff, J., McFadgen, B.G. & Chagué-Goff, C. (2004). Sedimentary differences between the 2002 Easter storm and the 15th-century Okoropunga tsunami, southeastern North Island, New Zealand. *Marine Geology*, 204, 235-250.

Goff, J.R., Lane, E. & Arnold, J. (2009). The tsunami geomorphology of coastal dunes. *Natural Hazards and Earth System Sciences*, 9(3), 847-854.

Goodman-Tchernov, B.N., Dey, H.W., Reinhardt, E.G., McCoy, F. & Mart, Y. (2009). Tsunami waves generated by the Santorini eruption reached Eastern Mediterranean shores. *Geology*, 37(10), 943-946.

Goto, K., Chavanich, S.A., Imamura, F., Kunthasap, P., Matsui, T., Minoura, K., Sugawara, D. & Yanagisawa, H. (2007). Distribution, origin and transport process of boulders deposited by the 2004 Indian Ocean tsunami at Pakarang Cape, Thailand. *Sedimentary Geology*, 202(4), 821-837.

Goto, K., Okada, K. & Imamura, F. (2009). Characteristics and hydrodynamics of boulders transported by storm waves at Kudaka Island, Japan. *Marine Geology*, 262, 14-24.

Haslinger F., Kissling, E., Ansorge J., Hatzfeld, D., Papadimitriou, E., Karakostas, V., Makropoulos, K., Kahle, H.-G. & Peter, Y. (1999). 3D crustal structure from local earthquake tomography around the Gulf of Arta (Ionian region, NW Greece). *Tectonophysics,* 304(3), 201-218.

Hawkes, A.D., Bird, M., Cowie, S., Grundy-Warr, C., Horton, B.P., Hwai, A.T.S., Law, L., Macgregor, C., Nott, J., Ong, J.E., Rigg, J., Robinson, R., Tan-Mullins, M., Sa, T.-T., Yasin, Z. & Aik, L.W. (2007). Sediments deposited by the 2004 Indian Ocean Tsunami along the Malaysia–Thailand Peninsula. *Marine Geology,* 242, 169–190.

Hearty, P.J. (1997). Boulder Deposits from Large Waves during the Last Interglaciation on North Eleuthera Island, Bahamas. *Quaternary Research*, 48, 326–338.

Helene, O. & Yamashita, M.T. (2006). Understanding the tsunami with a simple model. *European Journal of Physics*, 4, 855-863.

Hellenic Military Geographical Service (HMGS) (1987). TM 1:50.000, sheets Vonitsa & Lefkada.

Hellenic Navy Hydrographic Service (HNHS) (1983). Bathymetrical chart 1:50.000, sheet Amvrakikos Gulf.

Hindson, R.A. & Andrade, C. (1999). Sedimentation and hydrodynamic processes associated with the tsunami generated by the 1755 Lisbon earthquake. *Quaternary International*, 56, 27-38.

Jagodzinski, R., Sternal, B., Szczucinski, W. & Lorenc, S. (2009). Heavy Minerals in 2004 Tsunami Deposits on Kho Khao Island, Thailand. *Polish Journal of Environmental Studies*, 18(1), 103-110.

Jankaew, K., Atwater, B.F., Sawai, Y., Choowong, M., Charoentitirat, T., Martin, M.E. & Prendergast, A. (2008). Medieval forewarning of the 2004 Indian Ocean tsunami in Thailand. *Nature*, 455, 1228-1231.

Karakostas, V.G., Papadimitriou, E.E. & Papazachos, C.B. (2004). Properties of the 2003 Lefkada, Ionian Islands, Greece, earthquake seismic sequence and seismicity triggering. *Bulletin of the Seismological Society of America*, 94(5), 1976-1981.

Keating, B.H., Helsley, C., Waheed, Z. & Dominey-Howes, D. (2005). 2004 Indian Ocean Tsunami on the Maldives Islands: Initial Observations. *Science of Tsunami Hazards*, 23(2), 19-70.

Kelletat, D. (2005). Neue Beobachtungen zu Paläo-Tsunami im Mittelmeergebiet: Mallorca und Bucht von Alanya, türkische Südküste. In: Beck, N. (ed.), *Neue Ergebnisse der Meeres- und Küstenforschung. Beiträge der 23. Jahrestagung des Arbeitskreises ''Geographie der Meere und Küsten'' (AMK), Koblenz, 28–30 April 2005*. *Schriften des Arbeitskreises Landes- und Volkskunde Koblenz (ALV),* 4, 1–14.

Kelletat, D. & Schellmann, G. (2002). Tsunamis on Cyprus: field evidences and 14C dating results. *Zeitschrift für Geomorphologie N.F. Suppl.-Vol.*, 137, 19-34.

Kelletat, D. & Scheffers, A. (2003). Chevron-shaped accumulations along the coastlines of Australia as potential tsunami evidences? *Science of Tsunami Hazards*, 21(3), 174-188.

Kokinou, E., Papadimitriou, E., Karakostas, V., Kamberis, E. & Vallianatos, F. (2006). The Kefalonia Transform Zone (offshore Western Greece) with special emphasis to its prolongation towards the Ionian Abyssal Plain. *Marine Geophysical Researches*, 27(4), 241-252.

Kontopoulos, N. & Avramidis, P. (2003). A late Holocene record of environmental changes from the Aliki lagoon, Egion, North Peloponnesus, Greece. *Quaternary International*, 111, 75-90.

Kortekaas, S. (2002). *Tsunamis, storms and earthquakes: Distinguishing coastal flooding events.* Unbublished PhD thesis, Coventry University.

Kortekaas, S. & Dawson, A.G. (2007). Distinguishing tsunami and storm deposits: An example from Martinhal, SW Portugal. *Sedimentary Geology*, 200, 208–221.

Kraft, J.C., Aschenbrenner, S.E. & Rapp, G. (1977). Paleogeographic Reconstructions of Coastal Aegean Archaeological Sites. *Science*, 195, 941-947.

Kraft, J.C., Kayan, İ. & Erol, O. (1980). Geomorphic Reconstructions in the Environs of Ancient Troy. *Science*, 209, 776-782.

Liew, S.C., Gupta, A., Wong, P.P. & Kwoh, L.K. (2010). Recovery from a large tsunami mapped over time: The Aceh coast, Sumatra. *Geomorphology*, 114(4), 520-529.

Lionello, P., Malanotte-Rizzoli, P. & Boscolo, R. (eds) (2006). *Mediterranean Climate Variability. Developments in Earth & Environmental Sciences, 4*. Amsterdam, 438 pp.

Louvari, E., Kiratzi, A.A. & Papazachos, B.C. (1999) The Cephalonia Transform Fault and its extension to western Lefkada Island (Greece). *Tectonophysics*, 308, 223-236.

Luque, L., Lario, J., Civis, J., Silva, P.G., Zazo, C., Goy, J.L. & Dabrio, C.J. (2002). Sedimentary record of a tsunami during Roman times, Bay of Cadiz, Spain. *Journal of Quaternary Science*, 17(5-6), 623–631.

Mamo, B., Strotz, L. & Dominey-Howes, D. (2009). Tsunami sediments and their foraminiferal assemblages. *Earth-Science Reviews*, 96(4), 263-278.

Maouche, S., Morhange, C. & Meghraoui, M. (2009). Large boulder accumulation on the Algerian coast evidence tsunami events in the western Mediterranean. *Marine Geology*, 262, 96-104.

Mastronuzzi, G. & Sanso, P. (2000). Boulders transport by catastrophic waves along the Ionian coast of Apulia (southern Italy). *Marine Geology*, 170, 93-103.

Mastronuzzi, G. & Sanso, P. (2004). Large Boulder accumulations by extreme waves along the Adriatic coast of southern Apulia (Italy). *Quaternary International*, 120, 173-184.

May, S.M. (2006). *Szenarien zur Palaäogegraphie der Küstenebene von Mytikas (Akarnanien, Nordwestgriechenland) – Ursachen und Folgen des holozänen Küstenwandels.* Unpublished diploma thesis, Philipps-Universität Marburg.

May, S.M., Vött, A., Brückner, H. & Brockmüller, S. (2007). Evidence of tsunamigenic impact on Actio headland near Preveza, NW Greece. *Coastline Reports*, 9, 115-125.

May, S.M., Vött, A., Brückner, H., Herd, R. & Lang, F. (2008a). Geoarchaeological studies in the environs of the ancient dam of Glosses, Akarnania, NW Greece. *Geo-Öko,* 29(1-2), 89-113.

May, S.M., Vött, A., Sakellariou, D., Kapsimalis, V., Herd, R. & Brückner, H. (2008b). On- and offshore tsunami traces around Actio Headland (NW Greece). *Geophysical Research Abstracts,* 10, EGU2008-A-11034.

May, S.M., Willershäuser, T. & Vött, A. (in press). Boulder transport by high-energy wave events at Cap Bon (NE Tunisia). *Coastline Reports.*

McClusky, S., Balassanian, S., Barka, A., Demir, C., Ergintav, S., Georgiev, I., Gurkan, O., Hamburger, M., Hurst, K., Kahle, H., Kastens, K., Kekelidze, G., King, R., Kotzev, V., Lenk, O., Mahmoud, S., Mishin, A., Nadariya, M., Ouzounis, A., Paradissis, D., Peter, Y., Prilepin, M., Reilinger, R., Sanli, I., Seeger, H., Tealeb, A., Toksoz, M.N. & Veis, G. (2000). Global Positioning System constraints on plate kinematics and dynamics in the eastern Mediterranean and Caucasus. *Journal of Geophysical Research-Solid Earth*, 105(3), 5695–5719.

McCoy, F.W. & Heiken, G. (2000). Tsunami Generated by the Late Bronze Age Eruption of Thera (Santorini), Greece. *Pure and Applied Geophysics*, 157, 1227–1256.

McGranahan D.A., Balk, D. & Anderson, B. (2007). The rising tide: assessing the risks of climate change and human settlements in low elevation coastal zones. *Environment and Urbanization*, 19, 17–39.

Minoura, K., Imamura, F., Kuran, U., Nakamura, T., Papadopoulos, G.A., Takahashi, T. & Yalciner, A.C. (2000). Discovery of Minoan tsunami deposits. *Geology*, 28(1), 59-62.

Monecke, K., Finger, W., Klarer, D., Kongko, W., AcAdoo, B.G., Moore, A.L. & Sudrajat, S.U. (2008). A 1,000-year sediment record of tsunami recurrence in northern Sumatra. *Nature*, 455, 1232-1234.

Morhange, C., Marriner, N. & Pirazzoli, P.A. (2006). Evidence of Late-Holocene Tsunami Events in Lebanon. *Zeitschrift für Geomorphologie N.F. Suppl. Vol.*, 146, 81-95.

Morton, R.A. (2009). Historical Changes in the Mississippi-Alabama Barrier-Island Chain and the Roles of Extreme Storms, Sea Level, and Human Activities. *Journal of Coastal Research*, 24(6), 1587-1600.

Morton, R.A. & Sallenger Jr., A.H. (2003). Morphological Impacts of Extreme Storms on Sandy Beaches and Barriers. *Journal of Coastal Research*, 19(3), 560-573.

Morton, R.A., Gelfenbaum, G. & Jaffe, B.E. (2007). Physical criteria for distinguishing sandy tsunami and storm deposits using modern examples. *Sedimentary Geology*, 200, 184–207.

Morton, R.A., Richmond, B.M., Jaffe, B.E. & Gelfenbaum, G. (2008a). Coarse-clast ridge complexes of the Caribbean: A preliminary basis for distinguishing tsunami and storm-wave origins. *Journal of Sedimentary Research,* 78(9-10), 624-637.

Morton, R.A., Goff, J.R. & Nichol, S.L. (2008b). Hydrodynamic implications of textural trends in sand deposits of the 2004 tsunami in Sri Lanka. *Sedimentary Geology,* 207(1-4), 56-64.

Nanayama, F. (2008). Sedimentary Characteristics and Depositional Processes of Onshore Tsunami Deposits: An Example of Sedimentation Associated with the 12 July 1993 Hokkaido-Nansei-oki Earthquake Tsunami. In: Shiki, T., Tsuji, Y., Yamazaki, T. & Minoura, K. (eds.), *Tsunamiites*. Amsterdam, 63-80.

Nanayama, F., Shigeno, K., Satake, K., Shimokawa, K., Koitabashi, S., Miyasaka, S. & Ishii, M. (2000). Sedimentary differences between the 1993 Hokkaido-nansei-oki tsunami and the 1959 Miyakojima typhoon at Taisei, southwestern Hokkaido, northern Japan. *Sedimentary Geology*, 135(1-4), 255-264.

Narayana, A.C., Tatavarti, R., Shinu, N. & Subeer, A. (2007). Tsunami of December 26, 2004 on the southwest coast of India: Post-tsunami geomorphic and sediment characteristics. *Marine Geology*, 242, 155–168.

National and Atmospheric Administration (NASA) (2006). Modis Satellite Image. http://rapidfire.sci.gsfc.nasa.gov/.01/2006.

National and Atmospheric Administration (NASA) (2006). SRTM elevation data. http://www2.jpl.nasa.gov/srtm/.01/2006.

National and Atmospheric Administration (NOAA). http://www.ngdc.noaa.gov/hazard/tsu_db.shtml.

National Observatory of Athens (NOA). http://www.gein.noa.gr/services/tsunami.htm.

Nichol, S.L., Goff, J.R., Devoy, R.J.N., Chagué-Goff, C., Hayward, B. & James, I. (2007). Lagoon subsidence and tsunami on the West Coast of New Zealand. *Sedimentary Geology*, 200, 248–262.

Nott, J. (1997). Extremely high-energy wave deposits inside the Great Barrier Reef, Australia: determining the cause - tsunami or tropical cyclone. *Marine Geology*, 141, 193-207.

Nott, J. (2003). Tsunami or Storm Waves? - Determining the Origin of a Spectacular Field of Wave Emplaced Boulders Using Numerical Storm Surge and Wave Models and Hydrodynamic Transport Equations. *Journal of Coastal Research,* 19(2), 348-356.

Pantosti, D., Barbano, M.S., Smedile, A., Martini, P.M.D. & Tigano, G. (2008). Geological evidence of paleotsunamis at Torre degli Inglesi (northeast Sicily). *Geophysical Research Letters*, 35, L05311.

Papadopoulos, G.A. (2003). Tsunami Hazard in the Eastern Mediterranean: Strong Earthquakes and Tsunamis in the Corinth Gulf, Central Greece. *Natural Hazards*, 29, 437-464.

Papadopoulos, G.A., Karastathis, V.K., Ganas, A., Pavlides, S., Fokaefs, A. & Orfanogiannaki, K. (2003). The Lefkada, Ionian Sea (Greece), Shock, (Mw 6.2) of 14 August 2003: Evidence for the Characteristic Earthquake from Seismicity and Ground failures. *Earth, Planets and Space*, 55, 713-718.

Papazachos, B.C. & Dimitriu, P.P. (1991). Tsunamis In and Near Greece and Their Relation to the Earthquake Focal Mechanisms. *Natural Hazards*, 4, 161-170.

Papazachos, B. & Papazachou, C. (1997). Sea Waves associated with Earthquakes in Greece. In: Papazachos, B. & Papazachou, C. (eds.), *The Earthquakes of Greece*. Thessaloniki, 71-76.

Paris, R., Lavigne, F., Wassmer, P. & Sartohadi, J. (2007). Coastal sedimentation associated with the December 26, 2004 tsunami in Lhok Nga, west Banda Aceh (Sumatra, Indonesia). *Marine Geology*, 238, 93-106.

Paris, R., Wassmer, P., Sartohadi, J., Lavigne, F., Barthomeuf, B., Desgages, E., Grancher, D., Baumert, P., Vautier, F., Brunstein, D. & Gomez, C. (2009). Tsunamis as geomorphic crises: Lessons from the December 26, 2004 tsunami in Lhok Nga, West Banda Aceh (Sumatra, Indonesia). *Geomorphology*, 104(1-2), 59-72.

Pinegina, T.K. & Bourgeois, J. (2001). Historical and paleo-tsunami deposits on Kamchatka, Russia: long-term chronologies and long-distance correlations. *Natural Hazards and Earth System Sciences*, 1(4), 177–185.

Pirazzoli, P.A., Stiros, S.C., Arnold, M., Laborel, J. & Laborel-Geguen, F. (1999). Late Holocene coseismic vertical displacement and tsunami deposits near Kynos, Golf of Euboea, central Greece, *Physics and Chemistry of the Earth (A,)* 24(4), 361–367.

Reicherter, K. & Becker-Heidmann, P. (2009). Tsunami Deposits in the Western Mediterranean: Remains of the 1522 Almería Earthquake? In: Reicherter, K., Michetti, A.M. & Silva, P.G. (eds.), (2009), *Paleoseismology: Historical and prehistorical records of earthquake ground effects for seismic hazard assessment. Journal of the Geological Society of London, Special Publication,* 316, 217-235.

Reinhardt, E.G., Goodman, B.N., Boyce, J.I., Lopez, G., van Hengstum, P., Rink, W.J., Mart, Y. & Raban, A. (2006). The tsunami of 13 December A.D. 115 and the destruction of Herod the Great's harbor at Caesarea Maritima, Israel. *Geology,* 34(12), 1061-1064.

Robinson, E., Rowe, D.-A.C. & Khan, S. (2006). Wave-Emplaced Boulders on Jamaica's Rocky Shores. *Zeitschrift für Geomorphologie N.F. Suppl. Vol.*, 146, 39-57.

Sachpazi, M., Hirn, A., Clément, C., Haslinger, F., Laigle, M., Kissling, E., Charvis, P., Hello, Y., Lépine, J. C., Sapin, M. & Ansorge, J. (2000). Western Hellenic subduction and Cephalonia Transform: local earthquakes and plate transport and strain. *Tectonophysics,* 319(4), 301–319.

Satake, K. & Atwater, B.F. (2007). Long-Term Perspectives on Giant Earthquakes and Tsunamis at Subduction Zones. *Annual Review of Earth and Planetary Sciences*, 35(1), 349-374.

Scheffers, A. (2003). Boulders on the move: Beobachtungen aus der Karibik und dem westlichen Mittelmeergebiet. *Essener Geographische Arbeiten,* 35, 3-10.

Scheffers, A. (2005). Argumente und Methoden zur Unterscheidung von Sturm und Tsunami-Schutt und das Problem der Datierung von Paläo-Tsunamis. *Die Erde,* 136(4), 413-429.

Scheffers, A. & Kelletat, D. (2001). Hurricanes and Tsunamis - Dynamik und küstengestaltende Wirkungen. *Bamberger Geographische Schriften*, 20, 29-53.

Scheffers, A. & Kelletat, D. (2003). Sedimentologic and geomorphologic tsunami imprints worldwide - a review. *Earth-Science Reviews*, 63, 83-92.

Scheffers, A. & Kelletat, D. (2005). Tsunami Relics on the coastal landscape west of Lisbon, Portugal. *Science of Tsunami Hazards*, 23(1), 3-16.

Scheffers, A., & Scheffers, S. (2007). Tsunami deposits on the coastline of west Crete (Greece). *Earth and Planetary Science Letters,* 259, 613–624.

Scheffers, A., Scheffers, S. & Kelletat, D. (2005). Paleo-Tsunami Relics on the Southern and Central Antillean Island Arc. *Journal of Coastal Research*, 21, 263-273.

Scheffers, A., Kelletat, D., Vött, A., May, S.M. & Scheffers, S. (2008). Late Holocene tsunami traces on the western and southern coastlines of the Peloponnesus (Greece). *Earth and Planetary Science Letters,* 269(1-2), 271-279.

Scheidegger, A. E. (1994). Hazards: singularities in geomorphic systems. *Geomorphology*, 10(1-4), 19-25.

Schielein, P., Zschau, J., Woith, H. & Schellmann, G. (2007). Tsunamigefährdung im Mittelmeer - Eine Analyse geomorphologischer und historischer Zeugnisse. *Bamberger Geographische Schriften*, 22, 153-199.

Schriever, A. (2007). *Die Entwicklung des Acheloos-Deltas. Eine paläogeographisch-geoarchäologische Untersuchung zum holozänen Küstenwandel in Nordwest-Griechenland.* PhD thesis, Philipps-Universität Marburg, http://deposit.ddb.de/cgi-bin/dokserv?idn= 985957131.

Scicchitano, G., Monaco, C. & Tortorici, L. (2007). Large boulder deposits by tsunami waves along the Ionian coast of south-eastern Sicily (Italy). *Marine Geology,* 238(1-4), 75-91.

Shaw, B., Ambraseys, N.N., England, P.C., Floyd, M.A., Gorman, G.J., Higham, T.F.G., Jackson, J.A., Nocquet, J.M., Pain, C.C. & Piggott, M.D. (2008). Eastern Mediterranean tectonics and tsunami hazard inferred from the AD 365 earthquake. *Nature Geoscience*, 1(4), 268-276.

Soloviev, S.L. (1990). Tsunamigenic Zones in the Mediterranean Sea. *Natural Hazards*, 3, 183-202.

Soloviev, S.L., Solovieva, O.N., Go, C.N., Kim, K.S. & Shchetnikov, N.A. (2000). *Tsunamis in the Mediterranean Sea 2000 B.C.-2000 A.D.* Dordrecht.

Spiske, M., Böröcz, Z. & Bahlburg, H. (2008). The role of porosity in discriminating between tsunami and hurricane emplacement of boulders – A case study from the Lesser Antilles, southern Caribbean. *Earth and Planetary Science Letters*, 268(3-4), 384-396.

Srinivasalu, S., Thangadurai, N., Switzer, A.D., Mohan, V.R. & Ayyamperumal, T. (2007). Erosion and sedimentation in Kalpakkam (N Tamil Nadu, India) from the 26th December 2004 tsunami. *Marine Geology,* 240, 65-75.

Stanley, J.-D. & Bernasconi, M.P. (2006). Holocene Depositional Patterns and Evolution in Alexandria's Eastern Harbor, Egypt. *Journal of Coastal Research*, 22(2), 283-297.

Stefanakis, M.I. (2006). Natural Catastrophes in the Greek and Roman World: Loss or Gain? Four Cases of Seaquake-Generated Tsunamis. *Mediterranean Archaeology and Archaeometry,* 6*(*1), 61-88.

Stewart, I.S. & Morhange, C. (2009). Coastal Geomorphology and Sea-Level Change. In: Woodward, J.C. (ed.), *The Physical Geography of the Mediterranean*. Oxford, 385-412.

Sugawara, D., Minoura, K. & Imamura, F. (2008). Tsunamis and Tsunami Sedimentology. In: Shiki, T., Tsuji, Y., Yamazaki, T. & Minoura, K. (eds.), *Tsunamiites*. Amsterdam, 9-49.

Switzer, A.D. & Jones, B.G. (2008a). Large-scale washover sedimentation in a freshwater lagoon from the southeast Australian coast: sea-level change, tsunami or exceptionally large storm? *The Holocene*, 18(5), 787-803.

Switzer, A.D. & Jones, B.G. (2008b). Setup, Deposition, and Sedimentary Characteristics of Two Storm Overwash Deposits, Abrahams Bosom Beach, Southeastern Australia. *Journal of Coastal Research*, 24(1A), 189-200.

Switzer, A.D. & Burston, J.M. (2010). Competing mechanisms for boulder deposition on the southeast Australian coast. *Geomorphology*, 114, 42-54.

Switzer, A.D., Pucillo, K., Haredy, R.A., Jones, B.G. & Bryant, E.A. (2005). Sea Level, Storm, or Tsunami: Enigmatic Sand Sheet Deposits in a Sheltered Coastal Embayment from Southeastern New South Wales, Australia. *Journal of Coastal Research*, 21(4), 655–663.

Szczucinski, W., Niedzielski, P., Rachlewicz, G., Sobczynski, T., Ziona, A., Kowalski, A., Lorenc, S. & Siepak, J. (2005). Contamination of tsunami sediments in a coastal zone inundated by the 26 December 2004 tsunami in Thailand. *Environmental Geology*, 49(2), 321-331.

Tinti, S., Maramai, A. & Graziani, L. (2001). A new version of the European tsunami catalogue: updating and revision. *Natural Hazards and Earth System Sciences*, 1, 255–262.

Tinti, S., Maramai, A. & Graziani, L. (2004). The New Catalogue of Italian Tsunamis. *Natural Hazards*, 33, 439–465.

Tsunami Laboratory Novosibirsk (TLN). http://tsun.sscc.ru/On_line_Cat.htm.

Tuttle, M.P., Ruffman, A., Anderson, T. & Jeter, H. (2004). Distinguishing Tsunami from Storm Deposits in Eastern North America: The 1929 Grand Banks Tsunami versus the 1991 Halloween Storm. *Seismological Research Letters*, 75(1), 117-131.

U.S. Geological Survey (USGS) (2006). Earth Resources Observation & Science (EROS). http://edc. usgs.gov.01/2006.

Vött, A. (2006). *Holocene coastal changes of Akarnania, NW Greece. Palaeogeographies, sea level changes, extreme events and geoarchaeological aspects of past coastal landscapes.* Unpublished habilitation thesis, Philipps-Universität Marburg.

Vött, A. (2007). Relative sea level changes and regional tectonic evolution of seven coastal areas in NW Greece since the mid-Holocene. *Quaternary Science Reviews*, 26, 894–919.

Vött, A. & May, S.M. (2009). Auf den Spuren von Tsunamis im östlichen Mittelmeer. *Geographische Rundschau*, 61(12), 42-48.

Vött, A., Brückner, H., Handl, M. & Schriever, A. (2006a). Holocene palaeogeographies and the geoarchaeological setting of the Mytikas coastal plain (Akarnania, NW Greece). *Zeitschrift für Geomorphologie N.F. Suppl. Vol.* 142, 85-108.

Vött, A., Brückner, H., Handl, M. & Schriever, A. (2006b). Holocene palaeogeographies of the Astakos coastal plain (Akarnania, NW Greece). *Palaeogeography, Palaeoclimatology, Palaeoecology,* 239, 126–146.

Vött, A., Brückner, H., Schriever, A., Luther, J., Handl, M. & van der Borg, K. (2006c). Holocene Paleogeographies of the Palairos Coastal Plain (Akarnania, Northwest Greece) and their Geoarchaeological Implications. *Geoarchaeology,* 21(7), 649–664.

Vött, A., May, M., Brückner, H. & Brockmüller, S. (2006d). Sedimentary Evidence of Late Holocene Tsunami Events near Lefkada Island (NW Greece). *Zeitschrift für Geomorphologie N.F. Suppl.-Vol.*, 146, 139-172.

Vött, A., Brückner, H., May, M., Lang, F. & Brockmüller, S. (2007a). Late Holocene tsunami imprint at the entrance of the Ambrakian gulf (NW Greece). *Mediterranée,* 108, 43-57.

Vött, A., Schriever, A., Handl, M. & Brückner, H. (2007b). Holocene palaeogeographies of the central Acheloos River delta (NW Greece) in the vicinity of the ancient seaport Oiniadai. *Geodinamica Acta,* 20(4), 241-256.

Vött, A., Schriever, A., Handl, M. & Brückner, H. (2007c). Holocene Palaeogeographies of the Eastern Acheloos River Delta and the Lagoon of Etoliko (NW Greece). *Journal of Coastal Research*, 23(4), 1042-1066.

Vött, A., Brückner, H., May, M., Lang, F., Herd, R. & Brockmüller, S. (2008). Strong tsunami impact on the Bay of Aghios Nikolaos and its environs (NW Greece) during Classical-Hellenistic times. *Quaternary International,* 181(1), 105-122.

Vött, A., Brückner, H., Brockmüller, S., Handl, M., May, S.M., Gaki-Papanastassiou, K., Herd, R., Lang, F., Maroukian, H., Nelle, O. & Papanastassiou, D. (2009a). Traces of Holocene tsunamis across the Sound of Lefkada, NW Greece. *Global and Planetary Change,* 66(1-2), 112-128.

Vött, A., Brückner, H., May, S.M., Sakellariou, D., Nelle, O., Lang, F., Kapsimalis, V., Jahns, S., Herd, R., Handl, M. & Fountoulis, I. (2009b). The Lake Voulkaria (Akarnania, NW Greece) palaeoenvironmental archive - a sediment trap for multiple tsunami impact since the mid-Holocene. *Zeitschrift für Geomorphologie N.F.,* 53(SI 1), 1-37.

Vouvalidis, K., Syrides, G. & Albanakis, K.S. (2005). Holocene Morphology of the Thessaloniki Bay: Impact of sea level rise. *Zeitschrift für Geomorphologie N.F. Suppl. Vol.*, 137, 147-158.

Wallner, J. (2008). *Holozäne Landschaftsentwicklung am Lago Budi, Chile (38,9°S) – Paläo-limnologisch/paläoseismische Untersuchungen an Lagunensedimenten*. PhD thesis, Friedrich-Schiller-Universität Jena, http://deposit.ddb.de/cgi-bin/dokserv?idn=988862433.

Wang, P. & Horwitz, M.H. (2007). Erosional and depositional characteristics of regional overwash deposits caused by multiple hurricanes. *Sedimentology*, 54(3), 545-564.

Weiss, R., Bourgeois, J., Eipert, A., Higman, B., MacInnes, B. & Martin, M.E. (2008). *Differences between Tsunamis and Storms – Implications for Sedimentology.* Paper presented at the 26th IAS Meeting of Sedimentology, Abstract Book, Bochum, Germany.

Williams, H.F.L. (2009). Stratigraphy, Sedimentology, and Microfossil Content of Hurricane Rita Storm Surge Deposits in Southwest Louisiana. *Journal of Coastal Research*, 25(4), 1041-1051.

Williams, D.M. & Hall, A.M. (2004). Cliff-top megaclast deposits of Ireland, a record of extreme waves in the North Atlantic—storms or tsunamis? *Marine Geology,* 206, 101–117.

Wong, P.P. (2009). Impacts and Recovery from a Large Tsunami: Coasts of Aceh. *Polish Journal of Environmental Studies,* 18(1), 5-16.

Woodroffe, C. (2003). *Coasts - form, processes and evolution*. Cambridge, 623 pp.

Wortel, M.J.R. & Spakman, W. (2000). Subduction and Slab Detachment in the Mediterranean-Carpathian Region. *Science*, 290, 1910-1917.

Chapter II

Geomorphology and geomorphodynamics in the Lefkada – Preveza coastal zone – controls of coastal evolution and coastal change

2.1 STUDY BACKGROUND

Theoretically, the evolution of landscapes relates to the dynamic equilibrium between the contributing geomorphic processes which tend to create a state of natural balance between them (SCHEIDEGGER 1994). Since coastlines are subject to continuous morphological changes this is also true for coastal systems tending to adjust towards or oscillate around the formation of coastal equilibrium conditions over greater time periods. These time scales superimpose the natural variability of seasonal and episodic near-shore processes and involve an equilibrium morphology that changes over time (WOODROFFE 2003, FITZGERALD et al. 2008). After BIRD (2008) equilibrium conditions depend on the considered timescale and may be of cyclic or dynamic nature – while cyclic equilibrium is influenced by disturbances and the subsequent return to its original condition, dynamic equilibrium implies changes without losing the balance between its driving forces. However, the balancing trend can acyclically (and/or cyclically) be disturbed by alterations of these morphodynamic circumstances, forcing the coastal system to a recurrent reorganization. Besides the interacting effects of a number of operating morphodynamic processes, such as sediment supply, sea level evolution and/or tectonic subsidence or uplift, they are exposed to storm surges and tsunami (ORFORD et al. 1991, ANDRADE 1992, WOODROFFE & NASH 1995, MORTON & SALLENGER 2003, WOODROFFE 2003, ANDRADE et al. 2004, DAVIDSON-ARNOTT 2005, FITZGERALD et al. 2008, MORTON 2009). These coastal hazards can be regarded as singularities in geomorphic systems since they abruptly change initial conditions and involve sudden changes in long term behavior (SCHEIDEGGER 1994). The effects of these extreme wave events may have considerable influences on the coastal geomorphic system (GOFF et al. 2009, MAMO et al. 2009, PARIS et al. 2009, WONG 2009, LIEW et al. 2010). Up to now, the contribution of extreme wave events to coastal change throughout time is not well understood and may also be underestimated. Consequently, geo-scientific research on the evolution of coastal areas has to consider both long-term and episodic, impulsive littoral processes.

The morphological pattern of coastal areas stores comprehensive information about its geodynamic evolution and the contributing morphodynamic processes. Geo-scientific investigations thus have to consider the recent geomorphodynamic and geomorphological situation of a study area. In turn, when implementing geo-scientific studies on palaeo-event deposits, the interpretation of the sedimentary record demands a comprehensive understanding of its geographical context. Without knowledge about the continuous gradual coastal processes and related coastline changes, the interpretation and even the detection of event deposits is difficult.

For the Lefkada – Preveza coastal zone, comprehensive coastal changes can be inferred. According to the investigations of VÖTT et al. (2006, 2007, 2008, 2009), the study area not only experienced widespread coastal changes – it was also repeatedly affected by extreme wave and in particular tsunami events, which contributed to the evolution of the present coastline. The interaction of gradual and sudden coastal processes is thus evident for the study area. Therefore, within the context of coastal change in the study area, this study aims (i) to map the geomorphological inventory of the different geodynamic processes in the investigated area, (ii) to deduce the related processes and their interacting effects on coastal evolution, and (iii) to discuss the contribution of gradual, long-term and episodically occurring sudden changes in coastal evolution.

2.2 STUDY AREA

The study area (Fig. 2-1) comprises the coastal zone between the northern part of Lefkada Island, one of the Ionian Islands, and Aktium Headland, situated south of Preveza, NW Greece. Lefkada Island is separated from the Greek mainland of Akarnania by the shallow lagoonal environment of the Lefkada Lagoon and the Sound of Lefkada. To the north-west and north, the Lefkada Lagoon is sealed off from the open Ionian Sea by an extensive barrier beach system. This barrier beach system can be divided into a western (Gyrapetra barrier beach) and an eastern (Aghia Mavra barrier beach) part. To the north-east, the barrier beach is forming a spit, extending into the southern part of the Bay of Aghios Nikolaos.

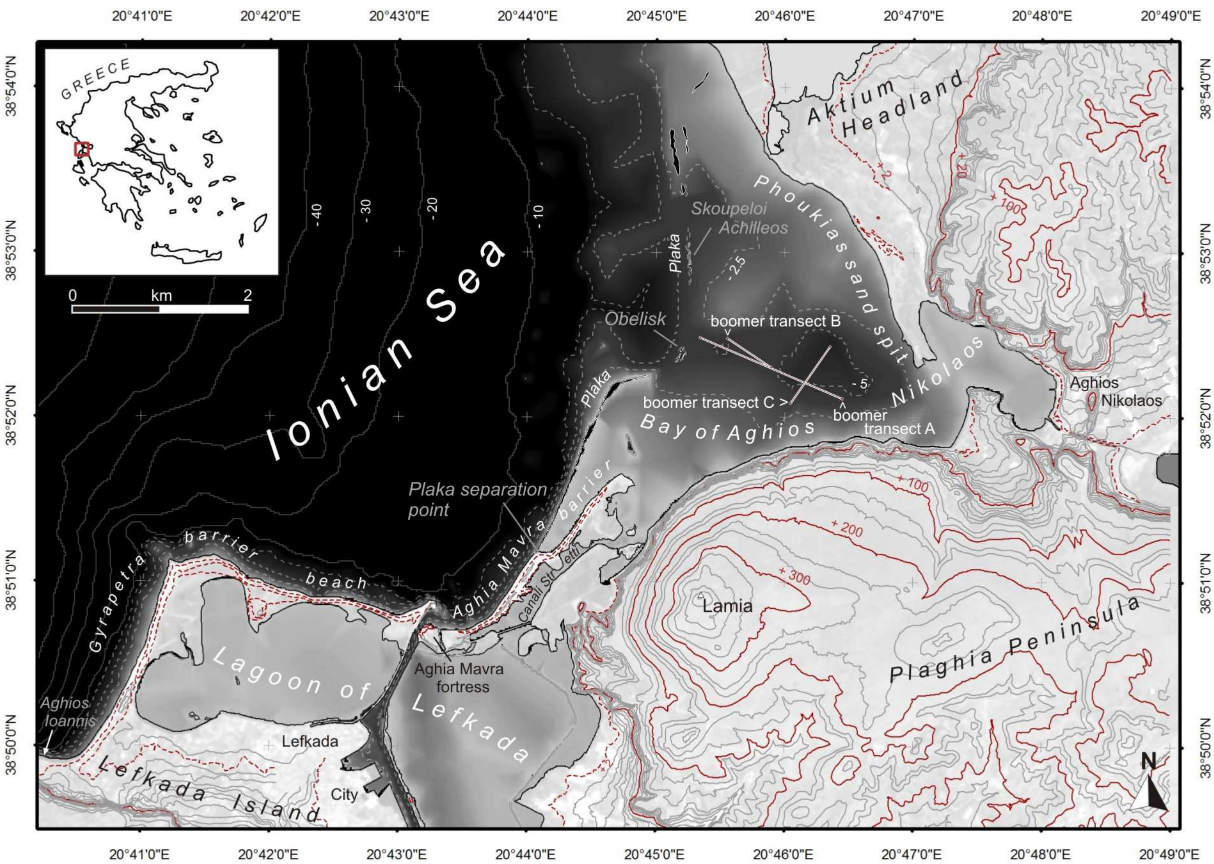

Fig. 2-1: Overview of the study area, comprising the northern part of the Lefkada Lagoon and the Bay of Aghios Nikolaos [map based on Aster satellite image 2003 (USGS), TM 1:50.000 sheets Vonitsa & Lefkada (HMGS), bathymetrical chart Amvrakikos Gulf (HNHS) and SRTM elevation data (NASA)].

The Bay of Aghios Nikolaos is separated from the open Ionian Sea by the remains of a comprehensive beachrock sequence, the so called Plaka, which is partly submerged and fragmented. Situated in direct prolongation of the Lefkada barrier beach spit, it most likely represents an older part of the spit system. However, it protects the Bay of Aghios Nikolaos from the open Ionian Sea and considerably reduces wave energy to its leeward side. To the east, the Bay of Aghios Nikolaos is characterized by a funnel-like topography. The northern part of the Bay of Aghios Nikolaos is bordered by southern Aktium Headland, which is surrounded by the Strait of Preveza to the north and the Ambrakian Gulf to the east. Beginning in the southern part of Aktium Headland, the Phoukias sand spit stretches several hundred meters into the central part of the Bay of Aghios Nikolaos.

Situated in the north-western part of Greece, the study area is exposed to the northern part of the Hellenic Arc (see also Fig. 1-1a, b) where the Adriatic microplate is subducted by the Aegean microplate. The Cefalonia transform fault (CF) and the Lefkada transform fault (LF), situated west of the Ionian Islands Cefalonia and Lefkada, connects this zone of subduction with an area of continent-continent collision beginning off the southern epirotic coast (Fig. 1-1a). The CF and the LF show a remarkably high seismic activity and have been responsible for numerous strong earthquakes during history (COCARD et al. 1999, LOUVARI et al. 1999, SACHPAZI et al. 2000, PAPADOPOULOS et al. 2003, BENETATOS et al. 2005). Therefore, the study area belongs to the seismically most active regions of the Mediterranean. According to PAPAZACHOS & DIMITRIU (1991) and SOLOVIEV (1990), it thus owns a high tsunamigenic potential.

2.3 METHODS

For the analysis of the geomorphological situation, the related geomorphodynamic processes and littoral morphodynamics, the visual interpretation of satellite images, combined with field observations, represents a powerful tool. For the southern study area, comprising the northern part of Lefkada Island and the Lefkada Lagoon, satellite images and photos from 1970 (Corona satellite image, *USGS*) and 2005 (*Google Earth*) as well as aerial photographs from 1945 and 1985 (*HMGS*) were used for multitemporal interpretation. For the northern part of the study area, constituted by the Bay of Aghios Nikolaos and Aktium Headland, available satellite data comprised the years 1970 (Corona satellite image, *USGS*), 1985 (aerial photograph, *HMGS*) and 2003 (*Google Earth*). Available satellite data was georeferenced using *ArcGIS (ESRI)* and *Global Mapper* software. Mapping of coastal changes and geomorphological features was carried out using *ArcGIS*. Additionally, two historical maps were used for the Lefkada area, documenting the coastal situation in 1864 (*Royal British Hydrographic Office*) and between 1905 - 1913 (VON MARÉES 1907, VON SEIDLITZ 1927). Geomorphological field survey was carried out along the shorelines of the study area during several summer field campaigns. Elevation transects were realized to study morphological characteristics of the Phoukias spit using a Leica SR 530 differential GPS system.

In order to investigate sublittoral and submarine morphology, scuba diving surveys were carried out along the Lefkada barrier beach system, along the Plaka and in the Bay of Aghios Nikolaos (scuba diving surveys were realized by R. Grapmayer and U. Ewelt). Underwater structures may also be detected in satellite images and aerial photographs since the intensity of submarine reflection depends on the characteristics of the seabed. Although no direct information about the sediment surface is available, seabed structures can be detected. Additionally, offshore geophysical studies were carried out in summer 2007 in cooperation with the Hellenic Centre for Marine Research (HCMR). Marine geophysical instrumentation during the campaign incorporated a side-scan sonar system and a boomer-type sub-bottom profiler (*GeoAcoustics Ltd*., GB), composed of a signal generator (*GEM*) and a catamaran type tow-fish. The latter is being pulled behind the vessel and floating on the sea surface, enabling the survey at very shallow waters. The Boomer was operated at a frequency of 0.7-1.5 kHz, a signal energy of 120 Joule and a firing rate of 250 milliseconds (4 times per second). Recording and processing was conducted with a Delph Seismic+ (*Triton Elics Int*., USA) acquisition and processing system. Sub-bottom profiling systems provide information of the subsurficial sedimentary structure, such as thickness of sub-bottom sediment layers and distribution of sedimentary boundaries.

2.4 RESULTS

2.4.1 GEOMORPHOLOGY

The Lefkada barrier beach

The Lagoon of Lefkada is separated from the Ionian Sea by an extensive barrier beach system, which is forming a spit stretching northwards into the southern part of the Bay of Aghios Nikolaos. The barrier beach system can be subdivided into a western (Gyrapetra barrier beach, west of the Aghia Mavra fortress) and an eastern part (Aghia Mavra barrier beach, east of the Aghia Mavra fortress) (see Fig. 2-1). Along the entire coastline, the barrier beach is mainly consisting of coarse sand and gravel, showing almost perfect rounding of components (Fig. 2-3b). Several DGPS elevation transects were carried out across the barrier beach. According to all elevation profiles (Fig. 2-2) the barrier beach is characterized by a steep seaward, swash-affected side and a slightly dipping landward side which is typical for numerous barrier beaches all over the world (WOODROFFE 2003, FITZGERALD et al. 2008). The top of the beach ridge is located at between ~20 - 40 m profile length, indicating a broad wave affected swash-zone (Fig. 2-3a, c). Generally, the top of the beach ridge was encountered between 3 and 4 m a.s.l., but elevations of up to 5 m a.s.l. were measured in the south-western part of the barrier. Transect 1, carried out in the western part of the Gyrapetra barrier beach system, is additionally characterized by a second elevation at ~160 - 180 m distance from the sea. Since the geomorphological characteristics are comparable to the present ridge at ~40 m, the elevation may represent a former beach ridge, which was superimposed by the present barrier beach. These findings point to a westward shift of the coastline, documenting a local regression of the sea throughout time.

In most parts, the recent beach ridge is, at its seaward side, continuously accompanied by beachrock which is covered by the present unconsolidated beach sediments (Fig. 2-3a, c) and dominates the sublittoral sea floor at most places. In the north-eastern part of the Aghia Mavra barrier beach system the present unconsolidated beach sediment is separated from the underlying beachrock (Plaka separation point, Fig. 2-1 and Fig. 2-3b). Here, the beachrock continues in north-eastern direction, forming the Plaka. The present barrier beach, in contrast, is shifting to the east and again turns north-eastwards after 200 m, where it proceeds parallel some 200 – 300 m to the east of the Plaka.

Elevation transects 3 – 8 were carried out in the north-eastern part of the Aghia Mavra barrier beach system, in the vicinity of the Plaka separation point. Here, the barrier beach is characterized by a sequence of several ridges (Fig. 2-2). In contrast to transect 2 carried out in the south-western part of the Aghia Mavra barrier beach, overall height of the barrier does not exceed 3 m and the barrier beach appears more structured. In elevation transects 3 – 7, several former beach ridges can be observed, pointing to the accretion of beach ridges during the evolution of the barrier. In transects 3 and 4, a well defined elevation at ~70 – 80 m distance from the sea characterizes the beach profile (ridge 1, red label). To the west, this former beach ridge is superimposed by a sequence of younger ridges the formation of which was related to a local regression of the sea. As illustrated in Fig. 2-2, ridge 1 cannot be followed in the northern transects 5 – 8. Instead, its crest is turning to the south-east where it disappears in the direction of the Canali Stretti fan structure. Here, the south-western margin of the fan is located in its south-eastern prolongation.

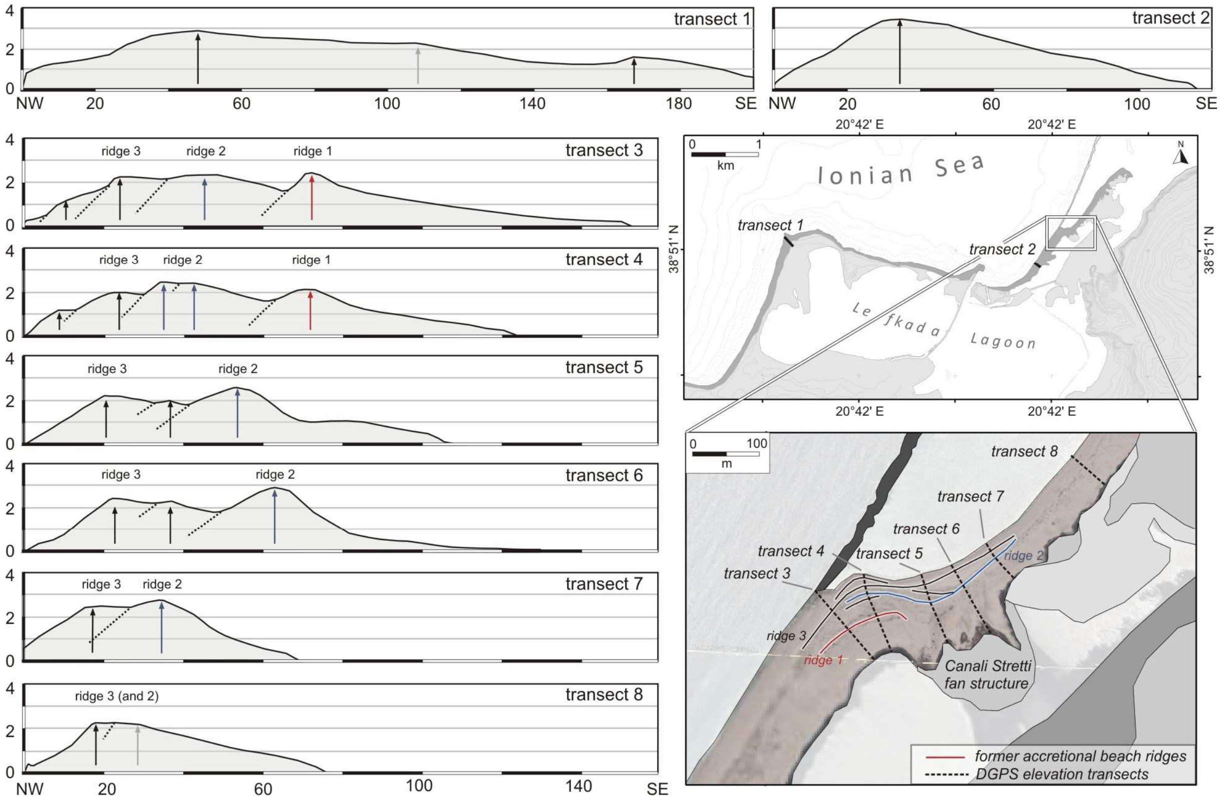

Fig. 2-2: Elevation profiles along the Lefkada barrier beach. Transect 1 was conducted in the western part of the barrier beach (Gyrapetra barrier beach). Transects 2 – 8 were carried out in the eastern part of the barrier beach (Aghia Mavra barrier beach), transects 3 – 8 in the vicinity of the Plaka separation point.

In contrast to ridge 1, at least two main younger ridges can continuously be identified in transects 3 – 7 (blue and black labels). Here, ridge 2 (blue label) is superimposed by the accretion of ridge 3 (black label) and some other, minor ridge structures. Ridge 1 and ridge 2 converge to the north and the topography is characterized by only one ridge crest in transect 8. In this part of the barrier beach system, the barrier is significantly narrower and less developed than in the other parts of the study area.

Particularly the landward side of the south-western part of the Aghia Mavra beach ridge is paved with numerous small slab-formed sandstone pebbles (Fig. 2-3f-h). Their size is up to > 20 cm and all of the pebbles are indicated by edge rounding. The occurrence of the sandstone pebbles is restricted to the area between the southernmost washover-like structure and some 150 m south of the Plaka separation point. According to the well rounded edges, these slabs were shaped in the sublittoral zone as well and must have been transported across the barrier beach by a washover event. In the north-eastern part of the Aghia Mavra barrier beach which is indicated by lower elevations, no pebbles were encountered. A comparable distribution is observed for larger dislocated beachrock blocks and slabs, which were found, partly imbricated, on top of the Aghia Mavra barrier beach system and which apparently origin from *in-situ* beachrock in the sublittoral and/or eulittoral zone (Fig. 2-3d, e).

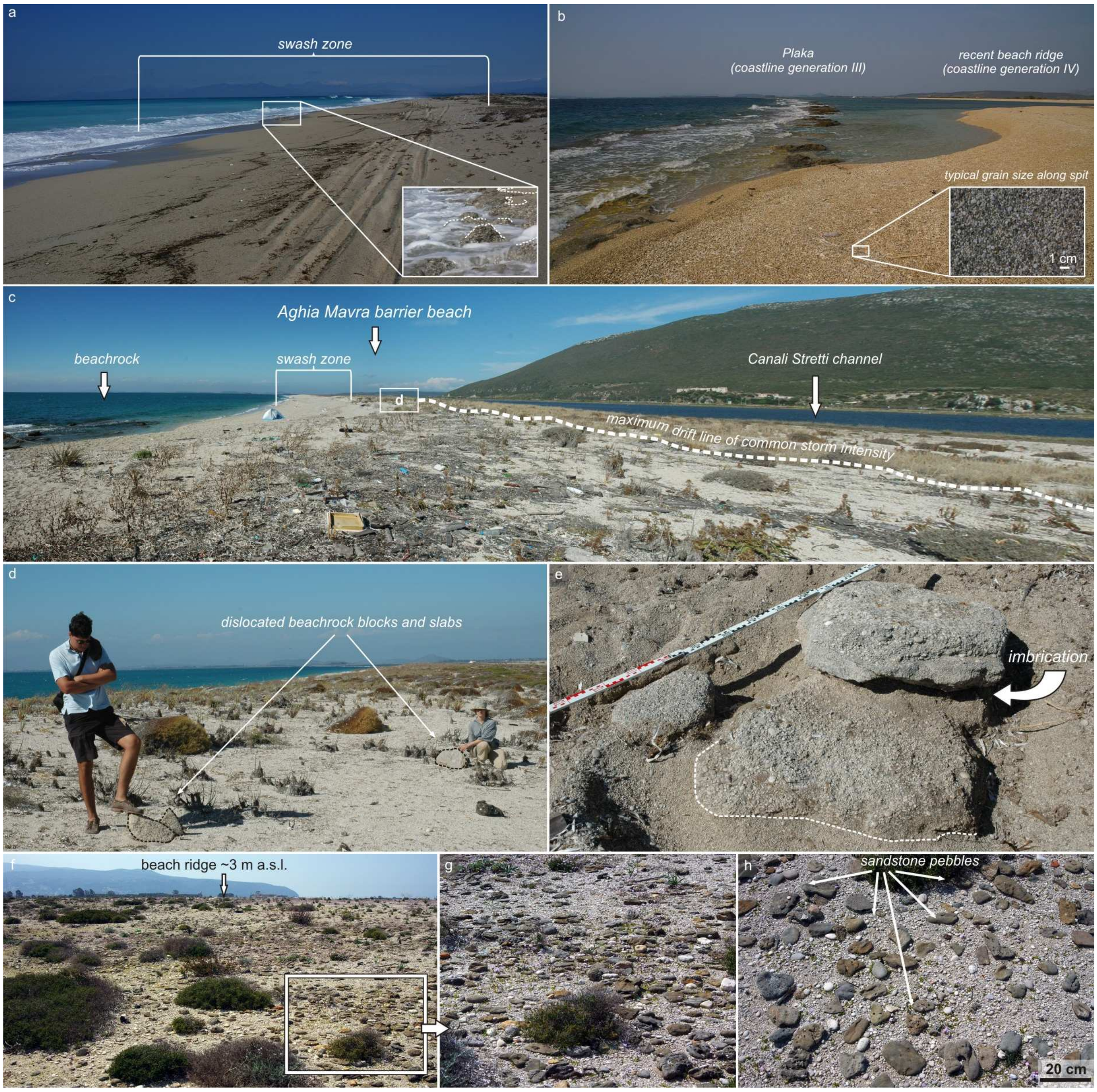

Fig. 2-3: a) Beach at the Gyrapetra barrier beach. Note wide swash zone and accompanying beachrock (inlay). b) In the north-eastern part of the Aghia Mavra barrier beach the present beach ridge is separated from the Plaka and proceeds some 200-300 m east. Inlay illustrates typical grain size and perfect rounding of components along the spit. c) Typical beach ridge at the Aghia Mavra barrier beach. Common storm drift line marked by white area. d) - h) Dislocated beachrock slabs and blocks (d, e) and rounded sandstone pebbles (f - h) found in and restricted to the south-western part of the Aghia Mavra barrier beach.

These blocks must have been transported across the swash zone and on top of the beach ridge by wave action, pointing to larger washover events in the past. The occurrence of these beachrock slabs and blocks is, comparable to the occurrence of the smaller sandstone pebbles, restricted to the south-western part of the Aghia Mavra barrier beach.

Fig. 2-4: Sediment supply of the Lefkada barrier beach system: a) Landslide close to the western shore of Lefkada Island (white box). b) Landsat 5 TM satellite image (GLCF) of northern Lefkada Island and the study area showing intense sediment transport off western Lefkada.

Several parts of the Lefkada barrier beach system are presently affected by coastal erosion. In particular, this is true for the very western part of the barrier beach, close to the northern tip of Lefkada Island. Here, the coastal road leading to Aghios Ioannis (see Fig. 2-1) is partly eroded and undercut by wave action. For the entire Lefkada barrier beach system, sediment supply is related to coastal erosion along the steep western and north-western shoreline of Lefkada Island. Here, besides the erosion of *in-situ* bedrock, sediment is provided by the accumulation of unconsolidated sediment due to recurring strong earthquakes along the Cefalonia and the Lefkada transform fault, which in turn cause extensive landslides and rock falls along the coast. According to the investigations of ROUSSAKIS et al. (2008), the coastal erosion is related to a decreasing sediment supply at the western Lefkada shore, which is the provenance area for the sediments accumulating along the Lefkada barrier beach system (Fig. 2-4).

Washover structures along the Lefkada barrier beach

Along the Lefkada barrier beach system, several lobe- or triangle-like geomorphological structures extend from the beach ridge into the Lagoon of Lefkada (Fig. 2-5). Fan-like structures stretching from barrier beaches into backbeach areas are generally interpreted as (i) washover fans, resulting from the flow of water and sediment (overwash) over the crest of the beach or (ii) scour fans, formed during breaching of the barrier beach (ANDRADE 1992, KRAUS 2003, DONNELLY et al. 2006, YULIANTO et al. 2007, GOFF et al. 2009). Consequently, these structures area assumed to result from sea water inundation during extreme wave events and the accompanied accumulation of sediments in the Lagoon of Lefkada.

The most extensive fan structure is situated in the western part of the Lefkada Lagoon (Fig. 2-5, Gyra washover). Due to area calculations based on satellite images the subaerial fan surface extends over an area of ~390.000 m². However, it can be assumed that, together with the area lying below sea level, the Gyra fan comprises at least 660.000 m². For the fan structure situated in the eastern part of the Lefkada Lagoon (Teki washover), a distinct calculation of the spatial dimensions is complicated due to anthropogenic modifications of the local morphology along the *Canali Stretti* (see Fig. 2-1). Nevertheless, its southern part is showing distinct lobe-like fan structures and comprises at least ~50.000 m². For the Canali Stretti fan structure in the north-eastern part of the Lefkada Lagoon, an extension of ~19.000 m² can be assumed.

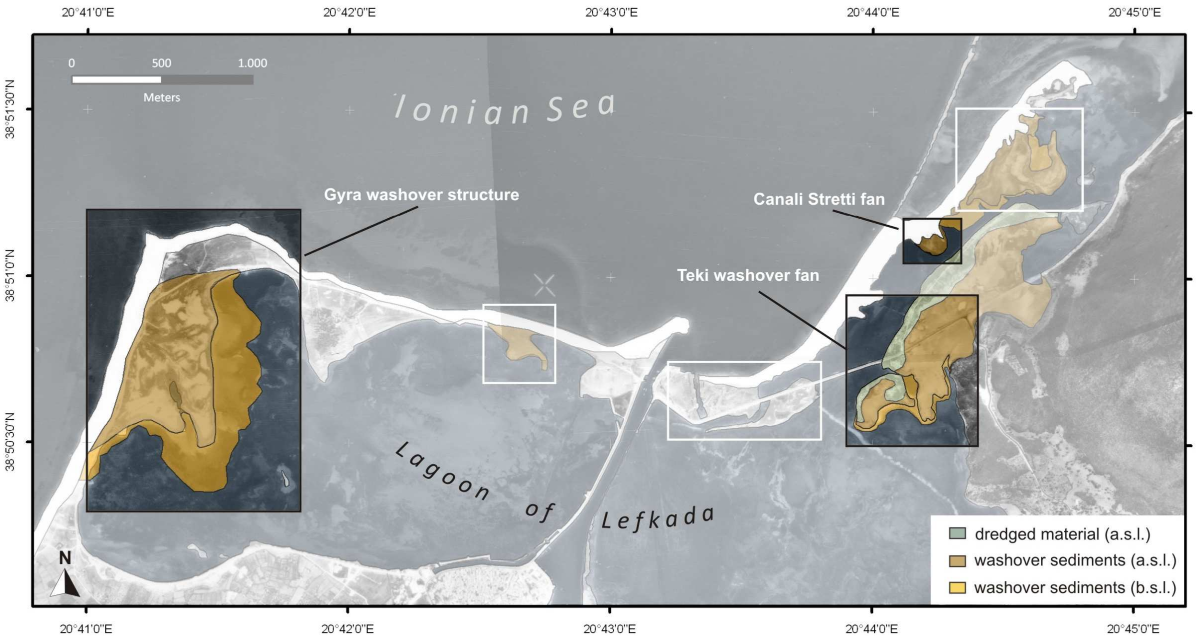

Fig. 2-5: Location of washover- and/or scour fan structures along the Lefkada barrier beach system, reaching into the Lagoon of Lefkada [map based on Aerial Photo 1985 (HMGS)].

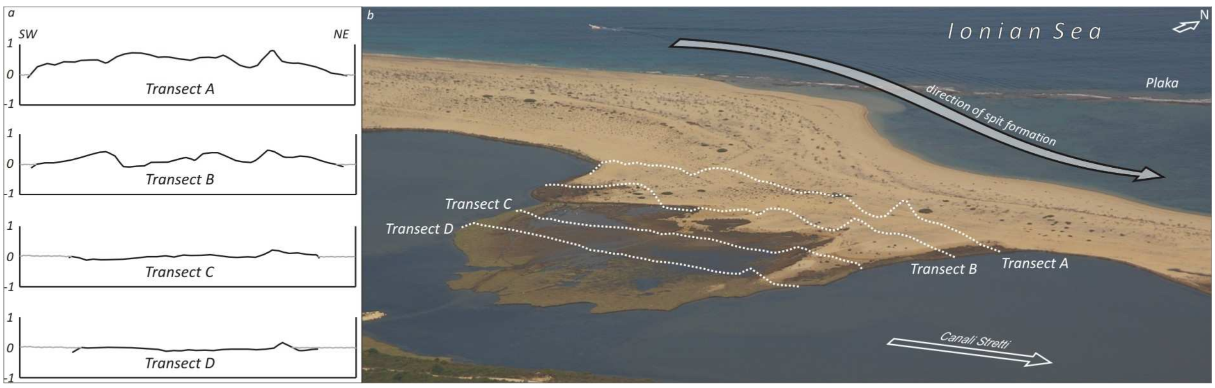

Fig. 2-6: The Canali Stretti fan as seen from the Lamia Mountain (a) and DGPS elevation transects carried out perpendicularly across the fan structure (b). As elevation profiles A - D show, the north-eastern and south-western margins of the fan structure are characterized by distinct ridge-like elevations, extending from the present beach into the lagoonal area.

On top of the Canali Stretti fan structure, four DGPS elevation profiles, crossing the fan in perpendicular direction from south-west to north-east, were conducted in order to document its morphological characteristics. As Fig. 2-6 shows, the fan structure exhibits a distinct topography, and several lobe-like structures within the washover fan can be observed. The westernmost elevation profiles (transect A and in particular transect B) illustrate at least three lobe-like elevation ridges, stretching perpendicular to the recent beach into the former Canali Stretti. In contrast, the morphology along elevation transects C and D is less pronounced. Here, due to the backbarrier position and the semi terrestrial to lagoonal environment, the lobe-like ridges are partly buried by the (sub-) recent accumulation of fine grained sediments and marsh vegetation. Nevertheless, the southern and in particular the northern margin of the fan structure is characterized by south-east stretching ridges.

The Plaka beachrock system

In the north-eastern part of the Lagoon of Lefkada, the recent, unconsolidated beach ridge is separated from the underlying beachrock (Fig. 2-3b). Here, the beachrock basement continues in north-eastern direction forming the Plaka. The spit system is shifting to the east and proceeds in north-eastern direction, some 200 – 300 m east of the Plaka. To the north, the Plaka beachrock continues as a natural reef, although, in this part of the study area, it is fragmented and its surface is dipping below sea level. Nevertheless, the Plaka remains protect the Bay of Aghios Nikolaos from main wave action.

Scuba diving transects, carried out along the Lefkada spit system and the Plaka, revealed the existence of *in-situ* lying beachrock west of the barrier system down to a depth of 12 m b.s.l. (Fig. 2-7c-g). Along the entire investigated area, the beachrock sequence shows numerous cracks and breaks and exhibits a considerable degree of fragmentation (Fig. 2-7c, d). Considering the high seismic activity within the study area, the fragmentation of the beachrock is most likely related to the effects of earthquakes. Several morphological indicators along these transects document the effects of (bio-) erosional processes, which are bound to the sea level (palaeo-notch, Fig. 2-7e; rock pools or whirlpools, Fig. 2-7f).

Beachrocks are hard, cemented coastal sedimentary formations consisting of beach sediments and are assumed to be formed by carbonate precipitation within the main body of beach sediments, mainly due to supersaturation and degassing of CO_2 (KNIGHT 2007, VOUSDOUKAS et al. 2007). Up to now, the determination of the precise position of a beachrock body with respect to the sea level is difficult. This uncertainty is even higher when considering the possibility of an event-induced origin of beachrock occurrences, as recently proposed by VÖTT & MAY (2009). The role of beachrock in sea level research is thus not yet satisfactory solved, and its potential use as a sea level indicator is limited (KNIGHT 2007, KELLETAT 2006). Nevertheless, beachrock remains are interpreted to trace former beaches and beach configurations since the beachrock is assumed to form within the body of the beach (BERNIER & DALONGEVILLE 1996, FOUACHE et al. 2005, KNIGHT 2007, VOUSDOUKAS et al. 2007). Found in different depths b.s.l. with clear signs of erosion, they prove the successive rise of local relative sea level and the accompanied formation, shifting and subsequent erosion of a comprehensive beachrock sequence.

For the north-eastern part of the Lefkada Lagoon and the Bay of Aghios Nikolaos, at least three former coastline generations can be inferred from the satellite images, aerial photographs and bathymetric data (Fig. 2-7a, b). Coastline generation I, comparable to coastline generation II, is represented by submarine beachrock remains and follows the main branch of the Plaka approximately until the small island of Aghios Nikolaos. From here, it continues in northern direction at ~3 m b.s.l.

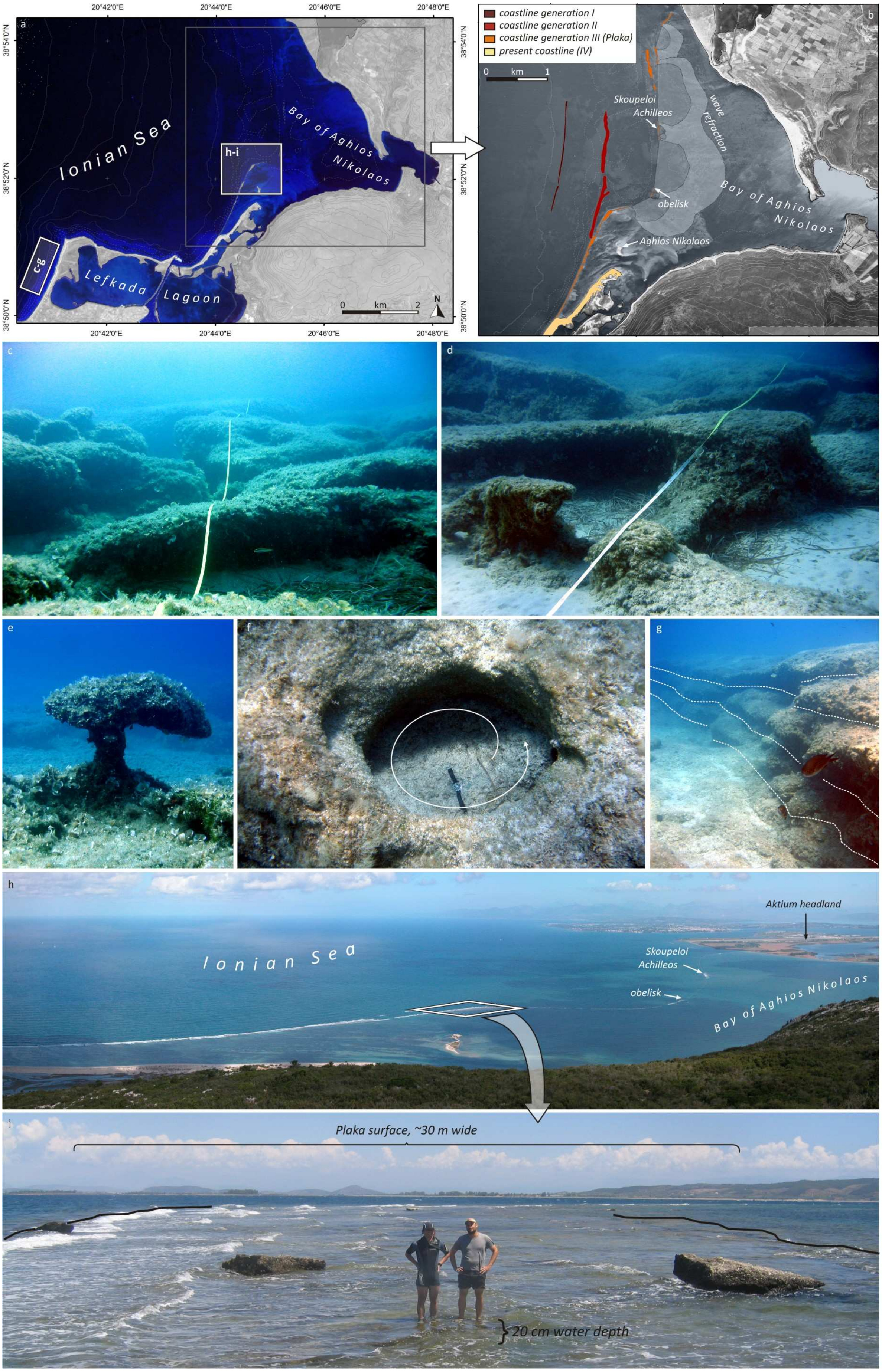
a
20°42'0"E
20°44'0"E
20°46'0"E
20°48'0"E
38°54'0"N
38°52'0"N
38°50'0"N
Ionian Sea
Bay of Aghios Nikolaos
h-i
c-g
Lefkada Lagoon
0 km 2
N
b
coastline generation I
coastline generation II
coastline generation III (Plaka)
present coastline (IV)
0 km 1
Skoupeloi Achilleos
wave refraction
obelisk
Aghios Nikolaos
Bay of Aghios Nikolaos
c
d
e
f
g
h
Aktium headland
Ionian Sea
Skoupeloi Achilleos
obelisk
Bay of Aghios Nikolaos
i
Plaka surface, ~30 m wide
20 cm water depth

Fig. 2-7 (previous page): Characteristics and occurrence of the extensive beachrock sequence. a) - b) Overview and former coastline generations as inferred from the interpretation of satellite images and aerial photographs [map based on Aster Satellite image 2003 (USGS) and aerial photos 1985 (HCMR)]. c)-g) Submarine morphological features of the beachrock sequence (all photos taken by R. Grapmayer and U. Ewelt): c)-d) In-situ beachrock between ~10 m – 5 m b.s.l. showing clear signs of erosion, e) submarine notch at ~7 m b.s.l., f) whirlpool eroded by wave-related currents at ~5 m b.s.l., g) horizontal layers of in-situ beachrock at ~4 m b.s.l. h)-i) Plaka surface in the western part of the Bay of Aghios Nikolaos. The beachrock platform is lying at around 0.20 m b.s.l.

Coastline generation III is represented by the main branch of the Plaka (Fig. 2-7h) and is shifting in north-eastward direction, west of the small island of Aghios Nikolaos. After ~600 m, it again turns northwards and constitutes reef-like submarine elevations, such as the *Skoupeloi Achilleos* or the obelisk area. Its beachrock surface is located at approximately 0.20 m a.s.l. (Fig. 2-7i). Apparently, this coastline shift is associated to the evolution of the north-eastern spit system. The recent coastline is situated south-eastwards of the main Plaka branch and constitutes coastline generation IV.

The Phoukias sand spit in southern Aktium Headland

The beachrock remains of the Plaka protect the Bay of Aghios Nikolaos from the open Ionian Sea. In some parts, the beachrock basement has been destroyed and is missing, for instance between the Plaka remains of *Skoupeloi Achilleos* and the obelisk (see Fig. 2-1 and Fig. 2-7b). Here, the related wave refraction in the Bay of Aghios Nikolaos results in a distinct influence on the shape of the Phoukias spit formation.

Particularly the northern part of the Phoukias sand spit shows pronounced morphological features. As documented in Fig. 2-8, several ridge-like structures can be observed and a simple relative succession and chronology of ridge evolution can be established by the visual interpretation of satellite images, aerial photographs and field observations. Two remarkable ridge generations can be distinguished. Considerable morphological differences between the two ridge generations can be inferred from the elevation profiles. For ridge generation I, at least two distinct ridges are identified (DGPS profile A-A^{l}). This ridge generation appears wider than the second ridge generation (ridge generation II) and is characterized by a well defined elevation, ca. 50 m wide and 0.70 m high, compared to the surrounding area. Additionally, the northernmost ridge of ridge generation I is characterized by a relatively steep, seaward orientated slope, whereas the landward (northern) side of the ridge exhibits a gently dipping surface. The surface of the ridge is textured by several smaller ridge-like elevations, reminding of current-generated ripple marks or dunes. To the north, several washover structures extend from ridge generation I into the low lying flat of the Limni Saltini. The lobes of these fan structures dip in northern direction and are, due to the temporary flooding of the Limni Saltini, buried by younger sediments. The second ridge of ridge generation I, however, is indicated by similar characteristics. To the south-west, the ridges run perpendicular to the coastline and are affected by coastal erosion.

Ridge generation II is attached to the south-eastern part of generation I and consists of a series of distinct elevations, up to 0.50 m high and 30 m wide, separated by narrow, low lying and swampy areas (DGPS profile B-B^{l}). In contrast to the ridges of ridge generation I, the ridges do not show an asymmetrical shape in cross sections. At least five ridges can be identified due to the interpretation of satellite images and field data, and elevation of the swales is decreasing in seaward direction about 20 cm. The southernmost and thus youngest ridges encounter the coastline in a flat angle and are exposed to coastal erosion. To the south-east, the ridge morphology is worse pronounced.

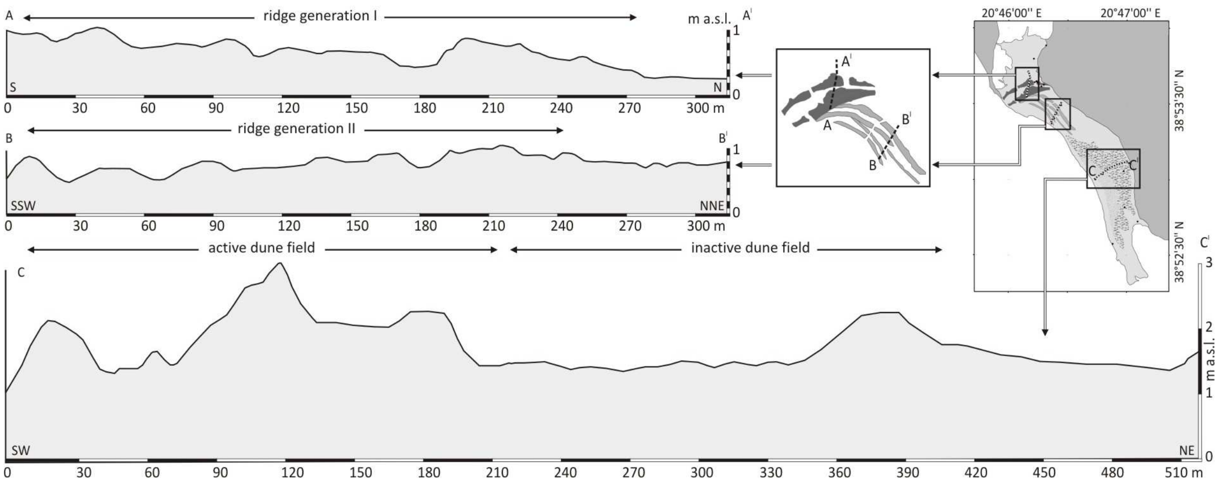

Fig. 2-8: DGPS transects carried out across the Phoukias sand spit. The northern part of the sand spit is characterized by two different ridge generations (A-A[I], B-B[I]). Transect C-C[I] represents the middle part of the spit and crosses an active dune field.

In the middle part of the spit system, an extensive dune field has formed on top of the spit's surface. DGPS profile C-C[I] illustrates the pronounced morphology of the dune system. The highest dunes reach elevations of up to 5 m a.s.l. and aeolian dynamics are still active. To the south and to the east, several smaller dunes have formed. Here, most of the dunes are characterized by vegetation cover and morphodynamic inactivity. However, dune accumulation must have started subsequent to the formation of the ridge generations and can be separated into several phases.

The Bay of Aghios Nikolaos - offshore geophysical studies

Several high resolution seismic (boomer) profiles were shot along the Lefkada barrier beach and in the Bay of Aghios Nikolaos (location of profiles depicted in Fig. 2-1). Fig. 2-9 illustrates seismic sub-bottom profiles A, B and C, carried out in the Bay of Aghios Nikolaos. Profile A is beginning west of the entrance to the Bay of Aghios Nikolaos and continuing towards the center of the Bay in eastern direction. Profile B is running parallel to and north of profile A. Profile C crosses profile A perpendicularly in its eastern part (see also Fig. 2-1). As the results show, sea floor topography is marked by a relatively monotonous, uniform surface in the inner Bay of Aghios Nikolaos, showing water depths of up to ~7.5 m b.s.l. Towards the west, the seafloor reaches ~4 m b.s.l. and is characterized by a pronounced morphology. Directly east of the submarine beachrock system represented by the Plaka remains at the entrance to the bay, the bathymetry is dipping towards the open Ionian Sea to around 10 m b.s.l. (transect B) and 7 m b.s.l. (transect A). Apparently, the area is characterized by a monotonous, uniform topography is restricted to the

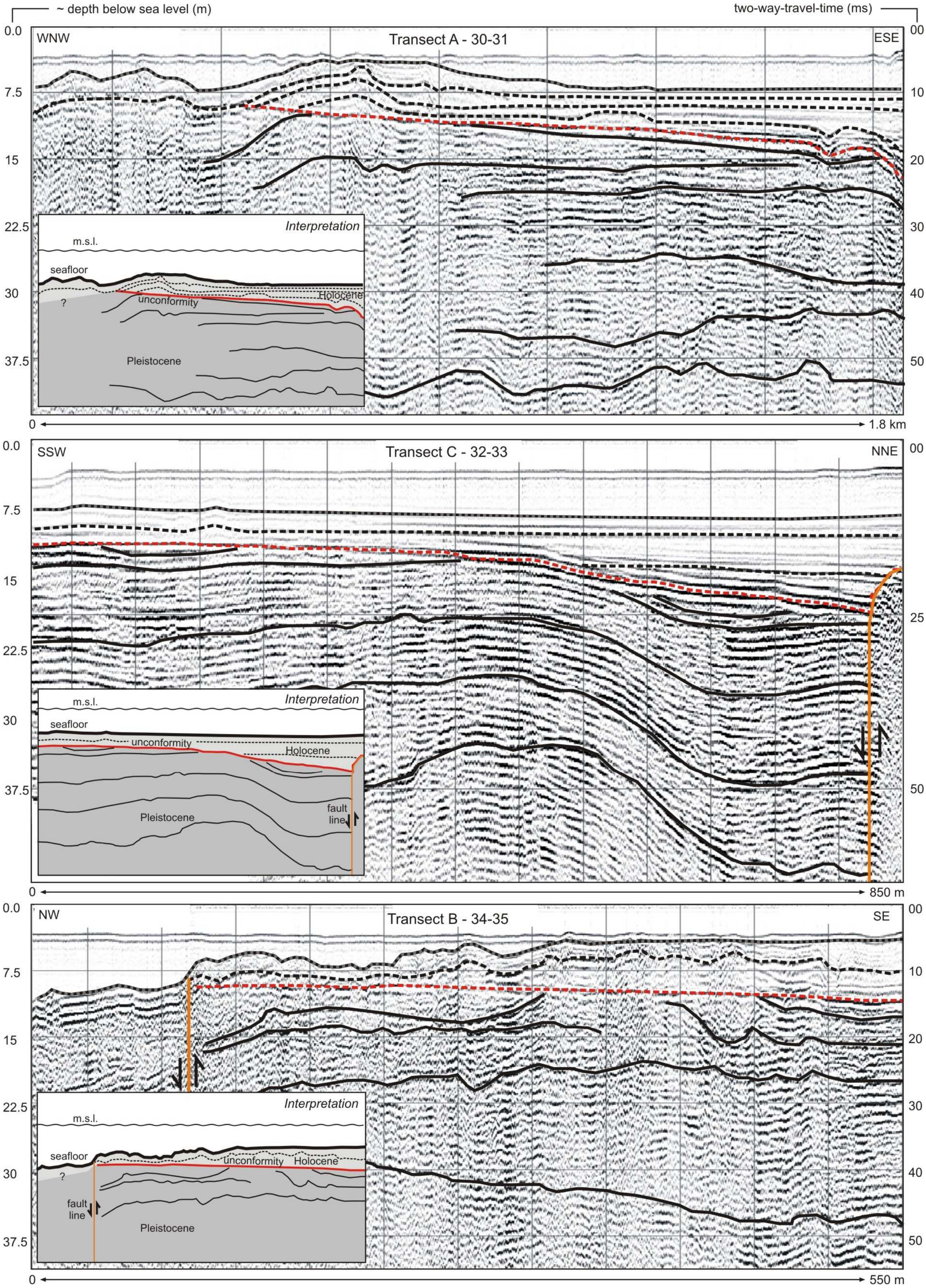

Fig. 2-9: Selected "boomer" profiles carried out in the Bay of Aghios Nikolaos. Vertical units represent two-way-travel-time in milliseconds (right) and corresponding depth b.s.l. (left). Horizontal units indicate number of shots during profiling, which is equivalent to the profile length. For location of profiles see Fig. 2-1.

basin like structure in the central part of the Bay of Aghios Nikolaos (see also Fig. 2-1). Here, fine grained, horizontal deposition must be assumed. The pronounced morphology in the western parts of transects A and C can be traced in the aerial photos as well and may be explained by the occurrence of thick meadows of *Posidonia* sp., which characterize the sea floor in the area.

According to all illustrated sub-bottom profiles, the sedimentary sequence in the Bay of Aghios Nikolaos can be separated into two main units. The lower thick bedded sequence most likely represents Pleistocene and possibly early Holocene sediments of different origin and structure.

This lower sequence is covered by a thinner unit, characterized by a horizontal orientation of boundaries, interpreted as the relatively undisturbed late Holocene sedimentary sequence. The base of the upper unit is marked by a sharp erosional unconformity (Fig. 2-9), cutting the underlying sedimentary sequence at several locations. Due to its land- (transect A) and north-eastward (transect C) dipping, it may not be interpreted as a normal transgressive unit due to sea level rise.

The north-western part of transect B and the north-eastern part of transect C display strong reflecting sub-seabed formations which minimize the penetration signal. In transect C, the lower, thick-bedded Pleistocene sequence is characterized by bulge-like increasing depths of boundaries in its middle part. To the east, boundaries show a flexure-like downward orientated trend until they encounter the disturbance area. Here, the erosional unconformity on top of the lower sequence is dipping towards the disturbance area as well. The abrupt change in the seismic stratigraphy of both profiles is thus assumed to be related to vertical movements along fault lines, intersecting the whole study area. The upper sequence is indicated by horizontal bedding, pointing to reduced crustal movements during the time of its deposition.

2.4.2 Geomorphodynamics

To the west and to the north, the Lefkada barrier beach system is exposed to the open Ionian Sea. It is influenced by intense and continuous wave activity and coastal currents, but it is also assumed to be affected by high-energy wave events. In order to estimate long-term coastal processes and coastal changes, (sub-) recent littoral morphodynamics are investigated by the interpretation of multitemporal satellite data, aerial photographs and historical maps.

The Lefkada barrier beach

In addition to the satellite images illustrated in Fig. 2-11, two historical maps illustrating the investigated area were analyzed and interpreted (Fig. 2-10). Fig. 2-10a represents a nautical map which was published by the *Royal British Hydrographic Office* and which is based on a bathymetrical survey carried out in 1864. The map depicted in Fig. 2-10b is based on topographical and geological investigations carried out by W. von Marées between 1905 and 1913.

Although at least for the older map from 1864 a topographical accuracy cannot be inferred, several conclusions can be made concerning the coastal configuration around 150 years ago. For the south-western part of the Aghia Mavra barrier beach system, no remarkable changes are observed. In contrast, the north-eastern part of the Aghia Mavra barrier beach system north of the Plaka separation point shows considerable changes – here, two former water passages can be assumed within the spit system, connecting the Canali Stretti with the lagoonal area east of the Plaka. A continuous spit system to the north of the Plaka separation point thus did not exist in the middle of the 19th century. In contrast, several island-like elevations are depicted in the map, most probably representing gravel bars or sand and gravel banks. In 1911, northward spit progradation had advanced several hundred meters (Fig. 2-10b). Only one narrow inlet to the Canali Stretti can be inferred from the map. The advancing spit shows typical, recurved haken-like structures of sediment accretion. Moreover, spit progradation and sediment accretion can be assumed north of the narrow interrupting water passage. Here, the sand and/or gravel bars and banks depicted in the map from 1864 form secondary cells of the developing barrier beach.

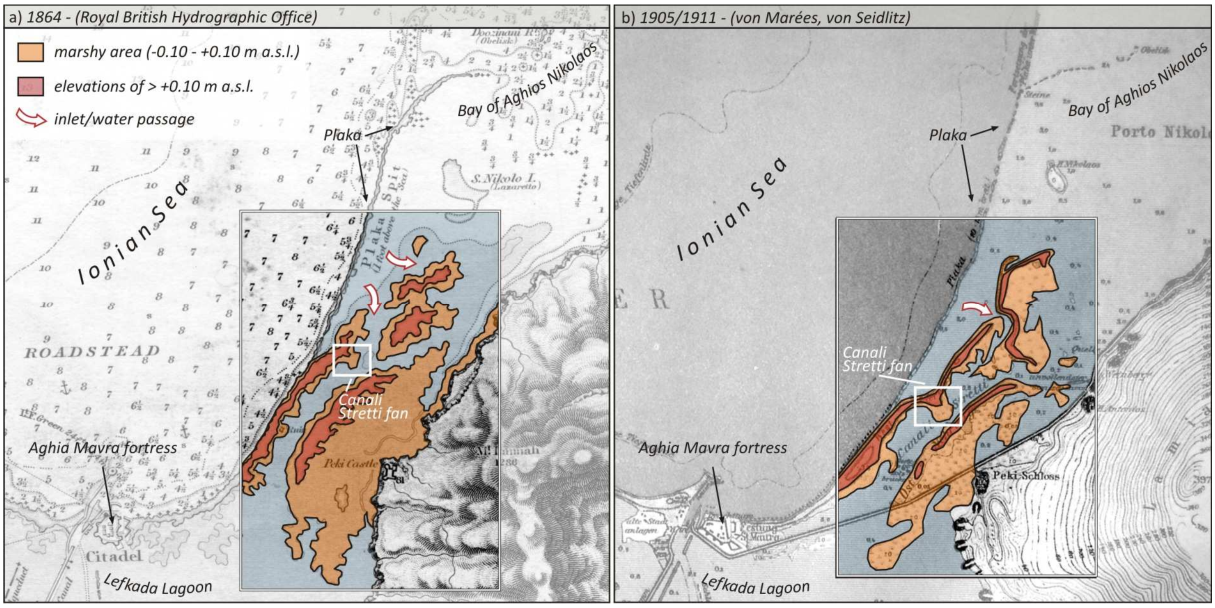

Fig. 2-10: Historical maps showing the eastern part of the Lefkada barrier beach system. a) Nautical map from 1864 (Royal British Hydrographic Office). b) Topographical map from 1905/1911 (VON MARÉES 1907, VON SEIDLITZ 1927). Differences in the north-eastern part of the Aghia Mavra barrier beach can be inferred, pointing to a re-establishment of coastal balance.

Fig. 2-11 illustrates the coastal evolution of the north-eastern part of the Lefkada spit system for the period between 1945 and 2003. In this part of the spit, the recent beach is separated from the Plaka beachrock and proceeds 200-300 m east of the Plaka. Nevertheless, it shows high morphodynamic activity which is manifested in a distinct coastal longshore sediment drift, directed from south-west to north-east. For the meantime of 58 years, several main areas of accumulation and erosion can be detected along the spit (Fig. 2-11a, b). In the south-western part, at the point of detachment of the Plaka and the beach ridge, spit progradation of ~100 m can be observed due to continuous sediment accumulation. A comparable amount of sediment accumulation is documented from the very end of the spit in the north-eastern part. In contrast, sediment erosion along the investigated spit area is concentrated in the middle part of the spit. Here, along a distance of ~450 m, the coastline retreated up to 35 m. Assuming a comparable south-northward directed longshore current and a constant accumulation rate throughout time, a spit progradation of ~1.5 m/a can be deduced.

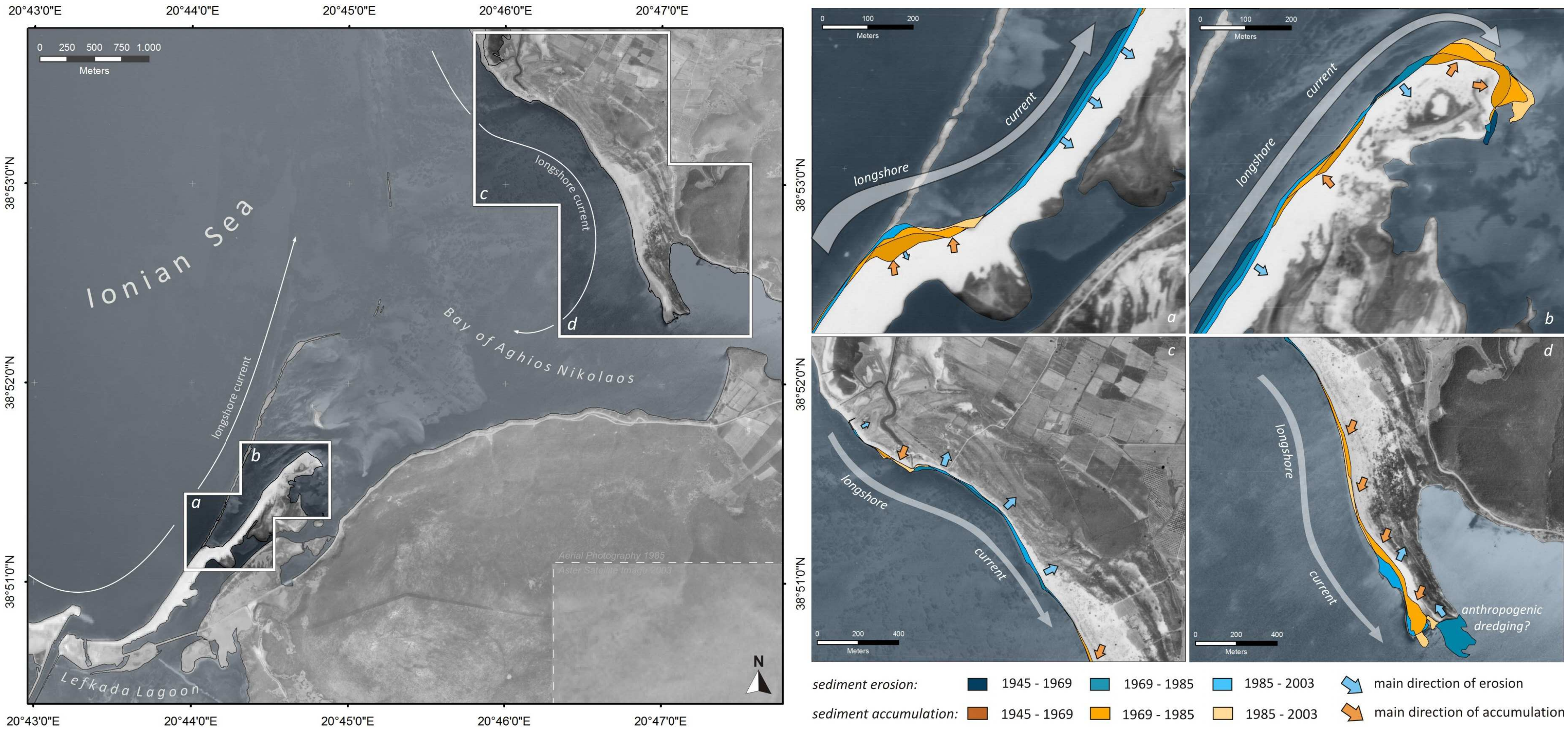

Fig. 2-11: Overview of the study area (map based on Aerial Photo 1985, HMGS) and areas of sediment accumulation and erosion during different time periods along the Aghia Mavra barrier beach (inlays a and b) and the Phoukias sand spit in the Bay of Aghios Nikolaos (inlays c and d), based on comparison of aerial photos and satellite data from 1945, 1969, 1985 and 2003.

Regarding the spit evolution during the last 60 years, an accentuation of the morphological configuration can be observed in the south-western, a balancing, compensational trend in the north-eastern part of the investigated spit. Due to the constant sediment accumulation, the detachment area of the Plaka and the recent spit system has moved ~100 m to the north.

Although the washover structures in the older map from 1864 are only rudimentarily indicated by lobe-like extensions from the barrier beach, it is assumed that all washover structures already existed in the middle of the 19th century. No changes of the washovers' configuration and dimension are thus assumed during the last 150 years. Only for the northernmost structure, a different formation may be assumed since the lobe like structure is located approximately in the area of the gravel and/or sandbars and banks detected in 1864.

Southern Aktium Headland

North of the Limni Saltini's outlet, (sub-) recent coastal erosion has formed a natural cliff, up to 2 m high (Fig. 2-12a, c). Along the outcropping cliff a red soil can be observed, which developed in the upper part of a Pleistocene sedimentary sequence. At some places cemented marine and/or aeolian deposits crop out, which may correlate with upcoming aeolianite sequences near Preveza. The outcropping sandstone is eroded and the eroded components are transported southwards by littoral drift. (Sub-) recent sediment accumulation is restricted to the southern Phoukias spit and the area close to the outlet of the Limni Saltini. Here, the eroded Pleistocene sandstones are incorporated into the recent beach sediments (Fig. 2-12b).

Fig. 2-12: The western shore of Aktium Headland: a) Active cliff about 400 m north of Limni Saltini's outlet. Note outcropping and eroded aeolianite of Pleistocene age. b) Outcrop of intensely weathered Pleistocene sediments with well developed red soil. c) Aeolianite slabs from a) incorporated into the recent sandy beach sediments further south. d) Thin layer of Holocene beach sands covering the deeply weathered Pleistocene sequence. This boundary is dipping to the south.

The morphodynamic activity of the Phoukias spit was estimated by investigating multitemporal aerial photos and satellite images. As Fig. 2-11 shows, morphodynamic activity led to both erosion and accumulation at the western coast of the spit during the last 50 years. In general, intense erosion can be observed in the northern part of the Phoukias spit and the adjacent coastline to the north. South of Limni Saltini's outlet, in the northern and middle part of the Phoukias spit system several meters of the beach have been eroded between 1969 and 2003.

Towards the south, sediment accretion has shifted the coastline up to 30 m west- and southwards. Between 1969 and 1985, erosion of the southernmost spit area took place. As the southward progradation of the spit would hinder the use of the inner Bay of Aghios Nikolaos as a fishing harbour, the area most likely was dredged by the inhabitants. Subsequently, the very end of the spit again extended about 70 m to the south.

Altogether, a north-south directed sediment transport can be determined, which is due to the coastal longshore drift. In this respect, the formation of ridge generation II in the northern spit area may be ascribed to similar longshore currents in the past. A relation between intense coastal erosion in the north and constant sediment accumulation in the Phoukias area is likely, which resulted in the accretion of beach ridges and a local regression of the sea.

2.5 INTERPRETATION AND DISCUSSION

Investigations on the study area's geomorphology and geomorphodynamic activity document considerable coastal changes throughout time. At present, a state of coastal balance cannot be assumed for the sub-recent and present coastal configuration, as highly active gradual coastal processes point to a re-organization of the coastal configuration and a re-installation of coastal balance. From a conceptual point of view, cyclic or metastable equilibrium conditions can thus be deduced for the overall evolution of the Lefkada barrier beach system (see for instance WOODROFFE 2003, BIRD 2008). Based on the presented results, three major controls of coastal evolution and coastal morphodynamics may have contributed to the coastal changes in the study area, reflecting the complex interplay of (i) continuously (gradually) operating processes of long-term coastal (re-)adjustment, (ii) the participation of active tectonics, and (iii) the impact of high magnitude extreme wave events. The contribution and significance of these controlling mechanisms is discussed in the following.

2.5.1 GRADUAL COASTAL PROCESSES

The extensive beachrock system along the Lefkada barrier beach and at the western margin of the Bay of Aghios Nikolaos is interpreted to reflect the occurrence of former beaches and beach configurations (BERNIER & DALONGEVILLE 1996, FOUACHE et al. 2005, KNIGHT 2007, VOUSDOUKAS et al. 2007). It documents the successive evolution of former beach ridge sequences in south-northward direction and at least one, probably two or more former coastlines which formed due to the gradual sea level evolution and the related gradual process of coastal longshore drift and by coastal conditions close to a state of equilibrium. Although little is known about the evolution of the beachrock system, previous findings from the eastern Lefkada Lagoon suggest that the formation of the barrier beach system took place before the beginning of the 5th millennium BC (VÖTT et al. 2008). These authors carried out geomorphological investigations in the Lefkada coastal zone by analyzing several vibracores from the backbeach area and found lagoonal conditions at around 5300 cal BC in the Bay of Aghios Nikolaos as well as lagoonal deposition in the northern Lefkada Lagoon before ~4000 cal BC. These findings fit well to the evolution of numerous coastal areas, where the onset of dominating gradual littoral processes, such as the formation of barrier beach systems due to longshore drift or the progradation of fluvial deltas, is documented at around 5000 cal BC and is assumed to be related to the deceleration of eustatic sea level rise (FAIRBANKS 1989, STANLEY & WARNE 1994, BRÜCKNER et al. 2005, VÖTT 2007, ENGEL et al. 2009). It can be assumed that the establishment of a lagoonal environment in the Bay of Aghios Nikolaos was linked, due to gradual coastal processes, to the formation of one of the former coastlines which are now represented by the submarine beachrock remains.

In the middle of the 19th century the north-eastern part of the Aghia Mavra barrier beach was characterized by a discontinuous configuration. Since then, it underwent a considerable reorganization, and spit formation due to gradual littoral drift and spit progradation of ~100 m within the last 50 years is documented. Assuming comparable progradation rates in the past, the evolution of a spit branch of 2 km length, comparable to the main branch of the Plaka, and 1.3 km length, comparable to the recent spit branch, would thus require ~1300 years and ~850 years, respectively. However, it can be assumed that sandbanks and sandbars attributed to the evolution of the north-eastern part of the Aghia Mavra spit system. The period of time of the spit's formation thus may be considerably shorter. It can be assumed that this gradual process of longshore drift influenced the area for several hundred or even thousand years, although, however, no information about the consistency of sediment supply, accumulation processes and coastal erosion is available for a longer period of time.

At least for the recent past, coastal erosion at the western part of the Lefkada barrier beach system caused by changing sediment supply at the western shore of Lefkada Island is documented by the investigations of ROUSSAKIS et al. (2008). For the evolution of barrier beach systems, sediment supply and the interaction of erosion and accumulation represents one dominant factor (ORFORD et al. 1991, WOODROFFE & NASH 1995, MORTON 2009), which may result in the segmentation, the re-assemblage and/or the breakdown of the barrier (ORFORD et al. 1991). Also for the Lefkada barrier beach system alterations of sediment supply along the western shore of Lefkada may involve geomorphological changes (ROUSSAKIS et al. 2008). In this context, the recurrent re-organization of the Lefkada barrier beach system may be linked to periodically and/or aperiodically occurring breakdowns due to changing sediment supply. Considering the state of coastal equilibrium which is assumed for the former Plaka coastline west of the Bay of Aghios Nikolaos, sediment supply is assumed to have been constant for a considerable period in the past. During this period, most probably comprising several hundreds or even thousand years, gradual modifications were not capable of disturbing the entire spit system. Comparable influence must be attributed to the effects of the gradual eustatic sea level evolution, generally causing a gradual adjustment of the coastline (MORTON 2009).

At present, a high morphodynamic activity is documented for the Phoukias sand spit. In its northern part, morphology is dominated by two ridge generations. Due to the interpretation of the present morphological configuration, generation I was accumulated prior to generation II and coastal erosion took place subsequent to the formation of ridge generations I and II and is still going on. If attributed to common longshore processes, the formation of ridge generation I cannot be explained by the present coastal configuration, since it perpendicularly encounters the present coastline. Therefore, assuming a formation due to gradual, regular coastal processes, intense coastal erosion at the western shore of Aktium Headland and sediment accumulation and sediment accretion along the Phoukias sand spit are inferred and point to remarkable gradually induced coastal changes. However, morphological characteristics between the two ridge generations are of considerable difference, and ridge generation I exhibits washover structures on its landward site. Different processes, such as the influence of extreme wave events, may thus have contributed to the formation of ridge generation I.

Nevertheless, the onset of ridge formation in the Phoukias area is linked to a considerable disturbance of the coastal system. Altogether, a south-eastward shifting of the coastline is inferred throughout time. Since the beachrock system in the western part of the Bay of Aghios Nikolaos is interpreted to correspond to at least one former coastline generation, the area of the present Phoukias spit was situated, at that time, in a corresponding backbeach position. Consequently, the formation of the Phoukias spit must have taken place subsequent to the breakdown of the former coastline.

Summarizing the presented findings, a considerably high gradual littoral morphodynamic activity is documented for the study area. This is true not only for the present situation – it is also assumed for several earlier periods of time, during which, for instance, the Plaka coastline evolved. Gradual coastal morphodynamic activity, comprising sediment erosion, transport and accumulation, is closely related to sediment supply and relative sea level rise. It is apparent for the entire Lefkada barrier beach system and the Phoukias sand spit and characterized the coastal system throughout time.

2.5.2 Tectonics

In contrast to the gradually operating coastal processes, sudden tectonic uplift and/or subsidence due to strong earthquakes may exert a strong control on the coastal system. The existence of major fault lines in the study area is documented by the results of the offshore geophysical studies, indicating at least one fault line crossing the Bay of Aghios Nikolaos from south-east to north-west. Previous terrestrial geophysical investigations document fault lines along the eastern margin of the Lefkada Lagoon at the transition to the Plaghia peninsula. These fault lines can be assumed to extend in northern direction and cross the Aghia Mavra beach ridge system from north to south (Vött et al. 2008). They reflect the overall tectonic situation of the study area which is characterized by a system of fault lines, and crustal motions accompanied by rapid uplift or subsidence (EERI 2003, Papadopoulos et al. 2003, Papathanassiou et al. 2005).

Further evidence for tectonic uplift of the northern Lefkada area has been presented by Vött et al. (2009) who report on *Lithophaga* sp. boreholes and corals in ~12 m a.s.l. dated to the last interglacial sea level high stand and a possibly slightly uplifted Holocene notch at Aghios Ioannis. Moreover, Vött (2007) investigated submerged notches at the southern Plaghia peninsula documenting co-seismic subsidence in post-Roman times. Co-seismic subsidence may also have participated in the submergence of the mole of the Corinthians (Murray 1988) and the remains of a Hellenistic to Roman bridge (Négris 1904) in the inner Lefkada Sound. As shown by Vött (2007), the hereby indicated relative sea level rise of up to 3 m during the last 2500 years agrees with the relative sea level evolution of the adjacent coasts of Akarnania.

Thereby, the contribution of tectonic controls such as (i) sudden tectonic uplift and/or subsidence or (ii) tectonic-related processes (e.g. liquefaction) on the coastal evolution in the study area is evident and must be assumed to have resulted in more enduring disturbances of the coastal balance (NIXON et al. 2009, WONG 2009). Moreover, co-seismic uplift and/or subsidence is often accompanied by the occurrence of tsunami waves (ALTINOK et al. 2001, BOURGEOIS & JOHNSON 2001, KELSEY et al. 2002, CISTERNAS et al. 2005, MELTZNER et al. 2006)

2.5.3 EXTREME WAVE EVENTS - TSUNAMIS

The existence of washover and scour structures in the northern part of the Lefkada Lagoon documents the occurrence of strong storms and/or tsunami events in the study area. They have formed by the marine induced inundation of the Lagoon of Lefkada, which must have been accompanied by high transportation energy and considerable flow velocity of water masses. According to the interpretation of satellite images, aerial photos and historical maps it can be concluded that the washover structures have not been modified by younger events since about ~150 years, and no additional washover structures have formed. Storm surges of common intensity with annually, decadal or even centennial recurrence intervals thus did not affect near coastal morphology within this period. This is also true for five tsunami events which are reported to have taken place within the last ~150 years. Therefore, only extreme wave events of exceptional intensity and very likely tsunamigenic origin are capable to significantly inundate the backbeach area, to alter near coastal morphology by the formation of washover or scour structures, and to leave considerable imprints in near coastal geological archives.

The Gyra washover in the western Lagoon of Lefkada and the Teki washover structure in the eastern part of the Lefkada Lagoon comprise 660.000 m² and 158.000 m², respectively, and both washover structures stretch several hundred meters into the Lefkada Lagoon. Inundation distance has frequently been used as a diagnostic criterion to distinguish between a storm- or tsunami-induced origin of the washover (TUTTLE et al. 2004, KORTEKAAS & DAWSON 2007, MORTON et al. 2007, SWITZER & JONES 2008a, BAHLBURG 2008), and the maximum marine inundation distance and the lateral dimension of washover deposits are reported to be larger when induced by a tsunami event (MORTON et al. 2007). Comparable, storm-generated sizes of the inundated area have only been reported from coastal zones which are affected by tropical cyclones – for instance, in 2008 tropical cyclone Nargis flooded almost the entire Irrawaddy delta plain in Burma (BAHLBURG 2008). Therefore at least the Gyra washover in the western Lagoon of Lefkada and the Teki washover structure in the eastern part of the Lefkada Lagoon can be attributed to tsunami inundation.

Specifically, for the Canali Stretti fan structure and the adjacent part of the barrier beach, DGPS transects document (i) ridge-like elevations at the fan's lateral margins and (ii) the interruption of the oldest beach ridge of the eastwards lying barrier. From a geomorphological point of view, the breaching of barrier beaches involves the interruption of previously existing beach ridges and, in many cases, the accumulation of sediment in the prolongation of the breached inlet's margins, which in turn represent the lateral limits of the scour fan (ANDRADE 1992, KRAUS 2003, GOFF et al. 2009). Considering the present morphology, the Canali Stretti fan structure represents a scour fan rather than a washover fan. The barrier beach was breached during an extreme wave event, involving the destruction of the oldest beach ridge, the opening of a water inlet and the formation of the scour fan in the lagoonal area to the east. Subsequently, the inlet was closed by longshore sediment transport, which is represented by the existence of younger, continuous beach ridges. However, for this smaller and younger Canali Stretti fan, a storm induced origin may be considered as well.

Finally, two different interpretations of the sharp landwards dipping erosional surface detected in the high resolution seismic profiles may be considered. First, it may be interpreted as a normal erosional surface which formed due to long term terrestrial conditions and erosion during the last glacial and the successive deposition of lagoonal and/or marine sediments above. Second, it may also mark an abrupt erosional event (personal comm. D. SAKELLARIOU 2010). Thus it may also reflect erosional effects induced by a tsunami entering the Bay of Aghios Nikolaos which would coincide with the presence of tsunami deposits on the surrounding land area (see also following *Chapters 3* and *4*). However, further evidence is needed to verify this interpretation.

In summary, the presented findings show that coastal changes may be induced by both gradual and impulsive processes. However, the most extensive coastal changes in the Lefkada-Preveza coastal zone are assumed to be triggered by sudden, impulsive disturbances, such as co-seismic subsidence and/or extreme wave events, in particular tsunamis, whereas gradual changes are considered to be of minor importance. Thereby these results corroborate that extreme wave events are capable of disturbing and altering coastal configurations and coastal morphology (ANDRADE et al. 1992, BEHRE 2004, BIRD 2008, GOFF et al. 2008, MAMO et al. 2009). Although large parts of the coastal erosion which occurred during the 2004 Indian Ocean Tsunami were compensated by gradual coastal processes within a few years (CHOOWONG et al. 2009, WONG 2009, LIEW et al. 2010), the results from the study area show that more enduring disturbances of the coastal system can be expected for coastal systems characterized by barrier beaches. Here, large parts of the barrier beach and the former backbarrier lagoonal environments may disappear during the event (see also LIEW et al. 2010), particularly when accompanied by tectonic movements (WONG 2009).

2.6 CONCLUSIONS

Comprehensive investigations on the coastal morphology and (sub-) recent coastal morphodynamics have been carried out. As shown in detail, the results provide substantial information about the study area's coastal evolution:

a) For the study area, remarkable coastal changes are documented. Several former coastlines have been detected by the investigations on the beachrock system at the western margin of the Bay of Aghios Nikolaos. The most prominent palaeo-coastline generation is represented by the Plaka.

b) At present, a considerably high morphodynamic activity and littoral dynamic is manifested for the Lefkada barrier beach system and the Phoukias sand spit.

c) For several periods in time, the barrier beach coastline must have been in or close to a state of equilibrium, which can be described as a state of dynamic equilibrium over a distinct period of time. A state of a cyclic equilibrium may be inferred for the entire barrier system when considering the evolution based on a different time scale.

d) Several disturbances forced the system to a recurrent reorganization. For the barrier beach system, in particular for the north-eastern part, a temporary breakdown of the barrier beach is documented. The most recent disturbance must have taken place before the middle of the 19th century. Since then, the coastline is in a state of re-organisation.

e) For south-western Aktium Headland, intense coastal erosion is inferred. The accumulation of the spit system went along with the coastal retreat to the north. Two different ridge generations indicate different geomorphodynamics and a different coastal configuration during their formation.

f) The influence of tectonically induced vertical crustal movements is likely since several fault lines cross the barrier beach system. Moreover, the occurrence of extreme wave events is apparent, and tsunami frequency is similar or even higher compared to the frequency of exceptionally large storms. A contribution of episodic, impulsive controls to the documented coastal changes is more than likely (for detailed investigations see *Chapters 3 and 4*).

g) Genetic morphology allows insight in the development of coastal systems. The coastal system is controlled by a number of influences. Considerable influence on the coastal evolution must be attributed to tectonic processes, to gradual coastal processes and to tsunami events.

h) In general, coastal change may be controlled by impulsively occurring disturbances. These sudden disturbances may be represented by tectonics or extreme wave events. They may be described as geomorphic singularities, during which the initial conditions of the coastal system are cyclically or acyclically changed and the system is forced to re-establish a state of balance. Thus, the coastline is the result of recurring disturbances and subsequent masking and mimicking by gradual coastal evolution.

2.7 REFERENCES

Altinok, Y., Tinti, S., Alpar, B., Yalçiner, A.C., Ersoy, S., Bortolucci, E., Armigliato, A., (2001). The Tsunami of August 17, 1999 in Izmit Bay, Turkey. *Natural Hazards*, 24, 133–146.

Andrade, C. (1992). Tsunami Generated Forms in the Algarve Barrier Islands (South Portugal). *Science of Tsunami Hazards*, 10(1), 21-34.

Andrade, C., Freitas, M.C., Moreno, J. & Craveiro, S.C. (2004). Stratigraphical evidence of Late Holocene barrier breaching and extreme storms in lagoonal sediments of Ria Formosa, Algarve, Portugal. *Marine Geology*, 210(1-4), 339-362.

Bahlburg, H. (2008). Storm and tsunami deposits in light of cyclone Nargis, Burma, May 2 and 3, 2008. Paper presented at the 26th IAS Meeting of Sedimentology, Abstract Book, Bochum, Germany.

Behre, K.-E. (2004). Coastal development, sea-level change and settlement history during the later Holocene in the Clay District of Lower Saxony (Niedersachsen), northern Germany. *Quaternary International,* 112(1), 37-53.

Benetatos, C., Kiratzi, A., Roumelioti, Z., Stavrakakis, G., Drakatos, G., & Latoussakis, I. (2005). The 14 August 2003 Lefkada Island (Greece) earthquake: Focal mechanisms of the mainshock and of the aftershock sequence. *Journal of Seismology*, 9, 171–190.

Bernier, P. & Dalongeville, R. (1996). Mediterranean Coastal Changes Recorded in Beach-Rock Cementation. *Zeitschrift für Geomorphologie N.F. Suppl. Vol.*, 102, 185-198.

Bird, E. (2008). *Coastal Geomorphology – An Introduction*. New York, 411 pp.

Bourgeois, J. & Johnson, S.Y. (2001). Geologic evidence of earthquakes at the Snohomish delta, Washington, in the past 1200 yr. *Geological Society of America Bulletin*, 113(4), 482-494.

Brückner, H., Vött, A., Schriever, A. & Handl, M. (2005). Holocene delta progradation in the eastern Mediterranenan - case studies in their historical context. *Mediterranée*, 1(2), 95-106.

Choowong, M., Phantuwongraj, S., Charoentitirat, T., Chutakositkanon, V., Yumuang, S. & Charusiri, P. (2009). Beach recovery after 2004 Indian Ocean tsunami from Phang-nga, Thailand. *Geomorphology*, 104(3-4), 134-142.

Cisternas, M., Atwater, B.F., Torrejon, F., Sawai, Y., Machuca, G., Lagos, M., Eipert, A., Youlton, C., Salgado, I., Kamataki, T., Shishikura, M., Rajendran, C.P., Malik, J.K., Rizal, Y. & Husni, M. (2005). Predecessors of the giant 1960 Chile earthquake. *Nature*, 437, 404-407.

Cocard, M., Kahle, H.-G., Peter, Y., Geiger, A., Veis, G., Felekis, S., Paradissis, D. & Billiris, H. (1999). New constraints on the rapid crustal motion of the Aegean region: recent results inferred from GPS measurements (1993–1998) across the West Hellenic Arc, Greece. *Earth and Planetary Science Letters,* 172, 39–47.

Davidson-Arnott, R.G.D. (2005). Conceptual Model of the Effects of Sea Level Rise on Sandy Coasts. *Journal of Coastal Research,* 21(6), 1166-1172.

Donnelly, C., Kraus, N. & Larson, M. (2006) State of Knowledge on Measurement and Modelling of coastal Overwash. *Journal of Coastal Research*, 22(4), 965-991.

Earthquake Engineering Research Institute (EERI) (2003). Preliminary Observations on the August 14, 2003, Lefkada Island (Western Greece) Earthquake. EERI Special Earthquake Report, 11 p. — November 2003, http://www.eeri.org/lfe/pdf/greece_lefkada_eeri_pre-liminary_rpt.pdf [access: January 01, 2010].

Engel, M., Knipping, M., Brückner, H., Kiderlen, M. & Kraft, J.C. (2009). Reconstructing middle to late Holocene palaeogeographies of the lower Messenian plain (southwestern Peloponnese, Greece): Coastline migration, vegetation history and sea level change. *Palaeogeography, Palaeoclimatology, Palaeoecology*, 284(3-4), 257-270.

Fairbanks, R.G. (1989). A 17,000-year glacio-eustatic sea level record: influence of glacial melting rates on the Younger Dryas event and deep-ocean circulation. *Nature*, 342, 637-642.

FitzGerald, D.M., Fenster, M.S., Argow, B.A. & Buynevich, I.V. (2008). Coastal Impacts Due to Sea-Level Rise. *Annual Review of Earth and Planetary Sciences,* 36(1), 601-647.

Fouache, E., Desruelles, S., Pavlopoulos, K., Dalongeville, R., Coquinot, Y., Peulvast, J.-P. & Potdevin, J.-L. (2005). Using beachrock as sea level indicators in the insular group of Mykonos, Delos and Rhenia (Cyclades, Greece). *Zeitschrift für Geomorphologie N.F. Suppl. Vol.*, 137, 37-43.

Global Land Cover Facility (GLCF) University of Maryland (2006). Landsat ETM+ satellite data (17.09.1989). http://www.landcover.org/index.shtml/. 01/2006.

Goff, J.R., McFadgen, B.G., Wells, A. & Hicks, M. (2008). Seismic signals in coastal dune systems. *Earth Science Reviews*, 89, 73–77.

Goff, J.R., Lane, E. & Arnold, J. (2009). The tsunami geomorphology of coastal dunes. *Natural Hazards and Earth System Sciences,* 9(3), 847-854.

Google Earth (2007). QuickBird satellite images (12.06.2003/19.12.2005, provided by Digital Globe) [access: December 2007]

Hellenic Military Geographical Service (HMGS) (1987). TM 1:50.000, sheets Vonitsa & Lefkada.

Hellenic Military Geographical Service (HMGS) (1945/1985). Aerial Photographs.

Hellenic Navy Hydrographic Service (HNHS) (1983). Bathymetrical chart 1:50.000, sheet Amvrakikos Gulf.

Kelletat, D. (2006). Beachrock as sea-level indicator? Remarks from a geomorphological point of view. *Journal of Coastal Research,* 22(6), 1558-1564.

Kelsey, H.M., Witter, R.C. & Hemphill-Haley, E. (2002). Plate-boundary earthquakes and tsunamis of the past 5500 yr, Sixes River estuary, southern Oregon. *Geological Society of America Bulletin*, 114(3), 298-314.

Knight, J. (2007). Beachrock Reconsidered. Discussion of: Kelletetat, D., 2006. Beachrock as Sea-Level Indicator? Remarks from a Geomorphological Point of View. ournal of Coastal Research, 22(6), 1558-1564. *Journal of Coastal Research,* 23(4), 1074-1078.

Kortekaas, S. & Dawson, A.G. (2007). Distinguishing tsunami and storm deposits: An example from Martinhal, SW Portugal. *Sedimentary Geology*, 200, 208–221.

Kraus, N.C. (2003). Analytical model of incipient breaching of coastal barriers. *Coastal Engineering Journal*, 45(4), 511–531.

Kraus, N.C., Militello, A. & Todoroff, G. (2002). Barrier Breaching Processes and Barrier Spit Breach, Stone Lagoon, California. *Shore & Beach,* 70(4), A714384.

Liew, S.C., Gupta, A., Wong, P.P. & Kwoh, L.K. (2010). Recovery from a large tsunami mapped over time: The Aceh coast, Sumatra. *Geomorphology*, 114(4), 520-529

Louvari, E., Kiratzi, A.A. & Papazachos, B.C. (1999) The Cephalonia Transform Fault and its extension to western Lefkada Island (Greece). *Tectonophysics*, 308, 223-236.

Mamo, B., Strotz, L. & Dominey-Howes, D. (2009). Tsunami sediments and their foraminiferal assemblages. *Earth-Science Reviews,* 96(4), 263-278.

Meltzner, A.J., Sieh, K., Abrams, M., Agnew, D.C., Hudnut, K.W., Avouac, J.-P. & Natawidjaja, D.H. (2006). Uplift and subsidence associated with the great Aceh-Andaman earthquake 2004. *Journal of Geophysical Research*, 111, B02407.

Morton, R.A. (2009). Historical Changes in the Mississippi-Alabama Barrier-Island Chain and the Roles of Extreme Storms, Sea Level, and Human Activities. *Journal of Coastal Research,* 24(6), 1587-1600.

Morton, R.A. & Sallenger Jr., A.H. (2003). Morphological Impacts of Extreme Storms on Sandy Beaches and Barriers. *Journal of Coastal Research*, 19(3), 560-573.

Morton, R. A., Gelfenbaum, G. & Jaffe, B.E. (2007). Physical criteria for distinguishing sandy tsunami and storm deposits using modern examples. *Sedimentary Geology*, 200, 184–207.

Murray, W.M. (1982). *The coastal sites of western Akarnania: a topographical-historical survey*. PhD Thesis, University of Pennsylvania.

National and Atmospheric Administration (NASA) (2006). SRTM elevation data. http://www2.jpl.nasa.gov/srtm/. 01/2006.

Négris, P. (1904). Vestiges antiques submergés. *Athener Mitteilungen*, 29, 340–369.

Nixon, F.C., Reinhardt, E.G. & Rothaus, R. (2009). Foraminifera and tidal notches: Dating neotectonic events at Korphos, Greece. *Marine Geology,* 257(1-4), 41-53.

Orford, J.D., Carter, R.W.G. & Jennings, S.C. (1991). Coarse clastic barrier environments: Evolution and implications for quaternary sea level interpretation. *Quaternary International,* 9, 87-104.

Papadopoulos, G.A., Karastathis, V.K., Ganas, A., Pavlides, S., Fokaefs, A. & Orfanogiannaki, K. (2003). The Lefkada, Ionian Sea (Greece), Shock, (Mw 6.2) of 14 August 2003: Evidence for the Characteristic Earthquake from Seismicity and Ground failures. *Earth, Planets and Space,* 55, 713-718.

Papathanassiou, G., Pavlides, S. & Ganas, A. (2005). The 2003 Lefkada earthquake: Field observations and preliminary microzonation map based on liquefaction potential index for the town of Lefkada. *Engineering Geology,* 82(1), 12-31.

Papazachos, B.C. & Dimitriu, P.P. (1991). Tsunamis in and near Greece and their relation to the earthquake focal mechanisms. *Natural Hazards,* 4, 161-170.

Paris, R., Wassmer, P., Sartohadi, J., Lavigne, F., Barthomeuf, B., Desgages, E., Grancher, D., Baumert, P., Vautier, F., Brunstein, D. & Gomez, C. (2009). Tsunamis as geomorphic crises: Lessons from the December 26, 2004 tsunami in Lhok Nga, West Banda Aceh (Sumatra, Indonesia). *Geomorphology*, 104(1-2), 59-72.

Roussakis, G., Sakellariou, D., Georgiou, P., Anagnostou, C. & Lykousis, V. (2008). Coastal erosion along the western and northern shore of lefkada island. *4MMCZ*, 337-346.

Sachpazi, M., Hirn, A., Clément, C., Haslinger, F., Laigle, M., Kissling, E., Charvis, P., Hello, Y., Lépine, J. C., Sapin, M. & Ansorge, J. (2000) Western Hellenic subduction and Cephalonia Transform: local earthquakes and plate transport and strain. *Tectonophysics,* 319(4), 301–319.

Scheidegger, A.E. (1994). Hazards: singularities in geomorphic systems. *Geomorphology*, 10(1-4), 19-25.

Soloviev, S.L. (1990). Tsunamigenic Zones in the Mediterranean Sea. *Natural Hazards,* 3, 183-202.

Stanley, D.J. & Warne, A.G. (1994). Worldwide Initiation of Holocene Marine Deltas by Deceleration of Sea-Level. *Science*, 265, 228-231.

Switzer, A.D. & Jones, B.G. (2008). Large-scale washover sedimentation in a freshwater lagoon from the southeast Australian coast: sea-level change, tsunami or exceptionally large storm? *The Holocene*, 18(5), 787-803.

Tuttle, M.P., Ruffman, A., Anderson, T. & Jeter, H. (2004). Distinguishing Tsunami from Storm Deposits in Eastern North America: The 1929 Grand Banks Tsunami versus the 1991 Halloween Storm. *Seismological Research Letters*, 75(1), 117-131.

U.S. Geological Survey (USGS) (2006). Earth Resources Observation & Science (EROS). Corona satellite images and Aster satellite data. http://edc.usgs.gov.01/2006.

von Marées, W. (1907*). Karten von Leukas. Beiträge zur Frage Leukas-Ithaka*. Berlin.

von Seidlitz, W. (1927). Geologische Untersuchung der Inselnatur von Leukas. In: Dörpfeld, W. (ed.), *Alt-Ithaka. Ein Beitrag zur Homer-Frage, 2 Volumes*. München, 352-372.

Vött, A. (2007). Relative sea level changes and regional tectonic evolution of seven coastal areas in NW Greece since the mid-Holocene. *Quaternary Science Reviews,* 26, 894–919.

Vött, A. & May, S.M. (2009). Auf den Spuren von Tsunamis im östlichen Mittelmeer. *Geographische Rundschau,* 61(12), 42-48.

Vött, A., May, M., Brückner, H. & Brockmüller, S. (2006). Sedimentary Evidence of Late Holocene Tsunami Events near Lefkada Island (NW Greece). *Zeitschrift für Geomorphologie N.F. Suppl. Vol.*, 146, 139-172.

Vött, A., Brückner, H., May, M., Lang, F. & Brockmüller, S. (2007). Late Holocene tsunami imprint at the entrance of the Ambrakian gulf (NW Greece). *Mediterranée,* 108, 43-57.

Vött, A., Brückner, H., May, M., Lang, F., Herd, R. & Brockmüller, S. (2008). Strong tsunami impact on the Bay of Aghios Nikolaos and its environs (NW Greece) during Classical-Hellenistic times. *Quaternary International*, 181(1), 105-122.

Vött, A., Brückner, H., Brockmüller, S., Handl, M., May, S.M., Gaki-Papanastassiou, K., Herd, R., Lang, F., Maroukian, H., Nelle, O. & Papanastassiou, D. (2009). Traces of Holocene tsunamis across the Sound of Lefkada, NW Greece. *Global and Planetary Change,* 66(1-2), 112-128.

Vousdoukas, M.I., Velegrakis, A.F. & Plomaritis, T.A. (2007). Beachrock occurrence, characteristics, formation mechanisms and impacts. *Earth-Science Reviews,* 85(1-2), 23-46.

Wong, P.P. (2009). Impacts and Recovery from a Large Tsunami: Coasts of Aceh. *Polish Journal of Environmental Studies*, 18(1), 5-16.

Woodroffe, C. & Nash, D. (1995). Sea level. *Progress in Physical Geography*, 19(3): 391-398.

Woodroffe, C. (2003). *Coasts – form, processes and evolution*. Cambridge, 623 pp.

Yulianto, E., Prendergast, A.L., Jankaew, K., Eipert, A.A., Atwater, B.F., Cisternas, M., Fernando, S. & Tejakusuma, I. (2007). Tsunami scour-fan deposits in south-central Chile. *Quaternary International*, 167–168, 469.

Chapter III

Tsunami-induced coastal changes at Aktium Headland, NW-Greece - the evolution of the Phoukias sand spit

3.1 STUDY BACKGROUND

With the beginning of the deceleration of eustatic sea level rise in the middle Holocene, gradual coastal change around the world was increasingly dominated by the interacting effects of sediment erosion and sediment supply, local tectonics and sediment compaction (FAIRBANKS 1989, STANLEY & WARNE 1994, BARD et al. 1996). In addition to gradual coastal processes, the occurrence of extreme wave events, such as storm surges, tropical cyclones and tsunami, has induced considerable changes in coastal configuration, although affecting the coastline no longer than a few days or hours. Remarkable shoreline modifications are reported from exceptional storm surges induced by tropical cyclones in numerous coastal areas around the world (COCH 1994, MORTON & SALLENGER 2003, WANG & HORWITZ 2007), comprising the deposition of washover sediments in the backbeach area, beach erosion and barrier breaching. However, in most cases the coastal changes during common storm activity are restricted to the beach area. The devastating effects of tsunami events on coastal configuration particularly are documented by the 2004 Indian Ocean Tsunami (MAMO et al. 2009, PARIS et al. 2009, LIEW et al. 2010), comprising the destruction and disappearance of barrier beaches and backbeach lagoons. Consequently, one of the main objectives in coastal research is to decipher the contribution of these extreme wave events to coastal change. In particular, the distinguishability of storm and tsunami deposits in the geological record turned out to be a major challenge in the research on extreme wave events (e.g. FOSTER et al. 1991, DAWSON 1996, NOTT 1997, NANAYAMA et al. 2000, SCHEFFERS & KELLETAT 2001, KORTEKAAS 2002, GOFF et al. 2004, WILLIAMS & HALL 2004, SWITZER et al. 2005, DOMINEY-HOWES et al. 2006, DAWSON & STEWART 2007, KORTEKAAS & DAWSON 2007, MORTON ET AL. 2007, NANAYAMA 2008, SUGAWARA et al. 2008, SWITZER & JONES 2008a, 2008b, DONATO et al. 2008, MAMO et al. 2009), since it is important for an appropriate hazard assessment (MORTON et al. 2007, SATAKE & ATWATER 2007, MAMO et al. 2009).

As documented for numerous coastal areas in western Greece and the Aegean (KRAFT et al. 1980, BESONEN 1997, VOUVALIDIS et al. 2005, MAY 2006, VÖTT 2007, VÖTT et al. 2007b, BRÜCKNER et al. in press, ENGEL et al. 2009), the coastal morphology in the Lefkada – Preveza area implies comprehensive palaeogeographical changes throughout time. Particularly the evolution of the Phoukias sand spit situated in the south-western part of Aktium Headland (Fig. 5-1) has been accompanied by extensive coastline changes (see *Chapter 2*). Since the Lefkada – Preveza area is prone to one of the most active seismic zones in the Mediterranean tsunamis represent a considerable threat in the study area (SOLOVIEV 1990, PAPAZACHOS & DIMITRIU 1991). Previous findings point to the influence of extreme wave events and in particular of tsunamis on the local coastal morphology (VÖTT et al. 2006, 2007a, 2008, 2009a, 2009b, MAY et al. 2007, 2008).

Detailed geo-scientific investigations on (i) palaeo-event deposits in the sedimentary record and (ii) modern analogues, such as (sub) recent storm and tsunami deposits, help to better understand the main characteristics of extreme wave events and their imprints in geological archives. In turn, considering the (palaeo-) geographical context of the investigated area may help to improve the interpretation of extreme wave event deposits. The Phoukias sand spit represents an excellent geological archive – its sedimentary architecture stores information about its evolution and the evolution of the Bay of Aghios Nikolaos, which was accompanied by major coastal changes throughout time. Therefore, results of detailed sedimentary and geomorphological investigations of the Phoukias sand spit are presented in this chapter. This study aims (i) to decipher the palaeogeographical context of the study area, (ii) to document coastal changes related to the Phoukias spit's evolution, (iii) to determine the main reasons for the coastal changes and (iv) to verify and to decipher a possible influence of extreme wave events, in particular tsunamis, on the spit formation.

3.2 STUDY AREA

The Phoukias spit (Fig. 3-1), an accretional sand spit, is situated in the south-western part of Aktium Headland (NW Greece) (see also Fig. 1-2, Chapter 1). The northern part of Aktium Headland is separated from the Preveza area by the entrance to the Ambrakian Gulf, the so called Preveza Strait. To the south, the spit extends several hundred meters into the Bay of Aghios Nikolaos, a funnel like bay north-west of Lefkada. In its northern part, it is characterized by a sequence of beach ridge-like elevations. To the south, several dune fields, up to 8 m high, can be observed near the coast.

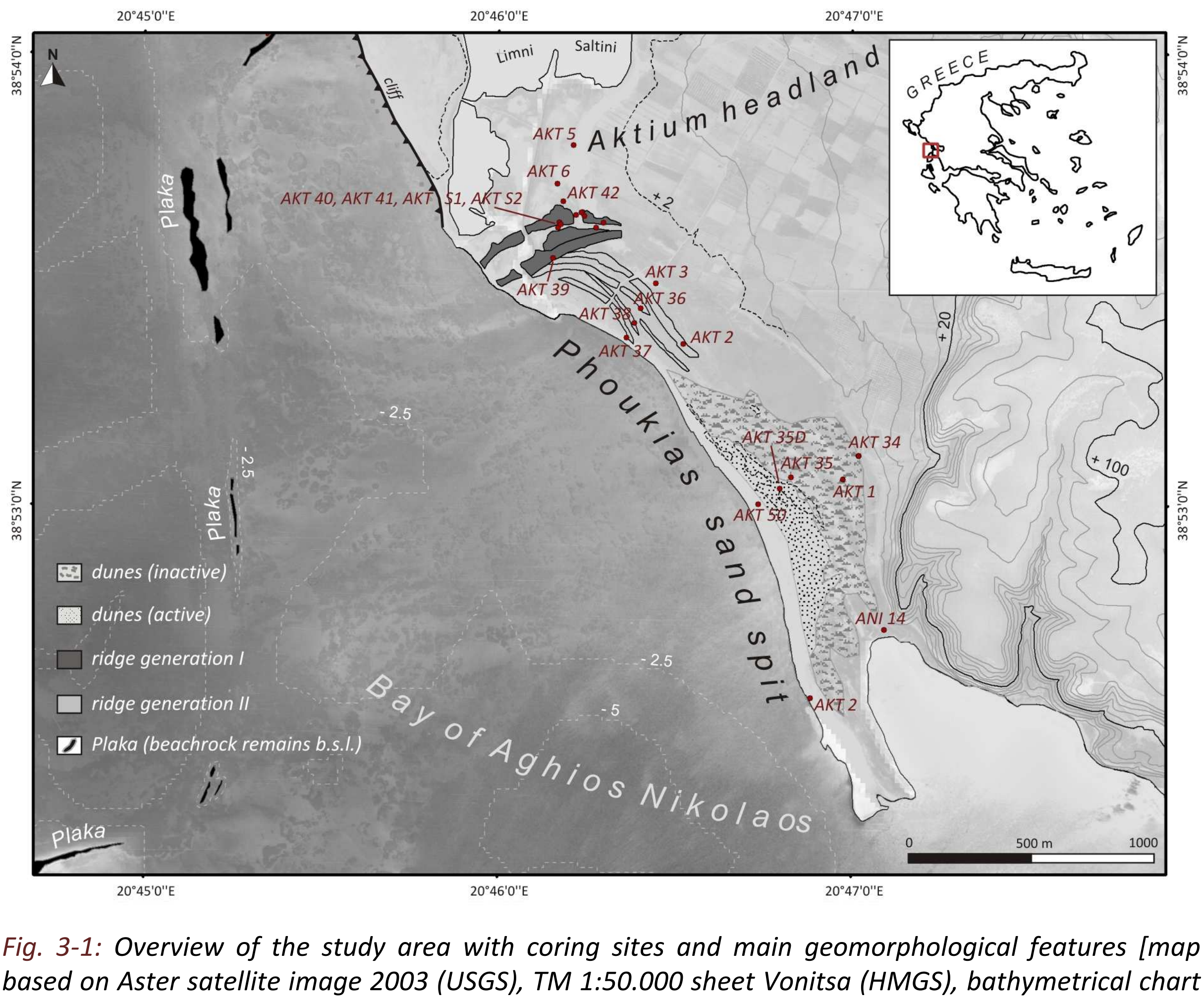

Fig. 3-1: Overview of the study area with coring sites and main geomorphological features [map based on Aster satellite image 2003 (USGS), TM 1:50.000 sheet Vonitsa (HMGS), bathymetrical chart Amvrakikos Gulf (HNHS) and SRTM elevation data (NASA)].

The Bay of Aghios Nikolaos is separated from the open Ionian Sea by the remains of a palaeo-coastline, the Plaka. This palaeo-coastline consists of beachrock, which is partly submerged, fragmented and, due to the effects of earthquakes, partly broken. However, it protects the Bay of Aghios Nikolaos from the open Ionian Sea and considerably reduces wave energy to its leeward side (see also *Chapter 1*, Fig. 1-2).

The area between Lefkada Island and Preveza is exposed to the northern part of the Hellenic Arc (see Fig. 1-1 a, b) where the Adriatic microplate is subducted by the Aegean microplate. The Cefalonia transform fault (CF) and the Lefkada transform fault (LF), situated west of the Ionian Islands Cefalonia and Lefkada, connects this zone of subduction with an area of continent-continent collision beginning off the southern epirotic coast (see also Fig. 1-1a) and exhibit a remarkably high seismic activity (COCARD et al. 1999, LOUVARI et al. 1999, SACHPAZI et al. 2000, PAPADOPOULOS et al. 2003, BENETATOS et al. 2005, KOKINOU et al. 2006). The study area thus belongs to the seismically most active regions of the Mediterranean.

3.3 METHODS

In this paper, detailed results of 17 vibracores and two sediment profiles carried out at the Phoukias sand spit in south-western Aktium Headland are presented (Fig. 3-1, for core data see also appendix A, B, C and E). Supplementary field work comprised DGPS measurements. Vibracorings were performed by means of an Atlas Copco Cobra mk 1 corer and sediment cores of 5 cm and 6 cm diameter. Sediment trenches were dug out in the northern part of the study area to follow the sedimentary stratigraphy, such as bedding structures, along several meters and to improve the idea of the internal sedimentary structure. Vibracore and sediment profiles were documented, recorded (colour, grain size and rounding, texture, carbonate content as recommended by Ad-hoc ARBEITSGRUPPE BODEN (2005), macrofaunal remains) and sampled in the field. Sedimentary and geochemical analyses were conducted in the laboratory. The air-dried and hand-pestled fine-grained fraction (< 2 mm) of the samples was analysed for Ca, Fe, Na, and K concentrations using atomic absorption spectrometry (Perkin Elmer A-Analyst 300) after digestion with concentrated HCl (37 %). $CaCO_3$ was measured applying the Scheibler method. Loss on ignition (LOI) was determined by oven-drying at 105 °C for 12 h and ignition in a muffle furnace at 550 °C for 4 h (BECK et al. 1995). In order to support the stratigraphical interpretation and to characterize the sedimentary units, wet-sieve pipette analysis (KÖHN 1928) was carried out to investigate the grain size distribution of sediment cores AKT 35, AKT 35c, AKT 3, AKT 6, AKT 39 and AKT 42 as well as sediment profile AKT S2. Samples were pre-treated with H_2O_2 (30 %) and 0.5 n $Na_4P_2O_7$ (55.7 g/l) to remove organic carbon and for aggregate dispersion. Processing of statistical values was carried out using GRADISTAT software (BLOTT & PYE 2001). Taphonomic investigations were carried out for core AKT 35 according to the analyses reported by DONATO et al. (2008). Macro- and microfaunal analyses were carried out for core AKT 35 in order to support textural and geochemical results, to verify the marine provenance of distinct sedimentary units and to determine sediment source areas. Samples (10 cm^3) were pre-treated with H_2O_2 (30%) for dispersion and sieved to isolate fractions of 63–125, 125–200, 200–400 and > 400 µm. Content of foraminifera and ostracods was investigated under a binocular and recorded semi-quantitatively, interpretation was mainly based on HANDL et al. (1999) and MURRAY (2006).

For the chronological framework, organic material and mollusc remains taken from the sediment samples were dated by the ^{14}C-AMS technique (Table 3-1). ^{14}C-AMS ages were corrected for a marine reservoir effect of 400 years if necessary (REIMER & MCCORMAC 2002) using CALIB 6.0

software and the dataset of REIMER et al. (2009). For plant remains identified as sea weed in the field marine calibration was carried out when $\delta^{13}C$-values were determined to 15 ‰ ± 3 ‰ (see e.g. WALKER 2005). Additionally, optically stimulated luminescence (OSL) dating of quartz minerals was carried out for sediment sequences of vibracores AKT 3 and AKT 36 as well as for dune profile AKT 35D to improve chronostratigraphical information and to cross-check ^{14}C-AMS ages (see also appendix D). To recover unbleached material for OSL samples from the vibracores, opaque PVC inliner cores were used. A parallel core was drilled and sampled for the determination of the dose rate. Sample preparation and luminescence measurements were carried out at the Marburg Luminescence Lab (MLL). First, samples were dry sieved. To remove carbonates, organic contents and clay samples were pre-treated with HCl (10 %), H_2O_2 (10 %) and $Na_2C_2O_4$. The quartz fraction was isolated by density separation using heavy liquids. Etching of obtained quartz grains was conducted using HF (40%) acid. For dating, the single-aliquot regenerative-dose (SAR) protocol after MURRAY & WINTLE (2000) was applied. All measurements were carried out on a Risø TL/OSL DA 20 reader, equipped with a $^{90}Sr/^{90}Y$ beta source delivering 0.1 Gy/s. The applicability of the SAR protocol was tested using dose-recovery and preheat-plateau tests. Small and large aliquots of 2 mm (for vibracore samples) and 8 mm (dune profile) were used. The quartz grains were stimulated by blue LED light at wavelength of 470 ± 30 nm, and signals were recorded in UV range using a Hoya U-340 optical filter (transmission 330 ± 40 nm). All aliquots were stimulated for 50 sec. at 125 °C. Following preheat plateau tests, the aliquots were heated at 260 °C (vibracore AKT 3b) and 240 °C (vibracore AKT 36b and dune profile AKT 35D) before optical stimulation. Finally, water content of the sediment sampled for OSL dating was estimated by analyzing loss of water in the laboratory and by interpreting signs of reduction and oxidation found within the sampled sediments (for detailed description of the OSL dating procedure see PREUSSER et al. 2008). The dose rate was estimated using high resolution gamma spectrometry and was carried out at the Faculty of Chemistry, Marburg University.

3.4 RESULTS

The investigated vibracores were drilled in different morphologic settings. In the ridge dominated northern part of the spit system, sediment profiles AKT S1 and AKT S2, vibracores AKT 39 – AKT 42 as well as vibracores AKT 3 and AKT 36 – AKT 38 were used for interpretation. To the northeast, vibracores AKT 5 and AKT 6 were conducted in a low lying and flat plain, which is temporarily flooded by the Limni Saltini and shows no pronounced elevations. In the middle and southern part of the spit, vibracores AKT 1, AKT 2, AKT 34, AKT 35 and AKT 50 as well as vibracores ANI 2 and ANI 14 were analyzed.

In the following, two key profiles (vibracores AKT 35 and ANI 2) are described in detail. They represent a comprehensible and characteristic picture of the Phoukias spit's sedimentary sequence. Based on these investigations, sediments of comparable or similar sedimentary and geochemical characteristics were summarized into nine stratigraphical units for all vibracores used in this study (Fig. 3-5). Therefore, they provide the basis for the interpretation of the sedimentary architecture of the Phoukias sand spit and reflect the evolution of the spit.

Vibracore profile AKT 35 (38°53'21.8487'' N, 20°46'28.8845'' E)

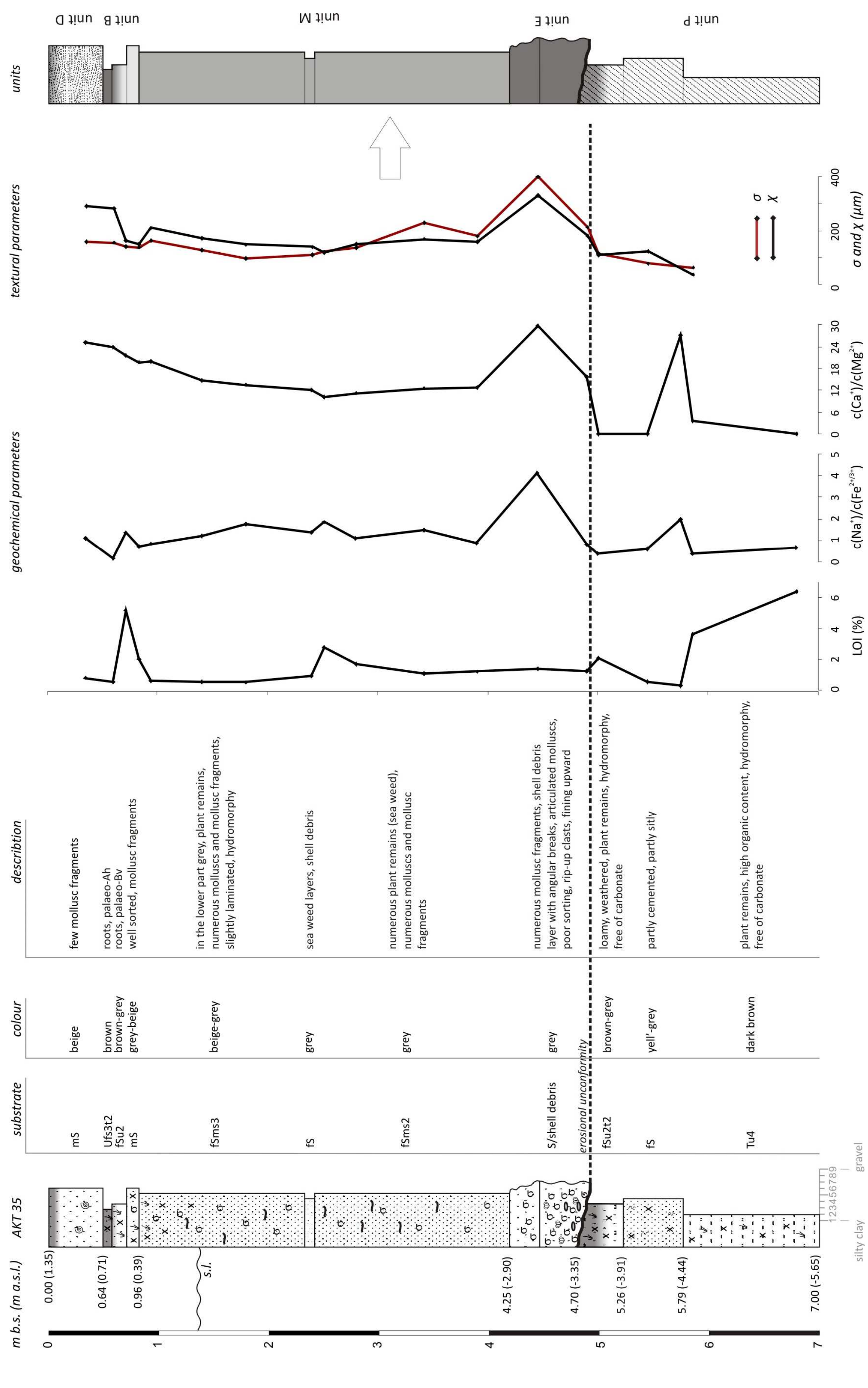

Fig. 3-2 (previous page): Sedimentary sequence and geochemical characteristics of vibracore profile AKT 35. The shell debris layer between 3.35 – 2.90 m b.s.l. marks the beginning of the marine sequence and is characterized by high carbonate contents, poor sorting and coarser grain size. Notes: b.s.l. – below mean sea level. a.s.l. – above mean sea level. s.l. – mean sea level. χ - mean grain size (µm). σ – sorting (standard deviation, µm). Grain size of cores is illustrated by different widths of core profile (1 – silty clay, 2 – clayey silt, 3 – sandy silt/silty sand, 4 – fine sand, 5 – fine and medium sand, 6 – medium sand, 7 – medium and coarse sand, 8 – coarse sand, 9 - gravel). For legend see Fig. 3-4.

3.4.1 Stratigraphy of vibracores AKT 35 and ANI 2

Vibracore AKT 35 (Fig. 3-2) was drilled in the central part of the Phoukias sand spit, in direct vicinity of an active dune system and about 200 m from the sea (see also Fig. 3-1). In the southern part of the Phoukias sand spit, vibracore ANI 2 (Fig. 3-4) was carried out on top of the sand spit reaching into the Bay of Aghios Nikolaos. With a depth of 18 m b.s. it is the deepest drilling in the study area.

Vibracore AKT 35

The sedimentary sequence of core AKT 35 starts with clayey (5.65 – 4.44 m b.s.l., below mean sea level) and sandy (4.44 – 3.91 m b.s.l.) sediments. From 3.91 m - 3.60 m b.s.l., greenish-grey, slightly silty and clayey fine sand with *in-situ* plant remains occurs. Sediments are characterized by relatively high clay contents of more than 10 % (Fig. 3-3, AKT 35/14 – AKT 35/15, AKT 35/18) and relatively high values of LOI. Here, the sediment is free of carbonate. Sample AKT 35/16 consists of very well sorted fine sand and shows clay contents of only ~6 %. Its geochemical characteristics are comparable to the surrounding sediments.

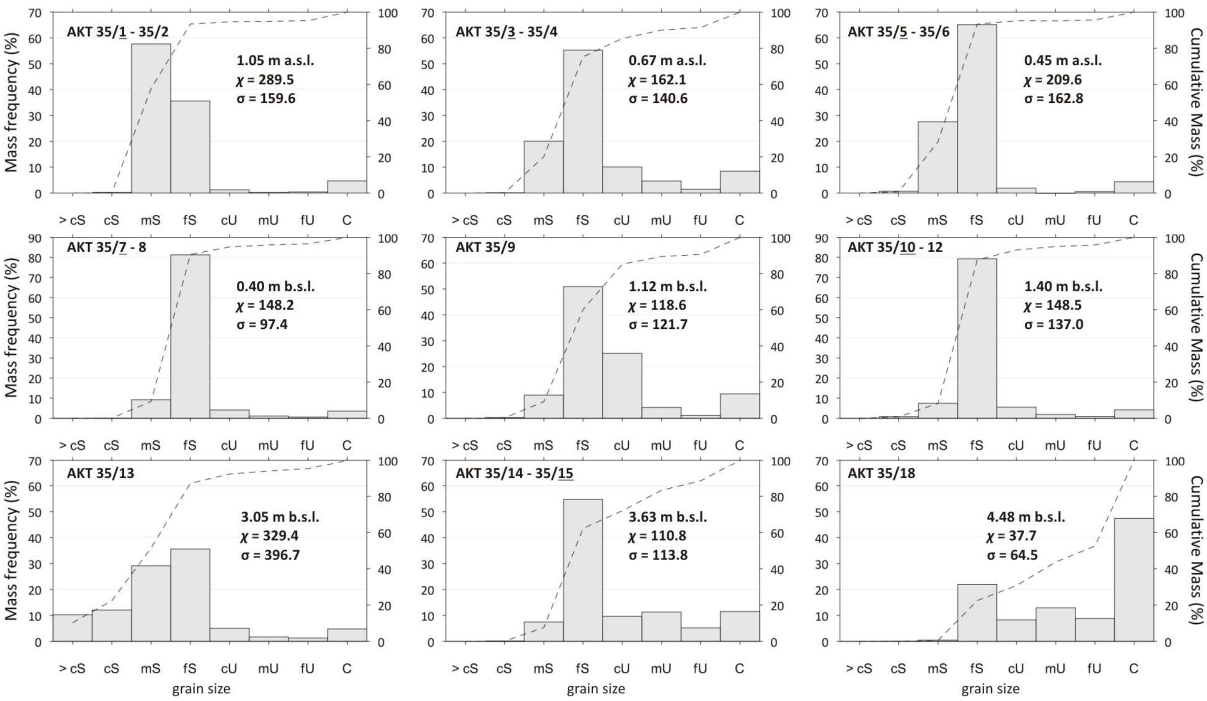

Fig. 3-3: Results of grain size analysis carried out for samples of vibracore profile AKT 35. For samples with similar or comparable grain size distribution only one plot was depicted (depicted sample underlined). Notes: b.s.l. – below mean sea level. a.s.l. – above mean sea level. s.l. – mean sea level. χ - mean grain size (µm). σ – sorting (standard deviation, µm).

The following sedimentary unit (3.35 m – 2.90 m b.s.l.) starts with a sharp erosional contact at 3.35 m b.s.l. The sediment mainly consists of grey sand with a high content of angular marine mollusc fragments. Articulated specimens were encountered as well. It is characterized by low LOI values and a high content of calcium carbonate. In contrast to all other sediments found for vibracore AKT 35, these sediments appear to be poorly sorted (Fig. 3-2 and Fig. 3-3, AKT 35/13). A clear fining-upward sequence can be identified at the transition to the overlying sediments. Moreover, small clasts of silty to clayey material could be detected, similar to the sediments from the underlying horizon.

The subsequent sediments (Fig. 3-3, AKT 35/7 – AKT 35/12, 2.90 m b.s.l. – 0.39 m a.s.l., above mean sea level) are marked by high contents of fine sand (50 – 81 %) accompanied by minor parts of medium sand (~10 %) and coarse silt (4 – 10 %). Only samples AKT 35/9 and AKT 35/11 show slightly higher contents of coarse silt and gravel. The sediments contain plant and sea weed and marine mollusc remains. Due to its overall good sorting and its high content of fine sand constant deposition in a morphodynamic regime of moderate energy is assumed. Above 0.65 m b.s.l., the marine sands show, in contrast to the underlying unweathered marine sequence, a brownish colour and high values of the Fe/Na ratio.

Increasing contents of medium sand (Fig. 3-3, 17 – 27 %, AKT 35/5 – AKT 35/6) are encountered above the well sorted, fine sandy sediments (0.39 m – 0.71 m a.s.l.). The upper part of this sequence shows considerably higher amount of silt and clay in samples AKT 35/3 and AKT 35/4 (Fig. 3-3, 0.50 m – 0.71 m a.s.l.). Moreover, LOI values increase. Subsequently, samples AKT 35/1 and AKT 35/2 mainly consist of well sorted medium sand and a minor part of fine sand (Fig. 3-3). In contrast to the underlying sequence, the sediment appears to be loose and dry and is characterized by low LOI values. Only few macroscopic mollusc remains were detected.

Vibracore ANI 2

At its base, vibracore ANI 2 begins with a sequence of homogenous clayey silt, containing few mollusc and plant remains (17.72 – 13.22 m b.s.l.). The sediments appear muddy and are of olive-grey colour. Geochemical parameters show high organic contents and low values of the Na/Fe ratio. Moreover, shell remains are significantly thinner than in the overlying sediments. At 13.22 m b.s.l., a sudden change in geochemical parameters is accompanied by the occurrence of a shell debris layer (13.22 m – 12.98 m b.s.l.), showing a fining upward trend. The shell debris layer is separated from the underlying sediments by an erosional unconformity.

Above, depositional circumstances considerably changed. The sedimentary sequence shows decreasing parts of clay and increasing parts of fine sand. An increasing number of marine mollusc remains, lower LOI values, a sudden increase in the Na/Fe-ratio, and sea weed was found (12.98 m – 11.11 m b.s.l.). Subsequently, a sequence of fine sandy to silty sediments follows. It shows a partly pronounced lamination and sea weed layers occur (11.11 m – 3.36 m b.s.l.). At 3.27 m b.s.l., lamination of the sediment stops and homogenous, well sorted fine sand is documented between 3.27 m – 1.85 m b.s.l. The following unit shows increasing contents of medium sand (1.65 m b.s.l. – 0.28 m a.s.l.). To the top, geochemical parameters point to a slight weathering of the sediments (0.24 m b.s.l. – 0.28 m a.s.l.).

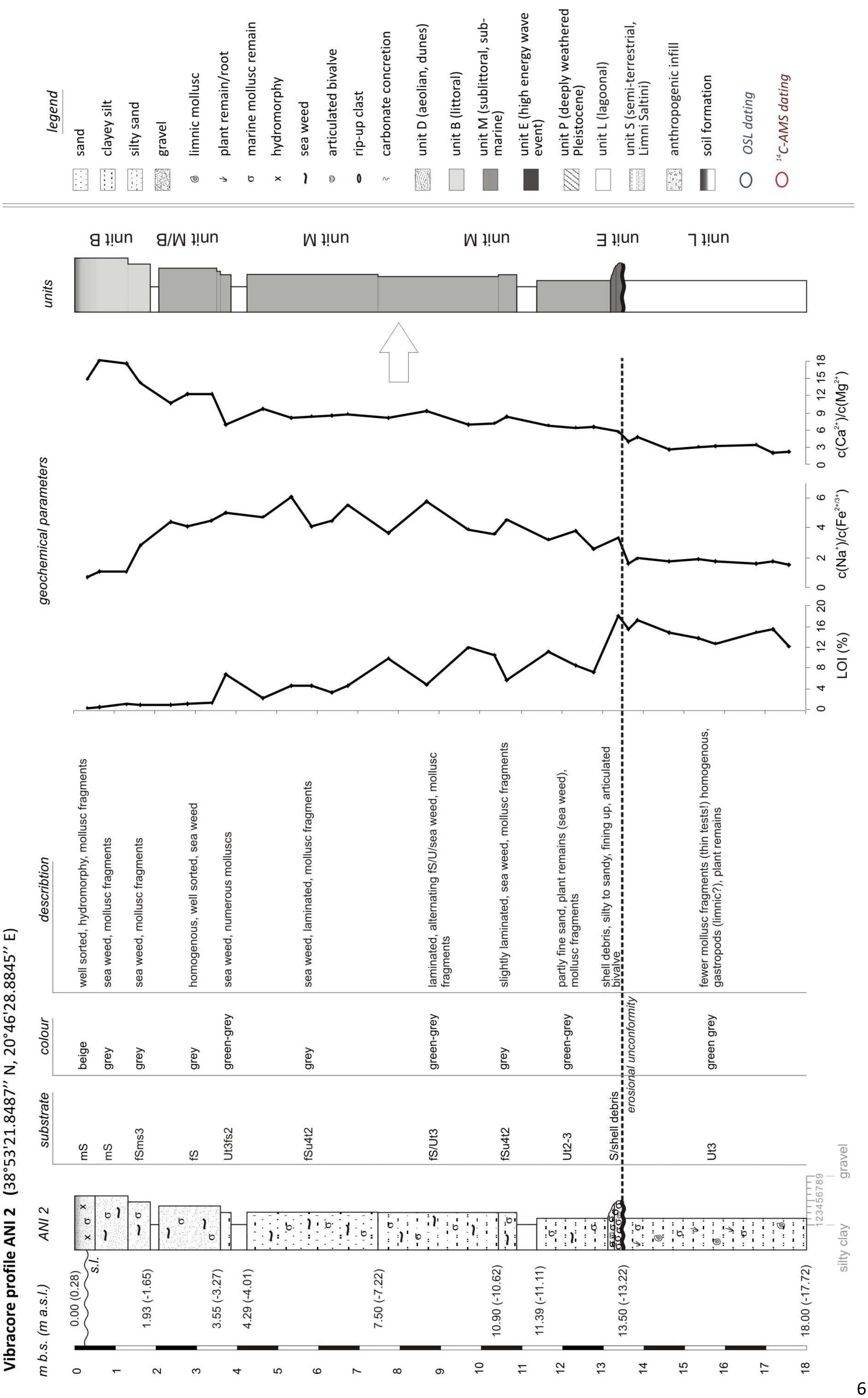
Vibracore profile ANI 2 (38°53'21.8487'' N, 20°46'28.8845'' E)
m b.s. (m a.s.l.)
ANI 2
substrate
colour
description
geochemical parameters
units
legend
0.00 (0.28)
1.93 (-1.65)
3.55 (-3.27)
4.29 (-4.01)
7.50 (-7.22)
10.90 (-10.62)
11.39 (-11.11)
13.50 (-13.22)
18.00 (-17.72)
s.l.
silty clay
gravel
123456789
mS
fSms3
fS
Ut3fs2
fSu4t2
fS/Ut3
Ut2-3
S/shell debris
Ut3
erosional unconformity
beige
grey
green-grey
green grey
well sorted, hydromorphy, mollusc fragments
sea weed, mollusc fragments
homogenous, well sorted, sea weed
sea weed, numerous molluscs
sea weed, laminated, mollusc fragments
laminated, alternating fS/U/sea weed, mollusc fragments
slightly laminated, sea weed, mollusc fragments
partly fine sand, plant remains (sea weed), mollusc fragments
shell debris, silty to sandy, fining up, articulated bivalve
fewer mollusc fragments (thin tests!) homogenous, gastropods (limnic?), plant remains
LOI (%)
c(Na⁺)/c(Fe²⁺/³⁺)
c(Ca²⁺)/c(Mg²⁺)
unit B
unit M/B
unit M
unit E
unit L
sand
clayey silt
silty sand
gravel
limnic mollusc
plant remain/root
marine mollusc remain
hydromorphy
sea weed
articulated bivalve
rip-up clast
carbonate concretion
unit D (aeolian, dunes)
unit B (littoral)
unit M (sublittoral, sub-marine)
unit E (high energy wave event)
unit P (deeply weathered Pleistocene)
unit L (lagoonal)
unit S (semi-terrestrial, Limni Saltini)
anthropogenic infill
soil formation
OSL dating
¹⁴C-AMS dating

Fig. 3-4 (previous page): Sedimentary sequence and geochemical characteristics of vibracore profile ANI 2 (see Fig. 3-1). In the lower part of the profile, geochemical characteristics considerably change subsequent to a normal graded shell debris layer, pointing to increased marine influence in the Bay of Aghios Nikolaos. The shell debris layer comprises sedimentary unit E. Notes: b.s.l. – below mean sea level. a.s.l. – above mean sea level. s.l. – mean sea level. Grain size of cores is illustrated by different widths of core profile (see caption of Fig. 3-2).

3.4.2 GENERALIZATION AND INTERPRETATION OF SEDIMENTARY UNITS

The sedimentary sequence of vibracores AKT 35 and ANI 2 is typical for the entire Phoukias sand spit. Although several minor differences between the vibracores exist, a generalization of the sedimentary sequence can be made (see Figs. 3-2 and 3-4). Thus, seven sedimentary units are summarized, each of them representing distinct sedimentary facies and depositional environments. The differentiation of the sedimentary units is based on their geochemical, sedimentary and visual characteristics (Fig. 3-5).

Unit P

The basal sedimentary sequence of vibracore AKT 35 is summarized in sedimentary unit P. Comparable sediments were found at the base of all investigated vibracores in the entire northern and middle part of the Phoukias sand spit. Due to its sedimentary and geochemical characteristics, unit P most likely represents intensely weathered pre-Holocene deposits of different origin. According to the abundant root-channels and plant remains, a former (semi-) terrestrial surface must have existed at least in some parts on top of this unit, which was accompanied by soil development and intense weathering. At most investigated sites, the top of this unit is marked by a clear erosional unconformity at the transition to the overlying deposits.

Unit L

In the southern part of the Phoukias sand spit, the base of the sedimentary sequence is comprised by sedimentary unit L instead of unit P, although vibracore profiles ANI 2 and ANI 14 have coring depths of 18 m and 13 m b.s., respectively. The sedimentary and geochemical findings point to reduced salt water influence for unit L and suggest a brackish-lagoonal palaeoenvironment, characterised by quiescent depositional conditions.

Unit M

In particular the cores in the middle part of the Phoukias sand spit are characterized by a sequence of sediments of marine origin which are, in contrast to the sediments of unit E, well sorted, fine grained (mainly fine sand) and homogeneous. In some parts, sea weed layers occur and a distinct lamination was encountered. These findings point to overall increased salt water influence for unit M, representing sublittoral, marine depositional conditions of different water depths. In some cases, the sublittoral sands were exposed to weathering processes and show, in contrast to the underlying unweathered marine sequence, a brownish colour and high values of the Fe/Na ratio.

Unit B

On top of unit M, increasing contents of medium sand represent establishing littoral conditions at many coring sites of the study area. These sediments are summarized in unit B. In many cases, in the upper part of this unit, higher parts of silt and clay were encountered (up to 20 %, e.g. samples AKT 35/3 and AKT 35/4, Fig. 3-3), evidencing soil formation.

Unit S

Unit S was not encountered in the key profiles AKT 35 and ANI 2 described above. However, in the northern part of the spit, sediments of unit E are covered by unit S, consisting of grey to brown, silty and clayey deposits. This unit is indicated by numerous plant- and root remains and exhibits clear signs of hydromorphy. In some parts, it contains minor parts of sand, most likely related to reworking of the underlying, sand-containing unit E. Accumulation of unit S is related to the temporary flooding of the area by the *Limni Saltini*.

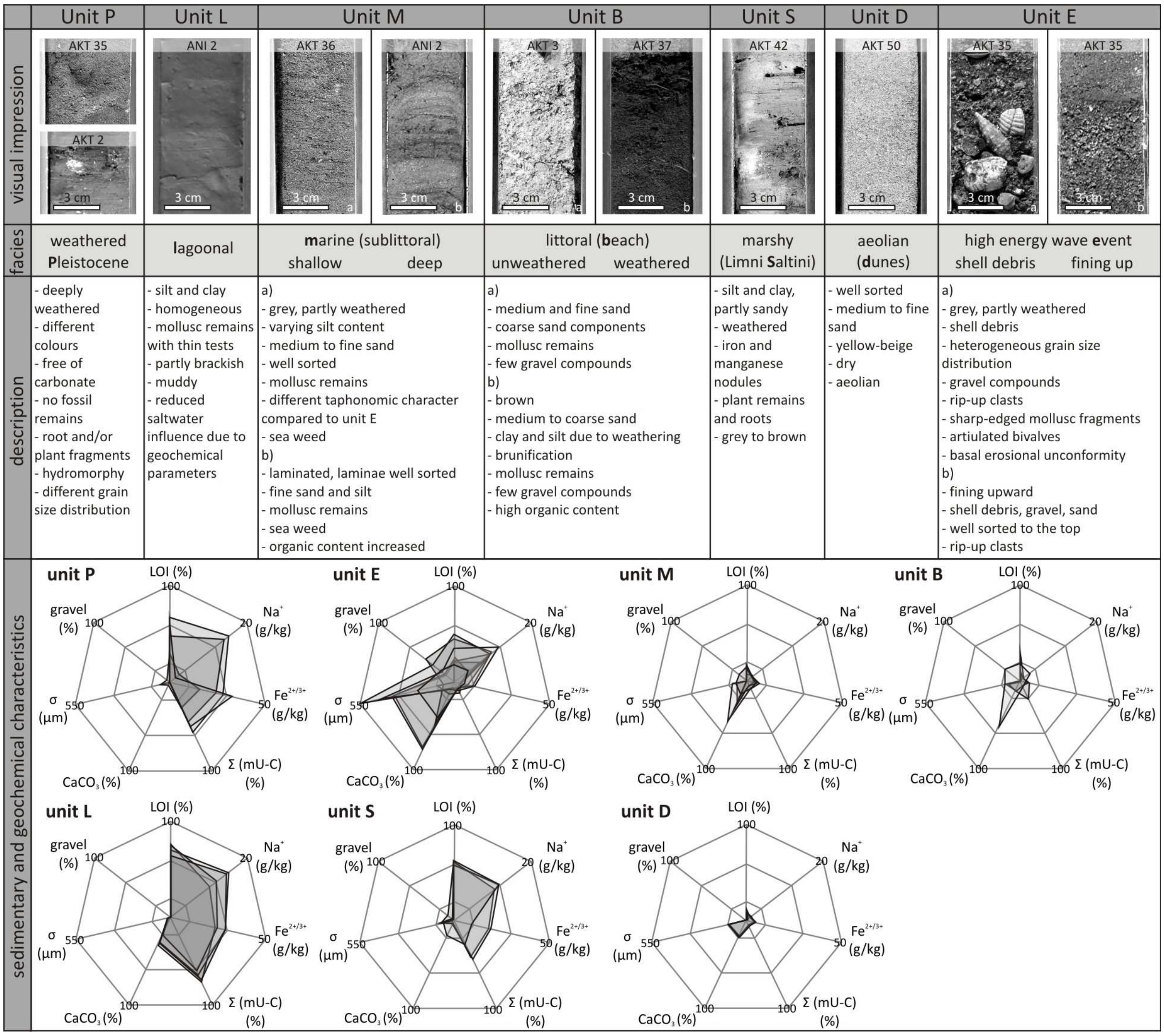

Fig. 3-5: Summarized characteristics of each sedimentary unit found in the study area. Each unit represents distinct depositional environments and sedimentary facies. Depicted spider diagrams abstract geochemical and textural characteristics. The high energy wave deposits of unit E clearly differ to all other units. Notes: σ – sorting (standard deviation).

Unit D

Unit D is restricted to the middle and southern part of the Phoukias sand spit, which is characterized by an extensive system of coastal dunes, up to 5 m high. It is found on top of units

M and B. This unit documents the deposition of dune related aeolian sediments, covering the littoral unit B.

Unit E

Unit E was encountered at numerous coring sites and consists, comparable to vibracore AKT 35, of a distinct shell debris layer. Typical characteristics for unit E are (i) a high content of angular marine mollusc fragments, (ii) low LOI values, (iii) a high content of calcium carbonate, and (iv) a heterogeneous grain size distribution consisting of sand and gravel. The overall poor sorting of the sediment is expressed in generally high standard deviations of grain size distribution. In most cases, unit E is separated from the underlying sediments by an erosional unconformity. A fining upward sequence characterizes the transition to the subsequent sedimentary unit. Unit E is different to all other units found within the stratigraphical sequence of the Phoukias spit (see Fig. 3-5). At numerous locations, unit E represents the beginning of the marine sequence of the Phoukias sand spit. Its sedimentary characteristics clearly point to a rapid deposition, related to turbulent, high energy wave dynamics. Therefore, detailed investigations were carried out for this stratigraphical unit for vibracore AKT 35 and sediment profile AKT S2, situated in the northern part of the Phoukias spit (see Fig. 3-1).

3.4.3 DETAILED INVESTIGATIONS ON EVENT UNIT E

In order to characterize the sediments of the high energy unit E in detail, comprehensive investigations were carried out for sediment profile AKT S2 and vibracore profile AKT 35. At coring site AKT 35 unit E starts with a sharp erosional contact at 3.35 m b.s.l., at sediment profile AKT S2, situated in the northern part of the spit, at 0.46 m b.s.l. For both event units, sedimentary characteristics are similar.

Macro- and microfaunal investigations on vibracore AKT 35

For macro- and microfaunal studies, parallel core AKT 35b was sampled and sixteen samples were investigated for micro- and macrofaunal content. Results of microfaunal analyses (foraminifers and ostracodes) are illustrated in Fig. 3-6. The documented species point to a shallow marine origin of the sediment, and no certain source region could be detected throughout the sequence. However, the lower part of unit E (samples AKT 35/12 MF – AKT 35/10 MF) is characterized by remarkably few findings of ostracod specimen in contrast to sediment samples AKT 35/3 MF – AKT 35/9 MF. For sample AKT 35/12 MF, only one individual of *Callistocythere* sp., *Loxoconcha stellifera* and *Pontocythere rubra* were found. For samples AKT 35/10 MF and AKT 35/11 MF, eight species with very low abundance were recovered from the sediment *(Cyprideis torosa, Aurila arborescens, Aurila* sp., *Cytheretta adriatica, Loxoconcha bairdi, Loxoconcha stellifera, Loxoconcha* sp., *Paradoxostoma* sp., *Pontosythere rubra, Pontocythere* sp., *Urocythereis margaritifera, Xestoleberis dispar).*

As ostracod and foraminiferal communities best develop under continuous and constant environmental conditions, high morphodynamics and a short sedimentation period can be assumed for the deposition of the related sedimentary units. These findings point to an event-induced origin.

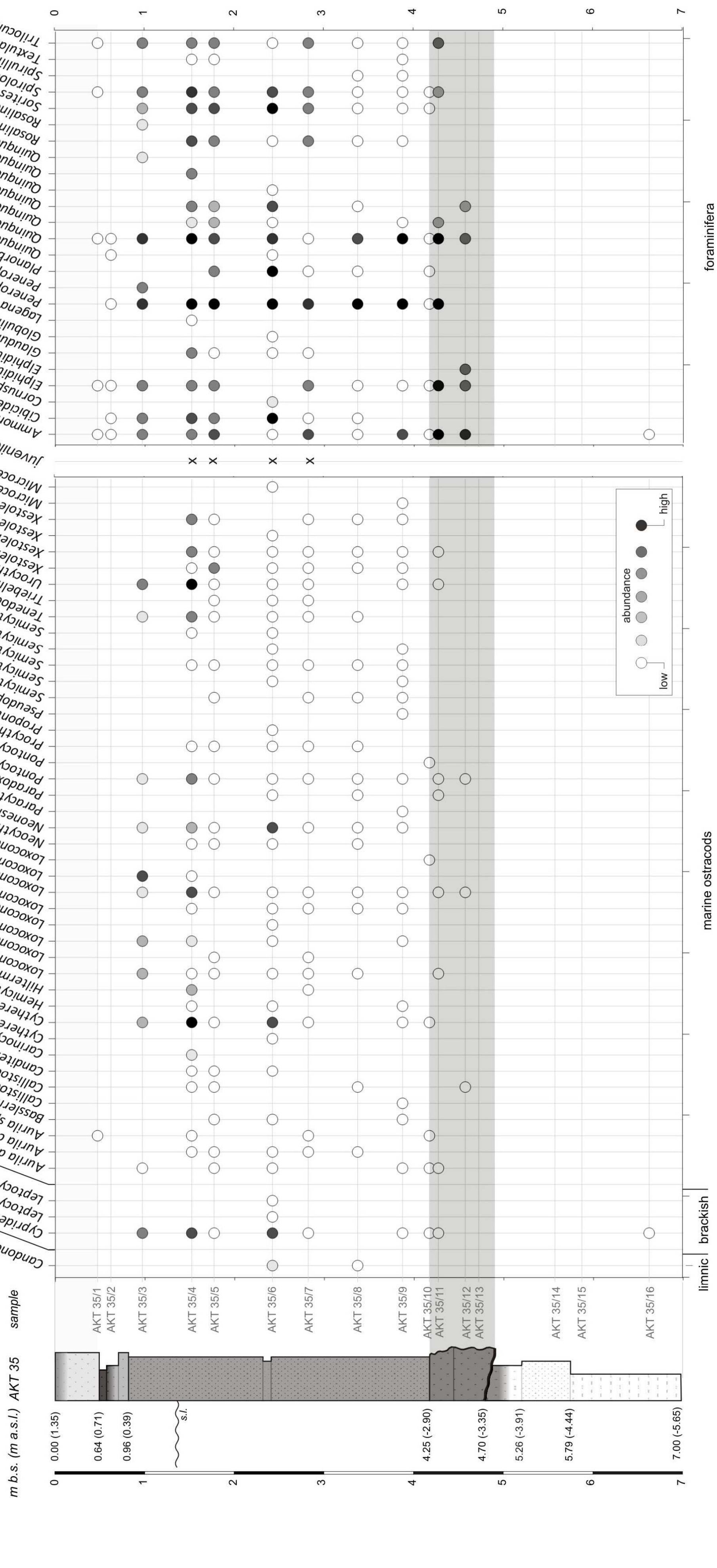

Fig. 3-6: *Results of microfaunal investigations carried out for vibracore AKT 35b. The deeply weathered sediments of unit P do not contain microfossils. The abundance of ostracod specimen and species considerably increases in the upper part of the marine sequence. A slight increase in foraminifera specimens and species may be inferred as well.*

Subsequently, abundance and diversity of detected species increase (AKT 35/9 MF – AKT 35/3 MF), and especially in samples AKT 35/6 MF – AKT 35/3 MF ostracods are abundant. In and subsequent to sample AKT 35/7 MF, several juvenile specimens were encountered. Therefore, within the profile's sequence, best environmental conditions for ostracod populations established during deposition of the upper 3 m of the profile, pointing to an autochthonous formation of the sediment. These results, from a geomorphodynamic point of view, suggest constant sublittoral depositional conditions in the upper part (above 3.00 m b.s.) of the marine unit of the profile.

In contrast, no considerable changes in foraminiferal assemblages can be detected, and shallow water species dominate throughout the whole profile. As to the distribution of the macrofaunal remains found in the sediment samples, again no differences in the source region of the marine sedimentary units can be detected throughout the profile. Increasing counts of specimen can be observed within unit E and directly following samples which is due to the shell debris character of the unit. Dominating shells found for the entire marine sequence are *Bittium latrellii*, *Hydrobia* sp., *Tricolia pullus* and the sessile genera *Vermetus* sp., all of them indicating shallow marine to lagoonal environments. Species exclusively found in the high energy layer are *Alvania discors, Ceritium vulgatum*, *Eulimella* sp., *Nassarius* sp., *Rissoa* cf. *variabilis*, *Truncularioipsis trunculus*, *Tricolia* cf. *tenius* and *Tricolia* sp., *Lucinella divaricata*, *Dosinia lupeus*, *Cerastoderma* sp. and *Venus verrucosa*.

Grain size distribution of unit E in vibracore AKT 35

Samples taken from parallel core AKT 35c (Fig. 3-7) document detailed analysis of the grain size distribution and grain size trend found for sedimentary unit E. The event deposit (unit E) can be subdivided into two general sedimentary subunits. Samples AKT 35c/1 - AKT 35c/3 represent the lower, samples AKT 35c/4 – AKT 35c/6 the upper part of the layer.

The lower part is characterized by a very heterogeneous grain size distribution, with high values of coarse material (> 2 mm, 20-30 %). In contrast to all other sedimentary units found for vibracore AKT 35 this points to a poor sorting during deposition (see also Fig. 3-2). Sample AKT 35c/1 mainly consists of medium and fine sand with 29 % and 36 %, respectively. Additionally, it shows a relatively high content of clay. Towards the overlying unit M, a considerable decrease in coarse grain sizes is apparent in the upper part of unit E (AKT 35c/4), and the sediment passes into well sorted fine to medium sand above 3.10 m b.s.l. (AKT 35c/5 and AKT 35c/6). A clear fining upward sequence (normal grading) thus can be identified, comprising the upper part of unit E.

Taphonomic investigations on shells of vibracore AKT 35

For core AKT 35c, the shell content of the samples from unit E was investigated for taphonomic characteristics. For the analysis, shell remains of > 2 mm were studied using a binocular microscope. The shell remains were grouped and counted based on the following characteristics: disarticulated whole valve, fragmented valve, fragment with angular breaks (no edge rounding), fragment with edgeless breaks (edge rounding), encrustations, dissolution and boring holes (Fig. 3-8 and 3-9).

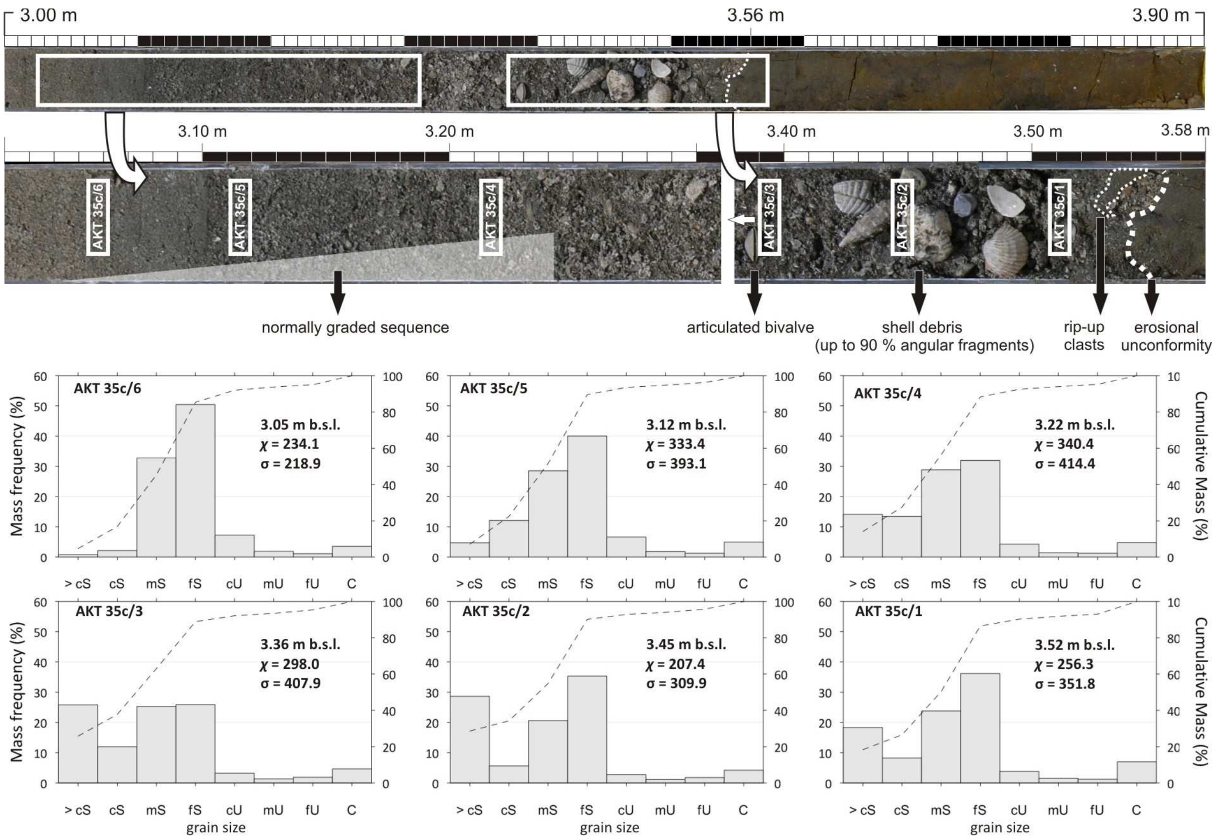

Fig. 3-7: Photography of the core section between 3.00 – 3.90 m b.s.l. of core AKT 35c, main sedimentary characteristics and detailed documentation of the event layer's grain size distribution (samples AKT 35c/1-AKT35c/6). Position of grain size samples is marked by white boxes. Event unit E can be separated into two subunits – a lower subunit of heterogeneous grain size distribution, and an upper subunit, indicated by a fining upward sequence. Notes: b.s.l. – below mean sea level. a.s.l. – above mean sea level. s.l. – mean sea level. χ - mean grain size (µm). σ – sorting (standard deviation, µm).

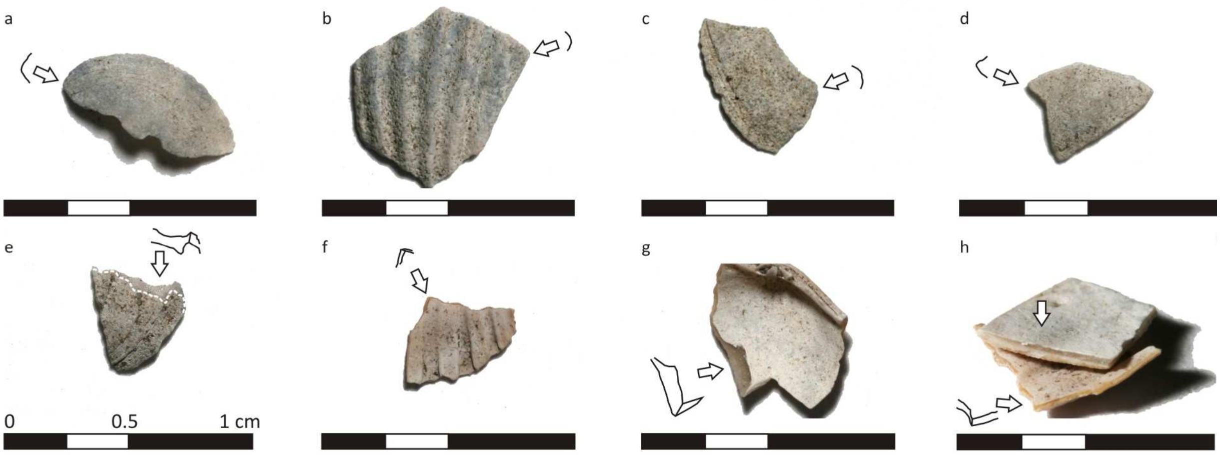

Fig. 3-8: Photographs of selected mollusc fragments with taphonomic characteristics used for classification (all Photos taken by T. Willershäuser). Pictures a), b), c) and d) illustrate edge-rounded mollusc fragments. Angular mollusc fragments are shown in e), f), g) and h). Within the event layer, up to 90 % of the fragments exhibit angular breaks and edges.

Sample AKT 35c/6 was not depicted in Fig. 3-9 due to its low shell debris content (n = 27). However, its taphonomic characteristics are similar to samples AKT 35c/1- AKT 35c/5. As a reference, sample AKT 35/11 was analyzed and compared to the samples from the high energy sediment layer. As Fig. 3-9 shows, all samples from unit E are characterized by a considerably high content of shell fragments (> 80 %) while the amount of whole valves is relatively low (< 20%). Moreover, 80 - 92 % of the investigated fragmented shell remains exhibit angular breaks and fracture surfaces as well as edges with sharp angles (Fig. 3-8 e-h). In contrast, only 8-20 % of the fragments show rounded or edgeless fracture surfaces (Fig. 3-8 a-d). In all samples, the amount of mollusc remains affected by dissolution does not exceed 10 %. The number of shell remains showing boring holes, encrustations and signs of dissolution is negligible. Due to the use of cores with 6 cm and 5 cm diameter, only limited sample material was available, and the content of articulated bivalves in the sediment may not be representative. Nevertheless, several articulated bivalves were found in unit E.

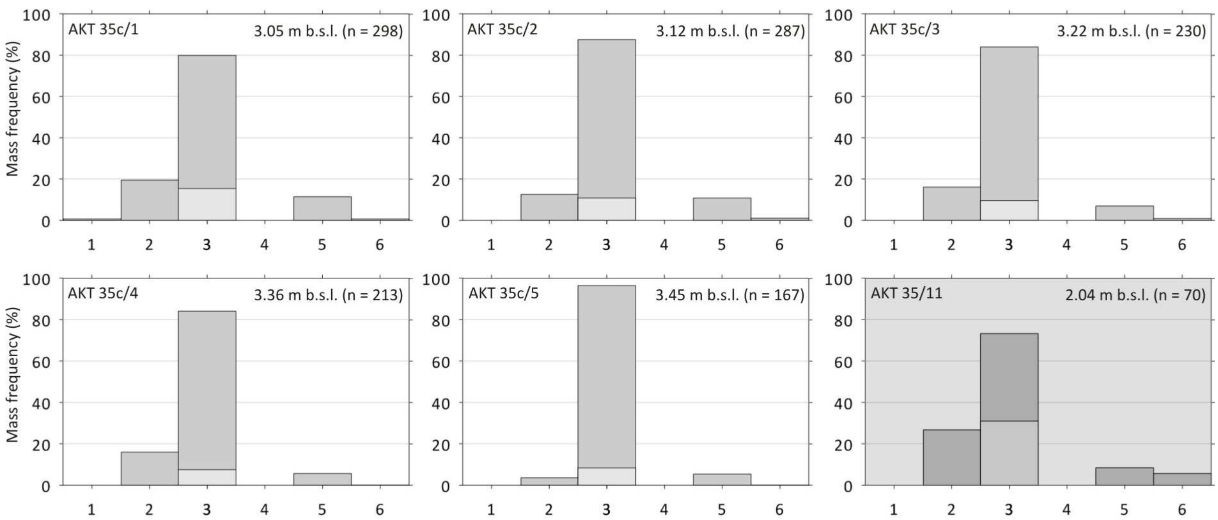

Fig. 3-9: Taphonomic characteristics of samples AKT 35c/1-AKT 35c/5 and reference sample AKT 35/11 (grey marked). x – Axis: 1 - articulated, 2 - whole valves, 3 - fragments (light grey: rounded breaks, dark grey: angular breaks), 4 - encrustations, 5 - dissolution and 6 - bore holes. A considerable difference in taphonomic characteristics can be observed between the samples of the assumed event layer and the sample from the sublittoral facies.

Reference sample AKT 35/11 was taken from sedimentary unit M (2.04 m b.s.l.) and is assumed to represent regular, sublittoral depositional conditions of low energy. A considerable difference in taphonomic characteristics can be observed between the samples of the high energy layer and the sample from the sublittoral facies. As illustrated in Fig. 3-9 it is characterized, compared to samples AKT 35c/1- AKT 35c/5, by higher parts of whole valves (~30 %) and edge-rounded mollusc fragments (> 40 % of all mollusc fragments). Moreover, the content of mollusc remains showing signs of dissolution and bore holes is noticeably higher.

Characteristics of event unit E in sediment profile AKT S2

In the northern part of the spit, similar to the findings documented for vibracore AKT 35, a shell debris layer was encountered above an erosional unconformity between 0.46 m – 0.21 m b.s.l. in sediment profile AKT S2 (Fig. 3-11, see also Fig. 3-1). Inside the trench the sedimentary stratigraphy is exposed along several meters. Although the depth of the shell debris layer is documented almost 3 m higher than in vibracore AKT 35, comparable findings have been observed.

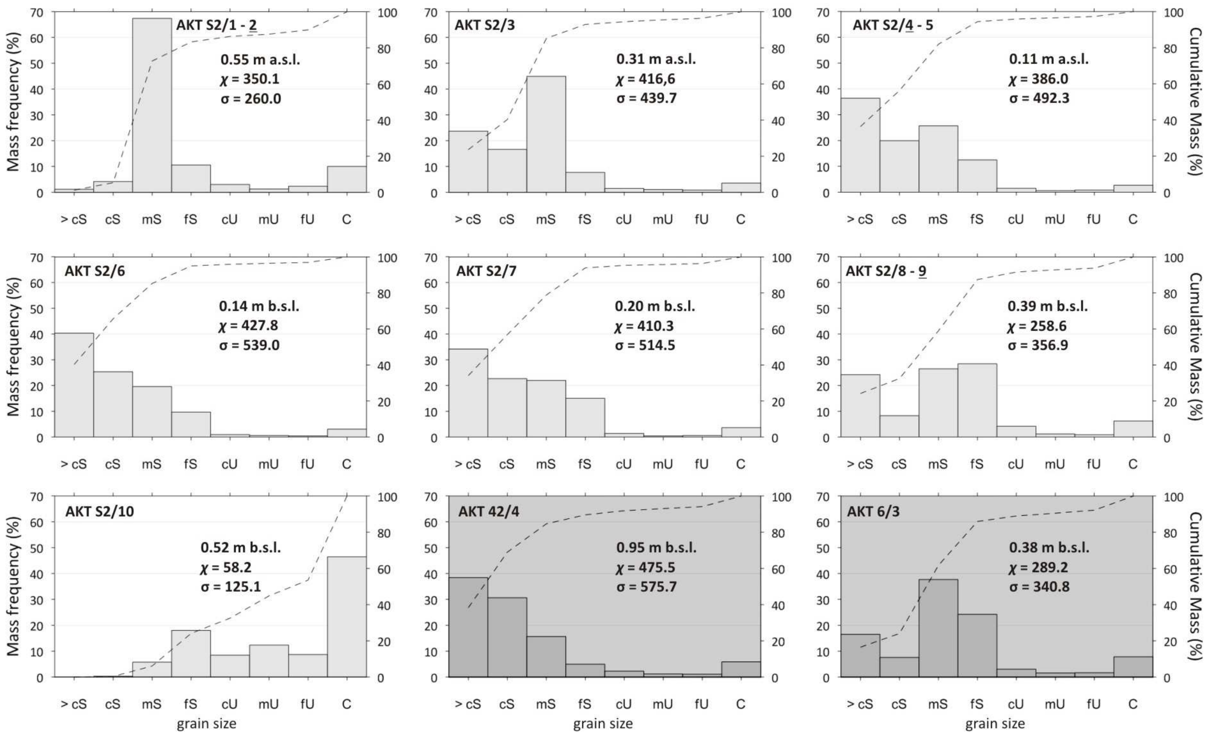

Fig. 3-10: Results of grain size analysis carried out for sediment profile AKT S2. The last two samples (grey background) represent examples of grain size analysis carried out for vibracores AKT 42 and AKT 6, in the northern part of vibracore transect A. The event deposit of unit E can be followed several hundred meters into the Limni Saltini plain and is thinning landward. Notes: b.s.l. – below mean sea level. a.s.l. – above mean sea level. s.l. – mean sea level. χ - mean grain size (µm). σ – sorting (standard deviation, µm).

Again, unit E can be subdivided into two general sedimentary units. The lower subunit (0.46 m – 0.21 m b.s.l.) is represented by grain size samples AKT S 2/8 and AKT S 2/9 (Fig. 3-10) and consists of shell debris, gravel, very well rounded, and a sandy matrix. The grain size analyses document the poor sorting of the sediment and indicate a bimodal grain size distribution. The upper subunit (0.21 m b.s.l. – 0.81 m a.s.l.) begins with a sequence of very well rounded gravel surrounded by a sandy matrix. Here, the grain size distribution (AKT S 2/6 – AKT S 2/7) shows an unimodal pattern dominated by sediment > 2 mm (34 and 40 %) and coarse sand (25 and 23 %).

Subsequently, the unit is characterized by decreasing gravel and increasing sand content (AKT S 2/3 – AKT S 2/5). The upper part of the unit (0.48 m – 0.81 m a.s.l., AKT S 2/1 and AKT S 2/2) consists of well sorted medium sand. Similar to the findings in vibracore AKT 35, the upper part is thus characterized by a clear fining upward sequence. Moreover, numerous articulated shells and abundant angular shell fragments were found within the sediment, which is comparable to the findings described for vibracore AKT 35 (see Fig. 3-3 and 3-7). In most cases, the articulated shells were filled with air or remains of fine grained, silty material of brown colour during excavation.

In the northern part of the spit, unit E constitutes the entire marine sequence covering the weathered former surface. As the results of the sediment cores carried out in this area show, unit E is thinning north- and landwards, respectively. Moreover, no gravelly sediments are found along the entire western shore of Aktium Headland. It is thus concluded that the provenance area of the deposits found in sediment profile AKT S2 is different to the transported sediment at the present western Aktium shore.

Fig. 3-11: Photographs of sediment profile AKT S2 (a) and the encountered shell debris layer of unit E (b, d). The shell debris layer contains abundant mollusc fragments and (!) articulated bivalves. Picture c) illustrates air-filled articulated bivalves that were washed out of the shell debris unit during digging and float in the ground water.

3.4.4 VIBRACORE TRANSECTS AND CHRONOSTRATIGRAPHICAL INTERPRETATION

Based on the above presented results, the internal structure of the Phoukias sand spit is illustrated along four vibracore transects. A stratigraphical correlation between single cores, along the core transects as well as between the core transects is realized. Together with the available results of the ^{14}C-AMS (Table 3-1) and the OSL datings (Table 3-2), a consistent chronostratigraphical picture of the spit formation is established.

Vibracore transect A

In the very northern part of the Phoukias sand spit, vibracore transect A (Fig. 3-12a) comprises, from south-west to north-east, vibracores AKT 39, AKT 40 and AKT 41, sediment profiles AKT S1 and AKT S2 as well as vibracores AKT 42, AKT 6 and AKT 5.

The stratigraphy described for sediment profile AKT S2, due to the findings in vibracores AKT 39, AKT 40, AKT 41 and AKT 42 was well as sediment profile AKT S1, can be assumed for the entire ridge-dominated south-western part of transect A, belonging to ridge generation I (see also *Chapter 2*). In the north-eastern part of transect A, vibracores AKT 42, AKT 6 and AKT 5 show a slightly different but comparable stratigraphical sequence. Vibracore AKT 6 was carried out in the adjacent low lying plain, ~100 m north of the northernmost ridge-like elevation. Here, the transition from the deeply weathered former surface (unit P) to the overlying coarse grained marine sequence (unit E) was detected at 0.41 m b.s.l. Unit E is thinner compared to sediment profile AKT S2 but consists of a shell debris layer, containing well rounded gravel and a sandy matrix (sample AKT 6/3, Fig. 3-10), and a subsequent layer out of sand and gravel with mollusc fragments. Due to the temporary flooding of the site it is covered by the sediments of unit S.

For vibracore AKT 42, situated between vibracore AKT 6 and sediment profile AKT S2, a similar sequence was found. As Fig. 3-10 shows, grain size distribution of sample AKT 42/4 is similar to the grain size distribution of the lower part of unit E in sediment profile AKT S2. Here, unit E shows a thickness of 87 cm (1.01 m – 0.14 m b.s.l.). At coring site AKT 5 (170 m northeast of AKT 6, 270 m north of the northernmost ridge), a thin layer of marine origin, containing mollusc fragments, was encountered at 0.27 m – 0.20 m b.s.l. Within the lower part of the subsequent unit, well rounded isolated pieces of fine gravel were detected. Therefore, a northward and thus landward thinning of the event unit E described for sediment profile AKT S2 can be assumed, reaching at least 270 m inland. These findings clearly indicate the washover-character of the sequence and document its event induced origin.

*Tab. 3-1: ^{14}C-AMS dating results used for the chronological interpretation of the stratigraphy. Notes: unid. plant remains - unidentified plant remains. artic. mollusc - articulated mollusc. Lab. No. – laboratory number, University of Erlangen-Nürnberg (ERL), University of Kiel (KIA), University of Utrecht (UTC). * - marine reservoir correction with 400 years of reservoir age. ";" - there are several possible age intervals because of multiple intersections with the calibration curve; oldest and youngest age depicted.*

Sample	Depth (m b.s.l.)	Lab. No.	Sample description	δ^{13}C (ppm)	^{14}C age (BP)	1σ max-min (cal BC/AD)	2σ max-min (cal BC/AD)
AKT 2/9 PR	1.60	KIA31674	unid. plant remains	-5.18	4160 ± 31	2872; 2679 BC	2879-2632 BC
AKT 3/5 PR	0.54	KIA34003	unid. plant remains	-9.30	2880 ± 25	1113; 1012 BC	1188; 946 BC
AKT 35/9 PR	1.11	KIA34004	unid. plant remains	-15.20	1690 ± 25	*661-711 AD	*636-763 AD
AKT 35/12 M	2.51	KIA34005	articulated mollusc	1.34	2065 ± 30	*264-361 AD	*228-416 AD
AKT 35/15 PR	3.64	KIA34006	unid. plant remains	-10.65	4275 ± 45	3000; 2780 BC	3019; 2703 BC
AKT 37/11 PR	1.24	KIA34007	unid. plant remains sea weed?	-17.03	1840 ± 25	132;214 AD *515-605 AD	88; 240 AD *460-629 AD
AKT 37/14 PR	2.04	KIA34008	unid. plant remains	-7.36	3290 ± 25	1608; 1503 BC	1624-1503 BC
AKT 38/8+ PR	1.65	KIA34009	unid. plant remains	-9.06	3305 ± 25	1615; 1532 BC	1662; 1513 BC
AKT S2/9 M	0.44	KIA39794	articulated mollusc	2,27	4200 ± 25	*2398-2290 BC	*2447; 2239 BC
AKT S2/9+ M	0.45	KIA39795	articulated mollusc	-8,42	3495 ± 25	*1472-1403 BC	*1506-1371 BC
AKT S2/10 PR	0.54	KIA39793	unid. plant remains	-13,25	3555 ± 35	1952;1783 BC	2015; 1772 BC
ANI 2/7 PR	3.25	UTC13679	wood remains	-24,80	113 ± 41	1688; 1926 AD	1676; 1954 AD
ANI 2/12 PR	6.25	UTC13678	sea weed	-18.00	1003 ± 46	*1314-1395 AD	*1286-1430 AD
ANI 2/16++ PR	10.00	ERL9794	sea weed	-14,40	1499 ± 40	*825-943 AD	*781-994 AD
ANI 2/21+ PR	12.59	KIA39792	unid. plant remains	-11.31	2250 ± 20	384; 234 BC *50-122 AD	390; 210 BC *9-149 AD
ANI 2/22+ M	13.20	KIA39790	articulated mollusc	-3,05	2450 ± 25	*190-101 BC	*248-41 BC
ANI 2/29 M	16.95	KIA39791	articulated mollusc	-4,56	4225 ± 25	*2439-2341 BC	*2462-2287 BC
ANI 14/7+ PR	2.89	KIA31664	sea weed	-13.83	1590 ± 29	*728-818 AD	*700-874 AD
ANI 14/11+ PR	4.88	KIA31665	sea weed	-12.85	2170 ± 27	*131-221 AD	*90-254 AD
ANI 14/25 M	11.16	KIA31676	artic. *Mytilus* sp.	-6.80	6745 ± 40	*5373-5280 BC	*5426-5226 BC

Along the ridge-dominated part of transect A, a well developed brown soil can be observed on top of the sedimentary sequence (see also Fig. 3-11). Due to the distinct formation of the related Ah and Bv soil horizons and the depth of related brunification and loamification, (i) a relatively long period of undisturbed subaerial weathering after deposition and (ii) a deposition of the sequence above sea level is assumed. The time of deposition of the sedimentary sequence thus must have occurred at least several hundred years ago, and no reworking occurred since then.

For sediment profile AKT S2, three samples were dated by ^{14}C-AMS to obtain a chronological framework for the evolution of the sedimentary sequence. From the deeply weathered former surface of unit P, a plant remain was dated to 2015; 1772 cal BC (AKT S2/10 PR, Tab. 3-1). Moreover, two articulated bivalves (*Cerastoderma glaucum*) were taken from the subsequent shell debris layer of event unit E. Sample AKT S2/9 M (1.25m b.s.) yielded an age of 2447; 2239 cal BC, sample AKT S2/9+ M (1.26 M b.s.) an age of 1506-1371 cal BC. For the latter sample, the δ^{13}C-value points to an influence of fresh water on the shell's carbonate composition, and an overestimation of the obtained age is likely (personal communication P.M. GROOTES 2009).

Vibracore transect B

Vibracore transect B (Fig. 3-12b) starts with vibracore AKT 3 and continues with corings AKT 36, AKT 38 and AKT 37 towards the south-west. The topography along transect B is characterized by a sequence of beach ridges, belonging to ridge generation II (see *Chapter 2*). Overall stratigraphy of transect B is comparable to the findings of vibracore transects A and C. Here, the former surface is dipping slightly towards the southeast to 1.31 m b.s.l. (AKT 36), 1.61 m b.s.l. (AKT 38) and 2.02 m b.s.l. (AKT 37). Its upper part is characterized by a clear erosional unconformity and, in most cases, followed by the sandy shell debris layer of event unit E. In all vibracores along transect B the following marine units represent submarine to littoral depositional conditions (unit M and B), and the accumulation of the sequence can be linked to the formation of ridge generation II (see also *Chapter 2*).

Tab. 3-2: OSL datings of parallel cores AKT 3b, AKT 36b and sediment profile AKT 35D. Notes: b.s. – depth below surface, Gy – gray (j/kg), yrs – years before present. For radionuclide values and age-depth plots see appendix D.

Sample	*Depth (m b.s.)*	*Equivalent dose (Gy)*	*Doserate ± Error (Gy/ka ± Gy)*	*Water content (%)*	*Grain size (µm)*	*OSL age (yrs)*	*Error (+- yrs)*
AKT 3b OSL 1	0.56-0.64	1.14 ± 0.08	0.59 ± 0.08	5+-5	150-200	1930	240
AKT 3b OSL 2	0.83-0.93	1.21 ± 0.07	0.56 ± 0.07	10+-5	150-200	2160	250
AKT 3b OSL 3	1.35-1.45	1.52 ± 0.08	0.55 ± 0.07	10+-5	150-200	2770	310
AKT 3b OSL 4	1.60-1.70	2.99 ± 0.21	1.31 ± 0.16	15+-5	125-180	2290	240
AKT 3b OSL 7	2.45-2.50	129.3 ± 7.01	1.16 ± 0.16	10+-5	38-63	111000	13900
AKT 3b OSL 8	2.80-2.95	109.34 ± 7.46	1.12 ± 0.17	10+-5	38-63	97500	12800
AKT 36b OSL 1	0.56-0.65	1.69 ± 0.16	0.75 ± 0.13	5+-5	150-200	2250	320
AKT 36b OSL 2	0.86-0.98	1.7 ± 0.06	0.71 ± 0.08	10+-5	125-180	2400	260
AKT 36b OSL 3	1.55-1.64	1.53 ± 0.05	0.67 ± 0.07	10+-5	150-200	2280	240
AKT 36b OSL 4	1.87-1.98	1.93 ± 0.1	0.77 ± 0.09	70+-5	125-180	2523	248
AKT 36b OSL 5	2.72-2.79	1.61 ± 0.05	0.70 ± 0.06	85+-5	150-200	2290	190
AKT 36b OSL 6	2.86-2.98	2.21 ± 0.11	0.72 ± 0.09	85+-5	38-63	3060	330
AKT 36b OSL 7	3.50-3.61	65.66 ± 11.15	0.90 ± 0.23	10+-5	150-200	73090	13950
AKT 36b OSL 8	3.86-3.98	81.19 ± 7.41	0.90 ± 0.14	10+-5	150-200	90370	11400
AKT 35D OSL 1	2.10	0.28 ± 0.05	0.53 ± 0.14	5+-5	150-200	528	109
AKT 35D OSL 2	1.70	0.37 ± 0.06	0.53 ± 0.15	5+-5	125-180	704	163
AKT 35D OSL 3	1.20	0.37 ± 0.05	0.51 ± 0.12	5+-5	150-200	719	133
AKT 35D OSL 4	0.70	0.17 ± 0.08	0.69 ± 0.47	5+-5	125-180	245	118
AKT 35D OSL 5	0.45	0.32 ± 0.11	0.71 ± 0.35	5+-5	150-200	453	162

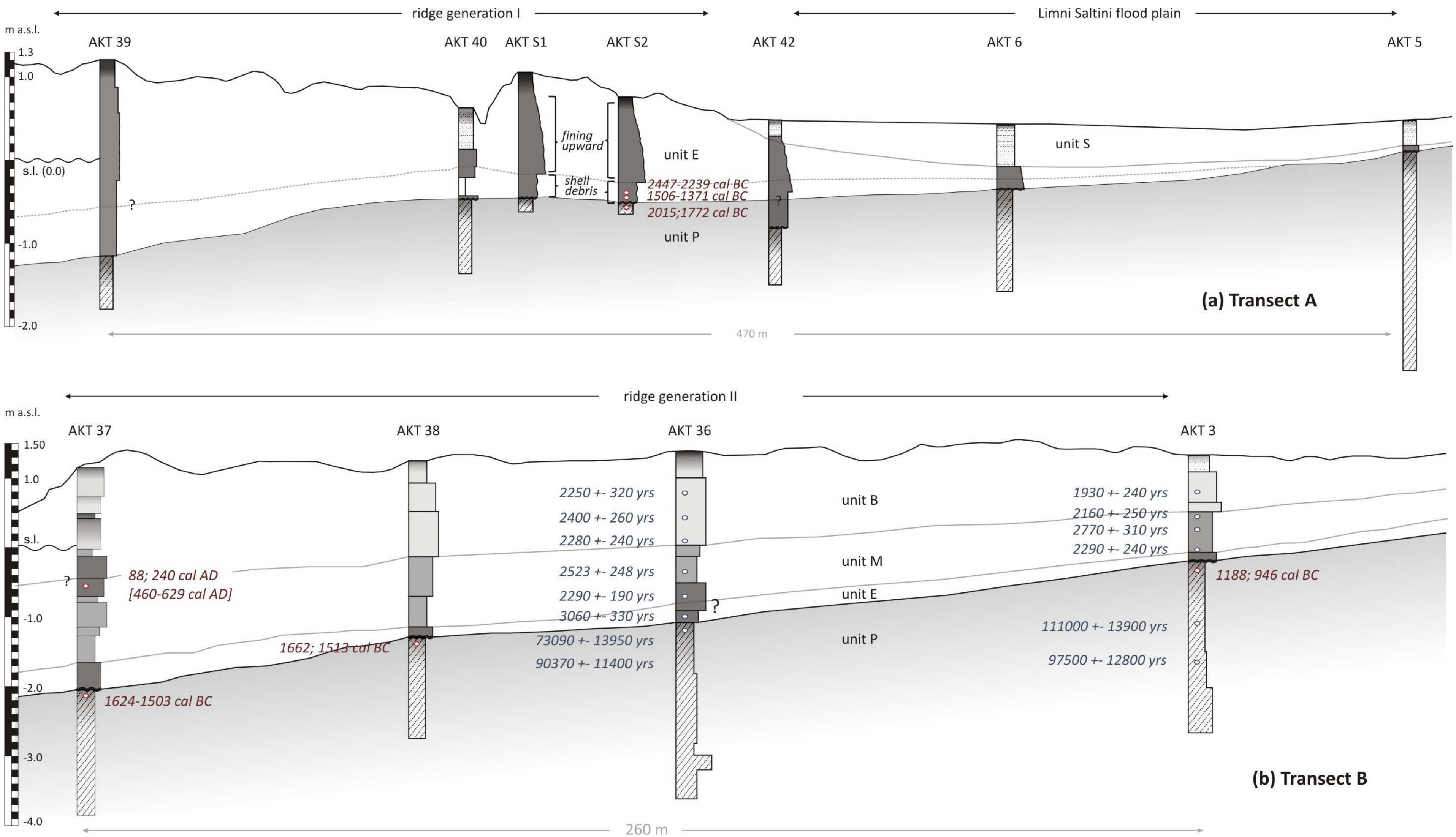

Fig. 3-12: Schematic illustration of vibracore transects A (a) and B (b). Available ^{14}C-AMS-dating results and OSL ages are integrated into the profiles. Overview and location of the vibracore profiles see Fig. 3-13. For Legend see Fig. 3-4.

Altogether, four ^{14}C-AMS datings exist for chronological interpretation of transect B. A plant remain found in core AKT 3, taken from right below the erosional unconformity, yielded an age of 1188; 946 cal BC (sample AKT 3/5 PR, 0.54 m b.s.l.). Two plant remains were taken from a comparable stratigraphical position (AKT 37/14 PR, 2.04 m b.s.l.; AKT 38/8+ PR, 1.65 m b.s.l.) and were dated to 1624-1503 cal BC and 1662; 1513 cal BC. From the overlying marine sequence, a plant remain (sample AKT 37/11 PR, 1.24 m b.s.l.) resulted in a terrestrial calibrated age of 88; 240 cal AD (marine calibrated age 460-629 cal AD).

OSL datings were carried out for parallel cores of vibracores AKT 3 and AKT 36 in order to crosscheck ^{14}C-AMS dating results and obtain depositional ages for both the lower deeply weathered sedimentary unit as well as the upper marine sequence above the erosional unconformity. For both vibracores, OSL dating results prove a Pleistocene age of deposition of the deeply weathered unit below the erosional unconformity, yielding ages between 111.000 +- 13.900 yrs. (AKT 3b OSL 7) and 73.090 +-13.950 yrs (AKT 36b OSL 8). Sedimentation of the marine unit at coring site AKT 3 took place between 2770 +-310 yrs (AKT 3b OSL 3) and 1930 +- 240 yrs (AKT 3b OSL 1), at AKT 36 between 3060 +- 330 yrs (AKT 36b OSL 6) and 2250 +- 320 yrs (AKT 36b OSL 1) (see Table 3-2, appendix D).

Vibracore transect C

Along vibracore transect C (AKT 34, AKT 1, AKT 35 and AKT 50), a comparable stratigraphy to vibracore transects A and B was found (Fig. 3-13a). The erosional unconformity on top of the former surface can be followed along the entire transect and is overlain by event unit E. Towards the west, the depth of this boundary is increasing to 1.03 m b.s.l. (AKT 34), 1.90 m b.s.l. (AKT 1), 3.35 m b.s.l. (AKT 35) and 5.10 m b.s.l. (AKT 50), documenting a westward dipping of the former surface. In contrast to the findings in vibracore transect B, the former surface shows a slightly steeper south-westward dipping. The well sorted sand of unit M is followed by coarser sediments of littoral unit B and, on top of unit B, aeolian unit D. A comparable succession is documented along the entire transect (Fig. 3-13a).

At vibracore transect C, plant remains taken from vibracore profile AKT 35 at 3.64 m b.s.l., just below the erosional unconformity, were dated to 3019-2703 cal BC (AKT 35/15 PR, Table 3-1). Above, an articulated marine mollusc (228-416 cal AD, AKT 35/12 M, 2.51 m b.s.l., Table 3-1) and a sea weed remain taken from 1.11 m b.s.l. (636-763 cal AD, AKT 35/9 PR, Table 3-1) were dated by ^{14}C-AMS. The *terminus ad* or *post quem* of ~ 2800 cal BC for the deposition of the event layer and the following marine sequence (sample AKT 35/15 PR, 3.64 m b.s.l., Table 3-1) is supported by the ^{14}C-AMS dating result of sample AKT 2/9 PR (plant remain, 1.60 m b.s.l., Table 3-1), taken from core AKT 2 some 700 m north of site AKT 35. Sampled from a comparable stratigraphical position, it yielded an age of 2879-2632 cal BC.

The uppermost unit (unit D) of vibracore AKT 35 corresponds to the formation of the adjacent dune field to the west. Here, sediment profile AKT 35 D was prepared some 100 m west of vibracore AKT 35, at the base of a major dune of 5 m elevation a.s.l. The profile was sampled for OSL dating and five OSL ages were obtained for the lower part of the dune. From a chronostratigraphical point of view, the profile can be divided into two units.

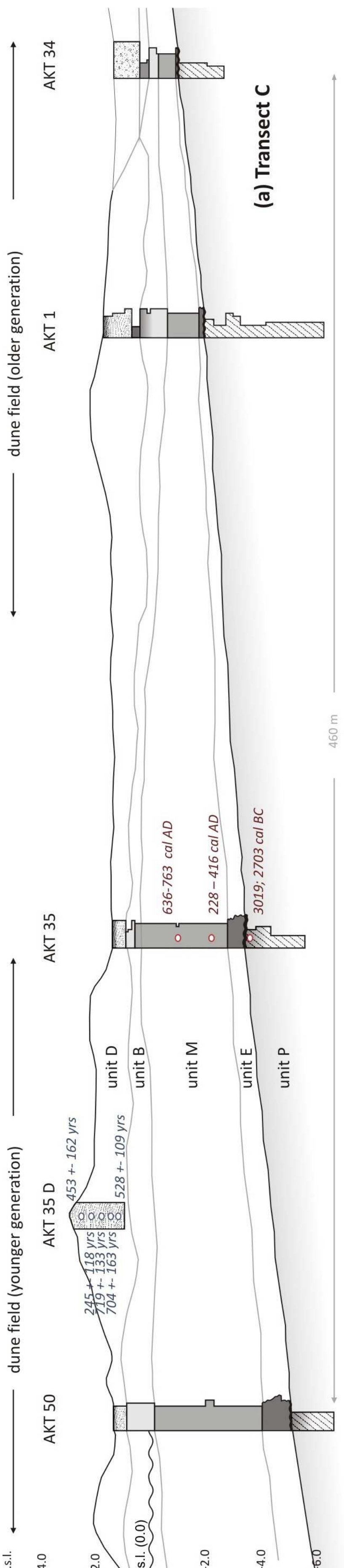

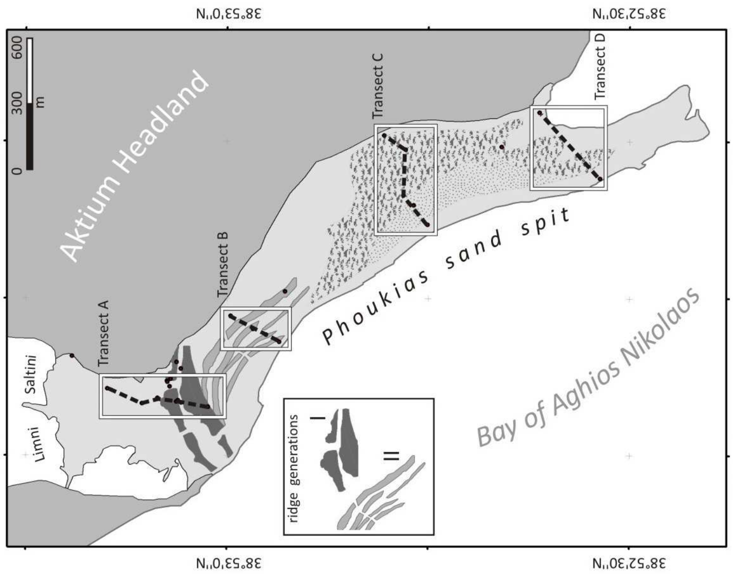

Fig. 3-13: Schematic illustra-tion of vibracore transects C (a) and D (b). Available ^{14}C-AMS-dating results and OSL ages are integrated into the profiles. For legend see Fig. 3-4.

Samples AKT 35 D-1, AKT 35 D-2 and AKT 35 D-3, taken from the lower part of the profile, show slightly older depositional ages of around 700 yrs than the above lying samples AKT 35 D-4 and AKT 35 D-5, showing ages of around 300 yrs (see also Tab. 3-2).

Vibracore transect D

In the southern part of the Phoukias sand spit, vibracore ANI 2 was drilled on top of the sand spit reaching into the Bay of Aghios Nikolaos. With a depth of 18 m b.s., it is the deepest drilling in the study area. Vibracore ANI 14 was brought down east of the extending sand spit close to the steep, westward dipping bedrock slope of southern Aktium Headland. Together with the results of transects B and C, the findings from coring sites ANI 2 and ANI 14 imply a dipping level of the former surface to the south and south-east and a subsurficial slope of the pre-Holocene topography.

For vibracores ANI 2 and ANI 14 nine ^{14}C-AMS datings exist for chronological interpretation. Sample ANI 2/29 M was taken from 16.95 m b.s.l. and proves brackish-lagoonal conditions at 2462-2287 cal BC. An articulated mollusc sampled from the lower part of the shell debris layer (13.20 m b.s.l.) found in vibracore ANI 2 was dated to 238 - 41 cal BC (ANI 2/22+ M). It thus provides a *terminus ad* or *post quem* for the deposition of the shell debris layer and the increase of saltwater influence in the Bay of Aghios Nikolaos. Above the shell debris layer, at 12.59 m b.s.l., a plant remain was dated to 390; 210 cal BC (terrestrial calibrated) or 9-149 cal AD (marine calibrated, ANI 2/21+ PR). Sample ANI 2/16++ PR (sea weed) was taken from 10.00 m b.s.l. and yielded an age of 781-994 cal AD, and sea weed remains from 6.25 m b.s.l. (ANI 2/12+ PR) resulted in an age of 1286-1430 cal AD. The age of sample ANI 2/7+ PR (3.25 m b.s.l.) was determined to 1676; 1954 cal AD. From core ANI 14 an articulated mollusc (*Mytilus* sp.) was sampled at 11.16 m b.s.l. and yielded an age of 5426-5226 cal BC (ANI 14/25 M). At 4.88 m b.s.l. (ANI 14/11+ PR) and 2.89 m b.s.l. (ANI 14/7+ PR) sea weed remains resulted in an age of 90-254 cal AD and 700-874 cal AD, respectively.

3.5 INTERPRETATION AND DISCUSSION

3.5.1 EVENT-INDUCED COASTAL CHANGES – EVIDENCE FOR TSUNAMI OR STORM?

As shown by the presented results, distinct event layers, summarized in sedimentary unit E, were encountered within the sedimentary sequence of several vibracores and sediment profiles in the Phoukias sand spit. At some places, they intercalate sublittoral deposits of long-term morphodynamics; at other places they represent the beginning of the marine sedimentary sequence. For the event units E found in vibracore AKT 35 and sediment profile AKT S2 detailed investigations revealed similar sedimentary characteristics. Unit E is characterized by (i) a clear erosional unconformity at its base, (ii) rip-up-clasts from the underlying sedimentary unit, (iii) a heterogeneous, partly bimodal grain size distribution and a poor sorting, (iv) a shell debris layer in its lower part, which is indicated by a high content of angular mollusc fragments and numerous articulated molluscs, (v) allochthonous microfaunal assemblages, (vi) a fining upward sequence in its upper part, and (vii) a clear thinning landward sequence, in particular in the northern part of the Phoukias spit. Thus, unit E accumulated under high energy morphodynamics and is assumed to be of extreme wave origin. In the following, a detailed discussion of the sedimentary characteristics found for the event layers is carried out to clarify its origin. The interpretation is mainly based on observations of tsunami and storm deposits found around the world.

The documented sedimentary characteristics of unit E represent typical depositional signatures which are generally used for the determination and differentiation of extreme wave events in the geological record (KORTEKAAS & DAWSON 2007, MORTON et al. 2007, SWITZER & JONES 2008a, MAMO et al. 2009). However, several studies on extreme wave event deposits have shown that a number of these signatures occur in both tsunami and storm layers and only confirm the marine origin of the sediment (MORTON et al. 2007, SWITZER & JONES 2008a). Thus, if encountered in a potential event deposit, a single sedimentary feature is not capable to appropriately distinguish between tsunami and storm; i.e. an independent, diagnostic criterion for the determination of the related hydrodynamic process does not exist.

The geochemical characteristics of an event deposit for instance may possibly not differ from the characteristics found for storm deposits or even for sublittoral sediments, accumulated due to constant low energy conditions. Nevertheless, the distribution of distinct elements within a sedimentary sequence provides useful information about the marine influence during its deposition and may trace marine inundation due to an extreme wave event in the geological record (see also CHAGUE-GOFF & GOFF 1999, 2002, FREITAS et al. 2003, NICHOL et al. 2007, VÖTT et al. 2009a). This is true for vibracore profile ANI 2, where a considerable change in geochemical characteristics and facies of the sedimentary sequence is documented for the event-related and subsequent units.

For the study area, microfaunal analyses have been carried out for core AKT 35. In general, the analysis of ostracod, diatom and foraminifera assemblages are capable of estimating the provenance of sediments and its palaeoenvironmental context (HAWKES et al. 2007, RUIZ et al. 2010, MAMO et al. 2009). Open marine species, such as planktonic and/or shelf species, indicate washover events and therefore storm and/or tsunami inundation if found in sediments intercalating the sedimentary sequence in backbeach positions, such as lagoons or paralic swamps (SEDGWICK & DAVIS 2003, TUTTLE et al. 2004, KORTEKAAS & DAWSON 2007, WILLIAMS 2009). However, in many cases, the macro- and microfaunal content of these sediments only proves its marine origin, since the macro- and microfaunal content of an event deposit is a product of its source (SWITZER & JONES 2008a). The foraminiferal assemblage found for the event layer thus does not remarkably differ from the content of the subsequent well sorted sediments of sublittoral origin. Nevertheless, considerable differences are observed in the findings of ostracod communities. Here, only few single individuals could be documented in the event related units, pointing to a rapid sedimentation related to an extreme wave event. In contrast, the overlying units are indicated, as expected, by a well developed, autochthonous ostracod association, showing different states of growth as well as juvenile species. The establishment of sublittoral conditions related to constant, moderated morphodynamics is thus proved for the upper 3.0 m - 3.5 m of the core.

In the study area, the base of unit E is associated with a sharp erosional contact at most investigated sites. Moreover, rip-up clasts were found in unit E at several coring sites. A sharp contact to the underlying unit, which is in most cases represented by the former, pre-event soil and/or a lagoonal surface, is known from both tsunami and storm deposits (NANAYAMA et al. 2000, SEDGWICK & DAVIS 2003, HAWKES et al. 2007, SUGAWARA et al. 2008, WILLIAMS 2009). The occurrence of erosional unconformities, documenting intense erosion of the covered substrate, in most cases is linked to tsunami events, although reports on basal erosion during storm events exist as well (WANG & HORWITZ 2007, WILLIAMS 2009). The strong erosive effects of inundation during extreme wave events involve the detachment of fragments from the underlying material. These so called rip-up clasts are incorporated into the event deposit and are reported to be a prominent feature of tsunami sediments, since they are absent in most investigated storm deposits (MORTON et al. 2007, KORTEKAAS & DAWSON 2007). The presence of rip-up clasts in unit E, as documented for cores AKT 35 and AKT 39 for instance, thus favours the tsunamigenic origin of the event layer. Moreover, intense erosion of the underlying material of unit P is suggested by slightly higher parts of silt and clay found in the lower part of unit E in vibracore AKT 35 and sediment profile AKT S2. Comparable findings have been presented by KORTEKAAS & DAWSON (2007) who investigated event deposits of the 1755 AD Lisbon tsunami in SW Portugal.

The lower part of the event deposit unit E is constituted by a shell debris layer. In general, shell debris layers may be ascribed to both tsunami and storm events (SEDGWICK & DAVIS 2003, FUJIWARA & KAMATAKI 2007, GUTIERRÉZ-MAS et al. 2009, VÖTT et al. 2009a, ENGEL et al. in review), but shell layers related to storm deposits are reported to be organized in thin laminae in most cases (MORTON et al. 2007). However, similar findings compared to the findings in the study area have been presented by NICHOL et al. (2007) from western New Zealand, who assume a tsunamigenic origin of a comparable shell debris unit. Moreover, the results of the taphonomic investigations show remarkable similarities compared to the investigations of DONATO et al. (2008), who carried out taphonomic analysis for known storm and tsunami deposits from the Sur Lagoon, Oman and Caesarea, Israel (see also REINHARDT et al. 2006). For vibracore AKT 35, considerable differences in the taphonomic characteristics of the samples from the event layer (unit E) and the reference sample from the assumed sublittoral unit (unit M) have been found. The shell content in the sediment taken from the assumed event layer was exposed to turbulent flow and high energy wave activity prevailed during deposition, and most of the shell remains from unit E were not exposed to marine abrasion and bio-destructive processes before their deposition. These findings suggest that a long period of reworking of most of the shell fragments from unit E, in contrast to unit M, can be excluded. Moreover, event unit E in sediment profile AKT S2 shows abundant articulated, air-filled molluscs, which were found in *ex-situ* position. It may be assumed that the articulated molluscs were alive during erosion, transport and deposition, pointing to a rapid, event-induced formation of the shell debris layer. Correlations between the lower part of unit E and the Oman tsunami layer (DONATO et al. 2008) are evident, although absolute values differ between the investigated sites. Though assemblages of articulated molluscs are known from storm deposits as well (e.g. BOYAJIAN & THAYER 1994), a tsunamigenic origin of unit E is assumed due to the abundant articulated molluscs and the remarkably high content of angular mollusc fragments within the sediment.

The poor sorting of the unit and the normally graded transition to the subsequent unit indicating declining transport energy during the process of wave inundation clearly document the event character of the unit (see e.g. TUTTLE et al. 2004, HAWKES et al. 2007, KORTEKAAS & DAWSON 2007, NICHOLS 2009, WILLIAMS 2009). In the north-western, ridge-dominated part of the spit, the event unit E constitutes the entire sedimentary sequence of the northernmost ridge of ridge generation I and can be followed up to ~300 m to the north (see Transect A, cores AKT 42, AKT 6, AKT 5). Unit E thus shows a typical thinning landward sequence. The washover-character of the unit is indicated by several fan-like structures as well, extending from the northern side of the older, northernmost ridge generation I. From both storm and tsunami deposits heterogeneous grain size distribution and graded sequences, normal and inverse, are reported (GELFENBAUM & JAFFE 2003, BAHLBURG & WEISS 2006, SUGAWARA et al. 2008, BESONEN et al. 2008, TUTTLE et al. 2004, SEDGWICK & DAVIS 2003, MOORE et al. 2006), and thinning landward sequences are known from both storm and tsunami inundation as well (NANAYAMA et al. 2000, MOORE et al. 2007, WILLIAMS 2009). However, most storm deposits are characterized by a sequence of numerous thin layers or laminae, typically more than 15, consisting of sandy material and showing inverse or normal grading (MORTON et al. 2007, SWITZER & JONES 2008a, WILLIAMS 2009). In contrast, tsunami deposits generally consist of only few subunits (TUTTLE et al. 2004, HAWKES et al. 2007, MORTON et al. 2007, NICHOL et al. 2007, CHOOWONG et al. 2008, NANAYAMA 2008). However, investigations on 2004 Indian Ocean tsunami deposits showed that lamination may also occur in tsunami deposits, especially when backwash deposits contribute to the sequence (PARIS et al. 2007, MORTON et al. 2008). No indication for thin-layered lamination and/or numerous subunits, which would assume a storm origin, could be observed. A tsunamigenic origin is thus assumed.

The deposition of unit E was accompanied by remarkable modifications of coastal configuration and considerable changes of coastal dynamics. It involved (i) the formation of ridge generation I and the related thinning landward unit in the northern part of the Phoukias spit, (ii) the subsequent coastal erosion to the north-west of the recent spit system which was accompanied by erosion of the western part of ridge generation I, (iii) the accumulation of ridge generation II in the central spit area, characterized by a local regression of the sea and (iv) the related formation of the Phoukias spit system, extending into the Bay of Aghios Nikolaos. Event unit E must have accumulated when the Plaka coastline became inactive. It is therefore assumed that the documented events contributed, at least partly, to the destruction of the former Plaka coastline.

As described above, the formation of the ridges in the northern Phoukias area are assumed to be related to the inferred event. In general, the formation of near-coastal ridges is attributed to regressive and/or transgressive littoral dynamics, related to the local morphodynamics and the local relative sea level evolution. However, the stratigraphical architecture of ridge generation I, comprising (i) the distinct shell debris layer with articulated, air filled molluscs, (ii) the subsequent, clear fining upward sequence, and (iii) the fining landward sequence of both units, is not known to be a typical characteristic of beach ridge sediments. Due to the different morphology and the morphological arrangement of both ridge generations, a different dynamic and a different direction of currents must be assumed for the formation of ridge generation I, in contrast to the sequence of ridges comprising ridge generation II. In addition to these findings, the lower part of the fining upward sequence at sediment profile AKT S2 consists of perfectly rounded gravel. At present, the western shore of Aktium Headland and thus the provenance area of the Phoukias spit's sediments is characterized, besides the eroded aeolianite slabs, by sandy deposits (see also *Chapter 2*). In contrast, the entire Lefkada barrier beach and most parts of the beachrock remains are dominated by perfectly rounded gravel, and gravel must be assumed to have dominated grain size along the former Plaka coastline. Therefore it is assumed that the gravel compounds found in unit E of ridge generation I and the related thinning landward sequence represents reworked material of the former Plaka barrier coastline. Ridge generation I is thus assumed to have formed during the inferred tsunami event. Sediments released by the destruction of the Plaka barrier beach were incorporated into the ridges of generation I.

According to VÖTT (2007) and MARKOVIC (2008), local relative sea level in the adjacent area never exceeded its present position during the Holocene. A relative sea level rise of ~ 2 - 3 m within the last 2000 years is evident for several coastal areas in the direct vicinity of the study area (VÖTT 2007). The well developed soil on top of unit E in the northern part of the Phoukias spit (for instance at sediment profile AKT S2) and the overall weathering of the sequence under oxidizing circumstances proves that in this part of the study area unit E was accumulated well above sea level. For the event layers from the northern (AKT S2) and middle part (AKT 35) of the Phoukias sand spit a broad range of typical empirical signatures known from tsunami deposits is evident. Assuming a storm generated formation of the event layers, a higher frequency of comparable units should be expected in the geological record, since several strong winter storms apparently must have taken place within the depositional history of the spit system. Considering (i) the dimension of coastal changes which are assumed to be related to the accumulation of units E, (ii) the sedimentary characteristics of units E in AKT S2 and AKT 35, (iii) the absence of comparable units within the sedimentary record, at least one major tsunami event is documented for the study area.

3.5.2 THE EVOLUTION OF THE PHOUKIAS SAND SPIT – EVIDENCE FOR TSUNAMI-INDUCED COASTAL CHANGES

As discussed above, distinct event layers are documented within the Phoukias sand spit's sedimentary architecture and summarized in unit E. Due to their sedimentary characteristics they are attributed to tsunami impact. A possible correlation and contemporaneous formation may be considered, for instance for event units E in core AKT 35 and sediment profile AKT S2.

According to the available tsunami catalogues, the occurrence of more than one tsunami event in the study area within the considered period of time is likely. For the regarded period of time three tsunami events are reported from the Ionian Sea, all of them related to well known supraregional events which affected large parts of the eastern Mediterranean. These tsunami events are related to (i) the eruption of the Thera volcano (Santorini) at ~1650 cal BC, (ii) the 373 cal BC earthquake in the Corinthian Gulf, and (iii) the 365 cal AD earthquake off western Crete (see also SOLOVIEV et al. 2000, STIROS 2001, STEFANAKIS 2006, VÖTT et al. 2006). According to VÖTT et al. (2006), several local tsunami events must be inferred to have taken place within the considered period of time. In addition to the tsunami catalogues, VÖTT et al. (2006, 2007a, 2008, 2009a, 2009b) report on several late Holocene tsunami impacts on the Bay of Aghios Nikolaos and on the Lefkada Lagoon based on geo-scientific investigations. The best documented events are reported to have taken place at around or after ~1000 BC, at around or after ~300 BC, and at around or after ~400 AD. However, several further tsunami events are assumed to have affected the study area as well - in the Phoukias area for instance at around or after 2400 BC and at ~800

AD, in the Bay of Aghios Nikolaos at ~1000 AD. As to the distinct event layers of unit E, its formation may correspond to either the ~1000 cal BC, the 300 cal BC event or the 400 AD event, which are assumed by the authors to have affected the study area and the adjacent coastal zones.

Tsunami induced coastal changes at ~1000 cal BC

For the northern part of the Phoukias sand spit, the OSL dating results from transect B clearly show Pleistocene depositional ages of the sedimentary base of the spit system (unit P). Deposition of these sediments is assumed to have occurred during the last interglacial. Along vibracore transects A and B the transition of Pleistocene and Holocene sediments is marked by an erosional unconformity followed by tsunamigenic event unit E (for details see *Chapter 3.4.3* and *Chapter 3.5.1*). According to the available ^{14}C-AMS ages (see Tab. 3-1), a former terrestrial surface persisted until at least ~1000 cal BC along transect B, involving the deep weathering of the Pleistocene sediments. Moreover, all ^{14}C-AMS ages from the weathered surface represent *termini ad* or *post quem* for the deposition of event unit E and the onset of marine conditions.

Along transect A, ridge generation I dominates the present morphology and is entirely constituted by event unit E. Since the articulated bivalves taken from event unit E were filled with air during excavation, it may be assumed (i) that the molluscs were alive during transport, (ii) that the obtained ^{14}C-AMS ages represent depositional ages of the sedimentary unit and (iii) that the ^{14}C-AMS ages, keeping in mind the marine reservoir effect, determine the date of the extreme wave event. However, the age of sample AKT S2/9 M (2447; 2239 cal BC) is several hundred years older than the plant remain taken from the underlying former surface (AKT S2/10 PR, 2015; 1772 cal BC), documenting an age inversion. Together with the age of the second articulated mollusc (AKT S2/9+ M, 1506 - 1371 cal BC) it can thus not be assumed that the age of the dated articulated molluscs represent depositional ages of the sedimentary unit and the date of the corresponding event. Therefore, all dates represent *termini post quem* for the deposition of event unit E, and at least some of the articulated molluscs must have been already dead at the time they were eroded, transported and deposited. Assuming a major tsunami impact in the study area at around or shortly after 1000 cal BC as proposed by VÖTT et al. (2008), it is assumed that the deposition of unit E in the northern part of the Phoukias spit and the related formation of ridge generation I corresponds to this event. Moreover, coarse grained sediments of marine origin found in the Lake Voulkaria (JAHNS 2005, VÖTT et al. 2006, 2009b) may correspond to the same tsunami event.

According to the OSL dating results, sedimentation of the marine unit at coring site AKT 3 took place between 2770 +-310 yrs (AKT 3b OSL 3) and 1930 +- 240 yrs (AKT 3b OSL 1), at AKT 36 between 3060 +- 330 yrs (AKT 36b OSL 6) and 2250 +- 320 yrs (AKT 36b OSL 1). Generally, all OSL ages represent maximum ages of deposition, due to the fact that a possible overestimation of the age may occur from incomplete bleaching of the sediment during deposition. Due to different provenance areas of the investigated sediment, each sample may be indicated by different signal characteristics, resulting in different variations of the emitted signals and different error ranges. Further uncertainties may arise from radioactive imbalances and, from a methodological point of view, from the determination of the dose rate, which was performed by sampling a parallel core. However, due to the characteristics of the samples, no indication for incomplete bleaching of the samples was found. Moreover, MURARI et al. (2007) report on pre-depositional zeroing of the luminescence of tsunami laid sands from the 2004 Indian Ocean tsunami, which can be ascribed to constant reworking and bleaching of the near-surface sands mobilized during the event. The available OSL results are thus considered to be reliable. Since bleaching of the sediment during the process of sampling and preparation is excluded, an underestimation of the ages can be excluded either way. Therefore, the deposition of the marine units at coring site AKT 36 started around or after 3060 +- 330 yrs, at site AKT 3 around or after 2770 +-310 yrs.

As shown in Tab. 3-2, age inversions are within error ranges and dating results are consistent. According to these findings, the main period of deposition of the marine sequence can be limited to between ~3300 yrs and ~1700 yrs BP. Assuming a ~ 1000 cal BC event as proposed by the results of sediment profile AKT S2, the OSL ages represent the beginning of marine sedimentation which started immediately after the event and the related deposition of ridge generation I. The ridges of ridge generation II may have formed as a result of the event-induced ingression of the sea, and the onset of (i) erosion at the western shore of Aktium Headland, (ii) southward directed longshore drift, and (iii) littoral activity and ridge accretion in the northern Phoukias area.

The ^{14}C-AMS dating of sample AKT 37/11 PR (1.24 m b.s.l.) yielded a terrestrial calibrated age of 88; 240 cal AD (marine calibrated age 460-629 cal AD). It proves that the upper part of the marine sequence, at least at coring site AKT 37, is younger than ~2000 yrs, which is generally supporting the presented OSL chronology. However, a slight change in morphodynamics may be inferred from coarser grain sizes which are associated to the plant remains of sample AKT 37/11 PR. Thus, a post ~200 AD high-energy wave event, depending on the calibration, may also be considered to have influenced the stratigraphy of transect B.

Regarding the error range of the OSL dating results, it may be interpreted that all datings show similar or at least comparable ages (see also appendix D). Therefore, similar or at least comparable depositional ages of ~2400 - 2200 yrs may be assumed for the entire marine sequence along transect B, which may be explained by either an event-induced accumulation of the entire sequence or a rapid accretion of ridge generation II due to longshore drift. As Table 3-2 and appendix D shows, considerable differences exist (i) between the dose-rate of sample AKT 3b OSL 4 (~1.31 gy/ka) and the dose-rates for samples AKT 3b OSL 1, AKT 3b OSL 2 and AKT 3b OSL 3 (~0.55 – 0.59 gy/ka) and (ii) between the radionuclide values (U, Th, K) of samples AKT 3b OSL 1 and AKT 3b OSL 2 and samples AKT 3b OSL 3, AKT 3b OSL 4 (see appendix D). These differences point to a different provenance of the lower and upper part of the marine sediments in profile AKT 3b and suggest a successive rather than a contemporaneous, episodic deposition of the entire sedimentary sequence. Moreover, a slight diminution of ages to the top is documented for the ages of core AKT 3b. Differences in the provenance area of the sediments comprising the stratigraphy of core AKT 36b must also be inferred from the differences in radionuclide values (see appendix D).

Tsunami induced coastal changes at around or after 300 cal BC

In the southern part of the Phoukias spit, the rising sea level resulted, at least since mid-Holocene, in the establishment of brackish-lagoonal conditions in the Bay of Aghios Nikolaos, while the former terrestrial surface persisted in the northern spit area. Up to now, little is known about the age and evolution of the Plaka remains, protecting the Bay of Aghios Nikolaos from the open Ionian Sea. However, the Plaka is assumed to represent a former shoreline (see also VÖTT et al. 2008; *Chapter 2*). The establishment of the lagoonal environment in the Bay of Aghios Nikolaos was linked to the formation of this former coastline. According to the ^{14}C-AMS dating of sample ANI 14/25 M, taken from the base of vibracore ANI 14, lagoonal conditions have already been established at around 5426-5226 cal BC and are also documented around 2462-2287 cal BC (ANI 2/29 M). In the northern Lefkada Lagoon comparable results date the beginning of lagoonal conditions to the 5th millennium BC (VÖTT et al. 2006, see also *Chapter 2*).

A considerable change in the sedimentary and geochemical characteristics of the sedimentary sequence at coring site ANI 2 is related to the deposition of the normal graded shell debris layer on top of the brackish-lagoonal sequence (13.10 – 13.22 b.s.l.). Above, marine influence on the Bay of Aghios Nikolaos must have significantly increased and considerable environmental changes are assumed to have taken place, which can only be explained by the breakdown of the Plaka coastline. These changes are documented, due to the geochemical investigations, by increased saltwater influence and the subsequent successive onset of higher morphodynamic activity. An articulated mollusc (*Dosinia exoleta*) was sampled from the event-related shell-debris layer in ANI 2 (13.10 - 13.22 m b.s.l.) and yielded an age of 248-41 cal BC. Thus, event unit E is considered to have formed around or after 248-41 cal BC. These findings are supported by the ^{14}C-AMS dating of sample ANI 2/21+ PR, taken some 50 cm above the shell debris layer, which yielded an terrestrial calibrated age of 390; 210 cal BC (marine calibrated age 9-149 cal AD]. The possibly slightly older age may be explained by a probable reworking of the plant material. A contribution of the inferred tsunami event at ~248-41 cal BC to the breakdown of the former Plaka coastline is likely.

The inferred event at around or after 248-41 cal BC (ANI 2/22+ M) fit well to the findings of VÖTT el al. (2006, 2007a, 2008, 2009b), who present several indications for a high energy wave event at around or after ~ 300 cal BC in the investigated and adjacent area. At the western shore of the Lake Voulkaria, a wood fragment taken out of an event-related coarse-clastic layer of marine origin was dated to 405; 204 cal BC. This event layer most likely was deposited in and is restricted to the former Cleopatra channel, which connected the Bay of Aghios Nikolaos and the Lake Voulkaria during antiquity (see VÖTT et al. 2009b for detail). An extreme wave event producing coarse grained deposits at the western shore of the Lake Voulkaria apparently must have affected the investigated area in the southern part of the Phoukias spit. Moreover, previous findings from a small beach at the northern shore of the inner Bay of Aghios Nikolaos suggest a high energy wave impact after 557–395 cal BC and a subsequent reduction of wave dynamics in the Bay of Aghios Nikolaos (VÖTT et al. 2008). These findings may be explained by the inferred post 300 cal BC tsunami and the subsequently beginning advance of the Phoukias spit, which is corresponding to the beginning of increased morphodynamics at vibracore site ANI 2 and involved the related wave protection in the inner part of the bay.

Marine conditions, due to the north-southward direction of sediment transport, continued for a longer period of time than in the northern part (Transects C and D). In vibracore transect D, the sedimentary sequence points to a successive, gradual change of coastal morphodynamics from wave-unaffected, clayey to silty units (deeper-water, distal to the spit front) to sand-dominated units (sublittoral and littoral, shallow water, proximal to the spit front). The related gradual shift of morphodynamic conditions is dated to the end of the first millennium AD and thus, typical for an advancing sand spit, post-dates the onset in the northern spit area. Afterwards, high sedimentation rates can be inferred at coring site ANI 2 which is expressed in successively increasing grain sizes and lamination of the sediments in the middle part of the core. Regarding the position of vibracore ANI 2, the deposition of this unit can be attributed to the advancing spit formation and its extension into the Bay of Aghios Nikolaos. At site ANI 14 datings do not show comparable high sedimentation rates. Here, due to the adjacent outcropping bedrock, littoral conditions took place after or at around ~800 cal AD (ANI 14/7+ PR). At the same time, shallow water conditions led to the deposition of the laminated unit in core ANI 2. In the very southern part of the spit, sediment accretion and spit formation, which formed the southern spit extension stretching into the Bay of Aghios Nikolaos proceeded during medieval and modern times and is still going on.

According to VÖTT et al. (2007a), the changing morphodynamic conditions documented for cores ANI 2 and ANI 14 and especially the incipient occurrence of sea weed layers in the sedimentary record of core ANI 2 (above ~11 m b.s.l.) may also be related to a younger high energy wave event at around 300 cal AD, which involved the breakdown of the Plaka coastline. However, due to the sedimentary results presented in this study, increased marine influence and thus the breakdown of the Plaka coastline is assumed to have taken place earlier, at ~300 – 200 cal BC. The related change of environmental conditions was accompanied by a considerable increase in sediment accumulation rates and may also be responsible for the inferred changes of morphodynamic activity in cores ANI 2 and ANI 14.

Evidence for a tsunami event from the central part of the Phoukias sand spit

Further to the south, at transect C, the former terrestrial surface (unit P) persisted until at least ~2700 cal BC (AKT 35/15 PR: 3019 –2703 cal BC, also AKT 2/9 PR: 2879-2632 cal BC). The ages serve as a *termini ad* or *post quem* for the deposition of tsunamigenic event unit E, which is unconformably covering unit P. For transect C, an articulated marine mollusc (AKT 35/12 M: 228 – 416 cal AD) and a sea weed remain (AKT 35/9 PR: 636-763 cal AD), taken from a sequence of well sorted fine sand (unit M), point to regular sublittoral conditions since at least ~300 cal AD. The possibly similar age of the upper sample may be explained due to reworking of the plant remains. For the deposition of unit E, the age represents a *terminus ante quem* as well – the ~300 cal BC event, which was found for the southern part of the spit, can be assumed to have triggered the deposition of the event unit E along vibracore transect C. Regarding the well sorted sand in the upper part of sediment profile AKT S2, which is interpreted to be part of the event unit, the exact determination of the upper limit of unit E in vibracore AKT 35 is difficult. It thus may be assumed that parts of the well sorted sand above the shell debris layer and the subsequent normal graded sequence also belong to event unit E. In this case, it may be possible that the obtained age of ~300 cal AD represents a *terminus ad* or *post quem* for unit E. A younger event around or after 300 cal AD thus cannot be excluded to be responsible for the deposition of unit E at coring site AKT 35 and along vibracore transect C. However, the evolution of autochthonous ostracod associations at coring site AKT 35 is proved for the upper 3 m of the sedimentary sequence and is assumed to be related to the establishment of normal, sublittoral conditions. Indication of a developing autochthonous ostracod association can already be inferred from the increasing number of ostracod species found for the lower part of the well sorted fine sand. Moreover, taphonomic investigations document differences between the event unit E and the subsequent well sorted sands of unit M (sample AKT 35/11, ~3.39 m b.s./2.04 m b.s.l.). Thus, an event-related formation of the well sorted fine sand covering unit E must be doubted and a *terminus ante quem* of ~300 cal AD is assumed for the deposition of unit E.

OSL datings of a dune profile close to vibracore AKT 35 in the western part of transect C suggest a maximum age of ~700 yrs for the presently active dune field in the middle part of the Phoukias sand spit. The lower part of the dune (AKT 35 D OSL-1, AKT 35 D OSL-2 and AKT 35 D OSL-3) seems to be slightly older than the upper part of the dune (AKT 35 D- OSL 4 and AKT 35 D- OSL 5), showing ages of around 300 yrs. Therefore it can be assumed that (i) dune formation started shortly before, around or after ~700 yrs, (ii) aeolian deposition, at least at site AKT 35 D, may be reactivated at around 300 yrs and (iii) marine conditions at transect C must have ended some time before 1300 AD (700 yrs), most likely due to the accretional formation of the Phoukias sand spit.

According to the presented dating results, the Phoukias sand spit formed during the last ~3000 years. Since the existence of the Plaka coastline would not allow the formation of an accretional sand spit in the lagoonal area to the east, the Phoukias sand spit did not exist at the time when the Plaka represented an active littoral system. Initiation of the spit's formation must have taken place subsequent to the destruction of the Plaka and the related shifting of the coastline. It thus can be concluded, that the Plaka represented an active littoral system until at least and became inactive after ~1000 BC. Coastal configuration in the area of the Bay of Aghios Nikolaos thus must have considerably changed since middle Holocene.

The succession of different facies within the sedimentary architecture of the Phoukias sand spit reflects its geomorphodynamic evolution. Distinct event units have been found in several investigated cores and sediment profiles and show comparable or even similar sedimentary characteristics, which point to a tsunamigenic origin (see *Chapter 3.5.1*). Therefore, the presented sedimentary sequence documents the interplay of both long-term morphodynamics and high-energy wave impacts. Due to the available dating results it must be assumed that at least two, probably three tsunami events contributed to the evolution of the Phoukias sand spit. Moreover, the presented findings indicate that at least one of the encountered tsunami events triggered the breakdown of the Plaka coastline.

In this context, discrepancies exist between the northern and southern part of the spit; whereas dating results of core ANI 2 point to a breakdown of the Plaka coastline and a related increase of marine influence on the Bay of Aghios Nikolaos at around or after ~300 cal BC, the formation of ridge generation I in the northern part of the spit (sediment profile AKT S2 and adjacent cores) and therefore a first marine inundation of the Phoukias area and a related disturbance of the

Plaka coastline must have occurred at around 1000 cal BC. Although the formation of event unit E at coring site AKT 35 and vibracore transect C in the central part of the spit may be attributed to a post 300 cal AD event, the triggering event here may be the post 300 cal BC event as well. Further (later) sedimentary changes in the subsequent sedimentary sequence, such as the presence of shell-rich sands in the southern spit area (ANI 2 and ANI 14, AKT 37), must relate to past morphodynamic changes as well – whether these changes have been induced by long-term littoral processes, such as a changing sediment supply and gradual sediment accretion, by tectonic subsidence or by the short-term effects of storms and/or tsunami events, as proposed by Vött et al. (2008), cannot be clarified (see also *Chapter 2)*.

3.6 CONCLUSIONS

Detailed geo-scientific investigations on the evolution of the Phoukias sand spit in SE Aktium Headland have been carried out. According to the presented results, the following can be concluded:

a) The Phoukias sand spit in south-western Aktium Headland represents an excellent geological archive. Its sedimentary architecture and morphological pattern store comprehensive information about the evolution of the Bay of Aghios Nikolaos and the former, north-eastern part of the Lefkada barrier beach system. Both long-term morphodynamics and high-energy wave impacts contributed to the formation of the Phoukias sand spit.

b) The study area was affected by remarkable coastal changes within the last 3000 years. Several phases of the coastal system's evolution can be reconstructed. These coastal changes involved (i) the breakdown of the former Plaka coastline, (ii) the onset of (open) marine conditions in the Bay of Aghios Nikolaos, and (iii) the formation of the Phoukias sand spit.

c) Within the stratigraphical sequence of the sand spit, distinct event layers were detected. A broad range of typical empirical signatures known to be characteristic for tsunami deposits is evident for the documented event units. A tsunamigenic origin of the investigated event layers is thus assumed.

d) At several sites, event deposits mark the beginning of changing morphodynamics. Therefore, at least two, probably three tsunami events considerably contributed to the coastal changes in the study area. Tsunami events are assumed to have taken place at ~1000 cal BC, at ~300 cal BC. A possible younger event occurred at ~ 300 cal AD.

In general, it can be concluded that

e) Comprehensive geo-scientific investigations and sedimentary analysis are important for the detection, the differentiation and the interpretation of event deposits. More studies on extreme wave event deposits are needed to improve knowledge and comparability. Apart from that, the palaeogeographical context helps to interpret the succession of the sedimentary sequence. Therefore, palaeo-event research should be linked to palaeoenvironmental investigations.

f) The dating of event deposits exhibits considerable difficulties. ^{14}C-AMS-datings of organic material in most cases represent *termini ante*, *ad* or *post quem* for the deposition of event layers, depending on the stratigraphical relation the material was sampled. Numerous datings are thus needed to narrow the time of deposition of event layers. In this study, reliable OSL ages helped to establish a local chronology of the Phoukias spit's sedimentary architecture. In combination with ^{14}C-AMS datings, OSL datings of sediment cores provide useful information about the depositional ages of (event-related) marine sediments. However, several restrictions and difficulties remain, which are partly ascribed to methodological problems.

g) Besides relative sea level evolution and gradual coastal processes, extreme wave events and in particular tsunami events are an important factor in coastal evolution and may contribute to coastal changes in general.

3.7 REFERENCES

Ad-hoc-Arbeitsgruppe Boden der Staatlichen Geologischen Dienste und der Bundesanstalt für Geowissenschaften und Rohstoffe (Ed.) (2005). *Bodenkundliche Kartieranleitung*. Stuttgart, 438 pp.

Bahlburg, H. & Weiss, R. (2007). Sedimentology of the December 26, 2004, Sumatra tsunami deposits in eastern India (Tamil Nadu) and Kenya. *International Journal of Earth Sciences,* 96(6), 1195-1209.

Bard, E., Hamelin, B., Arnold, M., Montaggioni, L., Cabioch, G., Faure, G. & Rougerie, F. (1996). Deglacial sea-level record from Tahiti corals and the timing of global meltwater discharge. *Nature*, 382, 241-244.

Beck, R., Burger, D. & Pfeffer, K.-H. (1995): Laborskript. *Kleinere Arbeiten aus dem Geographischen Institut der Universität Tübingen*, 11.

Benetatos, C., Kiratzi, A., Roumelioti, Z., Stavrakakis, G., Drakatos, G. & Latoussakis, I. (2005). The 14 August 2003 Lefkada Island (Greece) earthquake: Focal mechanisms of the mainshock and of the aftershock sequence. *Journal of Seismology,* 9, 171–190.

Besonen, M. R. (1997). *The Middle and Late Holocene Geology and Landscape Evolution of the Lower Acheron River Valley, Epirus, Greece.* M.Sc. thesis, University Of Minnesota.

Besonen, M.R., Bradley, R.S., Mudelsee, M., Abbott, M.B. & Francus, P. (2008). A 1,000-year, annually-resolved record of hurricane activity from Boston, Massachusetts. *Geophysical Research Letters,* 35, L14705.

Blott, S.J. & Pye, K. (2001). GRADISTAT: a grain size distribution and statistics package for the analysis of unconsolidated sediments. *Earth Surface Processes and Landforms*, 26, 1237-1248.

Boyajian, G.E. & Thayer, C.W. (1995). Clam Calamity: A Recent Supratidal Storm-Deposit as an Analog for Fossil Shell Beds. *Palaios*, 10(5), 484-489.

Brückner, H., Kelterbaum, D., Marunchak, O., Porotov, A. & Vött, A. (in press). The Holocene sea level story since 7500 BP – Lessons from the Eastern Mediterranean, the Black and the Azov Seas. *Quaternary International*, doi:10.1016/j.quaint.2008.11.016.

Chagué-Goff, C. & Goff, J.R. (1999). Geochemical and sedimentological signature of catastrophic salt water inundations (tsunami), New Zealand. *Quaternary Australia*, 17, 38-48.

Chagué-Goff, C., Dawson, S., Goff, J.R., Zachariasen, J., Berryman, K.R., Garnett, D.L., Waldron, H.M. & Mildenhall, D.C. (2002). A tsunami (ca. 6300 years BP) and other Holocene environmental changes, northern Hawke's Bay, New Zealand. *Sedimentary Geology*, 150(1-2), 89-102.

Choowong, M., Murakoshi, N., Hisada, K.-i., Charusiri, P., Charoentitirat, T., Chutakositkanon, V., Jankaew, K., Kanjanapayont, P. & Phantuwongraj, S. (2008). 2004 Indian Ocean tsunami inflow and outflow at Phuket, Thailand. *Marine Geology*, 248(3-4), 179-192.

Cocard, M., Kahle, H.-G., Peter, Y., Geiger, A., Veis, G., Felekis, S., Paradissis, D. & Billiris, H. (1999). New constraints on the rapid crustal motion of the Aegean region: recent results inferred from GPS measurements (1993–1998) across the West Hellenic Arc, Greece. *Earth and Planetary Science Letters,* 172, 39–47.

Coch, N.K. (1994). Geologic effects of hurricanes. *Geomorphology*, 10(1-4), 37-63.

Dawson, A.G. (1996). The Geological Significance of Tsunamis. *Zeitschrift für Geomorphologie N.F. Suppl. Vol.*, 102, 199-210.

Dawson, A.G. & Stewart, I. (2007). Tsunami deposits in the geological record. *Sedimentary Geology*, 200(3-4), 166-183.

Dominey-Howes, D.T.M., Humphreys, G.S. & Hesse, P.P. (2006). Tsunami and palaeotsunami depositional signatures and their potential value in understanding the late-Holocene tsunami record. *The Holocene*, 16(8), 1095-1107.

Donato, S.V., Reinhardt, E.G., Boyce, J.I., Rothaus, R. & Vosmer, T. (2008). Identifying tsunami deposits using bivalve shell taphonomy. *Geology*, 36(3), 199-202.

Engel, M., Knipping, M., Brückner, H., Kiderlen, M., & Kraft, J.C. (2009). Reconstructing middle to late Holocene palaeogeographies of the lower Messenian plain (southwestern Peloponnese, Greece): Coastline migration, vegetation history and sea level change. *Palaeogeography, Palaeoclimatology, Palaeoecology*, 284(3-4), 257-270.

Engel, M., Brückner, H., Wennrich, V., Scheffers, A., Kelletat, D., Vött, A., Schäbitz, F., Daut, G., Willershäuser, T. & May, S.M. (in review). The back-barrier record of eastern Bonaire (Netherlands Antilles): new insights into the palaeo-tsunami history of the southern Caribbean.

Fairbanks, R.G. (1989). A 17,000-year glacio-eustatic sea level record: influence of glacial melting rates on the Younger Dryas event and deep-ocean circulation. *Nature,* 342, 637-642.

Foster, D.L., Dawson, A.G., Dawson, S., Lees, J.A. & Mansfield, L. (1993). Tsunami Sedimentation Sequences In The Scilly Isles, South-West England. *Science of Tsunami Hazards,* 11(1), 35-45.

Freitas, M., Andrade, C., Rocha, F., Tassinari, C., Munha, J.M., Cruces, A., Vidinha, J. & Marques da Silva, C. (2003). Lateglacial and Holocene environmental changes in Portuguese coastal lagoons 1: the sedimentological and geochemical records of the Santo Andre coastal area. *The Holocene,* 13(3), 433-446.

Fujiwara, O. & Kamataki, T. (2007). Identification of tsunami deposits considering the tsunami waveform: An example of subaqueous tsunami deposits in Holocene shallow bay on southern Boso Peninsula, Central Japan. *Sedimentary Geology*, 200, 295–313.

Gelfenbaum, G. & Jaffe, B. (2003). Erosion and Sedimentation from the 17 July, 1998 Papua New Guinea Tsunami. *Pure and Applied Geophysics,* 160, 1969–1999.

Goff, J., McFadgen, B.G. & Chagué-Goff, C. (2004). Sedimentary differences between the 2002 Easter storm and the 15th-century Okoropunga tsunami, southeastern North Island, New Zealand. *Marine Geology*, 204, 235-250.

Gutiérrez-Mas, J.M., Juan, C. & Morales, J.A. (2009). Evidence of high-energy events in shelly layers interbedded in coastal Holocene sands in Cadiz Bay (south-west Spain). *Earth Surface Processes and Landforms,* 34, 810–823.

Handl, M., Mostafawi, N. & Brückner, H. (1999). Ostracodenforschung als Werkzeug der Paläogeographie. *Marburger Geographische Schriften,* 134, 116-153.

Hawkes, A.D., Bird, M., Cowie, S., Grundy-Warr, C., Horton, B.P., Hwai, A.T.S., Law, L., Macgregor, C., Nott, J., Ong, J.E., Rigg, J., Robinson, R., Tan-Mullins, M., Sa, T.-T., Yasin, Z. & Aik, L.W. (2007). Sediments deposited by the 2004 Indian Ocean Tsunami along the Malaysia–Thailand Peninsula. *Marine Geology,* 242, 169–190.

Hellenic Military Geographical Service (HMGS) (1987). TM 1:50.000, sheet Vonitsa.

Hellenic Navy Hydrographic Service (HNHS) (1983). Bathymetrical chart 1:50.000, sheet Amvrakikos Gulf.

Jahns, S. (2005). The Holocene history of vegetation and settlement at the coastal site of Lake Voulkaria in Acarnania, western Greece. *Vegetation History and Archaeobotany,* 14, 55-66.

Köhn, M. (1928): Bemerkungen zur mechanischen Bodenanalyse. III. Ein neuer Pipettierapparat. *Journal of Plant Nutrition and Soil Science*, 11(1), 50-54.

Kokinou, E., Papadimitriou, E., Karakostas, V., Kamberis, E. & Vallianatos, F. (2006). The Kefalonia Transform Zone (offshore Western Greece) with special emphasis to its prolongation towards the Ionian Abyssal Plain. *Marine Geophysical Researches,* 27(4), 241-252.

Kortekaas, S. (2002). *Tsunamis, storms and earthquakes: Distinguishing coastal flooding events.* Unpublished PhD thesis, Coventry University.

Kortekaas, S. & Dawson, A.G. (2007). Distinguishing tsunami and storm deposits: An example from Martinhal, SW Portugal. *Sedimentary Geology,* 200, 208–221.

Kraft, J.C., Kayan, İ. & Erol, O. (1980). Geomorphic Reconstructions in the Environs of Ancient Troy. *Science*, 209, 776-782.

Liew, S.C., Gupta, A., Wong, P.P. & Kwoh, L.K. (2010). Recovery from a large tsunami mapped over time: The Aceh coast, Sumatra. *Geomorphology*, 114(4), 520-529.

Louvari, E., Kiratzi, A.A. & Papazachos, B.C. (1999). The Cephalonia Transform Fault and its extension to western Lefkada Island (Greece). *Tectonophysics*, 308, 223-236.

Mamo, B., Strotz, L. & Dominey-Howes, D. (2009). Tsunami sediments and their foraminiferal assemblages. *Earth-Science Reviews*, 96(4), 263-278.

Marković, M. (2008). *Untersuchungen zu Neotektonik und relativen Meeresspiegelschwankungen im Holozän zwischen Leukas und Preveza (Nordwestgriechenland) auf der Grundlage von Küstensedimenten und geoarchäologischen Befunden*. Unpublished diploma thesis, Philipps-Universität Marburg.

May, S.M. (2006). *Szenarien zur Palaäogegraphie der Küstenebene von Mytikas (Akarnanien, Nordwestgriechenland) – Ursachen und Folgen des holozänen Küstenwandels*. Unpublished diploma thesis, Philipps-Universität Marburg.

May, S.M., Vött, A., Brückner, H. & Brockmüller, S. (2007). Evidence of tsunamigenic impact on Actio headland near Preveza, NW Greece. *Coastline Reports*, 9, 115-125.

May, S.M., Vött, A., Sakellariou, D., Kapsimalis, V., Herd, R. & Brückner, H. (2008). On- and offshore tsunami traces around Actio Headland (NW Greece). *Geophysical Research Abstracts*, 10, EGU2008-A-11034.

Moore, A., Nishimura, Y., Gelfenbaum, G., Kamataki, T. & Triyono, R. (2006). Sedimentary deposits of the 26 December 2004 tsunami on the northwest coast of Aceh, Indonesia. *Earth, Planets and Space*, 58, 253–258.

Moore, A.L., McAdoo, B.G. & Ruffman, A. (2007). Landward fining from multiple sources in a sand sheet deposited by the 1929 Grand Banks tsunami, Newfoundland. *Sedimentary Geology,* 200, 336–346.

Morton, R.A. & Sallenger Jr., A.H. (2003). Morphological Impacts of Extreme Storms on Sandy Beaches and Barriers. *Journal of Coastal Research*, 19(3), 560-573.

Morton, R.A., Gelfenbaum, G. & Jaffe, B.E. (2007). Physical criteria for distinguishing sandy tsunami and storm deposits using modern examples. *Sedimentary Geology*, 200, 184–207.

Morton, R.A., Goff, J.R., & Nichol, S.L. (2008). Hydrodynamic implications of textural trends in sand deposits of the 2004 tsunami in Sri Lanka. *Sedimentary Geology,* 207(1-4), 56-64.

Murari, M.K., Achyuthan, H. & Singhvi, A.K. (2007). Luminescence studies on the sediments laid down by the December 2004 tsunami event: Prospects for the dating of palaeo tsunamis and for the estimation of sediment fluxes. *Current Science*, 92(3), 367-371.

Murray, A.S. & Wintle, A.G. (2000). Luminescence dating of quartz using an improved single-aliquot regenerative-dose protocol. *Radiation Measurements*, 33, 57-73.

Murray, J.W. (2006). *Ecology and Applications of Benthic Foraminifers*. Cambridge, 439 pp.

Nanayama, F. (2008). Sedimentary Characteristics and Depositional Processes of Onshore Tsunami Deposits: An Example of Sedimentation Associated with the 12 July 1993 Hokkaido-Nansei-oki Earthquake Tsunami. In: Shiki, T., Tsuji, Y., Yamazaki, T. & Minoura, K. (eds.), *Tsunamiites*. Amsterdam, 63-80.

Nanayama, F., Shigeno, K., Satake, K., Shimokawa, K., Koitabashi, S., Miyasaka, S. & Ishii, M. (2000). Sedimentary differences between the 1993 Hokkaido-nansei-oki tsunami and the 1959 Miyakojima typhoon at Taisei, southwestern Hokkaido, northern Japan. *Sedimentary Geology*, 135(1-4), 255-264.

National and Atmospheric Administration (NASA) (2006). SRTM elevation data. http://www2.jpl.nasa.gov/srtm/.01/2006.

Nichol, S.L., Goff, J.R., Devoy, R.J.N., Chagué-Goff, C., Hayward, B. & James, I. (2007). Lagoon subsidence and tsunami on the West Coast of New Zealand. *Sedimentary Geology*, 200, 248–262.

Nichols, G. (2009). *Sedimentology and Stratigraphy*. Chichester, Hoboken, 419 pp.

Nott, J. (1997). Extremely high-energy wave deposits inside the Great Barrier Reef, Australia: determining the cause - tsunami or tropical cyclone. *Marine Geology*, 141, 193-207.

Papadopoulos, G.A., Karastathis, V.K., Ganas, A., Pavlides, S., Fokaefs, A. & Orfanogiannaki, K. (2003). The Lefkada, Ionian Sea (Greece), Shock, (Mw 6.2) of 14 August 2003: Evidence for the Characteristic Earthquake from Seismicity and Ground failures. *Earth, Planets and Space*, 55, 713-718.

Papazachos, B.C. & Dimitriu, P.P. (1991). Tsunamis In and Near Greece and Their Relation to the Earthquake Focal Mechanisms. *Natural Hazards*, 4, 161-170.

Paris, R., Lavigne, F., Wassmer, P. & Sartohadi, J. (2007). Coastal sedimentation associated with the December 26, 2004 tsunami in Lhok Nga, west Banda Aceh (Sumatra, Indonesia). *Marine Geology*, 238, 93-106.

Paris, R., Wassmer, P., Sartohadi, J., Lavigne, F., Barthomeuf, B., Desgages, E., Grancher, D., Baumert, P., Vautier, F., Brunstein, D. & Gomez, C. (2009). Tsunamis as geomorphic crises: Lessons from the December 26, 2004 tsunami in Lhok Nga, West Banda Aceh (Sumatra, Indonesia). *Geomorphology*, 104(1-2), 59-72.

Preusser, F., Degering, D., Fuchs, M., Hilgers, A., Kadereit, A., Klasen, N., Krbetschek, M., Richter, D. & Spencer, J.Q.G. (2008). Luminescence dating: basics, methods and applications. *Eiszeitalter und Gegenwart/Quaternary Science Journal,* 57(1-2), 95-149.

Reimer, P.J. & McCormac, F.G. (2002). Marine Radiocarbon Reservoir Corrections for the Mediterranean and Aegean Seas. *Radiocarbon*, 44(1), 159–166.

Reimer, P.J, Baillie, M.G.L., Bard, E., Bayliss, A., Beck, J.W., Blackwell, P.G., Bronk Ramsey, C., Buck, C.E., Burr, G.S., Edwards, R.L., Friedrich, M., Grootes, P.M., Guilderson, T.P., Hajdas, I., Heaton, T.J., Hogg, A.G., Hughen, K.A., Kaiser, K.F., Kromer, B., McCormac, F.G., Manning, S.W., Reimer, R.W., Richards, D.A., Southon, J.R., Talamo, S., Turney, C.S.M., van der Plicht, J. & Weyhenmeyer, C.E. (2009). IntCal09 and Marine09 Radiocarbon Age Calibration Curves, 0–50,000 Years cal BP. *Radiocarbon*, 51, 1111-1150.

Reinhardt, E.G., Goodman, B.N., Boyce, J.I., Lopez, G., van Hengstum, P., Rink, W.J., Mart, Y. & Raban, A. (2006). The tsunami of 13 December A.D. 115 and the destruction of Herod the Great's harbor at Caesarea Maritima, Israel. *Geology,* 34(12), 1061-1064.

Ruiz, F., Abad, M., Cáceres, L.M., Rodríguez Vidal, J., Carretero, M.I., Pozo, M. & González-Regalado, M.-L. (2010). Ostracods as tsunami tracers in Holocene sequences. *Quaternary Research,* 73(1), 130-135.

Sachpazi, M., Hirn, A., Clément, C., Haslinger, F., Laigle, M., Kissling, E., Charvis, P., Hello, Y., Lépine, J. C., Sapin, M. & Ansorge, J. (2000). Western Hellenic subduction and Cephalonia Transform: local earthquakes and plate transport and strain. *Tectonophysics,* 319(4), 301–319.

Satake, K. & Atwater, B.F. (2007). Long-Term Perspectives on Giant Earthquakes and Tsunamis at Subduction Zones. *Annual Review of Earth and Planetary Sciences,* 35(1), 349-374.

Scheffers, A. & Kelletat, D. (2001). Hurricanes and Tsunamis - Dynamik und küstengestaltende Wirkungen. *Bamberger Geographische Schriften*, 20, 29-53.

Sedgwick, P.E. & Davis, R.A. (2003). Stratigraphy of washover deposits in Florida: implications for recognition in the stratigraphic record. *Marine Geology,* 200(1-4), 31-48.

Soloviev, S.L. (1990). Tsunamigenic Zones in the Mediterranean Sea. *Natural Hazards*, 3, 183-202.

Soloviev, S.L., Solovieva, O.N., Go, C.N., Kim, K.S. & Shchetnikov, N.A. (2000). *Tsunamis in the Mediterranean Sea 2000 B.C.-2000 A.D.* Dordrecht.

Stanley, D.J. & Warne, A.G. (1994). Worldwide Initiation of Holocene Marine Deltas by Deceleration of Sea-Level Rise. *Science,* 265, 228-231.

Stefanakis, M.I. (2006). Natural Catastrophes in the Greek and Roman World: Loss or Gain? Four Cases of Seaquake-Generated Tsunamis. *Mediterranean Archaeology and Archaeometry,* 6*(*1), 61-88.

Stiros, S.C. (2001). The AD 365 Crete earthquake and possible seismic clustering during the fourth to sixth centuries AD in the Eastern Mediterranean: a review of historial and archaeological data. *Journal of Structural Geology*, 23, 545-562.

Sugawara, D., Minoura, K. & Imamura, F. (2008). Tsunamis and Tsunami Sedimentology. In: Shiki, T., Tsuji, Y., Yamazaki, T. & Minoura, K. (eds.), *Tsunamiites*. Amsterdam, 9-49.

Switzer, A.D. & Jones, B.G. (2008a). Large-scale washover sedimentation in a freshwater lagoon from the southeast Australian coast: sea-level change, tsunami or exceptionally large storm? *The Holocene*, 18(5), 787-803.

Switzer, A.D. & Jones, B.G. (2008b). Setup, Deposition, and Sedimentary Characteristics of Two Storm Overwash Deposits, Abrahams Bosom Beach, Southeastern Australia. *Journal of Coastal Research*, 24(1A), 189-200.

Switzer, A.D., Pucillo, K., Haredy, R.A., Jones, B.G. & Bryant, E.A. (2005). Sea Level, Storm, or Tsunami: Enigmatic Sand Sheet Deposits in a Sheltered Coastal Embayment from Southeastern New South Wales, Australia. *Journal of Coastal Research,* 21(4), 655–663.

Tuttle, M.P., Ruffman, A., Anderson, T. & Jeter, H. (2004). Distinguishing Tsunami from Storm Deposits in Eastern North America: The 1929 Grand Banks Tsunami versus the 1991 Halloween Storm. *Seismological Research Letters,* 75(1), 117-131.

U.S. Geological Survey (USGS) (2006). Earth Resources Observation & Science (EROS). Aster satellite data. http://edc.usgs.gov.01/2006.

Vött, A. (2007). Relative sea level changes and regional tectonic evolution of seven coastal areas in NW Greece since the mid-Holocene. *Quaternary Science Reviews,* 26, 894–919.

Vött, A., May, M., Brückner, H. & Brockmüller, S. (2006). Sedimentary Evidence of Late Holocene Tsunami Events near Lefkada Island (NW Greece). *Zeitschrift für Geomorphologie N.F. Suppl. Vol.*, 146, 139-172.

Vött, A., Brückner, H., May, M., Lang, F. & Brockmüller, S. (2007a). Late Holocene tsunami imprint at the entrance of the Ambrakian gulf (NW Greece). *Mediterranée,* 108, 43-57.

Vött, A., Schriever, A., Handl, M. & Brückner, H. (2007b). Holocene Palaeogeographies of the Eastern Acheloos River Delta and the Lagoon of Etoliko (NW Greece). *Journal of Coastal Research*, 23(4), 1042-1066.

Vött, A., Brückner, H., May, M., Lang, F., Herd, R. & Brockmüller, S. (2008). Strong tsunami impact on the Bay of Aghios Nikolaos and its environs (NW Greece) during Classical-Hellenistic times. *Quaternary International,* 181(1), 105-122.

Vött, A., Brückner, H., Brockmüller, S., Handl, M., May, S.M., Gaki-Papanastassiou, K., Herd, R., Lang, F., Maroukian, H., Nelle, O. & Papanastassiou, D. (2009a). Traces of Holocene tsunamis across the Sound of Lefkada, NW Greece. *Global and Planetary Change,* 66(1-2), 112-128.

Vött, A., Brückner, H., May, S.M., Sakellariou, D., Nelle, O., Lang, F., Kapsimalis, V., Jahns, S., Herd, R., Handl, M. & Fountoulis, I. (2009b). The Lake Voulkaria (Akarnania, NW Greece) palaeoenvironmental archive - a sediment trap for multiple tsunami impact since the mid-Holocene. *Zeitschrift für Geomorphologie N.F.,* 53(SI 1), 1-37.

Vouvalidis, K., Syrides, G. & Albanakis, K.S. (2005). Holocene Morphology of the Thessaloniki Bay: Impact of sea level rise. *Zeitschrift für Geomorphologie N.F. Suppl. Vol*, 137, 147-158.

Walker, M.J.C. (2005). *Quaternary Dating Methods*. Chichester, 286 pp.

Wang, P. & Horwitz, M.H. (2007). Erosional and depositional characteristics of regional overwash deposits caused by multiple hurricanes. *Sedimentology*, 54(3), 545-564.

Williams, H.F.L. (2009). Stratigraphy, Sedimentology, and Microfossil Content of Hurricane Rita Storm Surge Deposits in Southwest Louisiana. *Journal of Coastal Research,* 25(4), 1041-1051.

Williams, D.M. & Hall, A.M. (2004). Cliff-top megaclast deposits of Ireland, a record of extreme waves in the North Atlantic—storms or tsunamis? *Marine Geology,* 206, 101–117.

Chapter IV

Washover fans in the northern Lagoon of Lefkada – geomorphological and sedimentary evidence for extreme wave events

4.1 STUDY BACKGROUND

Fan-shaped sedimentary structures extending from barrier beach systems into backbeach coastal lagoons or coastal lowlands are described from numerous parts all over the world and represent an important feature of coastal morphology. In most cases, they are interpreted as (i) washover fans, resulting from the flow of water and sediment (overwash) over the crest of the beach or (ii) scour fans, formed during breaching of the barrier beach (LEATHERMAN & WILLIAMS 1977, ANDRADE 1992, KRAUS et al. 2002, DONNELLY et al. 2004, YULIANTO et al. 2007, GOFF et al. 2008, 2009). Since they are exclusively induced by high energy extreme wave events, their formation is attributed to the occurrence of tsunami, tropical cyclones, such as hurricanes, or extra-tropical winter storm surges (e.g. ANDRADE 1992, DAWSON 1996, SALLENGER 2000, SEDGWICK & DAVIS 2003, ANDRADE et al. 2004, DONNELLY & WOODRUFF 2007, WANG & HORWITZ 2007, YULIANTO et al. 2007, SWITZER & JONES 2008a, GOFF et al. 2009, WILLIAMS 2009). During the recent past, the number of geo-scientific studies dealing with the sedimentary characteristics of washover structures and focussing on their event induced origin has increased (e.g. TUTTLE et al. 2004, MORTON et al. 2007, SWITZER & JONES 2008b, WILLIAMS 2009). However, in many cases, problems with the unambiguous determination of their origin remain, where only the sedimentary record or the morphological structure, but no historical reports of the event itself are available. The distinguishability of tsunami and storm in the geological record therefore constitutes the main challenge of extreme wave event research. Against this background, detailed sedimentary analysis and descriptions of palaeo-washover structures and their sedimentary composition are required.

In this chapter, detailed sedimentary and geomorphological investigations of three washover structures in the northern Lagoon of Lefkada are presented. By means of a broad range of methods, detailed analyses of the washovers' sedimentary sequence are documented. Thereby, this study aims to (i) date major washover events and (ii) to determine the related hydrodynamic process (tsunami/storm) which induced the washover structures.

4.2 STUDY AREA

The area between Lefkada Island and the Bay of Aghios Nikolaos (NW Greece) is characterized by a comprehensive barrier beach system, separating the shallow Lagoon of Lefkada and the Lefkada Sound from the open Ionian Sea. The base of this barrier system is made up of beachrock down to approximately 12 m below present mean sea level (b.s.l.). Along the spit system, several washover fan structures, up to ~1 km long, stretch from the beach into the Lagoon of Lefkada (see also *Chapter 2*). Towards the north, the recent beach ridge is shifted eastwards and separated from its beachrock base. This beachrock base, the so called Plaka, is partly submerged, fragmented and, due to the effects of earthquakes, partly broken. Here, the remains of the Plaka represent a reef-like palaeo-coastline, protecting the Bay of Aghios Nikolaos from the open sea (see also *Chapter 2*).

The study area is exposed to the northern part of the subduction zone of the Hellenic Arc (Fig. 1a and 1b). To the north of the Hellenic Arc the Cefalonia transform fault (CF) and the Lefkada transform fault (LF) show a remarkably high seismic activity (COCARD et al. 1999, LOUVARI et al. 1999, SACHPAZI et al. 2000, PAPADOPOULOS et al. 2003, BENETATOS et al. 2005). Therefore, the study area belongs to the seismically most active regions of the Mediterranean and owns a high tsunamigenic potential (PAPAZACHOS & DIMITRIU 1991, SOLOVIEV 1990).

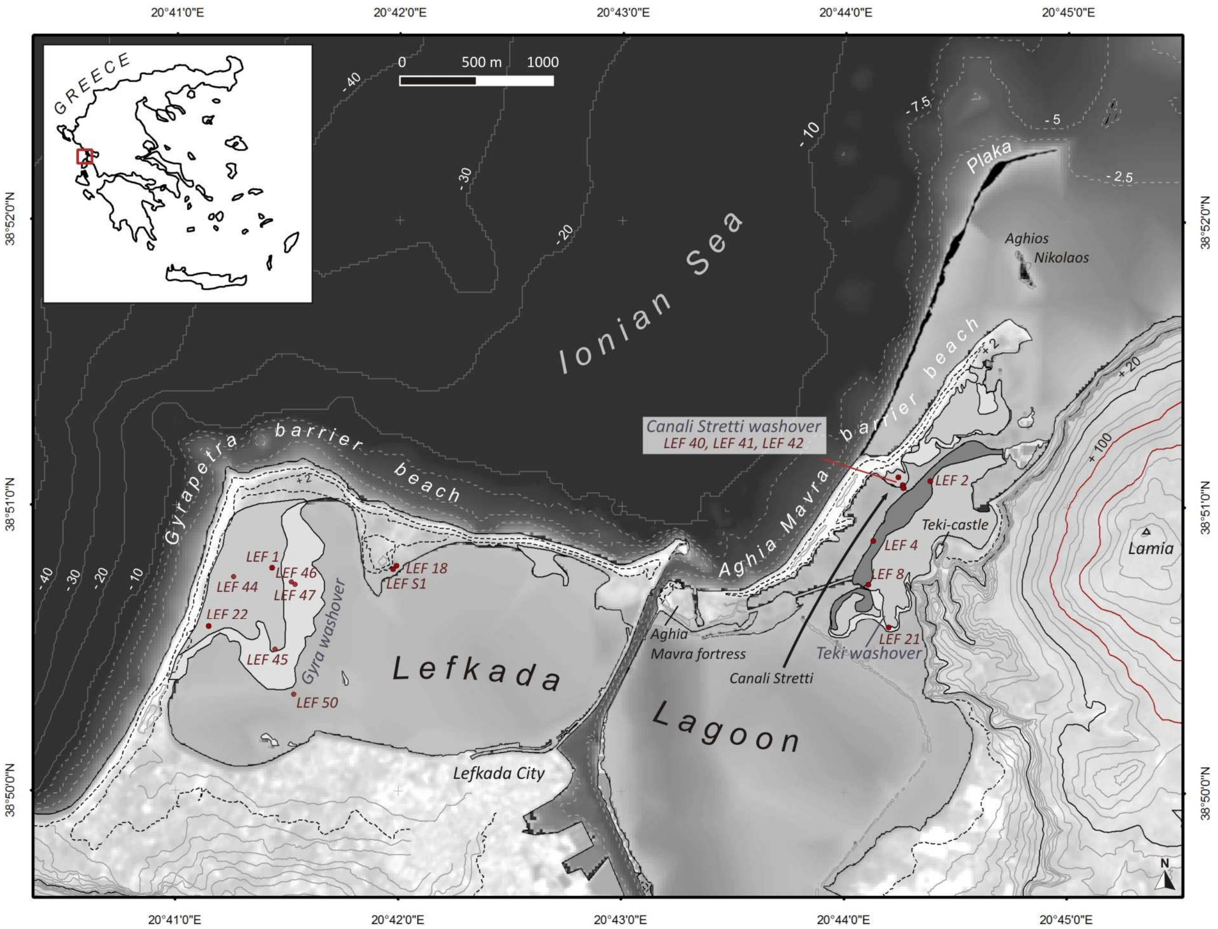

Fig. 4-1: Overview of the study area, comprising the northern part of the Lefkada Lagoon and the Lefkada barrier beach system [map based on Aster Satellite Image 2003 (USGS), TM 1:50.000 sheets Lefkada & Vonitsa (HMGS), Bathymetrical charts Amvrakikos Gulf & Lefkada channel (HNHS) and SRTM elevation data (NASA)].

4.3 METHODS

Field work comprised 10 vibracorings performed by means of an Atlas Copco Cobra mk 1 coring device and sediment cores of 5 cm and 6 cm diameter (for core data see appendix A, C and E). Additionally, on top of the washover structures and in the adjacent lagoonal areas, 7 sediment cores were obtained by pushing plastic tubes, 2 m long and 5 cm diameter, into the sediment by hand. In order to determine exact elevation and position of the sediment profiles and coring sites, DGPS-measurements were carried out using a Leica SR 530 differential GPS system. Elevation transects were realized to study morphological characteristics of washover structures. Supplementary field work comprised terrestrial geomorphological mappings as well as the examination of sediment profiles.

The vibracore and sediment profiles were documented, recorded (colour, grain size and rounding, texture, carbonate content as recommended by AD-HOC ARBEITSGRUPPE BODEN (2005), macrofaunal remains) and sampled in the field. Sedimentary, geochemical, macro- and microfaunal analyses were realized in the laboratory. Air-dried and hand-pestled fine-grained fraction (< 2 mm) of samples were analysed for Ca, Fe, Na, and K concentrations using atomic absorption spectrometry (Perkin Elmer A-Analyst 300) after digesting with concentrated HCl (37 %). $CaCO_3$ was measured following the Scheibler method. Loss on ignition (LOI) was determined by oven-drying at 105 °C for 12 h and ignition in a muffle furnace at 550 °C for 4 h (BECK et al. 1995). For core profile LEF 40, the anorganic element composition was determined using an ITRAX X-ray fluorescence (XRF) core scanner (Cox Analytical Systems). Semi-quantitative variations of elements from Al to U were analysed by scanning at 1 mm resolution and an exposure time of 20 sec. Presented count rates represent element amounts and an estimation of the relative concentrations in the sediment. Additionally, anorganic element composition was measured for selected core profiles (LEF 44, LEF 45, LEF 46 and LEF 50) by using a NITON XL3t 900 X-ray fluorescence (XRF) hand held elemental analyzer (Thermo Scientific). Here, scanning resolution was between 1 mm and several centimetres, exposure time was 30 sec.

Microfaunal analyses were carried out for cores LEF 21 and LEF 44 in order to support textural and geochemical results, to verify the marine provenance of distinct sedimentary units and to determine sediment source areas. Samples (10 cm^3) were pre-treated with H_2O_2 (30%) for dispersion and wet-sieved to isolate fractions of 63–125, 125–200, 200–400 and > 400 µm (core LEF 21). For core LEF 44 samples were sieved trough sieves of 63 µm and 125 µm. The foraminiferal content was investigated under a binocular microscope and recorded semi-quantitatively. At least 100 benthic forms were counted from each sample where sufficient concentrations were present. Any planktonic foraminifera encountered were additionally picked. Selected species were photographed using a JEOL JSM-6500F thermal field emission scanning microscope (FESEM). Identification of species was supported by original description and several key papers (AGIP 1982, CIMERMAN & LANGER 1991, SGARRELLA & MONCHARMONT ZEI 1993). Palaeoenvironmental interpretation of assemblages was inferred by a series of specific papers carried out on modern assemblages (e.g. SGARRELLA & MONCHARMONT ZEI 1993, MURRAY 2006).

For the chronological framework, organic material and mollusc remains taken from the sediment cores were dated by the ^{14}C-AMS technique (Table 4-1). ^{14}C-AMS ages were corrected for a marine reservoir effect of 400 years if necessary (REIMER & MCCORMAC 2002) using CALIB 6.0 software and the dataset of REIMER et al. (2009). For plant remains identified as sea weed in the field marine calibration was carried out when $\delta^{13}C$-values were determined to 15 ‰ ± 3 ‰ (see e.g. WALKER 2005).

4.4 RESULTS

4.4.1 THE LEFKADA WASHOVER SYSTEM

The northern part of the Lagoon of Lefkada is characterized by several fan-like washover or scour structures. In this study, detailed investigations on three of these structures have been carried out. The Gyra washover fan is situated in the western part of the Lefkada Lagoon and represents, with an area of 390.000 m² (area a.s.l., above mean sea level) and 660.000 m² (area a.s.l. and b.s.l., below mean sea level), the most extensive washover structure in the study area (see also *Chapter 2*).

In the eastern part of the Lefkada Lagoon, about 1.3 km east of the Aghia Mavra fortification, west of the Teki castle and 1 km to the south-east of the recent spit branch, distinct lobe-like washover structures can be observed, reaching southwards into the eastern part of the Lagoon of Lefkada (Teki washover structure). As described in *Chapter 2*, the adjacent marshy plain is separated from the recent beach system by a narrow water channel, the former *Canali Stretti*. Directly to the south of the channel, a beach ridge-like elevation can be observed, which is adjusted parallel to the recent beach barrier spit and which is interpreted as dredged material taken from the former channel (see Fig. 4-1 overview, black marked).

Fig. 4-2: Selected washover fan structures in the study area: a) The Gyra washover fan. On top of its subaerial surface, four sediment cores have been available for stratigraphical interpretation. Sediment cores LEF 46, LEF 47 and LEF 50 were conducted in the Lagoon of Lefkada. b) The Teki and Canali Stretti washover system seen from Lamia Mountain. At least two washover generations can be observed (W1 and W2). The formation of the ridge-like elevation to the east of the recent spit system most likely formed due to the (repeated) dredging of the Canali Stretti channel, especially subsequent to washover-events. c) The Canali Stretti scour fan seen from the Lamia Mountain.

Along the north-eastern part of the Lefkada beach ridge system, to the north-east of the Aghia Mavra fortification, several washover structures extend from the recent barrier beach into the area of the former *Canali Stretti* in south-eastern direction. In this study, investigations on the Canali Stretti fan structure were carried out (Fig. 4-2c). The fan structure most likely formed due to a breaching of the barrier beach as deduced from geomorphological investigations (see *Chapter 2*).

In the following, three key cores from each of the investigated washover fans [core LEF 44 (Gyra fan), core LEF 21 (Teki fan), and core LEF 40 (Canali Stretti fan)] are described in detail. Each core consists of a succession of different facies representing different depositional conditions. These form the base for a stratigraphic correlation along vibracore transects. In combination with nine ^{14}C-AMS datings (Table 4-1), this ultimately leads to the interpretation of the sedimentary architecture and the establishment of a chronostratigraphic framework for the investigated washovers.

4.4.2 The Gyra fan

Stratigraphy of vibracore profile LEF 44

Vibracore LEF 44 (Fig. 4-3, Fig. 4-4 and Fig. 4-5) was carried out in the middle part of the Gyra washover structure, about 250 m from the sea (see Fig. 4-1 and Fig 4-2). At its base, it consists of homogenous grey clayey silt, containing mollusc remains (1.37 – 0.93 m b.s.l.). These sediments are characterized by relatively low Ca- and Sr-, but high Fe-values, the latter indicating terrestrial influence during deposition.

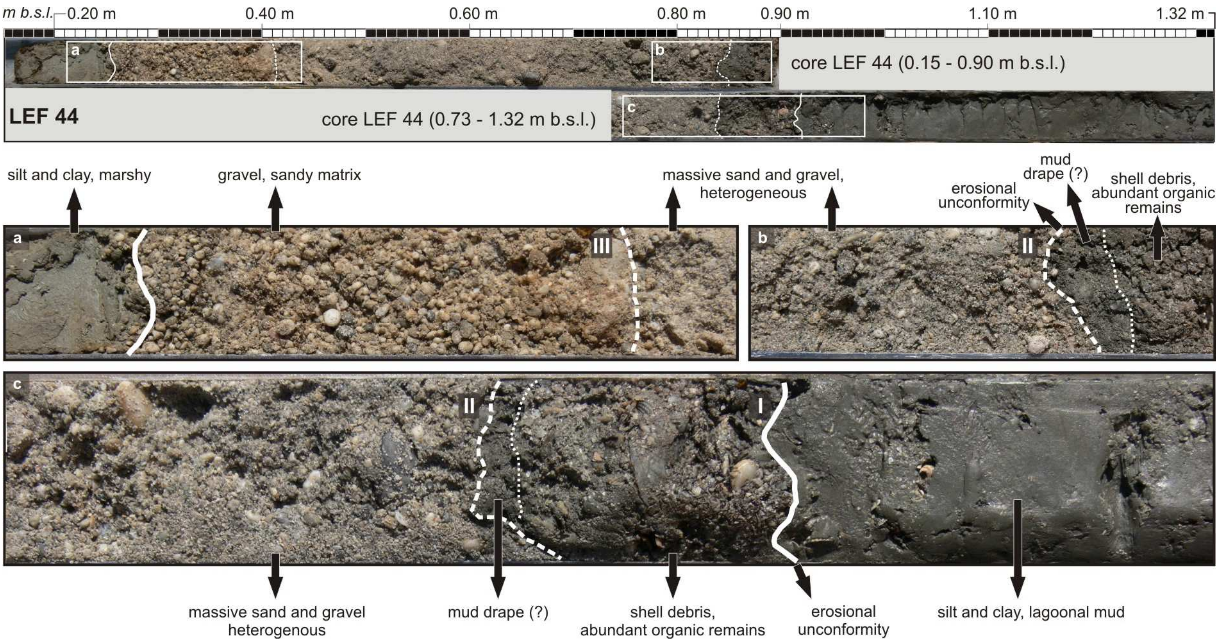

Fig. 4-3: Core section between 0.14 m and 1.32 m b.s.l. of vibracore LEF 44. On top of the lagoonal mud a coarse grained sequence of was found, comprising three different subunits (I, II, III). Interesting core sections are enlarged and main sedimentary characteristics depicted.

At 0.93 m b.s.l. depositional conditions suddenly change. The lagoonal mud is followed by a coarse grained sequence, which can be subdivided into three subunits (I, II and III, see Fig. 4-3). From 0.93 – 0.86 m b.s.l., a shell debris layer, poorly sorted, was encountered (subunit I). Due to its shell debris content it can be described as a bioclastic layer. Its matrix consists of clayey silt with a considerable part of sand. Moreover, it contains abundant small black components, which are interpreted as heavy minerals. The top of the bioclastic unit, at the transition to the overlying subunit, is marked by a thin mud-layer (0.86 – 0.85 m b.s.l.). Subsequently, a massive layer of sand and gravel is documented between 0.85 and 0.40 m b.s.l. (subunit II) This sedimentary unit is well separated from the underlying and overlying sediments and contains numerous mollusc remains. The gravel components, up to 2 cm, show a perfect grade of rounding. Based on the visual impression of the sediment, a bimodal grain size distribution is assumed. Several sea weed remains, but less shell debris and no heavy minerals were found in this layer. This unit is followed by a distinct gravel layer with a sandy matrix (0.40 – 0.24 m b.s.l., subunit III). Again, the gravel content is characterized by perfect rounding, but the size of the gravel compounds is considerably smaller compared to the underlying unit. For the coarse grained sequence entirely different geochemical characteristics are documented. The sequence is indicated by high Ca and Sr as well as low values of parameters indicating terrestrial influence, such as Fe, K and Ti. Increased values of the Sr/Fe ratio point to increased marine influence (see for instance VÖTT et al. 2002, NICHOL et al. 2007). Subsequently, the coarse grained sequence is covered by grey clayey silt, showing clear signs of hydromorphy and containing remains of roots and plants. These sediments represent the (sub-) recent, marshy depositional conditions.

Macro- and microfaunal investigations on vibracore LEF 44

In order to assess the provenance of the sedimentary units found for sediment profile LEF 44, detailed micropalaeontological analysis and macrofaunal observations were carried out for parallel cores LEF 44A and LEF 44B. Investigations were focused on the foraminiferal content of the sediments.

Altogether 15 sediment samples were analyzed throughout the sedimentary sequence. Results are depicted in Fig. 4-4. The lagoonal unit at the base of the profile is represented by sediment samples LEF 44A-7 and LEF 44B-4, LEF 44B-5, LEF 44B-6, LEF 44B-7 and LEF 44B-8. In all samples, the foraminiferal assemblage is composed by *Ammonia* spp., *Haynesina germanica*, *Haynesina depressula*, *Quinqueloculina* spp. *Affinetrina planciana* and *Aubignyna perlucida*, indicating a low energy, quiescent palaeoenvironment with deposition of muddy sediments. Few specimens of *Peneroplis pertusus* possibly reflect the existence of the adjacent barrier beach system. The lowermost sample, LEF 44B-7, shows slightly increased contents of fine sand. Here, the occurrence of *Peneroplis pertusus, Planorbulina mediterranensis* and *Cibicides lobatulus* may indicate increased marine influence, possibly due to minor washover-related sea water inundation.

With the beginning of subsequent coarse grained sedimentary sequence, an overall increased diversity in the foraminiferal assemblage is apparent. This is particularly true for the bioclastic unit at the base of the coarse grained sedimentary sequence, characterized by abundant shell debris, and the lower part of the subsequent massive sandy unit (see also Fig. 4-3, subunits I and II). Although the lagoonal species found in the samples below are still present, numerous additional benthic species appear in samples LEF 44A-6, LEF 44A-5 and LEF 44A-4 as well as LEF 44B-3. Here, *Peneroplis pertusus* and *Peneroplis planatus* are dominant, and several other (in most cases epiphytic) marine species, such as *Elphidium macellum*, *Elphidium crispum, Neocorbina posidonicola*, *Nubecularia lucifuga*, *Planorbulina mediterranensis, Sorites orbicularis,* and *Cibicides lobatulus* (MURRAY 2006). Some taxa like *Gaudryna* sp., *Uvigerina mediterranea* and *Cibicides refulgens* have been found which are typical for shelf-bathyal environments of greater water depths (MURRAY 2006).

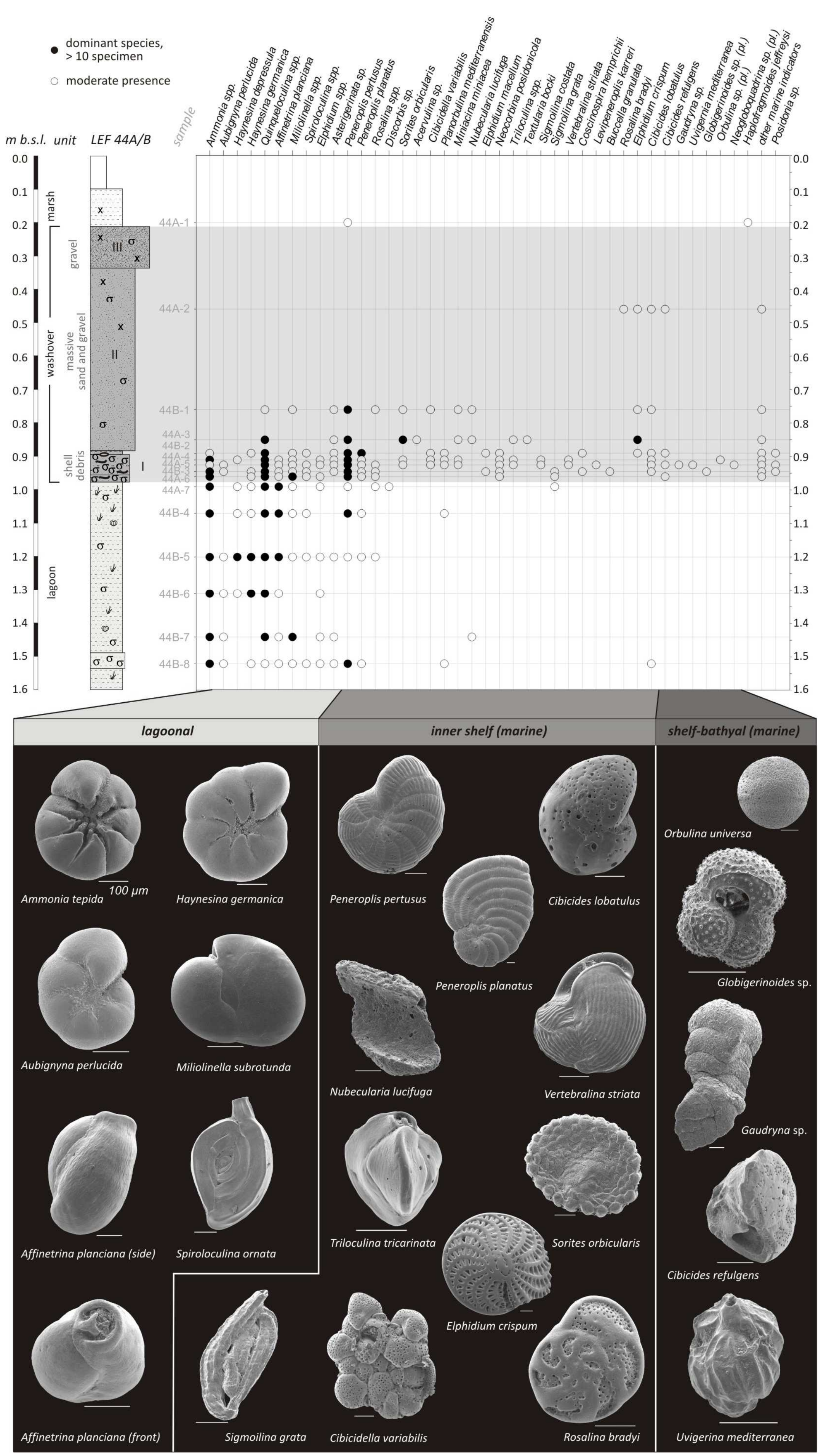

Fig. 4-4: Stratigraphy and results of microfaunal investigations carried out for parallel cores LEF 44A and LEF 44B. Stratigraphy slightly differs from core LEF 44. A distinct increase of diversity is documented from the lower part of the washover sequence. Here, a mixture of foraminiferal assemblages is evident, showing lagoonal species as well as abundant open marine species.

Moreover, the occurrence of planktonic tests, such as *Globigerinoides* sp., *Neogloboquadrina* sp. and *Orbulina* sp. point to an open-marine origin of the unit as well. Moreover, remains of sea urchins, fragments of bryozoa, a sponge spicule and several fibres of *Posidonia* sp. have been encountered, assuming a sublittoral provenance of the sediment. Altogether, a well preservation of the encountered foraminifera was observed.

The upper part of the profile is characterized by massive units of sand and gravel, indicating a littoral origin of the sediment. These units are represented by samples LEF 44A-2, LEF 44A-3 and LEF 44B-2. Besides several shallow marine taxa also documented for the underlying units, the dominance of the littoral species *Elphidium crispum* and *Cibicides lobatulus* pointing to the sublittoral and/or littoral provenance of the sediment as well (see also BARBANO et al. 2009, MAMO et al. 2009). Here, in contrast to the underlying subunit, the brackish-lagoonal species recede. The marshy environment during deposition of the uppermost fine grained sediments is indicated by the occurrence of *Haplofragmoides jeffreysi* in sample LEF 44A-1.

Coring site LEF 44 is situated in a backbeach position, ~200 m east of the current barrier beach. According to our findings, particularly the foraminiferal assemblage found for the lower part of the coarse grained deposits (subunit I and the lower part of subunit II, Fig. 4-3 and Fig. 4-4) is characterized by a mixture of different, partly open marine associations. An allochthonous origin of the deposit, related to a washover event, is thus manifested.

Stratigraphy of the Gyra washover structure

Vibracore transect A (Fig. 4-5b) comprises, from north-west to south-east, vibracores cores LEF 44 and LEF 1, lagoonal cores LEF 46 and LEF 47 as well as vibracore LEF 18 and sediment profile LEF S1, which were carried out some 800 m east of coring site LEF 1 on top of a triangle like peninsula (see also Fig. 4-1 for locations). Vibracore LEF 1 was carried out in the eastern part of the Gyra washover fan and represents the deepest drilling of transect A. At the base of the profile, (sub-) littoral sediments indicate a westward shift of the coastline, characterized by well sorted fine sand, few mollusc and sea weed remains as well as a geochemical distribution indicative of a marine environment. At the very base, the marine sands are cemented to beachrock or a beachrock-like sequence and represent the lower limit of the investigations. The littoral sediments are covered by lagoonal mud, similar to the sediments described from the lower part of vibracore LEF 44 (1.37 – 0.93 m b.s.l., see also Fig. 4-3).

Subsequently, the lagoonal mud is covered by the heterogeneous sequence of coarse grained sediments. Terrestrial indicators, such as the content of K, Fe and Ti show overall decreased values within the coarse deposits (see Fig. 4-5a). A contrary pattern is observed for the Ca- and Sr-values, indicating marine provenance (VÖTT et al. 2002, NICHOL et al. 2007). Within the coarse grained units above the lagoonal sediments considerably increased Ca- and Sr-contents are recognized. The lowermost section of the washover sequence represents a transitional horizon, which is indicated by a mixture of geochemical patterns reflecting both marine and terrestrial (lagoonal) environments. These findings are in good agreement with the results of the sedimentary and microfaunal analysis, which indicate (i) a mixing of different microfaunal associations and (ii) a mixture of autochthonous and allochthonous sediments.

For cores LEF 44 and LEF 1 a comparable succession of the coarse grained sedimentary sequence is documented. Due to the sedimentary and geochemical findings in lagoonal cores LEF 46 and LEF 47, carried out ~200 m south-east of coring site LEF 1, the coarse grained unit is thinning towards the east (Fig. 4-5a, b). Here, the lagoonal mud is covered by a sandy shell debris layer and a subsequent massive heterogeneous sand layer. The gravel unit found in cores LEF 1 and LEF 44 therefore most likely is restricted to the part of the subaerial washover structure which is lying above sea level. On top of the coarse material, fine grained sediments accumulated due to the current marshy (LEF 1 and LEF 44) or lagoonal environment (LEF 46 and LEF 47), which is, compared to the basal lagoonal unit, characterized by an analogue geochemical pattern (Fig. 4-5a, b).

About 800 m east of vibracore LEF 1, vibracore LEF 18 and sediment pit LEF S1 were carried out in the southern part of a triangular shaped peninsula (see also Fig. 4-1). Overall stratigraphy of vibracore LEF 18 is different from the findings encountered for the Gyra washover structure. Here, no lagoonal sequence was found at the base of the profile. In contrast, the lowermost part (3.64 - 1.04 m b.s.l.) is consisting of deeply weathered, well sorted silty fine sand. Towards the top of the unit (1.04 – 0.37 m b.s.l.), the content of silt and clay increases and clear signs of hydromorphy as well as the brown colour point to soil formation due to the existence of a former surface. Within the uppermost 20 cm of this unit, numerous ceramic fragments could be extracted from the sediment profiles. The former surface is separated from the subsequent sediments by a distinct erosional unconformity (0.37 m b.s.l.). Above this unconformity, a sand layer was found, containing numerous mollusc remains and gravel, showing perfect rounding (0.37 – 0.08 m b.s.l.). Again, due to the gravel content in the sediment, it must be assumed that the sediment is of sublittoral or littoral origin. Moreover, intraclasts consisting of sediment from the underlying unit could be found. These intraclasts are interpreted as rip-up clasts and point to erosion and high energy turbulent flow during deposition of the unit. The uppermost part of the profiles is characterized by the recent depositional conditions, showing abundant organic remains as well as root and plant fragments (0.08 m b.s.l. – 0.08 m a.s.l.). The massive sandy unit found at sites LEF 18 and LEF S1, on top of the deeply weathered former surface, is assumed to correspond to the massive sandy washover subunit II found in the sedimentary sequence of the Gyra washover fan.

Vibracore transect B (Fig. 4-5c) comprises, from north-west to south-east, vibracore LEF 44, core LEF 45 and lagoonal core LEF 50 (see Fig. 4-1 for location). The sedimentary sequence of core LEF 45, carried out on the very southern point of the Gyra washover structure, is comparable to the sequence found in vibracore LEF 44 (Fig. 4-6). For the coarse grained unit above the lagoonal mud, again three subunits with comparable characteristics are separated (subunits I, II and III, Fig. 4-6). Here, after deposition of the uppermost gravel layer, lagoonal conditions reestablished at coring site LEF 45: the gravel unit is covered by clayey silt (0.31 – 0.13 m b.s.l.), slightly sandy, which contains abundant shell remains in its upper part, similar to the deposits at the recent lagoonal shore. This unit is comparable to lagoonal unit at the base of the profile. From 0.13 m b.s.l. - 0.05 m a.s.l., a peat-like layer out of organic remains and clayey silt was found, corresponding to marshy and thus to the current depositional conditions.

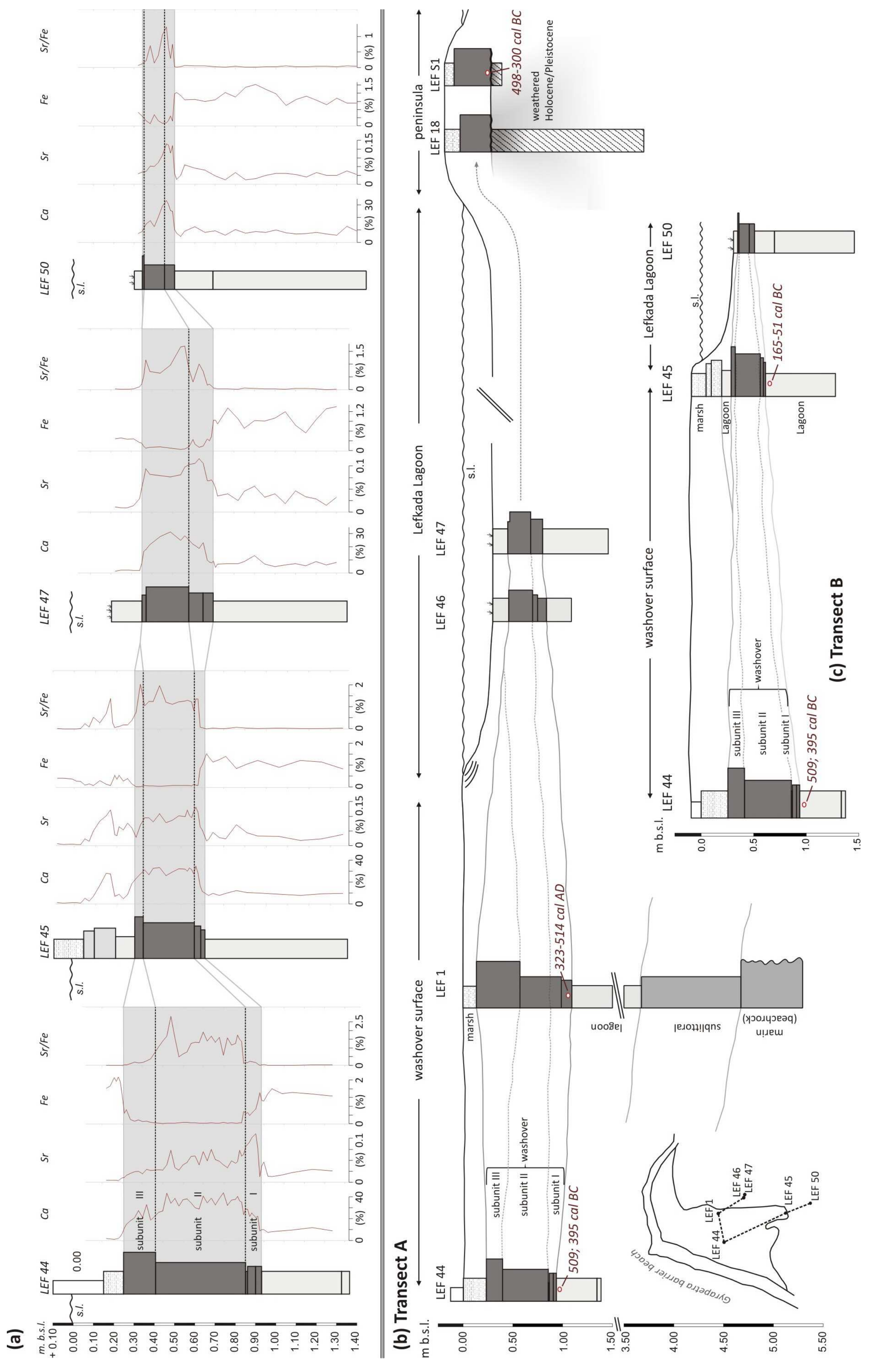
(a)
(b) Transect A
(c) Transect B
LEF 44
LEF 45
LEF 47
LEF 50
LEF 1
LEF 46
LEF 18
LEF S1
Ca
Sr
Fe
Sr/Fe
subunit III
subunit II
subunit I
washover
washover surface
Lefkada Lagoon
peninsula
marsh
lagoon
sublittoral
marin (beachrock)
weathered Holocene/Pleistocene
509; 395 cal BC
323-514 cal AD
498-300 cal BC
165-51 cal BC
Gyrapetra barrier beach
m b.s.l.
s.l.

Fig. 4-5 (previous page): a) Sediment cores carried out on top of the Gyra washover with selected geochemical proxis Ca, Sr, Fe, and Sr/Fe ratio. Different sedimentary units are characterized by a distinct distribution of elements. The marked washover unit is characterized by high Sr- and Ca-values. For the lower part of the washover sequence, a mixing of deposits from different depositional environments is documented. b) and c) Coring transects A and B carried out for the Gyra washover fan. Three distinct subunits within the washover sediment can be separated in cores LEF 44, LEF 1, LEF 45 and lagoonal core LEF 50. In lagoonal cores LEF 46 and LEF 47 only two subunits could be identified. The washover unit is characterized by a fining landward sequence (for legend see Fig. 4-7).

At coring site LEF 50, situated some 200 m south of site LEF 45 in the Lagoon of Lefkada, the coarse grained sedimentary units (subunits I, II and III) described for cores LEF 44 and LEF 45 are considerably thinner. Here, the uppermost gravel unit is represented by a thin gravel-containing layer, ~1 cm thick. Nevertheless, a coarse grained, massive sandy sequence (0.51 – 0.35 m b.s.l.) accumulated on top of the lagoonal mud, which can be divided into two subunits – a lower subunit, consisting of sand and silt with shell debris and abundant heavy minerals (0.51 – 0.45 m b.s.l.) and a subsequent upper unit, showing less shell debris and less heavy minerals (0.45 – 0.35 m b.s.l.). The uppermost 5 cm of the profile consist of silty sand and represent the reestablishment of the quiescent, lagoonal deposition.

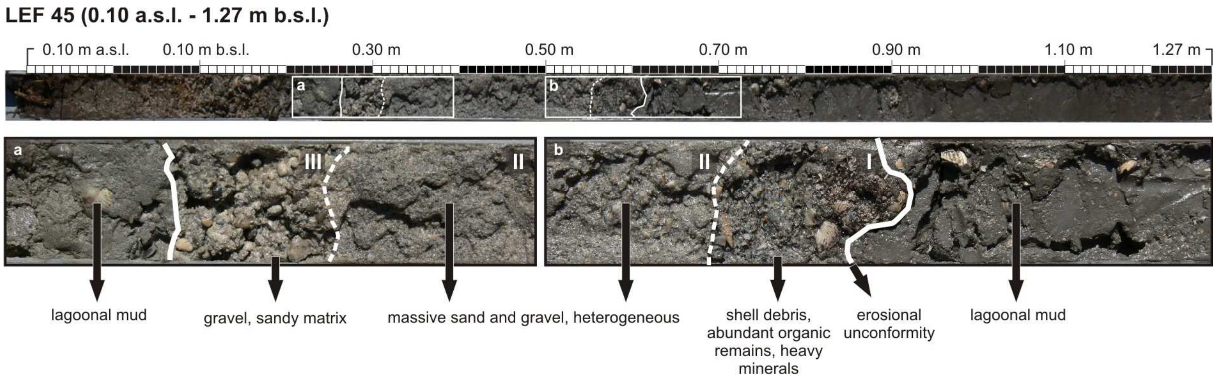

Fig. 4-6: Vibracore LEF 45, core section between 0.10 m a.s.l. and 1.27 m b.s.l. Comparable to core LEF 44, on top of the lagoonal mud a coarse grained sequence of was found, comprising three different subunits (I, II, III). Interesting core sections are enlarged and main sedimentary characteristics depicted.

The stratigraphical succession described for vibracore LEF 44 is clearly supported by the geochemical findings (Fig. 4-5a). The results show a remarkable difference between the washover deposits and the above and below lying deposits. Moreover, a similar geochemical pattern is recognized and allows a correlation of sedimentary units.

For a chronological Interpretation of core LEF 1 and vibracore transect A, a sea weed remain (LEF 1/4+ PR, Table 4-1) was sampled from 1.21 m b.s.l. It was dated by ^{14}C-AMS-technique to 323-514 cal AD. From the base of the coarse grained washover unit in sediment profile LEF S1, a mollusc test was dated to 498-300 cal BC (LEF S1/3 M, Table 4-1). Taken from the lowest part of the coarse grained sedimentary sequence above the lagoonal unit, the ages both represent *termini ad* or *post quem* for the deposition of the above lying washover sediments. Two ^{14}C-AMS datings exist for vibracore transect B. Plant remains taken from the lagoonal sediments below washover units date to 509; 395 cal BC (LEF 44/10+ PR, 0.98 m b.s.l.) and 165-51 cal BC (LEF 45/9 PR, 0.64 m b.s.l.).

*Tab. 4-1: ^{14}C-AMS dating results used for the chronological interpretation of the stratigraphy. Notes: unid. plant remains - unidentified plant remains. artic. – articulated mollusc. Lab. No. – laboratory number, University of Erlangen-Nürnberg (ERL), University of Kiel (KIA), University of California, Irvine (UCI), University of Utrecht (UTC). * - marine reservoir correction with 400 years of reservoir age. ";" - there are several possible age intervals because of multiple intersections with the calibration curve; oldest and youngest age depicted.*

Sample	*Depth (m b.s.l.)*	*Lab. No.*	*Sample description*	*δ^{13}C (ppm)*	*^{14}C age (BP)*	*1σ max-min (cal BC/AD)*	*2σ max-min (cal BC/AD)*
LEF 1/4+ PR	1.21	KIA28881	sea weed	-15.9	1965 ± 25	*368-448 AD	*323-514 AD
LEF 2/7 M	2.38	UTC1369	mollusc	0.3	2574 ± 37	*359-247 BC	*382-192 BC
LEF 2/14 M	5.53	UTC1369	mollusc	0.0	6257 ± 37	*4803-4705 BC	*4872-4666 BC
LEF 4/5 PR	1.42	Erl-9053	sea weed	-18.7	2093 ± 41	168; 54 BC *194-324 AD	342 BC; 0 AD *139-378 AD
LEF 4/7 M	2.10	Erl-9054	artic. *Dosinia exoleta*	-1.8	2709 ± 45	*517-385 BC	*647-356 BC
LEF 4/10 M	4.40	Erl-9799	artic. *Macoma* sp.	0.0	5104 ± 55	*3614-3470 BC	*3624-3370 BC
LEF 44/10+ PR	0.98	UCI73834	unid. plant remains	-	2375 ± 15	481; 397 BC	509; 395 BC
LEF 45/9 PR	0.64	UCI73835	unid. plant remains	-9.9	2085 ± 15	155; 55 BC	165-51 BC
LEF S1/3 M	-0.29	KIA39788	mollusc test	-7.93	2635 ± 30	*406-342 BC	*498-300 BC

4.4.3 THE TEKI FAN

Stratigraphy of vibracore profile LEF 21

Vibracore LEF 21 (Fig. 4-7) was carried out on top of the southernmost lobe of the Teki washover structure, some 820 m south-east of the present shoreline (Fig. 4-1 and 4-2). The base of vibracore profile LEF 21 begins with grey, well sorted fine sand of marine origin, containing minor parts of medium sand and mollusc remains (7.95 – 5.65 m b.s.l.) Between 5.65 – 5.19 m b.s.l., a unit of marine sand and gravel, very well rounded, was encountered. This unit is covered by well sorted medium sand (5.19 - 4.51 m b.s.l.). Here, plant and root remains are documented.

Subsequently, morphodynamic activity considerably decreased – above 4.51 m b.s.l clay and silt content increases and, according to the following unit out of grey clayey silt, lagoonal conditions established at coring site LEF 21 (4.51 – 1.39 m b.s.l.). Numerous plant and *in-situ* mollusc remains point to a swampy saltwater influenced environment. Compared to the underlying marine sediments, K- and Fe-values increase while the content of marine indicators, such as Na and Mg, recedes. Within the upper most part of the lagoonal unit, shell debris content considerably increases.

On top of the lagoonal mud, a sand and shell debris layer was found which contained numerous mollusc fragments and appeared slightly laminated (1.39 – 0.90 m b.s.l.). The sand and shell debris unit is followed by relatively well sorted fine and medium sand (0.90 – 0.58 m b.s.l.). Subsequently, morphodynamic activity decreased, and silt content within the sediment increases (0.58 m b.s.l. - surface). Here, the sediment consists of grey clayey silt, showing signs of hydromorphy. A considerable amount of fine sand is documented, most likely due to bioturbation and reworking of the underlying sandy unit, occurring during tide-related flooding. Due to the current prevailing semiterrestrial, marshy environmental conditions, the upper part of the sequence is affected by subaerial weathering.

Microfaunal investigations on vibracore LEF 21

For core LEF 21, microfaunal analyses were carried out for selected samples taken from the whole sedimentary sequence (Fig. 4-7, see also VÖTT et al. 2009a). The encountered ostracod and foraminifera species and genera are summarized in Fig. 4-3. Distinct differences in microfaunal assemblages can be observed between the fine-grained, lagoonal sediments and the coarse grained sedimentary units above and below.

The autochtonous, lagoonal deposits are characterized by overall low abundances of counted species and a significantly lower bio-diversity (LEF 21/9 – LEF 21/6). Foraminiferal assemblages here are dominated by *Ammonia beccarii* and *Elphidium* sp*.,* and fluctuations in salinity, oxygen content and acidity can be inferred from the investigations. However, for sample LEF 21/8, microfaunal assemblages point to a littoral, shallow marine environment, although sedimentary findings do not differ from the underlying and subsequent samples. An increased marine influence must be assumed for this part of the sedimentary sequence and may be explained by an extreme wave event, affecting the Lagoon of Lefkada (VÖTT et al. 2009a), or a temporary connection to the sea. Sample LEF 21/5 was taken from the sandy unit on top of the lagoonal mud and seems to represent a transition to the overlying unit. Overall microfaunal assemblage here points to shallow marine environmental conditions and an autochthonous community. Due to the prevailing occurrence of *Ammonia beccarii* in foraminiferal assemblages and a dominating ostracod association of *Loxoconcha* sp*., Xestoleberis* sp*. and Leptocythere lagunae,* a lagoonal environment still is assumed, but an at least episodical connection to the open Ionian Sea is likely (e.g. HANDL et al. 1999).

In contrast to the lagoonal sediments below, a high bio-diversity and high abundances of encountered species in foraminiferal and ostracod assemblages is typical for the coarse grained units of the upper part of the sediment profile. As illustrated in Fig. 4-7 these coarse grained units, representing a higher morphodynamic activity during deposition, are mainly dominated by (open) marine species. In some samples deep water species such as *Globulina* sp*. (*e.g. LEF 21/3, LEF 21/4) occur as well (see for instance KAMINSKI et al 2002).

According to MURRAY (1973, 2006), *Cibicides lobatulus*, *Cibicides* sp., *Planorbulina* sp. and also *Elphidium crispum* and *Polymorphina* sp. are of fully marine, partly littoral origin. Since these species are encountered inside the Sound of Lefkada and in sediments close to the present sea level, they clearly indicate an *ex-situ*, allochthonous assemblage. At least for the coarse grained units found in the upper part of the profile, on top of the lagoonal sequence, an allochthonous origin can thus be assumed. The uppermost two samples (LEF 21/2 and LEF 21/1) most likely represent reworked material from the underlying unit, which accumulated, due to the increasing silt content in the sediment, under reestablished lagoonal conditions.

In contrast, the only sample taken from the lower coarse grained unit (8.00 – 4.46 m b.s.) containing abundant ostracod species is sample LEF 21/13 (6.70 – 6.55 m b.s.). For samples LEF 21/14, LEF 21/11 and LEF 21/10, environmental conditions must have been inappropriate for the development of ostracod communities, most likely due to continuous wave dominated turbulent deposition. The microfaunal assemblages found in the lower part of the profile, characterized by marine sediments, thus do not point to a mixing of microfaunal associations. Most likely they are related to an autochthonous formation due to sublittoral or littoral conditions.

Vibracore profile LEF 21 (38°50.584' N, 20°44.157' E)

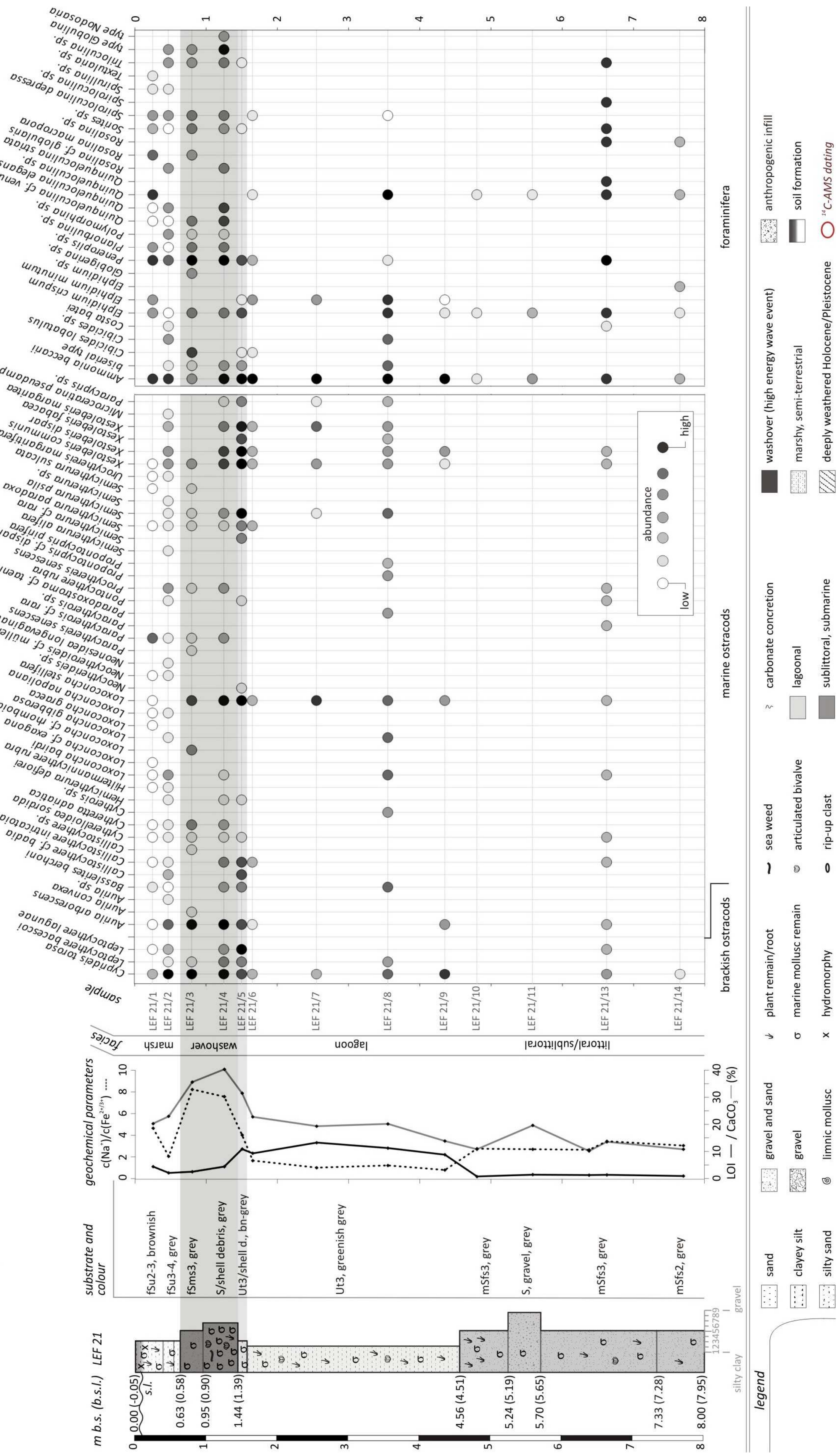

Fig. 4-7 (previous page): Sedimentary and geochemical characteristics of vibracore profile LEF 21 and results of microfaunal investigations. Comparable to the findings in cores LEF 44A and LEF 44B, a distinct increase of species diversity and abundance is documented for the washover sequence. Here, a mixture of foraminiferal assemblages is evident. Autochthonous assemblages are assumed for the lower sublittoral sands (LEF 21/13) and for the lagoonal sediments. Sample LEF 21/8 points to sea water inundation in the Lefkada Lagoon as well and may reflect an older extreme wave and washover event which affected the lagoonal environment. Grain size of cores is illustrated by different widths of core profile (1 – silty clay, 2 – clayey silt, 3 – sandy silt/silty sand, 4 – fine sand, 5 – fine and medium sand, 6 – medium sand, 7 – medium and coarse sand, 8 – coarse sand, 9 - gravel).

Stratigraphy of the Teki washover system

Fig. 4-8a illustrates a coring transect across the Teki washover. From north-east to south-west, coring sites LEF 2 and LEF 4 are situated in direct vicinity of the former *Canali Stretti* channel, on top of the ridge-like elevation to the south-east. Vibracore LEF 8 was conducted several hundred meters southwards of coring site LEF 4, in greater distance to the *Canali Stretti*. Additionally, vibracore LEF 21 was carried out at the southernmost point of the south-stretching washover lobe, reaching ~900 m into the Lagoon of Lefkada.

Similar to the findings at coring site LEF 21, at the base of sediment profiles LEF 2, LEF 4 and LEF 8 well sorted fine sand and/or gravel-rich sediments of marine origin are covered by muddy lagoonal deposits. On top of these sediments, coarse grained sediments accumulated along the entire transect. However, a correlation between the coring sites of this stratigraphical sequence is difficult due to its heterogeneity. Nevertheless, lagoonal conditions of low morphodynamic activity must have ended with the beginning of the coarse grained sequence.

At coring site LEF 4, the lagoonal mud is covered by grey fine sand containing few gravel components, very well rounded as well as numerous mollusc remains (2.02 – 1.15 m b.s.l.). Above, sediments contain considerable parts of gravel, very well rounded, pointing to its littoral provenance (1.15 – 0.53 m b.s.l.). The uppermost layer is characterized by a fining upward trend (0.53 – 0.26 m b.s.l.). Regarding the position of coring site LEF 4 these units, similar to vibracore LEF 21, are of allochthonous origin and interpreted as washover sediments. Above, clayey to silty fine sand occurs (0.26 – 0.08 m b.s.l.), which is covered by gravel in a silty matrix (0.08 m b.s.l. – 0.20 m a.s.l.). These two uppermost units most likely are due to anthropogenic dredging of the Canali Stretti channel.

The sedimentary sequence of sediment profile LEF 8 is comparable to the findings at coring site LEF 4. Here, above the lagoonal mud, fine sand and silt was deposited (1.74 – 1.29 m b.s.l.). Comparable to coring site LEF 4, the sand contains few gravel components, well rounded, and numerous mollusc remains. Subsequently, a layer of fine and medium gravel was found, originating from sublittoral or littoral environments. The gravel unit is followed by fine and medium sand (1.24 - 0.46 m b.s.l.). These two units may correspond to the uppermost coarse grained unit described for coring site LEF 4. The top of the profile (0.46 m b.s.l. – 0.11 m a.s.l.) is made up of gravel, containing numerous mollusc remains and, in its lower part, a sandy matrix.

At coring site LEF 2, subsequent to the lagoonal sediments, grey fine sand was encountered between 2.28 – 1.58 m b.s.l., containing few pieces of fine gravel, very well rounded. Due to its

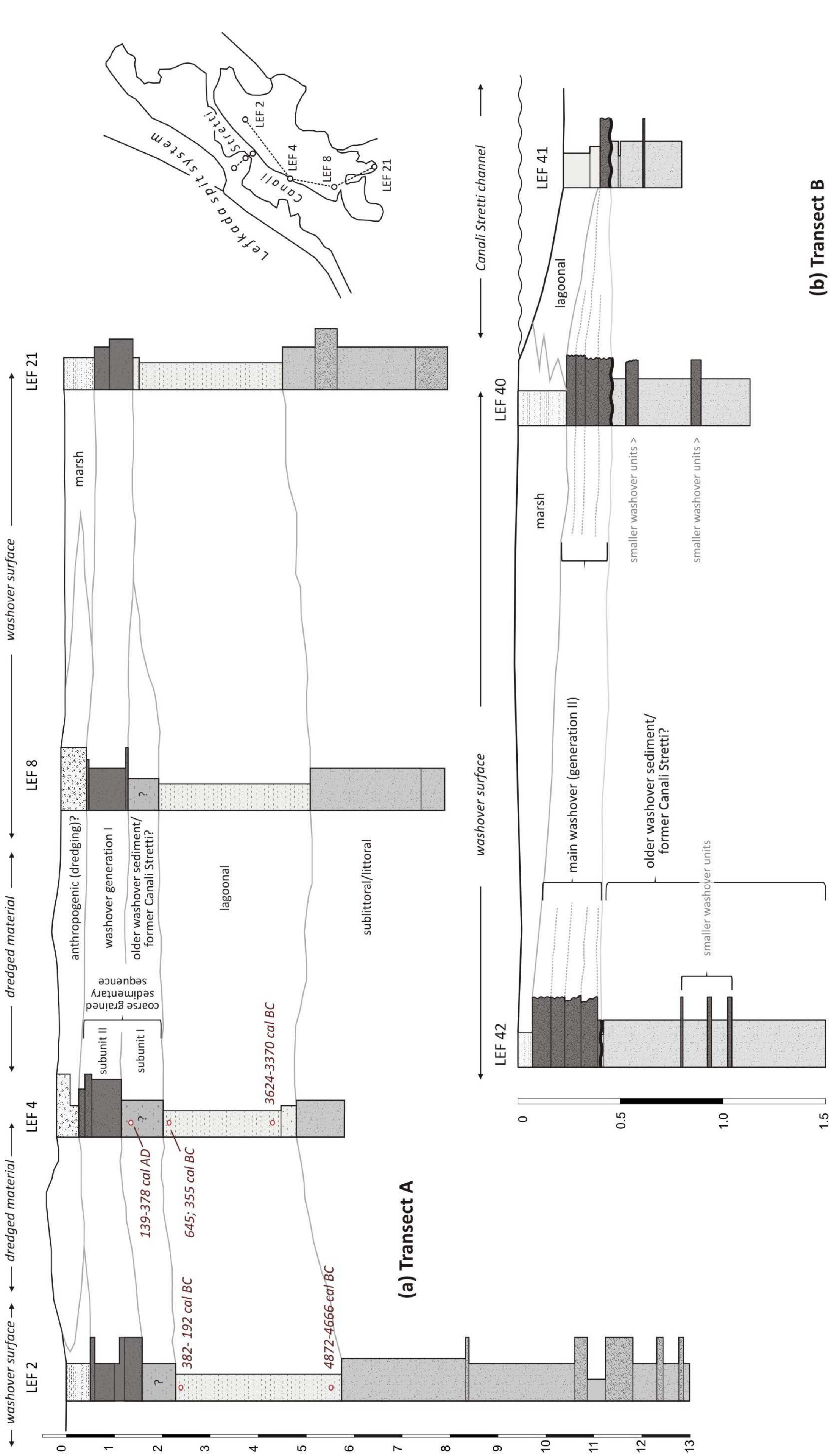
(a) Transect A
LEF 2
LEF 4
LEF 8
LEF 21
washover surface
dredged material
dredged material
washover surface
anthropogenic (dredging)?
washover generation I
older washover sediment/ former Canali Stretti?
lagoonal
sublittoral/littoral
marsh
coarse grained sedimentary sequence
subunit II
subunit I
382- 192 cal BC
4872-4666 cal BC
139-378 cal AD
645; 355 cal BC
3624-3370 cal BC
(b) Transect B
LEF 42
LEF 40
LEF 41
washover surface
Canali Stretti channel
main washover (generation II)
older washover sediment/ former Canali Stretti?
smaller washover units
smaller washover units >
marsh
lagoonal
Lefkada spit system
Canali Stretti
LEF 2
LEF 4
LEF 8
LEF 21

Fig. 4-8 (previous page): Vibracore transect A across the Teki washover structure (a, washover generation I) and transect B across the Canali Stretti fan structure (b, generation II). Several subunits within the washover sequences can be separated. The washover units are characterized by a fining landward sequence. Due to anthropogenic dredging of the channel, an interpretation of the uppermost units is problematic.

sedimentary characteristics, this unit can be correlated the lowermost, sandy part of the coarse grained sequence found in cores LEF 4 and LEF 8. Above, the coarse grained sequence is consisting of gravel, containing numerous mollusc fragments (1.58 – 1.21 m b.s.l.). The perfect rounding of the gravel components proves the littoral origin of the unit and points to an allochthonous origin. The gravel unit is covered by grey fine sand (1.21 – 0.59 m b.s.l.) and a layer of fine to medium gravel (0.59 – 0.50 m b.s.l.). The topmost unit out of fine sand is assumed to represent reworked material, which accumulated due to the present, marshy conditions and which is affected by brunification and initial soil development in its upper part.

Altogether, the coarse grained sequence on top of the lagoonal mud can be divided into a lower (subunit I) and an upper part (subunit II). Subunit I comprises the massive, lower sandy units in cores LEF 2, LEF 4 and LEF 8, subunit II several gravel-rich layers in cores LEF 2, LEF 4 and LEF 8, which are partly fining upward. At sediment profile LEF 21, the sequence of coarser sediments covering the lagoonal mud shows two distinct units as well. Both units are characterized by a heterogeneous, allochthonous microfaunal association. Here, the topmost part of the lagoonal sequence is characterized by a different microfaunal assemblage and increasing sand and shell debris content (see *Chapter 4.3.1*).

For a chronological interpretation of the vibracore transect, three ^{14}C-AMS-datings are available for vibracore profile LEF 4. Additionally, two dating results exist for vibracore LEF 2 (see also Table 4-1). The ^{14}C-AMS-datings of two articulated molluscs, taken from the lowermost part of the fine grained, lagoonal unit (LEF 2/14 M 5.53 m b.s.l.; LEF 4/10 M 4.40 m b.s.l.) document the onset of lagoonal conditions at 4872-4666 BC and 3624-3370 BC, respectively. At coring site LEF 4, the end of the lagoonal deposition is dated to around or after 645; 355 cal BC (LEF 4/7 M, 2.10 m b.s.l.), at coring site LEF 2 to around or after 382-192 cal BC (LEF 2/7 M, 2.38 m b.s.l.). Moreover, the subsequent sandy unit found in core LEF 4 (2.02-1.15 m b.s.l.) contained sea weed remains dated to 139-378 cal AD (LEF 4/5 PR, 1.40 m b.s.l.). However, due to the δ^{13}C-value of 18.7 ‰, also a terrestrial calibrated age of 342 BC; 0 AD may be considered but is not used for interpretation in this study.

4.4.4 The Canali Stretti fan

In contrast to the Gyra and the Teki washover fans, the Canali Stretti fan structure has been shown to be characterized by a much more pronounced morphology (see *Chapter 2*), which is additionally reflected in the DGPS transects A-D (Fig. 4-9). In combination with the interruption of the oldest beach ridge of the adjacent barrier beach system, these findings point to a breaching event of the adjacent barrier beach and the related formation of the fan (see also *Chapter 2*).

Sediment profiles LEF 42 and LEF 40 were carried out on top of the Canali Stretti fan structure, core LEF 41 in south-eastern prolongation in the middle of the former Canali Stretti channel, about 15 m south-east of coring site LEF 40. In Fig. 4-10a, the upper sections of cores LEF 40 and LEF 42 are illustrated. Fig. 4-8 b documents a coring transect along the coring sites LEF 42, LEF 40 and LEF 41.

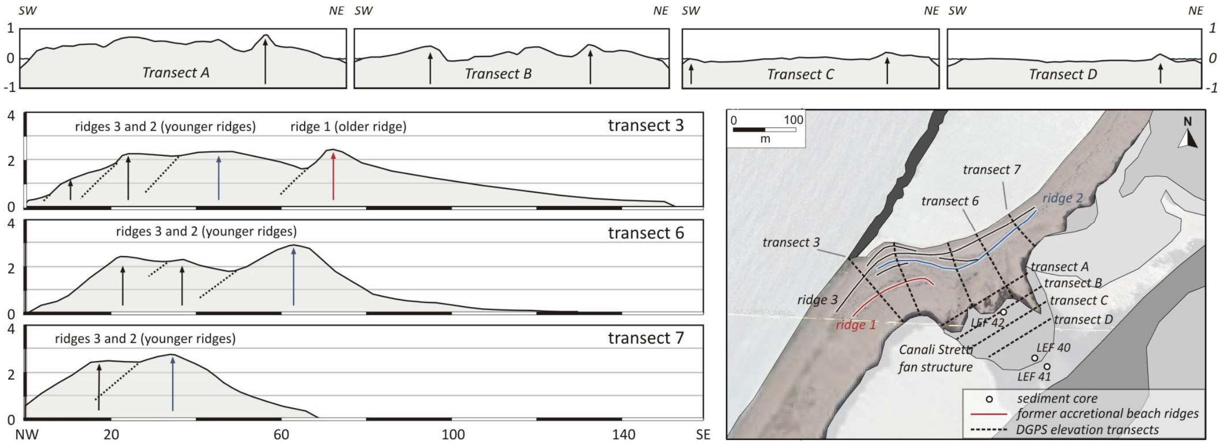

Fig. 4-9: The Canali Stretti fan structure with coring sites and locations of DGPS transects. Transects A-D were carried out on top of the fan surface, crossing the fan structure from south-west to north-east. Transects 3, 6 and 7 were conducted perpendicularly across the adjacent part of the barrier beach. As shown in Chapter 2, breaching of the barrier took place and involved (i) the interruption of the older ridge generation, (ii) the formation of the fan structure, and (iii) the subsequent closure of the breach by the accretion of younger ridges.

Sediment profile LEF 42 was obtained in the middle of the washover structure and has a length of 1.52 m. At its base (1.52 – 0.41 m b.s.l.), it consists of grey sand, containing numerous marine mollusc remains, sea weed and few gravel components. Between 0.81 - 0.79 m b.s.l. and 0.95 - 0.91 m b.s.l. the sand is intercalated by thin layers of fine gravel, originating from the (sub-) littoral zone west of the barrier beach. Several root remains were found in this unit. Between 0.42 and 0.41 m b.s.l., a layer of plant remains was found. The unit is comparable to the sandy sediments covering the lagoonal mud at coring site LEF 4 and LEF 2 (Teki washover structure, Fig. 4-8a).

At 0.41 m b.s.l., the thin layer of plant remains is abruptly covered by light grey sand. Here, no more root remains were encountered. At 0.39 m b.s.l., the thin sand layer is covered by the coarse-grained, gravelly sequence which can be divided into four subunits (see Fig. 4-10a). Its lower part (0.39 – 0.31 m b.s.l.) is made up of fine to medium gravel and has a sandy matrix. Above, between 0.31 – 0.24 m b.s.l., a unit of medium to coarse gravel was found. Here, the content of the sandy matrix decreases. From 0.24 – 0.17 m b.s.l., coarse sand, fine and medium gravel comprise subunit three. It is covered by another subunit, mainly consisting of medium gravel. At least the three lowermost subunits show a slight fining upward trend. Subsequently, the gravel unit is covered by brown-grey clayey silt (0.06 – 0.00 m b.s.l.), showing clear signs of hydromorphy and containing root- and plant remains. These fine grained, marshy sediments correspond to the current environmental and morphodynamic conditions and cover and flatten the lobe-like morphology of the fan.

Overall stratigraphy of sediment profiles LEF 40 and LEF 41 is comparable to the sequence shown for profile LEF 42. For sediment core LEF 40, XRF measurements were carried out in order to determine geochemical characteristics of the sedimentary sequence. Selected geochemical parameters are illustrated in Fig. 4-10b. The different sedimentary units found for core LEF 40 can be clearly separated by the distribution of the depicted geochemical parameters, and each unit is characterized by different contents of elements.

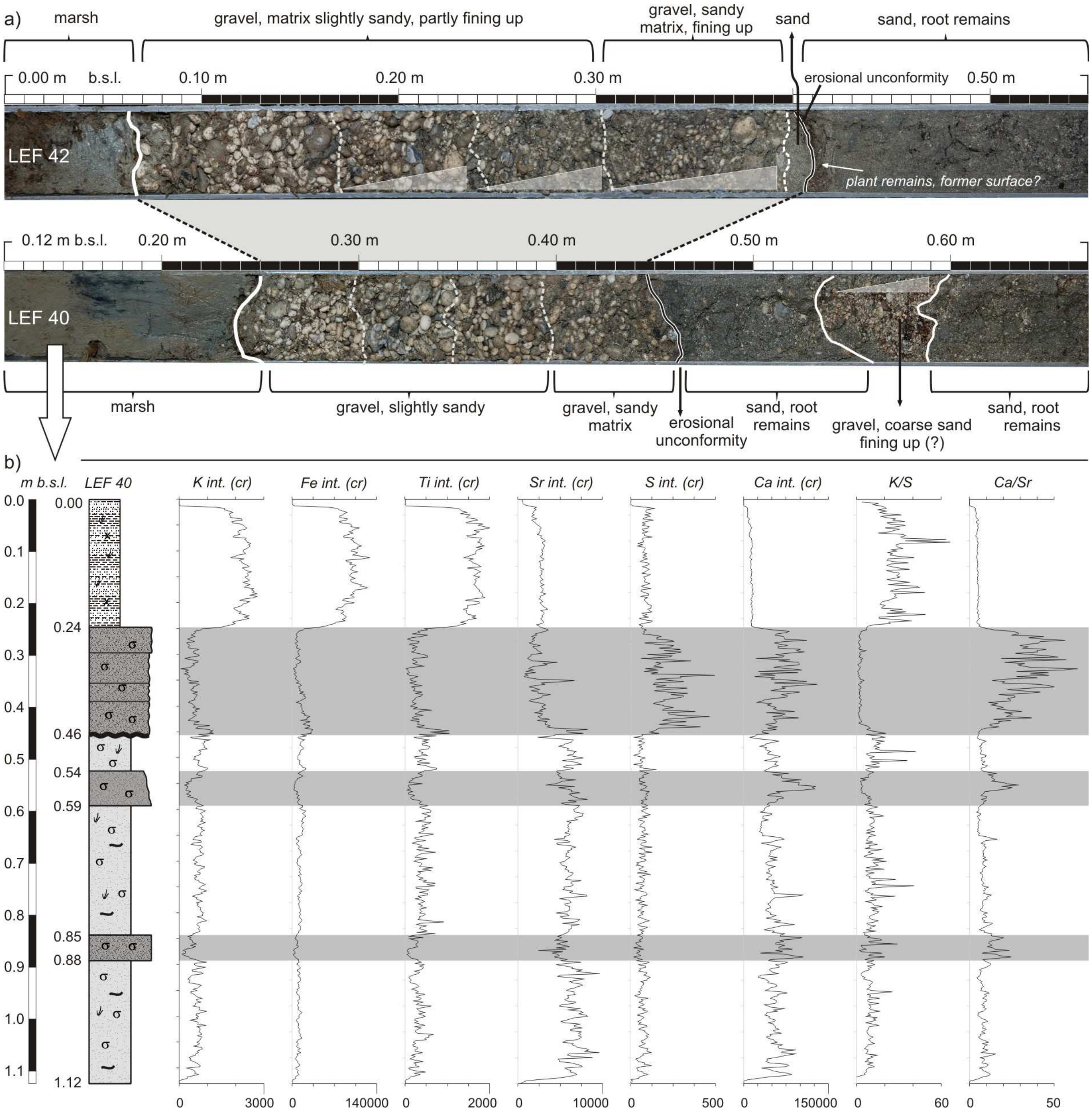

Fig. 4-10: a) Upper section of cores LEF 42 and LEF 40. The main gravel unit is consisting of four subunits, partly characterized by fining upward sequences. Below the main gravel unit sandy sediments were found, which are intercalated by at least two thin layers of coarse sand and fine gravel (LEF 40, e.g. 0.59 – 0.54 m b.s.l.). b) Sediment core LEF 40 and selected high-resolution proxies K, Fe, Ti, Sr, S and Ca. Different sedimentary units are characterized by a distinct distribution of elements. Besides the marked washover unit between 0.24 and 0.46 m b.s.l., two additional gravel-rich units, ~5 cm thick, can be detected in the lower part of the profile, intercalating the Canali Stretti unit. These units most likely correspond to washover events as well.

Similar to the findings in core LEF 42, two thin gravel units again intercalate the basal sandy unit (e.g. Fig. 4-10a, 0.59 – 0.54 m b.s.l., see also Fig. 4-8b). The main gravel unit is again separated into four subunits, and grain size distribution is comparable to the findings in sediment profile

LEF 42 (Fig. 4-10a). At the transition to the basal sandy unit, neither the layer of plant remains nor the subsequent sandy layer as described for core LEF 42 was encountered. Nevertheless, overall thickness of the coarse sequence is thinner (0.46 – 0.24 m b.s.l.). Within the coarse grained sequence, absolute values of rubidium (Rb), titanium (Ti), potassium (K) and iron (Fe) considerably decrease, allowing a clear differentiation between the above and below lying units. This is also true for the thin gravel layers found within the sandy unit at the profile's base. As high values of these elements in general indicate a terrestrial depositional environment or at least terrestrial influence, the characteristic distribution can be explained by the increased marine and the related reduced terrestrial influence during washover events. However, the decrease of bulk Rb, Ti, K and Fe-values may also be caused by the coarser particle size (e.g. VÖTT et al. 2002).

In contrast to the distribution of the elements characteristic for terrestrial sedimentation, a more heterogeneous distribution of the elements strontium (Sr), sulphur (S) and calcium (Ca), indicating marine influence, was detected. As Fig. 4-10b illustrates, S values are remarkably higher in the distinct washover unit compared to the above and below lying sedimentary units – including the thin gravel layers in the lower part of the profile. Moreover, the coarse grained sequence can be subdivided into a lower and an upper part, the latter showing lower S concentrations.

In contrast to the detected S concentrations, the profile's sequence is characterized by peaks of Ca values not only in the main gravelly unit but also in the two gravel layers intercalating the sandy unit at the base. Compared to the basal sandy unit the washover units are indicated by overall lower Sr abundances, although high Sr-contents in sediments generally point to increased marine influence. This fact may also be due to the increased particle size found for these units. In order to document a grain size independent distribution of selected elements, ratios of two elements have been calculated. As high K and Ti values point to increased terrestrial, high S and Sr values to increased marine influence, the K/S-ratio is assumed to represent grain size-independent information about variations in marine and terrestrial input, respectively. According to the results of the K/S ratio, a definite increased marine input can be assumed for all gravelly washover units. Additionally, the values for the Ca/Sr ratio clearly show differences between the sedimentary units. Here, all washover units are indicated by higher values and a distinct differentiation from the remaining units is documented.

Due to the adjacent Canali Stretti channel and the related frequent flooding of the coring site, the fine grained unit on top of the gravelly sequence shows an increasing thickness of 0.24 m. At coring site LEF 41, situated in the channel of the former Canali Stretti, the gravel unit was encountered between 0.23 – 0.13 m b.s.l. A subsequent anthropogenic disturbance of the sedimentary sequence, such as dredging in the former channel of Canali Stretti, is likely.

4.5 INTERPRETATION AND DISCUSSION

Along the Lefkada barrier beach system several major washover- and/or scour fan structures stretch into the Lagoon of Lefkada and represent important features of coastal morphology in the study area. In order to document their sedimentary architecture, chronological evolution and origin, altogether 14 sediment corings were investigated on top of and in direct vicinity of the three main washover structures, ultimately providing comprehensive insight into the palaeogeographical evolution of the Lefkada coastal zone.

4.5.1 The western part of the Lefkada Lagoon

The largest washover structure, the Gyra washover fan, is located in the western part of the Lagoon of Lefkada. At the base of the deepest corings, sediments of sublittoral or littoral origin were found. In all sediment profiles, the marine base is covered by a thick sequence of lagoonal mud, which is, due to the absence of coarse grained intercalating horizons, characterized by a relatively undisturbed sedimentation. According to these findings, (i) a local regression of the sea of at least 200 m and a related westward shifting of the Gyrapetra barrier beach, (ii) an accompanied establishment of lagoonal conditions east of the shifting barrier beach and (iii) a relatively long period of undisturbed lagoonal deposition is documented.

In all sediment profiles, the lagoonal sequence is covered by a distinct coarse-grained unit of allochthonous, sublittoral and/or littoral origin. Generally, the deposition of this unit may be explained by (i) temporarily establishing littoral conditions or (ii) by an event-induced transport of littoral material into the Lagoon of Lefkada, originating from the barrier beach or the foreshore area. According to the above described findings, a local regression of the sea is assumed for the Gyrapetra region due to gradual shoreline migration. Moreover, the local morphology does not point to former beach ridges in the investigated area but clearly indicates a lobe-like washover structure, stretching into the Lefkada Lagoon. The formation of the coarse grained unit on top of the lagoonal mud thus cannot be explained by a temporary eastward shifting of the barrier beach and a related re-establishment of littoral conditions – in contrast, it must be explained by an extensive washover event, which inundated at least the western part of the Lefkada Lagoon (see also Vött et al. 2006). According to the results of the investigated sediment cores, the following characteristics of the washover unit can be summarized:

(i) The sedimentary architecture of the main part of the washover structure can be subdivided into three sedimentary subunits.

(ii) The lowermost subunit (subunit I) comprises a mixture of lagoonal mud, sand and shell debris. In several sediment cores, heavy minerals are abundant, and the base of the subunit is characterized by a noticeable accumulation of organic remains. According to the microfaunal investigations, a mixture of foraminiferal assemblages is documented. Numerous fully marine species as well as lagoonal species were encountered, indicating the open marine provenance of the unit.

(iii) Subunit II consists of a massive layer of sand and gravel showing a heterogeneous, bimodal grain size distribution. Subunit III is represented by a distinct gravel layer, which is thinning towards the east. For both upper units, according to the perfectly rounded gravel compounds and the dominance of *Elphidium macellum* and *Elphidium crispum* in foraminiferal assemblages, a littoral provenance of the sediment is assumed.

(iv) In the lagoonal core profiles, the washover sequence is mainly built up by two subunits. Here, the topmost gravel layer is < 1 cm. Grain size in both units is finer compared to the findings from the central part of the washover. An overall fining and thinning landward (eastward) sequence is thus evident for the washover sequence.

(v) Vibracore LEF 18 and sediment profile LEF S1 show a distinct washover unit as well, which is comparable to the massive sand layer in the middle of the Gyra fan washover sequence (subunit II). Here, the event deposit covers a palaeosol, in which numerous ceramic fragments have been encountered. Several rip-up clasts from the underlying sedimentary unit point to intense erosion during deposition.

Numerous washover fans have been attributed to tsunami (ANDRADE 1992, GOFF ET AL. 2001, SWITZER et al. 2005, YULIANTO et al. 2007 GOFF et al. 2009) or extreme storm events (COCH 1994, MORTON & SALLENGER 2003, DONNELLY et al. 2004, WANG & HORWITZ 2007, WILLIAMS 2009), the latter in most cases reported from coastal zones affected by tropical cyclones. For the study area, the existence of tropical cyclones can be excluded and, besides tsunami, only exceptionally strong winter storms may theoretically have the energy to generate washover or breaching events along the Lefkada barrier beach system (see also WOODROFFE 2003: 461).

The Gyra washover structure comprises ~600.000 m³ and extends more than 1 km from the recent barrier beach into the Lefkada Lagoon. As documented in *Chapter 2,* the washover structures have not been affected by modifications at least during the last 150 a. In many studies, the lateral extension of the washover structure is used as a diagnostic criterion for the differentiation between tsunami and storm (TUTTLE et al. 2004, MORTON et al. 2007, SUGAWARA et al. 2008). In general, tsunami washover structures are reported to exhibit larger dimensions than storm induced washover structures (MORTON et al. 2007). For regions affected by tropical cyclones, however, storm-generated water inundation is documented to have similar or at least comparable dimensions (e.g. BAHLBURG 2008), and a related sediment accumulation can be considered. Whether exceptionally large winter storms in the study area are capable of generating washover structures of comparable dimension must be doubted. This is especially true when considering the long period of time the washover structures remained unmodified.

The marine origin of the washover sequence is clearly indicated by the microfaunal and sedimentary findings. For the Gyra washover fan, a distinct differentiation of three subunits (I, II and III, see Fig. 4-3) is evident, which can consistently be followed along the entire fan structure and is thinning landward. No fining upward sequence was found but instead, massive bedding of the two topmost units (subunits II and III) is documented, which is accompanied by a bimodal grain size distribution in the sandy layer (subunit II). These findings may point to multiple sediment sources (such as sublittoral and littoral environments) and are reported to be characteristic of several tsunami-induced deposits (e.g. FUJINO et al. 2008, SWITZER & JONES 2008a, MOORE et al. 2006). According to numerous findings all over the world, storm-induced washover systems are characterized by a number of thin layers and/or laminae, delta foreset stratification and subhorizontal, planar stratification with channel structures (LEATHERMAN & WILLIAMS 1977, SEDGWICK & DAVIS 2003, TUTTLE et al. 2004, KORTEKAAS & DAWSON 2007, MORTON et al. 2007, WILLIAMS 2009). Lamination within tsunami deposits for instance have been described by PARIS et al. (2007), CHOOWONG et al. (2008) and MORTON et al. (2008), who examined sediments deposited by the 2004 Indian Ocean tsunami and attribute these findings to the effects of backwash and/or waning phases during the event. Due to the topographical circumstances in the Lagoon of Lefkada, intense backwash induced currents can be excluded for the investigated locations. However, fewer (typically not more than 3 - 5) subunits are documented from several other tsunami deposits (NANAYAMA et al. 2000, BAHLBURG & WEISS 2007, HAWKES et al. 2007, MORTON et al. 2007, SUGAWARA et al. 2008).

Especially the lowermost subunit of the presented washover deposit (subunit I, Fig. 4-3 and Fig. 4-4) is indicated by a highly diverse foraminiferal assemblage and an increased number of species. Although numerous species of fully marine provenance have been encountered, the sediment here is still dominated by lagoonal species as well. A mixing of different microfaunal assemblages is thus documented, pointing to an allochthonous formation of the hosting sediment (HAWKES et al. 2007, MCMURTRY et al. 2007, RUIZ et al. 2010). Moreover, a mixing of different microfaunal assemblages is reported to be significant for tsunami deposits from numerous previous studies (DAWSON et al. 1995, ANDRADE et al. 1997, HINDSON & ANDRADE 1999, HINDSON et al. 1996, HAWKES et al. 2007, KORTEKAAS & DAWSON 2007, MCMURTY et al. 2007, MAMO et al. 2009, VÖTT et al. 2009a).

Additionally, several planktonic species and species indicative of deeper water were found within subunit I of the washover sediment. In contrast, the subsequent units of massive sand and gravel show typical characteristics of a littoral foraminiferal assemblage. In general, open marine species such as planktonic and/or shelf species indicate washover events and therefore storm and/or tsunami inundation if found in sediments intercalating the sedimentary sequence in backbeach positions, such as lagoons or paralic swamps (e.g. DAWSON et al. 1995, ANDRADE et al. 1997, TUTTLE et al. 2004, MAMO et al. 2009, RUIZ et al. 2010, WILLIAMS 2009). In many cases, comparable findings were used to support the tsunamigenic origin of sediments (DAWSON et al. 1996, ANDRADE et al. 1997, HINDSON & ANDRADE 1999, UCHIDA et al. 2005, NANAYAMA & SHIGENO 2006, DAWSON & STEWART 2007, MAMO et al. 2009). However, the macro- and microfaunal content of these sediments only proves its marine origin, since the macro- and microfaunal content of an event deposit is a product of its source.

A tsunami-induced washover event, in contrast to a storm induced event, would typically consist of few major impulses of sea water inundation, corresponding to the tsunami wave train. The characteristics of each flooding impulse considerably relate to several circumstances, such as near coastal bathymetry, slope of the coastal plain and shoreline morphology (MORTON et al. 2007). Particularly observations during the 2004 Indian Ocean Tsunami showed that most of the sediments in a tsunami deposit origins from the littoral zone, the beach and the adjacent area (see also SATO et al. 1995, MORTON et al. 2007). According to the same authors, the first tsunami inundation pulse is commonly characterized by minor energy, which is related to limited inundation depth and distance (see also CHOOWONG et al. 2008). The lower bioclastic subunit thus may be explained by the first, minor flooding impulse of a tsunami event. Here, erosion, reworking and mixing of the underlying lagoonal mud and the minor sediment load from the inundating water took place. It can be assumed that the second and subsequent flooding impulses would be characterized by increased turbulence and suspension and/or sediment load in the water column than the first inundation impulse, triggering thicker deposits in the geological record. Comparable observations have been presented by CHOOWONG et al. (2008) who examined deposits of the 2004 Indian Ocean Tsunami, and by FUJIWARA & KAMATAKI (2007) from offshore tsunami sediments off Boso Peninsula, Japan. In the Gyra washover region the massive sand layer and the following gravel layer most likely correspond to inundation periods related to waves from the middle of the tsunami wave train (such as waves 2, 3 or 4 during a tsunami event) and are characterized by a sublittoral and littoral provenance.

Further evidence for a tsunamigenic origin of the washover event may be derived from the existence of the mud-layer found in vibracore profile LEF 44, 1-2 cm thick and situated directly above the bioclastic unit. Moreover, rip-up clasts from the underlying former terrestrial surface were encountered in the massive sandy unit at vibracore site LEF 18. In general, mud layers or mud drapes are interpreted to form due to decreasing flow velocities subsequent to a major inundation impulse during a tsunami event. As internal mud layers and intraclasts from the eroded underlying sediments are reported to be a physical attribute found in numerous tsunami and only few storm deposits (e.g. MORTON et al. 2007, KORTEKASS & DAWSON 2007, SPISKE 2009, WILLIAMS 2009), a tsunami event is considered to be responsible for the formation of the Gyrapetra washover.

The sedimentary architecture of the Gyra fan structure is comprised of three distinct subunits. As has been shown above, a successive formation during one extreme wave event can be assumed. However, it may also be possible that several independent washover events contributed to the formation of the coarse grained sequence of subunits I, II and III. Due to the consistent morphology of the Gyra fan structure, a contemporaneous formation must be favoured. Moreover, no indication for intermittent soil formation, periods of subaerial weathering or periods of re-establishing lagoonal deposition was found on top of each subunit. Therefore, a successive deposition of the three subunits during one washover event is assumed, and each subunit corresponds to one inundation impulse during the event.

As to the chronological interpretation of the washover event, plant remains were taken from the underlying lagoonal unit (LEF 44/10+ PR and LEF 45/9 PR). Since a stratigraphical relation and a contemporaneous formation of the washover sediment is assumed, the younger age of 165-51 cal BC determines a *terminus post quem* for the deposition of the overlying washover sediments. Moreover, two ^{14}C-AMS-datings are available for vibracore transect A (LEF 1/4+ PR: 323-514 cal AD, LEF S1/3 M: 498-300 cal BC). Since the washover unit found in sediment core LEF 18 and profile LEF S1 is assumed to correspond to the same event, the age of sample LEF S1/3 M supports, due to a possible reworking of the bivalve test, the age obtained from core LEF 1. Within the former surface below the related erosional unconformity, several ceramic fragments have been encountered. Unfortunately, no age determination was possible due to the small size of the fragments. Nevertheless, these findings do not disagree with the assumed age of the washover event. A major washover event, triggered by a tsunami, thus occurred around or after 323-514 cal AD in the western part of the study area (see also VÖTT et al. 2006). Comparable to the findings of VÖTT et al. (2009b), who suggest tsunami related sediments at the south-western shore of the lake Voulkaria, the event may thus correspond to the well known eastern Mediterranean catastrophe at 365 AD (STIROS 2001, STEFANAKIS 2006).

4.5.2 THE EASTERN PART OF THE LEFKADA LAGOON

The coastal morphology in the eastern part of the Lefkada Lagoon is characterized by several fan-like washover structures as well. The so called *Canali Stretti*, a navigable channel leading from the central part of the Lagoon of Lefkada in north-eastern direction into the Bay of Aghios

Nikolaos, was used from antiquity until the beginning of the 19th century. At that time, particularly the washover dominated area was used to navigate across the Lefkada Sound. Since the construction of a navigable channel is most likely connected with dredging and overall maintenance, an anthropogenic influence on the existing morphology and stratigraphy has to be taken into account. Therefore, a careful interpretation of the sedimentary sequence and its chronological evolution is important. From a morphological point of view, the fan structures of the Teki fan and the considerably smaller Canali Stretti fan are assumed to correspond to at least two different washover generations (see also *Chapter 2*). At least for washover generation II, a formation during or subsequent to the use of the *Canali Stretti* channel can be assumed.

Washover generation I

In the north-eastern Lefkada Lagoon, open marine conditions persisted until the end of the 6th (Bay of Aghios Nikolaos) or the beginning of the 5th (northern Lefkada Lagoon) millennium BC and were followed, triggered by the formation of a barrier beach system to the north, by a long period of undisturbed quiescent lagoonal conditions (see also Vött et al. 2007). These findings are comparable to the evolution of numerous coastal areas, where the onset of dominating gradual littoral processes, such as the formation of barrier beach systems due to longshore drift or the progradation of fluvial deltas, is documented at around 5000 cal BC and is assumed to be related to the deceleration of eustatic sea level rise (Fairbanks 1989, Bard et al. 1996, Stanley & Warne 1994, Woodroffe & Nash 1995, Brückner et al. 2005, Vött 2007, Brückner et al. in press, Engel et al. 2009). Thus, the north-eastern part of the Lefkada Lagoon was affected by a northward regression of the sea, which occurred sometime before ~4000 cal BC.

At coring site LEF 21, microfaunal assemblages of the upper coarse grained units show a noticeably inhomogeneous spectrum and are assumed to be a mixture of different associations (Fig. 4-7, LEF 21/4 – LEF 21/1, above 1.30 m b.s.), which is comparable to the results documented for core LEF 44 in the Gyra region (see Fig. 4-4). The microfaunal investigations thus document an allochthonous origin of the marine sedimentary sequence found on top of the lagoonal mud. Regarding the location of coring site LEF 21, situated several hundred meters south of the barrier beach in the Lagoon of Lefkada, a formation due to a temporary establishment of regular sublittoral conditions must be excluded either way. The allochthonous coarse grained sequence found at coring site LEF 21 is interpreted to correlate with the coarse grained sequence encountered at all other drilling sites on top of the lagoonal sediments, comprising subunits I (lower sandy unit at sites LEF2, LEF 4 and LEF 8) and II (subsequent gravel rich layers). In all relevant cores, a comparable depth b.s.l. of the lower and upper limit of the sequence was found which may point to a contemporaneous formation.

For subunit I, increasing silt contents to the south (coring site LEF 8) indicate reduced morphodynamics during its deposition and may represent a fining landward sequence. The following gravelly sequence of subunit II can be divided into a lower and upper part. At coring site LEF 4, the lower gravel layer shows a sandy matrix while the upper gravel layer is characterized by a normal graded sequence indicating an *in-situ* formation without anthropogenic influence. Given a stratigraphical correlation of the allochthonous units in the upper part of cores LEF 4 and LEF 8, the lowermost gravel layer is thinning landward. Moreover, the upper normal graded gravel layer in core LEF 4 may correspond to the upper sandy layer in LEF 8. In this case, also a fining landward sequence is identified. However, the normal graded sequences within the coarse grained sedimentary sequence of subunit II indicate successive deposition of sediment load due to decreasing flow velocities (NICHOLS 2009). Since this flow-related formation is characteristic for depositional processes occurring during washover events these findings point to an extreme wave event origin of the deposit (see also HAWKES et al. 2007, MORTON et al. 2007). Due to the perfect rounding of the gravel components, a littoral provenance of the sediment is indicated which is in good agreement with the allochthonous foraminiferal assemblage found in the upper part of core LEF 21. Together with the prevailing washover dominated morphology, the deposition of the coarse grained sediments on top of the lagoonal mud must be attributed to at least one washover event (washover generation I), inundating the area from northern direction and reaching southwards into the Sound of Lefkada. A definite determination of its originating process is difficult - however, due to the absence of tropical cyclones in the study area and the dimension of washover generation I, we assume a tsunami-induced rather than a storm-induced origin for washover generation I.

For the evolution of the coarse grained sequence of subunits I and II several interpretations may be considered. First, it may be assumed that the two subunits formed independently and represent a succession of two washover events. Second, it may be possible that only the upper, gravel containing subunit II represents event deposits – in that case, the underlying subunit I can be interpreted to correspond to a former part of the Canali Stretti channel, though water currents in the channel must have been considerably stronger than at present. Third, also a contemporaneous deposition of subunits I and II triggered by the same event may be considered. In the latter case, the sequence of subunit I and II can be compared to the succession of subunits found for the Gyra fan, which is interpreted to correspond to different inundation impulses during one single tsunami-induced washover event.

Three ^{14}C-AMS datings are available for a chronological interpretation of the coarse grained sequence comprised by subunits I and II. Given a washover independent evolution of the lower subunit I, for instance due to the existence of the former *Canali Stretti* channel at coring sites LEF 2 and LEF 4 during antiquity, the ^{14}C-AMS age of sample LEF 4/5 PR documents the existence of the channel at 139-378 cal AD (see also Fig. 4-8). According to VÖTT et al. (2009a) the period of time of its formation coincides with the early period of time the *Canali Stretti* channel was used to navigate across the Sound of Lefkada. The sandy unit on top of the lagoonal mud thus may be interpreted as related to the *Canali Stretti* channel and to have accumulated due to the onset of the *Canali Stretti's* use in the middle of the 1st millennium BC. In this case, a washover event took place after 139-378 cal AD, involving the accumulation of, partly gravelly, subunit II and the allochthonous sandy sediments at coring site LEF 21. Alternatively, also a washover-induced formation of subunit I in cores LEF2, LEF 4 and LEF 8 as proposed by VÖTT et al. (2009a) may be taken into account. Assuming a contemporaneous, washover induced formation of this lower sandy subunit, a *terminus ad* or *post quem* for the washover event is determined to 139-378 cal AD as well. In either case, the extreme wave event, triggering the washover structure of generation I (Teki washover), may correlate to the tsunami event responsible for the Gyra washover system, which was determined to 323-514 cal AD (LEF 1/4+ PR) and may be related to the 365 AD Crete event (e.g. STIROS 2001, STEFANAKIS 2006).

Since a washover event, accumulating sand sheets at coring site LEF 21 and generating the washover lobes visible west of the Teki castle, must have affected the area of the former *Canali Stretti* channel as well, the re-use of the channel and the reconstitution of navigability across the Sound of Lefkada was only possible by dredging of the former channel area. Indeed, the navigability of the channel was interrupted several times between 500 BC and 200 AD (OBERHUMMER 1887, PARTSCH 1907, LEHMANN-HARTLEBEN 1923, see also VÖTT et al. 2009a). Along its southern shore, the shallow water channel is accompanied by a ridge-like elevation. This elevation is assumed to represent dredged material from the former *Canali Stretti* channel and indicates subsequent anthropogenic modifications of the backbeach morphology.

Washover generation II

The sedimentary sequence of the Canali Stretti fan structure (washover generation II) is well documented by the sediment profiles of cores LEF 42, LEF 40 and LEF 41. Here, the stratigraphical correlation allows a more detailed insight into the sedimentary architecture of the washover deposit and, comparable to the findings for the Gyra washover stratigraphy, a distinct stratigraphic correlation of the washover unit is possible.

Breaching of the adjacent barrier beach is inferred from the geomorphological investigations (*Chapter 4.4.4*, see also *Chapter 2*). The Canali Stretti fan structure is thus assumed to represent a scour fan rather than a washover fan, induced by an extreme wave event (for comparable findings see e.g. ANDRADE 1992, KRAUS 2003, GOFF et al. 2009). Apparently, the morphology of the Canali Stretti fan is related to the gravel unit on top of the lower sandy sediments, consisting of four subunits which are thinning land- or south-eastward. Grain size composition of each subunit is dominated by medium to fine gravel, clearly documenting the flow-related transport and deposition of beach material into the backbeach area. The lowermost subunits found for core LEF 42 are characterized by a fining upward grain size distribution. These normal graded sequences within the sedimentary units indicate the extreme wave event induced formation of the deposit, since they prove a successive deposition of sediment load due to decreasing flow velocities (NICHOLS 2009, see also HAWKES et al. 2007, MORTON et al. 2007). The existence of only four subunits within the Canali Stretti fan sedimentary sequence favours a tsunamigenic origin of the deposits, since storm generated washover deposits commonly are characterized by numerous thin layers and/or laminae, delta foreset stratification and subhorizontal, planar stratification (TUTTLE et al. 2004, KORTEKAAS & DAWSON 2007, MORTON et al. 2007). In contrast to the findings from the Gyrapetra region, no mud drapes or rip-up clasts have been found within the sediment. Given that washover or breaching deposits are always a product of their source and the incorporation of intraclasts is related to the characteristics of the underlying sedimentary unit, the absence of rip-up clasts within the breaching deposit cannot be used as a diagnostic criterion for a storm origin. However, turbulence during the event and related erosion of the underlying unit is documented by the considerably increased sand content within the lowermost sedimentary subunit of the washover sequence.

Below the washover sequence, sandy deposits were encountered, which are comparable to the lowermost sandy unit (subunit I) of the coarse grained sequence at coring sites LEF 2 and LEF 4, situated directly to the south of the *Canali Stretti*. At coring sites LEF 42 and LEF 40, several thin layers of coarse sand and gravel intercalate this sandy sequence. These layers are characterized by fining upward sequences as well. It is thus assumed that they were formed due to extreme wave events, most probably related to the overwash of the adjacent barrier beach. According to the smaller grain size, their minor thickness and the existence of only one comprising unit, the intensity of these events must have been considerably lower compared to the major washover sequence described above.

As documented, the geochemical pattern of core LEF 40 show distinct differences between all washover units and the above and below lying sediments. For instance, considerably higher $CaCO_3$ contents are observed in the washover sediments, which is interpreted to be related to numerous macro- and microfaunal remains and/or limestone gravel components in the sediment. However, the results also imply differences between the lower, thin bedded washover units and the uppermost thick event sequence. Here, a different pattern is documented by the S concentrations, which are remarkably higher in the main washover unit. High S values may correspond to the incorporation of organic material and the post-depositional formation of sulphat-aggregates in the sediment. Formation of these aggregates may be also linked to evaporation formed under subaerial conditions. It can thus be assumed that the uppermost washover unit was, at least partly, deposited above sea level. The two smaller washover units intercalating the lower sandy unit in turn most likely accumulated below water level and were not thick enough to be subaerially exposed, and no post-depositional S compounds have formed. For the thin gravel beds in the lower part minor changes of the backbeach morphology are assumed, while the deposition of the thick washover unit involved the formation of the fan structure and thus subsequent changes in depositional and environmental conditions. However, comparable results were presented by ENGEL et al. (in review) from the Caribbean, who report on a coarse grained, S rich event deposit and assume a tsunamigenic origin of the unit. Additionally, different provenance areas of the sediments comprising the uppermost washover unit and the thinner washover units at the base may be reflected by the S-distribution (see also CHAGUE-GOFF et al. 1999, ANDRADE et al. 2003, NICHOL et al. 2007).

As shown in *Chapter 2*, the formation of the Canali Stretti fan was related to a major disturbance of the north-eastern part of the Aghia Mavra barrier beach system and its temporary breakdown. However, the sedimentary and geochemical findings show that the breaching event and the formation of the Canali Stretti fan and, most likely, the disturbance and/or breakdown of the north-eastern part of the Aghia Mavra barrier beach system was triggered by an extreme wave event of high magnitude. Weather the lower intercalations were triggered by storm or tsunami events remains open. In either case, the magnitude of the related events was considerably lower.

For washover generation II, no ^{14}C-AMS results are available. At least relative chronological information is provided by the dating results of vibracore LEF 4 and the morphological interpretation of the two washover generations. Apparently, washover generation II is younger than washover generation I, which determines a post 139-378 cal AD formation. As documented in *Chapter 2*, the Canali Stretti fan structure is indicated in topographical maps from the middle of the 19th and the beginning of the 20th century. Therefore, the deposition of washover generation II took place before ~1850 cal AD. The formation of the Canali Stretti fan structure was related to a major disturbance of the coastal system, which must have occurred before the middle of the 19th century. Due to the sedimentary findings, a tsunami-induced formation is favoured. According to the available tsunami catalogues, possible related tsunami events took place at 1723, 1820 and 1825 AD (see also *Chapter 1,* VÖTT et al. 2006).

In a summary view, several similarities and differences were observed when comparing the different washover structures in the northern Lefkada Lagoon; first, the three washover fan structures differ in size and dimension. Moreover, only the smallest fan, the Canali Stretti fan, is characterized by a pronounced morphology. These differences may be explained by (i) different forming processes, e.g. the breaching or washover of the barrier beach, or (ii) a different age of the structure, which may involve an increased modification of the original morphology of older structures. For all washover structures, distinct subunits are documented. Three subunits were identified within the Gyra washover structure, up to five subunits within the Canali Stretti fan. For the Teki washover fan, at least two, probably three subunits can be separated. However, due to the ^{14}C-AMS dating results, two event generations contributed to the present coastal morphology. The older washover event was responsible for the formation of the Gyra and the Teki washover structures and is assumed to correspond to the well known 365 AD event, which was triggered by the catastrophic earthquake off western Crete. Formation of the younger washover generation must have taken place before 1850 AD and may be triggered by younger extreme wave events, probably corresponding to tsunami as well.

4.6 CONCLUSIONS

Detailed sedimentary, geochemical and microfaunal investigations were carried out on three fan-shaped washover structures in the northern Lefkada Lagoon. All washover structures consist of allochthonous, sublittoral and/or littoral sediments which have been transported into the backbeach area by high-energy wave dynamics. According to the presented results, the following can be concluded:

a) In the study area, washover and scour fan structures represent a prominent feature in coastal morphology. They are constituted of distinct event deposits determining the morphology of the structure.

b) The Gyra washover fan is build up of three sedimentary subunits. Each subunit is indicated by different sedimentary characteristics. Sedimentary and microfaunal investigations point to a tsunami-induced rather than a storm-induced formation of the washover fan. It is assumed that the subunits correspond to three major inundation phases during one tsunami event. Sediment transport and related deposition was largest during flooding impulses in the middle part of the tsunami wave train.

c) The formation of the Teki washover structure corresponds to an event induced flooding of the lagoonal area as well. A tsunamigenic formation of at least the upper allochthonous part of the sedimentary sequence is favoured. The navigability of the Canali Stretti during antiquity was interrupted by the corresponding washover event.

d) The formation of the Gyra washover fan took place at around or after 349 – 533 cal AD. The major washover event triggering the Teki washover structure took place later than 157 – 399 cal AD. Both washover structures therefore are assumed to be related to the same tsunami event. The 365 cal AD earthquake off western Crete is considered as a possible triggering source, since the related tsunami affected large parts of the eastern Mediterranean.

e) The smallest fan structure, the Canali Stretti fan, constitutes the youngest fan generation. It was triggered by a breaching event of the barrier beach. A tsunami-induced formation is favoured. Its formation was accompanied by a major disturbance of the coastal system, which must have occurred before the middle of the 19th century. Possible related tsunami events took place at 1723 AD, 1820 AD and 1825 AD.

In general, it can be stated that

f) Coring transects allow a comprehensive insight into the sedimentary architecture of washover structures, providing information about their origin. However, sediment trenches would allow studying the internal sedimentary structure in even more detail. Unfortunately, due to the high ground water level, trenches could not be carried out on top of the Gyra washover.

g) According to the presented results, only few washover and/or breaching events considerably altered the morphological pattern of the study area. Although the related changes must have taken place within hours, the resultant morphological structures persisted over several hundred to thousand years.

4.7 REFERENCES

Ad-hoc-Arbeitsgruppe Boden der Staatlichen Geologischen Dienste und der Bundesanstalt für Geowissenschaften und Rohstoffe (ed.) (2005). *Bodenkundliche Kartieranleitung*. Stuttgart, 438 pp.

AGIP (1982). Foraminiferi Padani (Terziario e Quaternario): Plate I–LII. Milano.

Andrade, C. (1992). Tsunami Generated Forms in the Algarve Barrier Islands (South Portugal). *Science of Tsunami Hazards*, 10(1), 21-34.

Andrade, C., Andrade, A.M., Kortekaas, S. & Dawson, A. (1997). Sedimentological traces of tsunamigenic overwash of the Martinhal lowland (Western Algarve, Portugal). *Seminário sobra a Zona Costeira do Algarve. Littoral ’97, Proceedings. International Symposium Eurocoast, July 1997, Faro, Portugal*, 11-17.

Andrade, C., Freitas, C., Miranda, J.M., Baptista, A.M., Cachao, M., Silva, P.G. & Munha, J. (2003). Recognizing possible tsunami sediments in the ultradissipative environment of the Tagus estuary (Portugal). In: Davis, R.A., Sallenger, A. & Howd, P. (eds.), *Crossing disciplinary boundaries – Proceedings of the international conference “Coastal Sediments 03” at Clearwater Beach, FL, USA, 18-23 May 2003 (CD-Rom)*.

Andrade, C., Freitas, M.C., Moreno, J. & Craveiro, S.C. (2004). Stratigraphical evidence of Late Holocene barrier breaching and extreme storms in lagoonal sediments of Ria Formosa, Algarve, Portugal. *Marine Geology*, 210(1-4), 339-362.

Bahlburg, H. (2008). Storm and tsunami deposits in light of cyclone Nargis, Burma, May 2 and 3, 2008. Paper presented at the 26th IAS Meeting of Sedimentology, Abstract Book, Bochum, Germany.

Bahlburg, H. & Weiss, R. (2007). Sedimentology of the December 26, 2004, Sumatra tsunami deposits in eastern India (Tamil Nadu) and Kenya. *International Journal of Earth Sciences*, 96(6), 1195-1209.

Barbano M.S., De Martini, P.M., Pantosti, D., Smedile, A., Del Carlo, P., Gerardi, F., Guarnieri, P. & Pirrotta, C. (2009). In search of tsunami deposits along the eastern coast of Sicily (Italy): state of the art. In: Guarnieri, P. (ed.), *Recent progress on Earthquake Geology,* (ISBN: 978-1-60876-147-0).

Bard, E., Hamelin, B., Arnold, M., Montaggioni, L., Cabioch, G., Faure, G. & Rougerie, F. (1996). Deglacial sea-level record from Tahiti corals and the timing of global meltwater discharge. *Nature*, 382, 241-244.

Beck, R., Burger, D. & Pfeffer, K.-H. (1995): Laborskript. *Kleinere Arbeiten aus dem Geographischen Institut der Universität Tübingen* 11.

Benetatos, C., Kiratzi, A., Roumelioti, Z., Stavrakakis, G., Drakatos, G. & Latoussakis, I. (2005). The 14 August 2003 Lefkada Island (Greece) earthquake: Focal mechanisms of the mainshock and of the aftershock sequence. *Journal of Seismology,* 9, 171–190.

Brückner, H., Vött, A., Schriever, A. & Handl, M. (2005). Holocene delta progradation in the eastern Mediterranenan - case studies in their historical context. *Mediterranée*, 1(2), 95-106.

Brückner, H., Kelterbaum, D., Marunchak, O., Porotov, A. & Vött, A. (in press). The Holocene sea level story since 7500 BP – Lessons from the Eastern Mediterranean, the Black and the Azov Seas. *Quaternary International*, doi:10.1016/j.quaint.2008.11.016.

Chagué-Goff, C. & Goff, J.R. (1999). Geochemical and sedimentological signature of catastrophic salt water inundations (tsunami), New Zealand. *Quaternary Australia*, 17, 38-48.

Choowong, M., Murakoshi, N., Hisada, K.-i., Charusiri, P., Charoentitirat, T., Chutakositkanon, V., Jankaew, K., Kanjanapayont, P. & Phantuwongraj, S. (2008). 2004 Indian Ocean tsunami inflow and outflow at Phuket, Thailand. *Marine Geology*, 248(3-4), 179-192.

Cimerman, F. & Langer, M.R. (1991). Mediterranean Foraminifera. *Academia Scientiarum et Artium Slovenica Classis IV*, 30.

Cocard, M., Kahle, H.-G., Peter, Y., Geiger, A., Veis, G., Felekis, S., Paradissis, D. & Billiris, H. (1999). New constraints on the rapid crustal motion of the Aegean region: recent results inferred from GPS measurements (1993–1998) across the West Hellenic Arc, Greece. *Earth and Planetary Science Letters,* 172, 39–47.

Coch, N.K. (1994). Geologic effects of hurricanes. *Geomorphology*, 10(1-4), 37-63.

Dawson, A. G. (1996). The Geological Significance of Tsunamis. *Zeitschrift für Geomorphologie N.F. Suppl. Vol.*, 102, 199-210.

Dawson, A.G. & Stewart, I. (2007). Tsunami deposits in the geological record. *Sedimentary Geology*, 200(3-4), 166-183.

Dawson, A.G., Hindson, R., Andrade, C., Freitas, C., Parish, R. & Bateman, M. (1995). Tsunami sedimentation associated with the Lisbon earthquake of 1 November AD 1755: Boca do Rio, Algarve, Portugal. *The Holocene*, 5(2), 209-215.

Donnelly, J.P. & Woodruff, J.D. (2007). Intense hurricane activity over the past 5,000 years controlled by El Nino and the West African monsoon. *Nature*, 447, 465-468.

Donnelly, J.P., Butler, J., Roll, S., Wengren, M. & Webb, T. (2004). A backbarrier overwash record of intense storms from Brigantine, New Jersey. *Marine Geology*, 210(1-4), 107-121.

Engel, M., Knipping, M., Brückner, H., Kiderlen, M. & Kraft, J.C. (2009). Reconstructing middle to late Holocene palaeogeographies of the lower Messenian plain (southwestern Peloponnese, Greece): Coastline migration, vegetation history and sea level change. *Palaeogeography, Palaeoclimatology, Palaeoecology*, 284(3-4), 257-270.

Engel, M., Brückner, H., Wennrich, V., Scheffers, A., Kelletat, D., Vött, A., Schäbitz, F., Daut, G., Willershäuser, T. & May, S.M. (in review). The back-barrier record of eastern Bonaire (Netherlands Antilles): new insights into the palaeo-tsunami history of the southern Caribbean.

Fairbanks, R.G. (1989). A 17,000-year glacio-eustatic sea level record: influence of glacial melting rates on the Younger Dryas event and deep-ocean circulation. *Nature*, 342, 637-642.

Fujino, S., Naruse, H., Suphawajruksakul, A., Jarupongsakul, T., Murayama, M. & Ichihara, T. (2008). Thickness and Grain-Size Distribution of Indian Ocean Tsunami Deposits at Khao Lak and Phra Thong Island, South-western Thailand. In: Shiki, T., Tsuji, Y., Yamazaki, T. & Minoura, K. (eds.), *Tsunamiites*. Amsterdam, pp. 123-132.

Fujiwara, O. & Kamataki, T. (2007). Identification of tsunami deposits considering the tsunami waveform: An example of subaqueous tsunami deposits in Holocene shallow bay on southern Boso Peninsula, Central Japan. *Sedimentary Geology*, 200, 295–313.

Goff, J., Chagué-Goff, C. & Nichol, S. (2001). Palaeotsunami deposits: a New Zealand perspective. *Sedimentary Geology*, 143, 1-6.

Goff, J., McFadgen, B.G. & Chagué-Goff, C. (2004). Sedimentary differences between the 2002 Easter storm and the 15th-century Okoropunga tsunami, southeastern North Island, New Zealand. *Marine Geology*, 204, 235-250.

Goff, J.R., McFadgen, B.G., Wells, A. & Hicks, M. (2008). Seismic signals in coastal dune systems. *Earth Science Reviews*, 89, 73–77.

Goff, J.R., Lane, E. & Arnold, J. (2009). The tsunami geomorphology of coastal dunes. *Natural Hazards and Earth System Sciences,* 9(3), 847-854.

Handl, M., Mostafawi, N. & Brückner, H. (1999). Ostracodenforschung als Werkzeug der Paläogeographie. *Marburger Geographische Schriften,* 134, 116-153.

Hawkes, A.D., Bird, M., Cowie, S., Grundy-Warr, C., Horton, B.P., Hwai, A.T.S., Law, L., Macgregor, C., Nott, J., Ong, J.E., Rigg, J., Robinson, R., Tan-Mullins, M., Sa, T.-T., Yasin, Z. & Aik, L.W. (2007). Sediments deposited by the 2004 Indian Ocean Tsunami along the Malaysia–Thailand Peninsula. *Marine Geology,* 242, 169–190.

Hellenic Military Geographical Service (HMGS) (1987). TM 1:50.000, sheet Vonitsa.

Hellenic Navy Hydrographic Service (HNHS) (1983). Bathymetrical chart 1:50.000, sheet Amvrakikos Gulf.

Hindson, R.A. & Andrade, C. (1999). Sedimentation and hydrodynamic processes associated with the tsunami generated by the 1755 Lisbon earthquake. *Quaternary International*, 56, 27-38.

Hindson, R.A., Andrade, C. & Dawson, A.G. (1996). Sedimentary processes associated with the tsunami generated by the 1755 Lisbon earthquake on the Algarve coast, Portugal. *Physics and Chemistry of the Earth*, 21(1-2), 57-63.

Kaminski, M.A., Aksu, A., Box, M., Hiscott, R.N., Filipescu, S. & Al-Salameen, M. (2002). Late Glacial to Holocene benthic foraminifera in the Marmara Sea: implications for Black Sea-Mediterranean Sea connections following the last deglaciation. *Marine Geology*, 190(1-2), 165-202.

Kortekaas, S. & Dawson, A.G. (2007). Distinguishing tsunami and storm deposits: An example from Martinhal, SW Portugal. *Sedimentary Geology*, 200, 208–221.

Kraus, N.C. (2003). Analytical Model of Incipient Breaching of Coastal Barriers. *Coastal Engineering Journal*, 45(4), 511–531.

Kraus, N.C., Militello, A., & Todoroff, G. (2002). Barrier Breaching Processes and Barrier Spit Breach, Stone Lagoon, California. *Shore & Beach*, 70(4), A714384.

Leatherman, S.P. & Williams, A.T. (1977). Lateral textural grading in overwash sediments. *Earth Surface Processes and Landforms,* 2(4), 333-341.

Lehmann-Hartleben, K. (1923). Die antiken Hafenanlagen des Mittelmeeres. *Klio-Beiheft* 14.

Louvari, E., Kiratzi, A.A. & Papazachos, B.C. (1999) The Cephalonia Transform Fault and its extension to western Lefkada Island (Greece). *Tectonophysics*, 308, 223-236.

Mamo, B., Strotz, L. & Dominey-Howes, D. (2009). Tsunami sediments and their foraminiferal assemblages. *Earth-Science Reviews,* 96(4), 263-278.

McMurtry, G.M., Tappin, D.R., Sedwick, P.N., Wilkinson, I., Fietzke, J. & Sellwood, B. (2007). Elevated marine deposits in Bermuda record a late Quaternary megatsunami. *Sedimentary Geology*, 200(3-4), 155-165.

Moore, A., Nishimura, Y., Gelfenbaum, G., Kamataki, T. & Triyono, R. (2006). Sedimentary deposits of the 26 December 2004 tsunami on the northwest coast of Aceh, Indonesia. *Earth Planets Space*, 58, 253–258.

Morton, R.A. & Sallenger Jr., A.H. (2003). Morphological Impacts of Extreme Storms on Sandy Beaches and Barriers. *Journal of Coastal Research*, 19(3), 560-573.

Morton, R.A., Gelfenbaum, G. & Jaffe, B.E. (2007). Physical criteria for distinguishing sandy tsunami and storm deposits using modern examples. *Sedimentary Geology*, 200, 184–207.

Morton, R.A., Goff, J.R., & Nichol, S.L. (2008). Hydrodynamic implications of textural trends in sand deposits of the 2004 tsunami in Sri Lanka. *Sedimentary Geology,* 207(1-4), 56-64.

Murray, J.W. (1973). *Distribution and ecology of living benthic foraminiferids*. London, 274 pp.

Murray, J.W. (2006). *Ecology and Applications of Benthic Foraminifers*. Cambridge, 439 pp.

Nanayama, F. & Shigeno, K. (2006). Inflow and outflow facies from the 1993 tsunami in southwest Hokkaido. *Sedimentary Geology,* 187(3-4), 139-158.

Nanayama, F., Shigeno, K., Satake, K., Shimokawa, K., Koitabashi, S., Miyasaka, S. & Ishii, M. (2000). Sedimentary differences between the 1993 Hokkaido-nansei-oki tsunami and the 1959 Miyakojima typhoon at Taisei, southwestern Hokkaido, northern Japan. *Sedimentary Geology*, 135(1-4), 255-264.

National and Atmospheric Administration (NASA) (2006). SRTM elevation data. http://www2.jpl.nasa.gov/srtm/.01/2006.

National and Atmospheric Administration (NOAA). http://www.ngdc.noaa.gov/hazard/tsu_db.shtml

National Observatory of Athens (NOA). http://www.gein.noa.gr/services/tsunami.htm

Nichol, S.L., Goff, J.R., Devoy, R.J.N., Chagué-Goff, C., Hayward, B. & James, I. (2007). Lagoon subsidence and tsunami on the West Coast of New Zealand. *Sedimentary Geology*, 200, 248–262.

Nichols, G. (2009). *Sedimentology and Stratigraphy*. Chichester, Hoboken, 419 pp.

Oberhummer, E. (1887). *Akarnanien, Ambrakia, Amphilochien, Leukas im Altertum*. München, 356 pp.

Papadopoulos, G.A., Karastathis, V.K., Ganas, A., Pavlides, S., Fokaefs, A. & Orfanogiannaki, K. (2003). The Lefkada, Ionian Sea (Greece), Shock, (Mw 6.2) of 14 August 2003: Evidence for the Characteristic Earthquake from Seismicity and Ground failures. *Earth, Planets and Space*, 55, 713-718.

Papazachos, B.C. & Dimitriu, P.P. (1991). Tsunamis In and Near Greece and Their Relation to the Earthquake Focal Mechanisms. *Natural Hazards*, 4, 161-170.

Paris, R., Lavigne, F., Wassmer, P. & Sartohadi, J. (2007). Coastal sedimentation associated with the December 26, 2004 tsunami in Lhok Nga, west Banda Aceh (Sumatra, Indonesia). *Marine Geology*, 238, 93-106.

Partsch, J. (1907). Das Alter der Inselnatur von Leukas. *Petermanns Geographische Mitteilungen,* 53, 269–278.

Reimer, P.J. & McCormac, F.G. (2002). Marine Radiocarbon Reservoir Corrections for the Mediterranean and Aegean Seas. *Radiocarbon*, 44(1), 159–166.

Reimer, P.J, Baillie, M.G.L., Bard, E., Bayliss, A., Beck, J.W., Blackwell, P.G., Bronk Ramsey, C., Buck, C.E., Burr, G.S., Edwards, R.L., Friedrich, M., Grootes, P.M., Guilderson, T.P., Hajdas, I., Heaton, T.J., Hogg, A.G., Hughen, K.A., Kaiser, K.F., Kromer, B., McCormac, F.G., Manning, S.W., Reimer, R.W., Richards, D.A., Southon, J.R., Talamo, S., Turney, C.S.M., van der Plicht, J. & Weyhenmeyer, C.E. (2009). IntCal09 and Marine09 Radiocarbon Age Calibration Curves, 0–50,000 Years cal BP. *Radiocarbon*, 51, 1111-1150.

Ruiz, F., Abad, M., Cáceres, L.M., Rodríguez Vidal, J., Carretero, M.I., Pozo, M. & González-Regalado, M.-L. (2010). Ostracods as tsunami tracers in Holocene sequences. *Quaternary Research,* 73(1), 130-135.

Sachpazi, M., Hirn, A., Clément, C., Haslinger, F., Laigle, M., Kissling, E., Charvis, P., Hello, Y., Lépine, J. C., Sapin, M. & Ansorge, J. (2000). Western Hellenic subduction and Cephalonia Transform: local earthquakes and plate transport and strain. *Tectonophysics,* 319(4), 301–319.

Sallenger Jr., A.H. (2000). Storm Impact Scale for Barrier Islands. *Journal of Coastal Research,* 16(3), 890-895.

Sato, H., Shimamoto, T., Tsutsumi, A. & Kawamoto, E. (1995). Onshore tsunami deposits caused by the 1993 Southwest Hokkaido and 1983 Japan Sea earthquakes. *Pure and Applied Geophysics,* 144(3), 693-717.

Sedgwick, P.E. & Davis, R.A. (2003). Stratigraphy of washover deposits in Florida: implications for recognition in the stratigraphic record. *Marine Geology,* 200(1-4), 31-48.

Sgarrella, F. & Moncharmont Zei, M. (1993). Benthic foraminifera of the Gulf of Naples (Italy): systematics and autoecology. *Bollettino della Società Paleontologica Italiana,* 32, 145–264.

Spiske, M. (2009). *Sedimentology and hydrodynamics of high-energy wave events*. PhD thesis, Wilhelms-Universität Münster.

Soloviev, S.L. (1990). Tsunamigenic Zones in the Mediterranean Sea. *Natural Hazards*, 3, 183-202.

Stanley, D.J. & Warne, A.G. (1994). Worldwide Initiation of Holocene Marine Deltas by Deceleration of Sea-Level Rise. *Science,* 265, 228-231.

Stefanakis, M.I. (2006). Natural Catastrophes in the Greek and Roman World: Loss or Gain? Four Cases of Seaquake-Generated Tsunamis. *Mediterranean Archaeology and Archaeometry,* 6(1), 61-88.

Stiros, S.C. (2001). The AD 365 Crete earthquake and possible seismic clustering during the fourth to sixth centuries AD in the Eastern Mediterranean: a review of historial and archaeological data. *Journal of Structural Geology,* 23, 545-562.

Sugawara, D., Minoura, K. & Imamura, F. (2008). Tsunamis and Tsunami Sedimentology. In: Shiki, T., Tsuji, Y., Yamazaki, T. & Minoura, K. (eds.), *Tsunamiites*. Amsterdam, 9-49.

Switzer, A.D., Pucillo, K., Haredy, R.A., Jones, B.G. & Bryant, E.A. (2005). Sea Level, Storm, or Tsunami: Enigmatic Sand Sheet Deposits in a Sheltered Coastal Embayment from Southeastern New South Wales, Australia. *Journal of Coastal Research,* 21(4), 655–663.

Switzer, A.D. & Jones, B.G. (2008a). Large-scale washover sedimentation in a freshwater lagoon from the southeast Australian coast: sea-level change, tsunami or exceptionally large storm? *The Holocene*, 18(5), 787-803.

Switzer, A.D. & Jones, B.G. (2008b). Setup, Deposition, and Sedimentary Characteristics of Two Storm Overwash Deposits, Abrahams Bosom Beach, Southeastern Australia. *Journal of Coastal Research*, 24(1A), 189-200.

Tuttle, M.P., Ruffman, A., Anderson, T. & Jeter, H. (2004). Distinguishing Tsunami from Storm Deposits in Eastern North America: The 1929 Grand Banks Tsunami versus the 1991 Halloween Storm. *Seismological Research Letters,* 75(1), 117-131.

U.S. Geological Survey (USGS) (2006). Earth Resources Observation & Science (EROS). Aster satellite data. http://edc.usgs.gov. 01/2006.

Uchida, J., Abe, K., Hasegawa, S., Fujiwara, O., Kamataki, T., Irizuki, T. & Hirakawa, K. (2005). Characteristics of faunal succession of foraminifera in tsunami-deposits and recognition of sauce area of particles — a case study of the Holocene tsunami deposits at Tateyama, Southern Part of the Boso Peninsula, Central Japan. *Abstract American Geophysical Union Fall Meeting,* #T11A-0361.

Vött, A. (2007). Relative sea level changes and regional tectonic evolution of seven coastal areas in NW Greece since the mid-Holocene. *Quaternary Science Reviews,* 26, 894–919.

Vött, A., Handl, M. & Brückner, H. (2002). Rekonstruktion holozäner Umweltbedingungen in Akarnanien (Nordwestgriechenland) mittels Diskriminanzanalyse von geochemischen Daten. *Geologica et Palaeontologica*, 36, 123-147.

Vött, A., May, M., Brückner, H. & Brockmüller, S. (2006). Sedimentary Evidence of Late Holocene Tsunami Events near Lefkada Island (NW Greece). *Zeitschrift für Geomorphologie N.F. Suppl. Vol.*, 146, 139-172.

Vött, A., Brückner, H., May, M., Lang, F. & Brockmüller, S. (2007). Late Holocene tsunami imprint at the entrance of the Ambrakian gulf (NW Greece). *Mediterranée,* 108, 43-57.

Vött, A., Brückner, H., Brockmüller, S., Handl, M., May, S.M., Gaki-Papanastassiou, K., Herd, R., Lang, F., Maroukian, H., Nelle, O. & Papanastassiou, D. (2009a). Traces of Holocene tsunamis across the Sound of Lefkada, NW Greece. *Global and Planetary Change,* 66(1-2), 112-128.

Vött, A., Brückner, H., May, S.M., Sakellariou, D., Nelle, O., Lang, F., Kapsimalis, V., Jahns, S., Herd, R., Handl, M. & Fountoulis, I. (2009b). The Lake Voulkaria (Akarnania, NW Greece) palaeoenvironmental archive - a sediment trap for multiple tsunami impact since the mid-Holocene. *Zeitschrift für Geomorphologie N.F.,* 53(SI 1), 1-37.

Walker, M.J.C. (2005). *Quaternary Dating Methods*. Chichester, 286 pp.

Wang, P. & Horwitz, M.H. (2007). Erosional and depositional characteristics of regional overwash deposits caused by multiple hurricanes. *Sedimentology*, 54(3), 545-564.

Williams, H.F.L. (2009). Stratigraphy, Sedimentology, and Microfossil Content of Hurricane Rita Storm Surge Deposits in Southwest Louisiana. *Journal of Coastal Research,* 25(4), 1041-1051.

Woodroffe, C. (2003). *Coasts – form processes and evolution*. Cambridge, 623 pp.

Woodroffe, C. & Nash, D. (1995). Sea level. *Progress in Physical Geography*, 19(3), 391-398.

Yulianto, E., Prendergast, A.L., Jankaew, K., Eipert, A.A., Atwater, B.F., Cisternas, M., Fernando, S. & Tejakusuma, I. (2007). Tsunami scour-fan deposits in south-central Chile. *Quaternary International*, 167–168, 469.

Chapter V

Block and boulder dislocation in the Lefkada coastal zone – evidence for extreme wave events of different intensity

5.1 STUDY BACKGROUND

Dislocated blocks and boulders constitute a prominent feature of coastal morphology along rocky shorelines worldwide. Besides fine-grained allochthonous marine sediments found in near-coast geological archives, those wave emplaced block deposits are attributed to extreme wave events, such as storm and/or tsunami (e.g. MASTRONUZZI & SANSO 2000, KELLETAT & SCHELLMANN 2002, WOODROFFE 2003, NOTT 2004, SCHEFFERS et al. 2005, HALL et al. 2006, SCICCHITANO et al. 2007, SCHEFFERS et al. 2009a, SWITZER & BURSTON 2010). However, in many cases the determination of the event source remains problematic and only the high-energy nature of the deposit is evident. Therefore, a debate on the distinguishability between tsunami and storm deposits in the geological record has evolved (e.g. KORTEKAAS & DAWSON 2007, MORTON et al. 2007, SWITZER & JONES 2008), and particularly the interpretation of block accumulations is a matter of intense discussion (e.g. NOTT 1997, SCHEFFERS & KELLETAT 2001; NOTT 2003a, 2003b, GOFF et al. 2004, WILLIAMS & HALL 2004, SCHEFFERS 2005; ROBINSON et al. 2006, MORTON et al. 2007, 2008, ROBINSON et al. 2008, SPISKE et al. 2008, SCHEFFERS et al 2009b, SWITZER & BURSTON 2009, MAY et al. in press). The application of hydraulic equations dealing with the wave energy necessary for the transportation of blocks, which may be helpful to estimate the event source and intensity, still exhibits considerable uncertainties (e.g. NOTT 1997, 2003a, 2003b, HANSOM et al. 2008, SWITZER & BURSTON 2010, IMAMURA et al. 2008, GOTO et al. 2009b, 2010, BENNER et al. in press). Since the determination of the event source and the ability to distinguish between tsunami- and storm-origin is important in palaeo-event research, analytical studies are required to improve our understanding of the geomorphological and sedimentary fingerprints of the different kinds of extreme wave events.

In this chapter, evidence of extreme wave-induced block accumulations of varying size found in different settings along the Lefkada barrier beach and its northern prolongation, the Plaka, is presented. Chronological aspects of the block movement and possible event sources are discussed. In contrast to tropical cyclones which can be excluded for the Mediterranean, the occurrence of tsunamis is likely due to the high seismic activity of the area (PAPAZACHOS & DIMITRIU 1991, BENETATOS et al. 2005). Besides tsunami events, only exceptionally large winter storms may be capable of dislocating large boulders in the study area.

5.2 STUDY AREA

The study area (Fig. 5-1) comprises the coastal zone between Lefkada Island, one of the Ionian Islands, and Aktium Headland, situated south of Preveza, NW Greece. The area between Lefkada and the Bay of Aghios Nikolaos is characterized by a comprehensive barrier beach system, separating the shallow Lagoon of Lefkada and the Lefkada Sound from the open Ionian Sea. The base of this barrier system is made up of beachrock down to approximately 12 m below present mean sea level (b.s.l). Towards the north, the recent beach ridge is shifted eastwards and separated from its beachrock base. This beachrock base, the so-called Plaka, is partly submerged, and, situated in direct prolongation of the Lefkada barrier beach, represents an older part of the spit system. Here, the remains of the Plaka represent a reef-like palaeo-coastline protecting the Bay of Aghios Nikolaos from the open sea and reducing wave energy to its leeward side (Fig. 5-1). On top of and along the Plaka and the Aghia Mavra barrier beach, the eastern part of the

Lefkada barrier beach system, wave-dislocated blocks and boulders represent a prominent feature in coastal and submarine morphology.

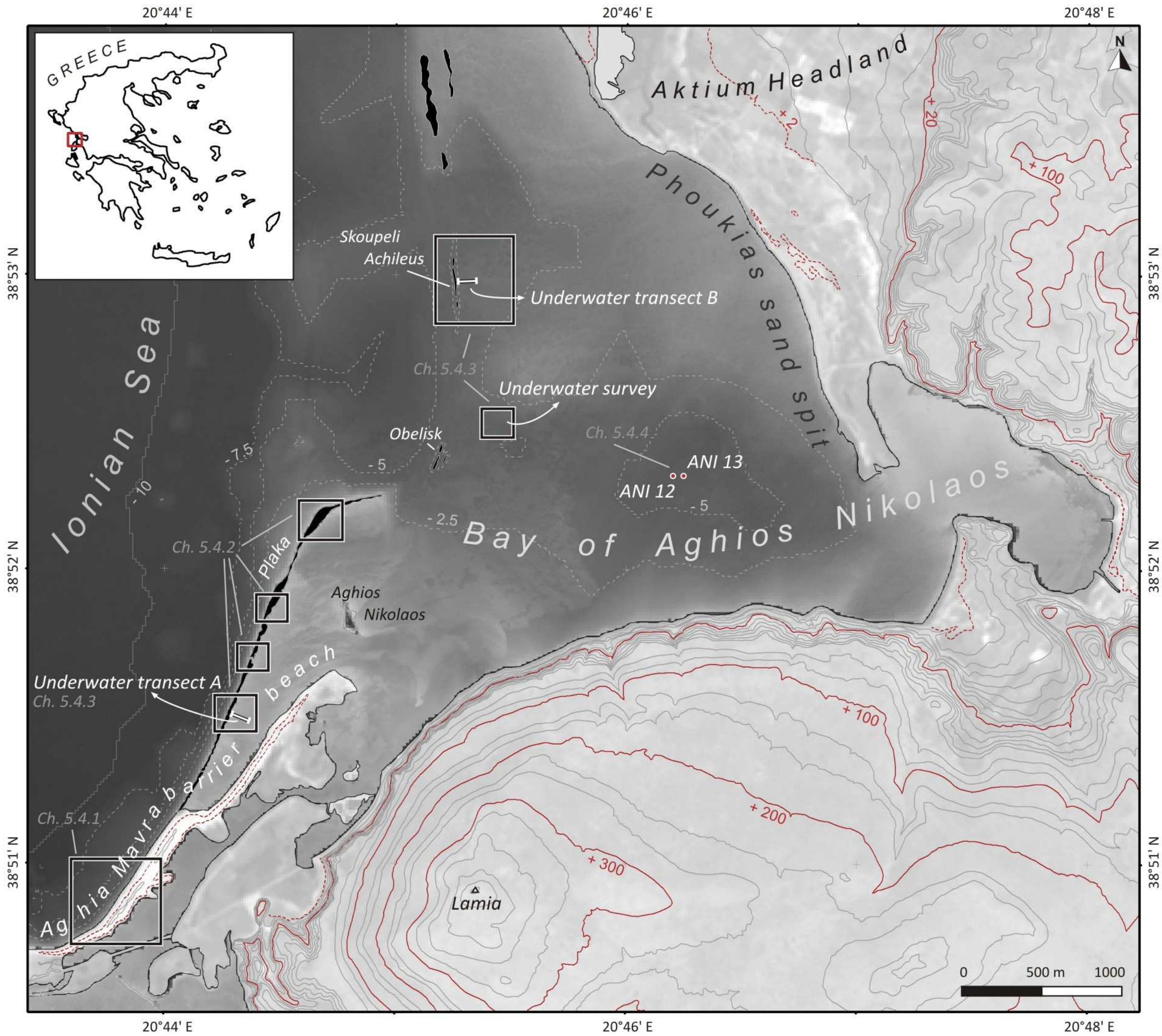

Fig. 5-1: Overview of the study area comprising the north-eastern part of the Lefkada barrier beach system, its northern prolongation, represented by the Plaka, and the Bay of Aghios Nikolaos [map based on Aster Satellite Image 2003 (USGS), Aerial photos 1985 & 1945 (HMGS), TM 1:50.000 sheets Lefkada & Vonitsa (HMGS), bathymetrical chart Amvrakikos Gulf (HNHS) and SRTM elevation data (NASA)]. Boxes mark sites of investigated block and boulder fields.

Situated in the north-western part of Greece, the study area is exposed to the northern part of the Hellenic Arc (see also Fig. 1-1 a, b). Here, the Cefalonia transform fault (CF) and the Lefkada transform fault (LF) are part of a triple junction area, connecting this zone of subduction with an area of continent-continent collision beginning off the southern Epirotic coast. Due to the remarkably high seismic activity of the CF and the LF (COCARD et al. 1999, LOUVARI et al. 1999, SACHPAZI et al. 2000, PAPADOPOULOS et al. 2003, BENETATOS et al. 2005) the study area belongs to the seismically most active regions of the Mediterranean and owns a high tsunamigenic potential (PAPAZACHOS & DIMITRIU 1991, SOLOVIEV 1990).

5.3 METHODS

During several field campaigns, geomorphological field surveys were carried out along the shorelines in the study area in order to document distribution and characteristics of block dislocation by extreme wave events. Investigated areas include the north-eastern part of the Lefkada barrier beach, the Plaka area and its northern prolongation, separating the Bay of Aghios Nikolaos from the open Ionian Sea. Survey was conducted along transects and subaqueous parts of the transects were studied by means of scuba diving. Geomorphological surveys along the subaerial part of the Plaka were conducted using a small motor boat.

Block fields detected during the geomorphological survey were documented and partly measured. In the Plaka area, sizes of selected boulders were estimated based on measurements of the x-, y- and z-axes using a measuring tape. All blocks and boulders were examined for rock pools on their surfaces. For weight calculation of the boulders, samples were brought to the laboratory. Volume of the samples was measured using the Archimedes principle of water displacement, and rock density was calculated together with the sample's weight. The weight of the boulders was extrapolated based on field measurements. For blocks and boulders where no samples were taken, rock density was estimated to ~2.2 g/cm³ (see also SCICCHITANO et al. 2007 for eastern Italy). In order to compare subaqueous block findings with the fine-grained sedimentary record in the Bay of Aghios Nikolaos, underwater corings were performed during scuba dives by pushing or pounding plastic pipes into the sea floor (see also appendix A, C, E).

For the chronological framework, organic material and mollusc remains taken from the sediment cores and from dislocated blocks were dated by ^{14}C-AMS (Table 5-1). ^{14}C-AMS ages were corrected for a marine reservoir effect of 400 years if necessary (REIMER & MCCORMAC 2002) using CALIB 6.0 software and the dataset of REIMER et al. (2009).

*Tab. 5-1: ^{14}C-AMS dating results used for the chronological interpretation in this study. Notes: b.s.l. – below mean sea level; unid. plant remains - unidentified plant remains; artic mollusc. – articulated mollusc; Lab. No. – laboratory number, University of Erlangen-Nürnberg (ERL), University of Kiel (KIA); * - marine reservoir correction with 400 years of reservoir age; ";" - there are several possible age intervals because of multiple intersections with the calibration curve; oldest and youngest age depicted.*

Sample	Depth (m b.s.l.)	Lab. No.	Sample description	δ^{13}C (ppm)	^{14}C age (BP)	1σ max-min (cal BC/AD)	2σ max-min (cal BC/AD)
AKT 12/2+ PR	7.62	ERL9798	unidentified plant	-13.2	585 ± 37	*1661;1802 AD	*1634-1830 AD
AKT 12/5 M	7.84	ERL9797	artic. *Dosinia exoleta*	-1.6	2353 ± 50	*95 BC - 43 AD	*166 BC-95 AD
PRN 1	3.00	KIA39796	unid. mollusc remains	0.03	>1954	modern	modern
PRN 3	2.90	KIA39797	unid. mollusc remains	0.12	>1954	modern	modern
PRN 4	2.80	KIA39798	unid. mollusc remains	7.18	2215 ± 30	*91-185 AD	*62-240 AD
PRN 5	4.20	KIA39799	unid. mollusc remains	0.0	570 ± 20	*1688;1803 AD	*1678-1816 AD

5.4 RESULTS

5.4.1 BLOCK TRANSPORT ALONG THE LEFKADA BARRIER BEACH

In the study area, block transport was documented along the entire Lefkada barrier beach system. Here, isolated blocks and block fields were detected especially at the seaward side and on top of the beach ridge. Along the Aghia Mavra beach ridge complex, detailed geomorphological surveys were carried out, including topographic DGPS measurements and morphometric analyses of dislocated beachrock slabs (see also Vött et al. 2008).

In the recent littoral zone, a block field of several beachrock slabs was detected. In some parts, the assemblage shows imbrication and several beachrock slabs are tilted or even turned upside down, indicated by bio-erosive features on the current lower surface. The largest measured slab was 3 m long and 2 m wide. Blocks and slabs apparently were torn out of the *in-situ* beachrock, existing in direct vicinity of the block field. Moreover, numerous beachrock blocks and slabs were encountered on top of the beach ridge. Most blocks are characterized by tubeworms and abundant boreholes from marine boring mussels on their surface, indicating their marine provenance. At many places, blocks are at least partly embedded into the unconsolidated beach ridge deposits. On top of the beach ridge, situated at ~3.50 m a.s.l. and ~30 m from the present shoreline, three imbricated beachrock slabs were encountered. The uppermost slab contained a large ceramic fragment integrated into the beachrock during the process of cementation. The ceramic fragment was dated to Classical–Hellenistic times (personal comm. F. Lang 2006, C. Melisch 2007) and represents a part of a well preserved roof tile.

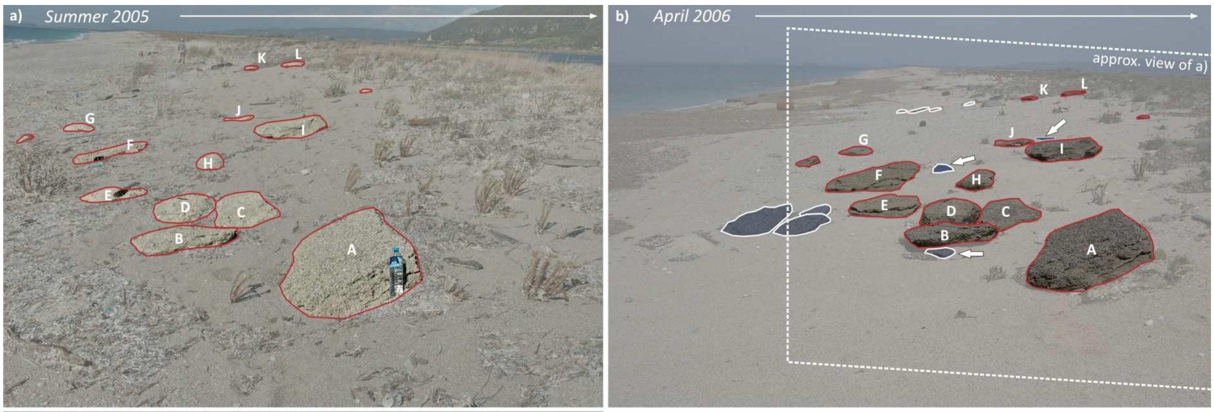

Fig. 5-2: Photo comparison of a block field at the Aghia Mavra barrier beach. While a number of blocks and/or slabs remained at their position (red frame) several blocks have been removed, others have been added to the assemblage (blue: 05-06; yellow: 06-08). Blocks marked by arrows were unambiguously dislocated during the investigated period. At least for the smaller components in block fields along the Lefkada barrier beach system a storm induced dislocation is proved.

A block field in the southern part of the beach ridge was photographed in 2005, 2006 and 2008 and photographs were compared in order to identify block dislocation due to common storm intensity. Results of the comparative analysis are depicted in Fig. 5-2 and show changes in the number of blocks, in the block assemblage and block distribution. However, the photos exhibit different perspectives, and a misinterpretation of the encountered changes may be considered due to the fact that some boulders may be covered by unconsolidated beach material. Nevertheless, particularly between 2006 and 2008, several smaller blocks accumulated at the seaward side of the beach ridge (yellow marked blocks, Fig. 5-2) in addition to the blocks existing in 2006 (red and blue marked blocks, Fig. 5-2). Some of the blocks documented in 2006 have been moved as well (for instance block B). However, most of the blocks and in particular the larger blocks (blocks A, I, F) did not change position within the entire period of time.

5.4.2 Boulder transport along the Plaka surface

The Plaka represents the remains of a former coastline running in north-north-eastern direction protecting the Bay of Aghios Nikolaos from the open Ionian Sea. It is completely made up of *in-situ* beachrock, which is, due to the seismo-tectonic activity of the area, fragmented and partly submerged (see also *Chapter 2*).

On top of the Plaka surface, numerous dislocated beachrock slabs and boulders of different size were encountered. The beachrock slabs and boulders were broken from the *in-situ* lying Plaka, uplifted and transported several meters landward, before they remained at their present position. Most probably, the rock slabs and blocks originate from the Plaka front area. The Plaka remains and most probably several dislocated boulders on top of the Plaka have been quarried in the past. They are present in numerous walls of older buildings in the study area (von Seidlitz 1927: 366f., Vött et al. 2008). However, as illustrated in Fig. 5-3b, boulders and boulder fields concentrate on four main locations at present.

Boulder field A consists of three main boulders. As Fig. 5-3e shows, the boulders are tilted and arranged in an imbrication train. Apparently, the westernmost boulder of the imbrication train is overturned, with the former surface facing downwards. This is indicated by well-developed rock pools found on the lower side of the block. According to our measurements it comprises ~14 m³ (xyz: 4.60 m x 3.50 m x 0.90 m). Due to calculations of the rock density, the weight of the boulder is estimated to ~30 t.

Boulder field B (Fig. 5-3b, f) is situated about 200 m north of boulder field A. Several boulders lie on top of the Plaka surface or, partly submerged, eastwards of the main part of the Plaka. At location C, one isolated boulder was encountered (Fig. 5-3g). Compared to the westernmost boulder at block field A, the size of the boulder is similar or even larger. Again, the boulder seems to be overturned by extreme wave action. It is worth noting that the position of the boulders did not change between 2003 and 2009.

Some 100 m north of the small island of Aghios Nikolaos, the Plaka trends to the east and is characterized by a broader surface, up to 100 m wide (Fig. 5-3b, h). Here, at least 6 major beachrock boulders and slabs constitute boulder field D. The beachrock slab depicted in Fig. 5-3j was calculated to around 5.5 m³ (xyz: 3.30 m x 3.10 m x 0.50 m) and ~12 t. As Fig. 5-3i shows, one major boulder broke into pieces during transportation or deposition, now forming two adjacent but isolated slabs of ~2 m³ (xyz: 1.90 m x 1.80 m x 0.65 m) and ~3 m³ (xyz: 2.10 m x 2.00 m x 0.6 m) size, respectively.

Assuming that the beachrock slab was intact before and at least during the initial phase of transportation, size and weight of the transported beachrock slab is estimated to around ~5 m³ and ~12 t.

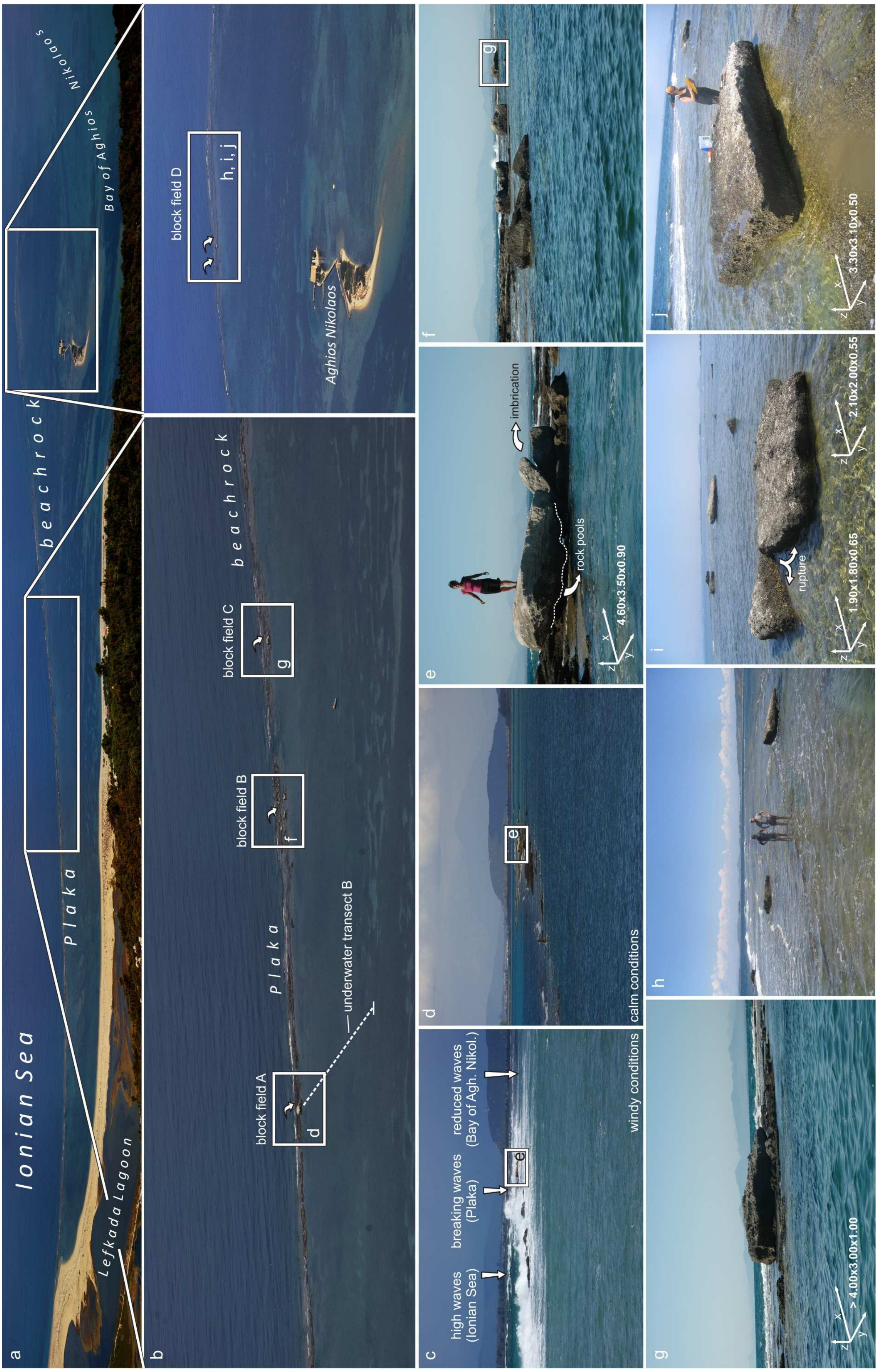
a
Ionian Sea
Lefkada Lagoon
Plaka
beachrock
Bay of Aghios Nikolaos
b
block field A
d
underwater transect B
Plaka
block field B
f
block field C
g
beachrock
block field D
h, i, j
Aghios Nikolaos
c
high waves (Ionian Sea)
breaking waves (Plaka)
reduced waves (Bay of Agh. Nikol.)
e
windy conditions
d
e
calm conditions
e
rock pools
imbrication
4.60x3.50x0.90
f
g
g
> 4.00x3.00x1.00
h
i
rupture
1.90x1.80x0.65
2.10x2.00x0.55
j
3.30x3.10x0.50

Fig. 5-3 (previous page): Dislocated boulders on top of the platform-like Plaka surface (a, b). At present, most boulders are assembled in four main boulder fields (b). Some boulders have been overturned (e), some cracked (i) during the process of the transport or during the impact on the surface. For location of block fields see Fig. 5-1.

5.4.3 Underwater surveys along the Plaka

Along two underwater transects, starting at the *in-situ* Plaka and reaching into the leeward area of the Bay of Aghios Nikolaos, numerous separate blocks und boulders east of the *in-situ* Plaka as well as ridges of isolated beachrock fragments down to 4 m water depth were discovered (Fig. 5-5 and Fig. 5-6, see also see Fig. 5-1).

Transect A

Transect A, 60 m long, is the northernmost transect and was carried out on the leeward side of an *in-situ* lying, submerged part of the former Plaka coastline called *Skoupeloi Achilleos*, situated in the western part of the Bay of Aghios Nikolaos (see Fig. 5-1). Up to about 20 m east of the Plaka, numerous isolated boulders of up to 10 m^3, some even 16 m^3, were detected (Fig. 5-5a, b). These boulders must have been transported from the *in-situ* lying Plaka. The boulder depicted in Fig. 5-5a was fractured during the process of the transport and/or during the impact on the sea floor. At some places, the boulders are tilted and show distinct imbrication (Fig. 5-5b). The surface of the boulder depicted in Fig. 5-5c, found at 16 m transect length in ~4 m water depth, showed a former whirlpool or rockpool structure, now densely covered with marine organisms. Since whirlpool and rockpool structures form due to continuous wave-induced currents, the hosting beachrock boulder thus origins from the windward side of the *in-situ* Plaka and was transported across the Plaka.

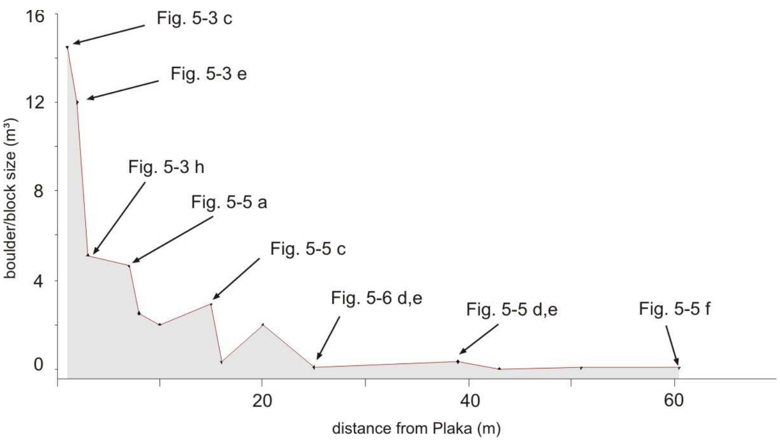

Fig. 5-4: Relation of block size and distance from the provenance area, found for the dislocated blocks and boulders along the Plaka surface and the underwater transects. The provenance area is assumed to be represented by the wave exposed western margin of the in-situ Plaka. For volume calculations see Fig. 5-3, Fig. 5-5 and Fig. 5-6.

A ridge of beachrock fragments, variable in size up to 1 m^3, was found around 40 m east of the Plaka (Fig. 5-5d, e). The ridge, situated in ~3 m water depth, is about 20–30m long and several meters wide. Dislocated blocks, up to 50 cm large, could be traced as far as ~60 m east of the *in-situ* Plaka along the transect (Fig. 5-5f). Without exception, the dislocated beachrock fragments are densely and homogeneously covered with algae and other marine organisms. Two mollusc remains were sampled from beachrock fragments found in the ridge at 40 m east of the *in-situ* Plaka. The samples were taken from the lower, downward facing surface of two beachrock slabs which were partly embedded into the sandy seafloor. ^{14}C-AMS datings of both molluscs resulted in modern ages meaning that the molluscs are younger than 1950 (see also Table 5-1).

Fig. 5-4 illustrates the relation between distance and calculated volume of the dislocated boulders and blocks found along the underwater transects. The exponential-like increase of block and boulder volume with decreasing distance to the Plaka indicates that the Plaka represents the provenance area for the encountered blocks. An exponential decrease of wave-induced transportation energy can be assumed on the leeward side of the Plaka.

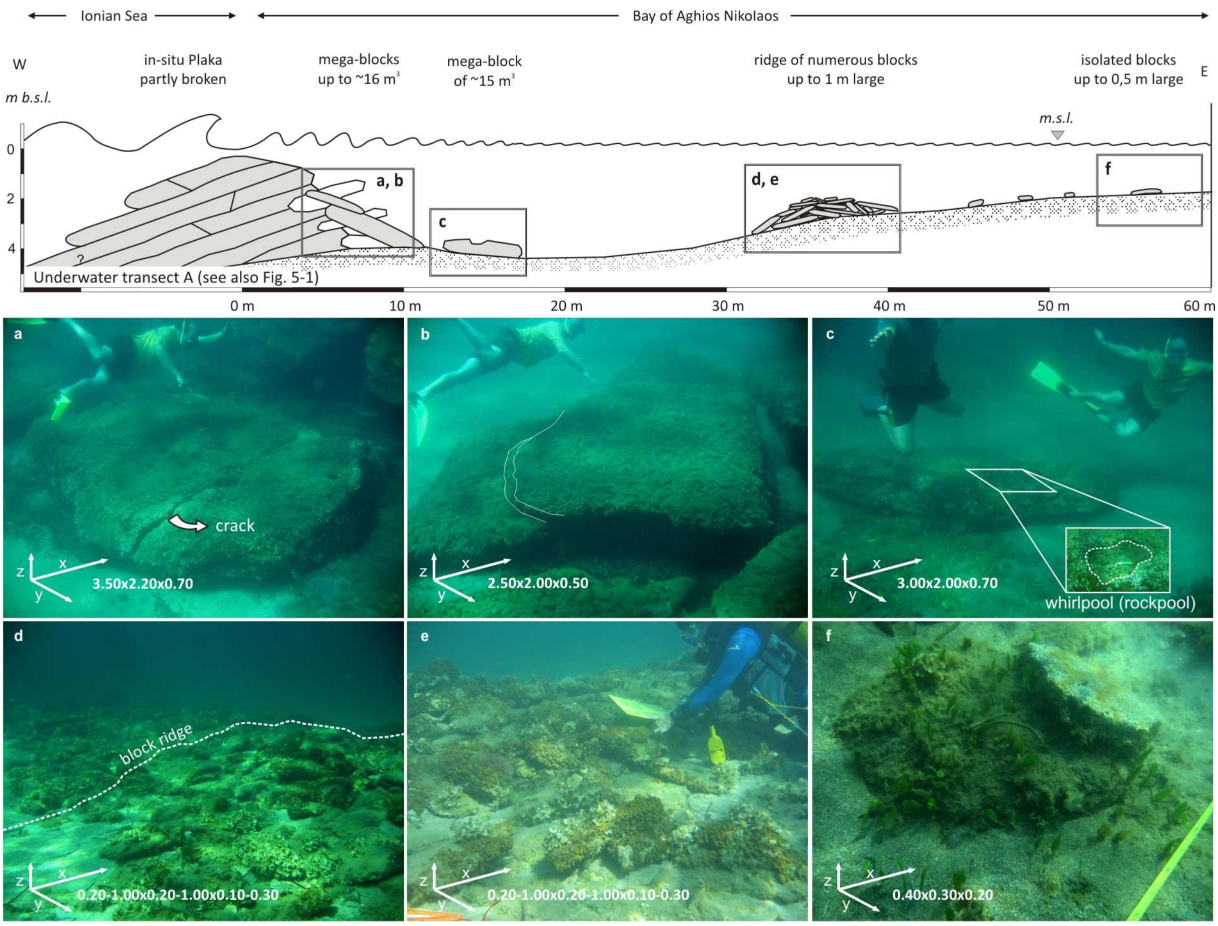

Fig. 5-5: Schematic profile of underwater transect A carried out east of Skoupeloi Achilleos (for location see Fig. 5-1). Photos illustrate a dislocated mega-block of ~10 m^3 at 18 m (a), a ridge of numerous blocks at ~40 m and (c) isolated beachrock slabs, up to 50 cm long, at 60 m east of the in-situ Plaka.

Transect B

Underwater transect B was carried out in the southern part of the Plaka, some 200 m north of the Plaka separation point. The transect starts at the southernmost block field A documented in Fig. 5-3e and stretches ~50 m into the lagoonal area to the east. About 10 m east of the *in-situ* Plaka, several isolated boulders of up to ~3 m³ were encountered (Fig. 5-6b). At 17 m profile length, size of dislocated boulders decreases to ~1.00 x 0.70 x 0.40 m maximum size (Fig. 5-6c), at around 25 m to < 1.00 m edge length (Fig. 5-6d, e). Here, the submarine surface is characterized by a block field with smaller beachrock blocks of up to 0.50 m length. The abundance of blocks decreases to the east – at 45 m east of the *in-situ* Plaka, only isolated beachrock blocks of smaller size were documented (Fig. 5-6f).

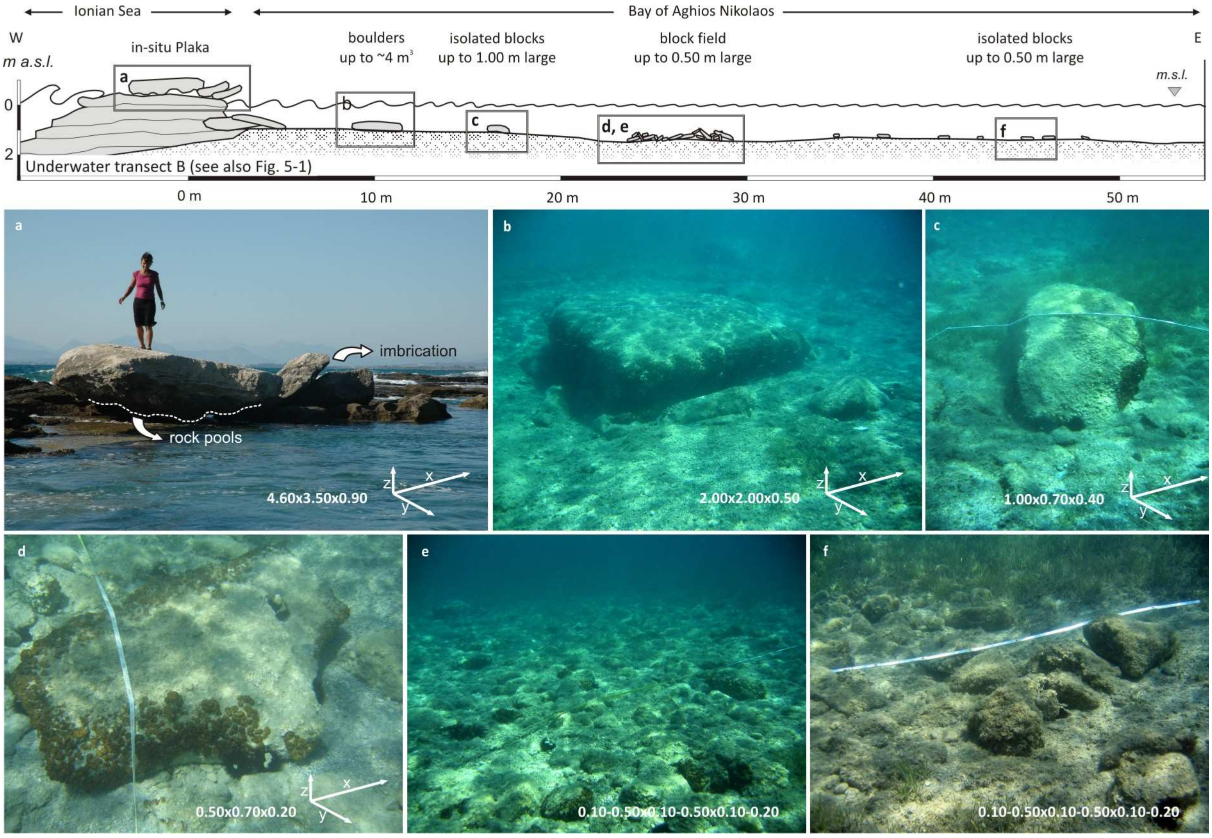

Fig. 5-6: Schematic profile of underwater transect B carried out east of the in-situ Plaka (for location see Fig. 5-1). Photos illustrate a dislocated mega-block of ~10 m³ at 18 m (a), a ridge of numerous blocks at ~40 m and (c) isolated beachrock slabs, up to 50 cm long, at 60 m east of the in-situ Plaka.

Further underwater block deposits

In the southern prolongation of the *Skoupeloi Achilleos* rise, *in-situ* beachrock remains were not encountered until the north-eastern tip of the Plaka, which is marked by an obelisk. For small fisher boats, this area is used as an entrance to the Bay of Aghios Nikolaos, since the reef-like beachrock barrier is missing here. Nevertheless, scuba diving surveys in this part of the Bay of Aghios Nikolaos revealed numerous huge beachrock plates and boulders, partly assembled to ramparts.

The detection of these ridges documents the existence of a former continuous beachrock structure which closed off the Bay of Aghios Nikolaos from the Ionian Sea. The beachrock remains of *Skoupeloi Achilleos* represent a relic of this former barrier. Sample PRN 4, a boring mollusc remain, was taken from the lower, downward facing surface of one smaller beachrock slab found within the field of beachrock plates, some 150 m east of the entrance to the Bay of Aghios Nikolaos. Since the lower surface of the slab was embedded into the sandy seabed and the mollusc is assumed to have been alive before the transport and deposition of the slab, the ^{14}C-AMS age of the mollusc remains of 53 - 235 cal AD (PRN 4, see Table 5-1) is considered to provide a *terminus ad* or *post quem* for the deposition of the beachrock slab and, most likely, of the entire assemblage

In addition to the mollusc samples taken from the beachrock ridge in transect A (samples PRN 1, PRN 3) and the above presented sample PRN 4, a fourth mollusc sample was taken from a comparable position several hundred meters north of *Skoupeloi Achilleos.* Here, the age of the mollusc was determined to 1678 - 1816 cal AD.

5.4.4 UNDERWATER CORES FROM THE BAY OF AGHIOS NIKOLAOS

In the central part of the Bay of Aghios Nikolaos, some 1200 m east of the obelisk, a circular depression is documented (see Fig. 5-1). Here, the sea floor is descending to ~7.50 m b.s.l. Two sediment cores ANI 12 and ANI 13 were obtained from the center of the circular depression in order to detect possible changes in the depositional pattern of the Bay of Aghios Nikolaos which may be related to the documented block transport at the Plaka to the west.

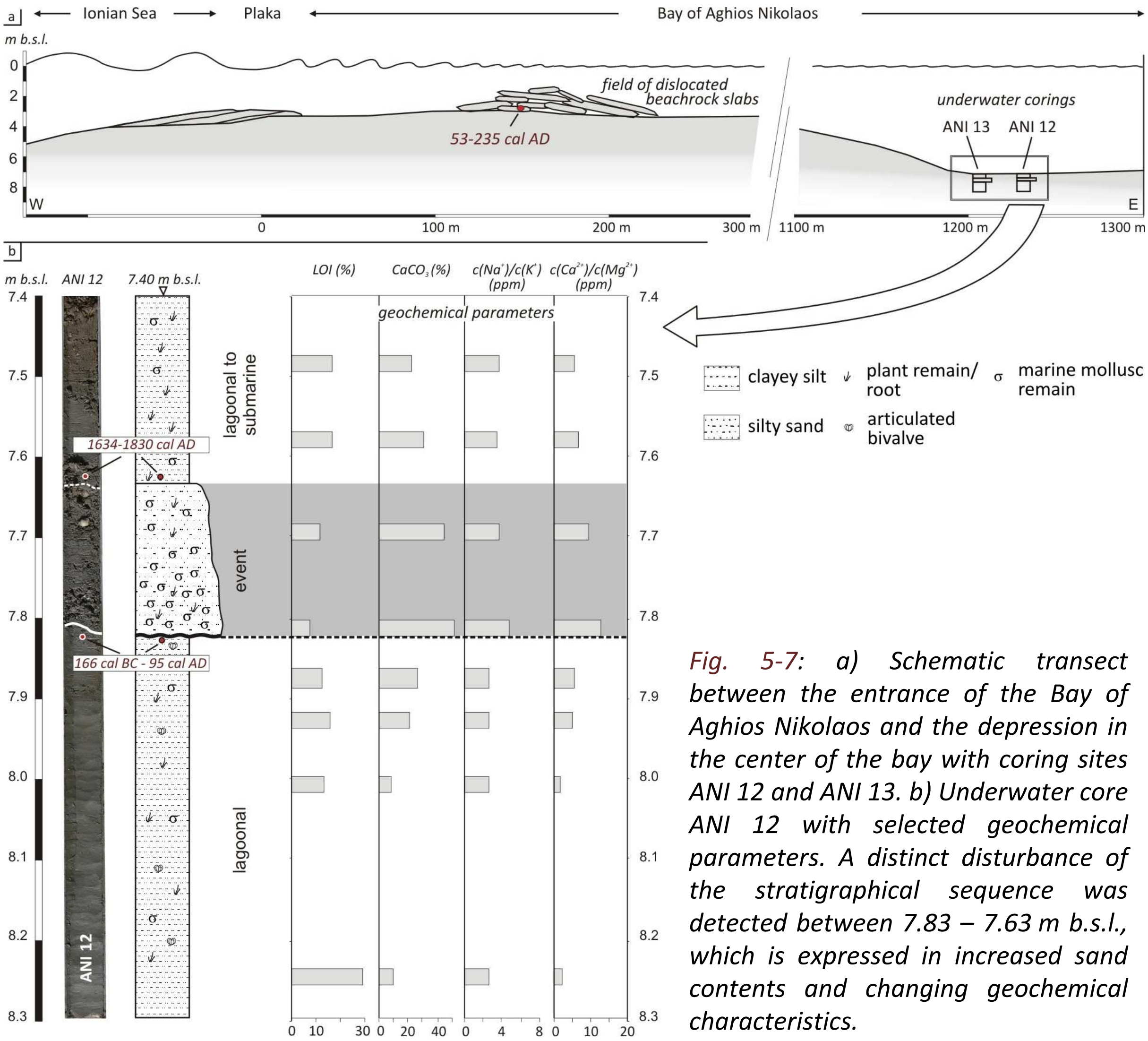

Fig. 5-7: a) Schematic transect between the entrance of the Bay of Aghios Nikolaos and the depression in the center of the bay with coring sites ANI 12 and ANI 13. b) Underwater core ANI 12 with selected geochemical parameters. A distinct disturbance of the stratigraphical sequence was detected between 7.83 – 7.63 m b.s.l., which is expressed in increased sand contents and changing geochemical characteristics.

Sediment core ANI 12 has a profile length of 0.89 m, sediment core ANI 13 of 0.85 m. Distance between the coring sites is approximately 20 m. Both core profiles show a similar sedimentary sequence. The base of core ANI 12 (Fig. 5-7) is characterized by a unit of grey, homogeneous clayey silt (8.29 m – 7.83 m b.s.l.), representing undisturbed, lagoonal or shallow marine depositional conditions of low energy. The low energy sequence is covered by a heterogeneous unit of silt, clay and fine sand (7.83 m – 7.63 m b.s.l.). Here, abundant shell debris and reworked (*ex-situ*) plant and/or root remains were found. Subsequently, the sandy unit is overlain by clayey to silty deposits, containing numerous root and plant remains found in *in-situ* position. Again, these sediments represent quiescent depositional conditions of a lagoonal environment.

As Fig. 5-7 shows, the Na content within the sandy unit shows a remarkable increase and remains relatively high within the subsequent sediment of re-establishing quiescent sedimentation. Within the sandy layer of disturbance, carbonate contents show elevated values and LOI values decrease. A distinct disturbance of the quiescent depositional conditions is therefore documented for the central part of the Bay of Aghios Nikolaos which was related to the accumulation of a heterogeneous, sandy shell debris unit.

An articulated specimen of *Dosinia exoleta* was found at 7.84 m b.s.l. and dated to 166 cal BC – 95 cal AD by ^{14}C-AMS technique. Taken from 1 cm below the intersecting sandy layer, it gives a *terminus post quem* for the disturbance of lagoonal sedimentation. Plant remains encountered directly above the sandy layer yielded and age of 1634–1830 cal AD (ANI 12/2+ PR, 7.62 m b.s.l.).

5.5 INTERPRETATION AND DISCUSSION

Fields of dislocated blocks and boulders are part of the entire coastline in the study area. All dislocated blocks and boulders derive from the comprehensive beachrock system, constituting the base of the Lefkada barrier beach, large parts of its foreshore area and the Plaka system to the north. In most cases, blocks and boulders are slab-shaped and were torn out of the *in-situ* beachrock, where (bio-) erosional processes weakened the beachrock structure. Rock density of dislocated blocks therefore can be estimated to ~2.00 – 2.50 g/cm³ for all transported blocks.

5.5.1 THE ORIGIN OF BLOCK AND BOULDER FIELDS IN THE STUDY AREA

On top of and in direct leeward vicinity of the Plaka, dislocated beachrock boulders are up to 16 m³ of size and more. Here, boulders were torn out of the seaward side of the *in-situ* Plaka, uplifted and transported several tens of meters across the beachrock platform before they remained at their present position. The imbrication of the blocks proves their extreme wave-generated displacement and deposition. Several boulders have been turned by wave action, indicated by rock pools at their lower surface, and some boulders have been broken during the transport. Moreover, at least for the cracked block found at block field D (Fig. 5-3i), a re-dislocation subsequent to the initial block transport and deposition can be excluded, since the configuration of the two block parts apparently documents their original post-transport position. Most likely, a re-dislocation would have resulted in a modification of this position, and a successive, stepwise shift of the beachrock slab without a change in the blocks' assemblage is unlikely. According to these findings, boulder transport occurred not only by a successive sliding motion across the Plaka platform – it must be assumed, that at least some boulders have been dislocated by floating, involving a disruption during their impact on the surface. Recurring field surveys document an unchanged position of the boulders during the last 6 years. This means that annually recurring winter storm activity of normal intensity does not shift or move the blocks, although, due to the low lying beachrock platform of the Plaka, most blocks are overflown by sea water and affected by wave action during winter storms (see also Fig. 5-3c).

Therefore, extreme wave events of exceptionally high intensity must be responsible for their dislocation. However, several authors refer to the importance of the pre-transport setting of dislocated boulders (e.g. NOTT 2003a, GOTO et al. 2009a, 2009b, BENNER et al. in press). A repeated transport of a boulder which is horizontally lying on top of the Plaka platform may require higher wave energies than its first disruption and dislocation from the seaward side of the *in-situ* Plaka. No information is available about the time of the boulders' dislocation.

A comparable pattern is documented by the underwater transects. Block deposits were encountered up to 60 m east of the *in-situ* Plaka and in up to 4 m water depth where they are not or little affected by regular wave action. The size of boulders in direct vicinity to the *in-situ* Plaka is comparable to the blocks found on top of the Plaka surface. Again, some of the blocks are indicated by impact-related cracks, and whirl- or rock pools point to a pre-transport wave- or sea level affected setting. The beachrock fragments and slabs comprising the ridges at ~30 – 40 m east of the *in-situ* lying Plaka are densely and homogeneously covered with marine algae and other marine organisms. This fact excludes that they are continuously moved by normal wave action or storms of annually recurrence frequency or comparable intensity. Although marine colonisation is known to take place quite rapidly, it is assumed that a stepwise, successive formation by continuous storm activity of the ridge of dislocated beachrock slabs encountered in underwater transect A would produce an inhomogeneous organic cover, since the assemblage of beachrock plates would recurrently be altered and/or enlarged. However, a sliding or shifting transport of the beachrock slabs, which is assumed for the movement of similar sized blocks across the Lefkada barrier beach, can be excluded for the underwater findings, since the area between the *in-situ* Plaka and the ridge is marked by a basin-like topography of up to 4.50 m water depth. Therefore, a floating transport of the beachrock fragments over a distance of up to 40 m and more must be assumed, which is expected only for exceptionally large storms and in particular tsunamis. Consequently, block dislocation and ridge assemblage must have been triggered by exceptionally large high energy wave events during the late Holocene.

Along the present Lefkada barrier beach, block fields and block deposits are characterized by considerably smaller block sizes. Most blocks were found on the seaward side and on top of the barrier beach and show maximum edge lengths of 1 m. Nevertheless, some beachrock slabs reach up to 1.50 m edge lengths. The comparison of photos taken from the same block field in 2005, 2006 and 2008 show that the number of blocks within the block field increased over the investigated period of time, although several uncertainties, such as a possible misinterpretation due to unconsolidated beach material covering smaller blocks, must be considered. It is thus assumed that recurring winter storms of regular intensity are capable of transporting smaller blocks and beachrock slabs of up to 1 m edge length some 30 m from the strandline and up to ~3 m on top of the beach ridge. However, also along the Lefkada barrier beach, the position of most of the blocks and in particular of the larger blocks has not been modified during the investigated period of time, and blocks remained at their position. This is also true for the beachrock slab hosting the ceramic fragment of Classical-Hellenistic times, which was found on the crest of the barrier beach. These findings prove that beachrock formation was in process during or after the 5th to 3rd centuries BC. Then, the beachrock was broken into plates and dislocated by marine water masses. For the dislocation of these blocks, extreme wave events of decadal or even centennial intensity are required. Whether their transport was triggered by tsunami or storm events remains open – regarding the remarkable short recurrence rates of tsunami events in the study area and adjacencies (see *Chapter 1*, VÖTT et al. 2006, SCHIELEIN et al. 2007), tsunami events are assumed to have contributed to the formation of these blocks as well.

Several studies have documented block and boulder transport due to extreme storms. However, in most cases, these findings are reported from areas which are affected by tropical cyclones. In Jamaica, for instance, a large boulder of approximately 80 t was moved 2 m during hurricane Dean in 2007 (ROBINSON et al. 2008), and storm dislocated boulders for instance are reported from Kudaka, Japan (GOTO et al. 2009a, 54 t), Hawaii (NOORMETS et al. 2002, 96 t) and Bonaire (SCHEFFERS & SCHEFFERS 2006, 25 t). From the temperate zone, block dislocation by storms was for instance reported from the western and northern part of Europe (WILLIAMS & HALL 2004, ETIENNE & PARIS 2008, HANSOM & HALL 2009) where extra-tropical North Atlantic cyclones involve strong winds and extreme wave heights, due to the related long fetch of the waves. These findings unambiguously document that storm waves are capable to lift and transport large boulders of even significantly larger size. However, it must be considered that storm energy may be considerably lower in the study area compared to the above mentioned localities. In this context, further investigations on wave heights and wave intensities during storm events in the eastern Ionian Sea are required which may evaluate the application of hydraulic equations to estimate the wave energy necessary for the transportation of the boulders (e.g. following the approach of NOTT 1997, 2003a, 2003b, IMAMURA et al. 2008, GOTO et al. 2009a, 2009b, 2010, BENNER et al. in press).

Due to the presented results, a floating transport of numerous of the dislocated blocks and boulders found on top of the Plaka surface and along the underwater transects must be assumed. Due to their considerably higher velocity, their greater inundation depth and the resulting increased drag and lift forces, the capability of tsunami waves to transport boulders, in particularly in by floating, is significantly higher (NOTT 2003a, BENNER et al. in press). As discussed in *Chapters 3* and *4*, investigations on the near coastal fine-grained geological record unambiguously indicate episodic high magnitude events of low frequency, and tsunami events are considered to have influenced the coastal evolution of the study area. Tsunami events are thus assumed to have contributed to the formation of boulder fields in the study area and are particularly considered to be responsible for dislocation of the larger boulders found on top of the Plaka and along the underwater transects. However, the influence of storms at least on the formation of block fields with smaller components along the Lefkada barrier beach is documented. Some block fields are assumed to be the product of several generations of extreme wave events, and both storms and tsunami may have contributed to their formation. Therefore, the occurrence of block fields and block assemblages in the study area is a product of both tsunami and storm. In this context, WOODROFFE (2003: 464) states that “it seems likely that similar morphology can result from several different causes (equifinality), and it will require further comparison to discriminate the cause of particular deposits”, which is particularly true for wave-dislocated boulder deposits along rocky shorelines.

5.5.2 Chronological implications

For the study area and the adjacent coastal zone recurrent disturbances of the coastal system are documented by investigations on (i) the geomorphological and the geomorphodynamic situation (*Chapter 2*) and (ii) on the fine-grained sedimentary record in near-coast geological archives (*Chapter 3* and *Chapter 4*). At least some of these disturbances are assumed to be triggered by tsunami events (see also Vött et al. 2006, 2007, 2008, 2009a, 2009b, May et al. 2007, 2008). A number of findings point to the tsunami-induced breakdown of the former Plaka coastline and a subsequent reorganization of the coastline at ~1000 cal BC and/or ~300 cal BC. For the northern part of the Lefkada Lagoon, a major washover event has shown to be most likely of tsunamigenic origin and was dated to ~300 AD. Moreover, tsunami catalogues report on a number of tsunami events which affected the study area, particularly since the beginning of the 18th century. Thus, both historical reports and sedimentary findings evidence the recurring impact of tsunami on the study area by now.

The ^{14}C-AMS dating of a mollusc fragment sampled from the embedded lower surface of a beachrock slab found in the ridge east of the entrance of the Bay of Aghios Nikolaos yielded an age of 53 - 235 cal AD (PRN 4). Assuming the death of the mollusc as a consequence of its transport and its embedding into the sandy sea floor it can be assumed that the beachrock slab was dislocated to its present position at around or after 53 - 235 cal AD. However, the dislocation of the beachrock slab may have occurred considerably later than the obtained ^{14}C-AMS age of the colonising mollusc, since the mollusc may have been dead before. About 1000 m east of the ridge, the sedimentary sequence of the underwater corings ANI 12 and ANI 13 document a distinct disturbance of depositional conditions in the central part of the Bay of Aghios Nikolaos. Here, quiescent, lagoon-like deposition is intercalated by a sandy layer which is characterized by shell debris and a considerably different geochemical pattern compared to the units above and below, and which must have accumulated after 166 cal BC - 46 cal AD (ANI 12/5 M). Therefore, a contemporaneous dislocation of the beachrock slab or even the formation of the ridge of beachrock slabs some 1000 m west of the drilling sites can be assumed. Moreover, a comparable age is assumed for the two main washover structures dominating the present coastal morphology in the northern part of the Lagoon of Lefkada (see *Chapter 4*). From the adjacent southern part of the Phoukias spit, a shell rich event deposit intercalating lagoonal deposits was dated to around or after 238 – 39 cal BC (see *Chapter 3*). The disturbance documented in the sedimentary record of core ANI 12 thus may also be related to the deposition of the event deposit found in the sedimentary sequence of the southern Phoukias spit. However, due to the δ^{13}C-value of ~7 ‰ of sample PRN 4, determination of the marine reservoir age may involve several uncertainties. Further comparable findings are needed to support the presented findings. The upper ^{14}C-AMS dating sampled from core ANI 12 yielded an age of 1634–1830 cal AD (ANI 12/2+ PR) and most likely represent sub-recent root remains.

Two fragments of colonising molluscs were sampled from the lower, sand-embedded side of two different beachrock plates which were found in the underwater block ridge east of *Skoupeloi Achilleos*. The samples were dated by ^{14}C-AMS and resulted in modern ages. Assuming that the mollusc died as a consequence of the block's transport and its embedding into the sea floor, the dislocation of the beachrock plates or at least of the two sampled plates took place after 1950.

However, it must also be considered that (i) dislocation of the beachrock plates occurred before 1950, but the lower side of the sampled plates was not entirely embedded into the seafloor and molluscs could colonise the plates after 1950, or (ii) dislocation of the beachrock plates occurred before 1950, but position of the fragments changed after 1950. These considerations are also true for sample PRN 5, which was taken from the lower, sand-embedded side of a beachrock slab found in a comparable assemblage of beachrock slabs several hundred meters north of *Skoupeloi Achilleos* and yielded an ^{14}C-AMS age of 1678 - 1816 cal AD. Younger events thus must also be considered to have triggered the dislocation of these beachrock slabs, and both tsunami and storm must be taken into account.

For the largest boulders found on top of and in direct vicinity of the Plaka, no direct chronological information is available. Nevertheless, dislocation of these boulders must have taken place after the former Plaka coastline became inactive. According to the findings presented in *Chapter 3*, a first disturbance of this former coastline occurred at around or after 1000 cal BC, though clear evidence for the breakdown of the barrier is documented not before ~300 cal BC. Thus, the Plaka boulder fields are definitely younger than 1000 BC and most probably even younger than ~300 cal BC. A contribution of (i) the tsunami at around or after ~300 AD triggering large washover fans in the Lefkada Lagoon (*Chapter 4*) and (ii) the extreme wave event involving the last major disturbance of the Lefkada barrier beach (*Chapter 2*) seems to be likely.

5.6 CONCLUSIONS

Within this study, subaerial and subaqueous investigations on boulder and block fields along the Lefkada barrier beach and the Plaka were carried out. Moreover, underwater corings were performed in order to link relate/link these coarse grained event deposits with the sedimentary record of fine grained, near-coast geological archives. According to the presented results, the following can be concluded:

a) Transport of the larger boulders found on top of the Plaka surface and along the underwater transects occurred not only by a successive sliding motion across the Plaka platform. A floating transport is assumed for numerous of the dislocated blocks and boulders which favours a tsunamigenic origin.

b) The position of the larger boulders on top of the Plaka surface remained unchanged during the last 6 years. Winter storm activity of normal intensity does not shift or move the blocks and only extreme wave events of exceptionally high intensity, in particular tsunami, are considered to be responsible for their dislocation.

c) Recurring winter storms of regular, annual or decadal intensity are capable of transporting smaller blocks and beachrock slabs of up to 1 m edge length and contribute to the block fields along the present Lefkada barrier beach.

d) For the formation of the block and boulder fields in the study area both tsunami and storm events must be taken into account. Present morphology is thus the result of an interrelation of both processes.

e) The Plaka boulder fields are younger than 1000 BC, most probably even younger than ~300 cal BC. Block and boulder dislocation may be triggered by tsunami events which are inferred from investigations on fine grained offshore (this study) and near-coast (*Chapters 3* and *4*) geological archives in the study area. Older events occurred at ~300 BC and at ~300 AD. Additionally, younger extreme wave events, for instance the event which involved the most recent major disturbance of the Lefkada barrier beach system, must be assumed to have dislocated blocks and boulders.

f) The question of determining and localizing the event source and the ability to distinguish between tsunami and storm origin is important in palaeo-event research; determining the forming process of palaeo-boulder and block fields along rocky shorelines remains a main challenge in extreme wave event research. However, the contribution of tsunami events to the boulder and block fields documented in this study is assumed.

g) Further analytical studies are required to improve our understanding of the geomorphological and sedimentological fingerprints of the different kinds of extreme wave event deposits. For the investigated area, these studies may focus on chronological aspects of the boulder fields' evolution, providing a link to the well documented fine-grained sedimentary record of near-coast geological archives. Additionally, investigations on the intensity of storm events in the Ionian Sea may be of particular interest.

5.7 REFERENCES

Benetatos, C., Kiratzi, A., Roumelioti, Z., Stavrakakis, G., Drakatos, G. & Latoussakis, I. (2005). The 14 August 2003 Lefkada Island (Greece) earthquake: Focal mechanisms of the mainshock and of the aftershock sequence. *Journal of Seismology,* 9, 171–190.

Benner, R., Browne, T., Brückner, H., Kelletat, D. & Scheffers, A. (in press). Boulder Transport by Waves: Progress in Physical Modeling. Zeitschrift für Geomorphologie, SI.

Cocard, M., Kahle, H.-G., Peter, Y., Geiger, A., Veis, G., Felekis, S., Paradissis, D. & Billiris, H. (1999). New constraints on the rapid crustal motion of the Aegean region: recent results inferred from GPS measurements (1993–1998) across the West Hellenic Arc, Greece. *Earth and Planetary Science Letters,* 172, 39–47.

Etienne, S. & Paris, R. (2008). Boulder accumulations related to storms on the south coast of the Reykjanes Peninsula (Iceland). In: Mastronuzzi, G., Pignatelli, C., Sansò, P., Milella, M. & Selleri, G. (eds.), *2nd International Tsunami Field Symposium, 22-27 September 2008, Ostuni - Puglia (Italy) and Lefkada (Ionian Islands, Greece), Abstract Book*. GI^{2}S Coast Research Publication, 6, 33-35.

Goff, J., McFadgen, B.G. & Chagué-Goff, C. (2004). Sedimentary differences between the 2002 Easter storm and the 15th-century Okoropunga tsunami, southeastern North Island, New Zealand. *Marine Geology,* 204, 235-250.

Goto, K., Okada, K. & Imamura, F. (2009a). Characteristics and hydrodynamics of boulders transported by storm waves at Kudaka Island, Japan. *Marine Geology*, 262, 14-24.

Goto, K., Okada, K. & Imamura, F. (2009b). Importance of the Initial Waveform and Coastal Profile for Tsunami Transport of Boulders. *Polish Journal of Environmental Studies,* 18(1), 53-61.

Goto, K., Okada, K. & Imamura, F. (2010). Numerical analysis of boulder transport by the 2004 Indian Ocean tsunami at Pakarang Cape, Thailand. *Marine Geology*, 268(1-4), 97-105.

Hall, A.M., Hansom, J.D., Williams, D.M. & Jarvis, J. (2006). Distribution, geomorphology and lithofacies of cliff-top storm deposits: Examples from the high-energy coasts of Scotland and Ireland. *Marine Geology,* 232(3-4), 131-155.

Hansom, J.D. & Hall, A.M. (2009). Magnitude and frequency of extra-tropical North Atlantic cyclones: A chronology from cliff-top storm deposits. *Quaternary International,* 195(1-2), 42-52.

Hansom, J.D., Barltrop, N.D.P. & Hall, A.M. (2008). Modelling the processes of cliff-top erosion and deposition under extreme storm waves. *Marine Geology,* 253(1-2), 36-50.

Hellenic Military Geographical Service (HMGS) (1987). TM 1:50.000, sheets Vonitsa & Lefkada.

Hellenic Navy Hydrographic Service (HNHS) (1983). Bathymetrical chart 1:50.000, sheet Amvrakikos Gulf.

Imamura, F., Goto, K. & Ohkubo, S. (2008). A numerical model for the transport of a boulder by tsunami. *Journal of Geophysical Research*, 113, C01008.

Kelletat, D. & Schellmann, G. (2002). Tsunamis on Cyprus: field evidences and 14C dating results. *Zeitschrift für Geomorphologie N.F. Suppl. Vol.*, 137, 19-34.

Kortekaas, S. (2002). *Tsunamis, storms and earthquakes: Distinguishing coastal flooding events.* PhD thesis, Coventry University.

Kortekaas, S. & Dawson, A.G. (2007). Distinguishing tsunami and storm deposits: An example from Martinhal, SW Portugal. *Sedimentary Geology*, 200, 208–221.

Louvari, E., Kiratzi, A.A. & Papazachos, B.C. (1999) The Cephalonia Transform Fault and its extension to western Lefkada Island (Greece). *Tectonophysics*, 308, 223-236.

Mastronuzzi, G. & Sanso, P. (2000). Boulders transport by catastrophic waves along the Ionian coast of Apulia (southern Italy). *Marine Geology,* 170, 93-103.

May, S.M., Vött, A., Brückner, H. & Brockmüller, S. (2007). Evidence of tsunamigenic impact on Actio headland near Preveza, NW Greece. *Coastline Reports*, 9, 115-125.

May, S.M., Vött, A., Sakellariou, D., Kapsimalis, V., Herd, R. & Brückner, H. (2008). On- and offshore tsunami traces around Actio Headland (NW Greece). *Geophysical Research Abstracts*, 10, EGU2008-A-11034.

May, S.M., Willershäuser, T. & Vött, A. (in press). Boulder transport by high-energy wave events at Cap Bon (NE Tunisia). *Coastline Reports*.

Morton, R.A., Gelfenbaum, G. & Jaffe, B.E. (2007). Physical criteria for distinguishing sandy tsunami and storm deposits using modern examples. *Sedimentary Geology*, 200, 184–207.

Morton, R.A., Richmond, B.M., Jaffe, B.E. & Gelfenbaum G. (2008): Coarse-Clast Ridge Complexes of the Caribbean: A Preliminary Basis for Distinguishing Tsunami and Storm-Wave Origins. *Journal of Sedimentary Research*, 78(9), 624-637.

National and Atmospheric Administration (NASA) (2006). SRTM elevation data. http://www2.jpl. nasa.gov/srtm/.01/2006.

Noormets R., Felton E.A. & Crook, K.A.W. (2002). Sedimentology of rocky shorelines: 2 – Shoreline megaclasts on the north shore of Oahu, Hawaii – origins and history. *Sedimentary Geology*, 150, 31-45.

Nott, J. (1997). Extremely high-energy wave deposits inside the Great Barrier Reef, Australia: determining the cause - tsunami or tropical cyclone. *Marine Geology*, 141, 193-207.

Nott, J. (2003a). Tsunami or Storm Waves? - Determining the Origin of a Spectacular Field of Wave Emplaced Boulders Using Numerical Storm Surge and Wave Models and Hydrodynamic Transport Equations. *Journal of Coastal Research,* 19(2), 348-356.

Nott, J. (2003b). Waves, coastal boulder deposits and the importance of the pre-transport setting. *Earth and Planetary Science Letters*, 210, 269-276.

Nott, J. (2004). The tsunami hypothesis – comparisons of the field evidence against the effects, on the Western Australian coast, of some of the most powerful storms on Earth. *Marine Geology,* 208, 1-12.

Papadopoulos, G.A., Karastathis, V.K., Ganas, A., Pavlides, S., Fokaefs, A. & Orfanogiannaki, K. (2003). The Lefkada, Ionian Sea (Greece), Shock, (Mw 6.2) of 14 August 2003: Evidence for the Characteristic Earthquake from Seismicity and Ground failures. *Earth, Planets and Space,* 55, 713-718.

Papazachos, B.C. & Dimitriu, P.P. (1991). Tsunamis In and Near Greece and Their Relation to the Earthquake Focal Mechanisms. *Natural Hazards*, 4, 161-170.

Reimer, P.J. & McCormac, F.G. (2002). Marine Radiocarbon Reservoir Corrections for the Mediterranean and Aegean Seas. *Radiocarbon*, 44(1), 159–166.

Reimer, P.J, Baillie, M.G.L., Bard, E., Bayliss, A., Beck, J.W., Blackwell, P.G., Bronk Ramsey, C., Buck, C.E., Burr, G.S., Edwards, R.L., Friedrich, M., Grootes, P.M., Guilderson, T.P., Hajdas, I., Heaton, T.J., Hogg, A.G., Hughen, K.A., Kaiser, K.F., Kromer, B., McCormac, F.G., Manning, S.W., Reimer, R.W., Richards, D.A., Southon, J.R., Talamo, S., Turney, C.S.M., van der Plicht, J. & Weyhenmeyer, C.E. (2009). IntCal09 and Marine09 Radiocarbon Age Calibration Curves, 0–50,000 Years cal BP. *Radiocarbon*, 51, 1111-1150.

Robinson, E., Khan, S., Rowe, D.A. & Coutou, R. (2008). Size of shoreline boulders moved and emplaced by recent hurricanes, Jamaica. In: Mastronuzzi, G., Pignatelli, C., Sansò, P., Milella, M. & Selleri, G. (eds.), *2nd International Tsunami Field Symposium, 22-27 September 2008, Ostuni - Puglia (Italy) and Lefkada (Ionian Islands, Greece), Abstract Book*. GI^2S Coast Research Publication, 6, 135-138.

Robinson, E., Rowe, D.-A.C. & Khan, S. (2006). Wave-Emplaced Boulders on Jamaica's Rocky Shores. *Zeitschrift für Geomorphologie N.F. Suppl.-Vol.*, 146, 39-57.

Sachpazi, M., Hirn, A., Clément, C., Haslinger, F., Laigle, M., Kissling, E., Charvis, P., Hello, Y., Lépine, J. C., Sapin, M. & Ansorge, J. (2000). Western Hellenic subduction and Cephalonia Transform: local earthquakes and plate transport and strain. *Tectonophysics,* 319(4), 301–319.

Scheffers, A. & Kelletat, D. (2001): Hurricanes und Tsunamis: Dynamik und küstengestaltende Wirkungen. *Bamberger Geographische Schriften*, 20, 29-53.

Scheffers, A. & Scheffers, S. (2006): Documentation of Hurricane Ivan on the Coastline of Bonaire. *Journal of Coastal Research*, 22(6), 1437-1450.

Scheffers, A. (2005): Coastal Response to Extreme Wave Events – Hurricanes and Tsunami on Bonaire. A Contribution to IGCP 495. *Essener Geographische Arbeiten*, 37.

Scheffers, A., Scheffers, S. & Kelletat, D. (2005): Paleo-Tsunami Relics on the Southern and Central Antillean Island Arc. *Journal of Coastal Research*, 21(2), 263-273.

Scheffers, A., Kelletat, D. & Engel, M. (2009a): Die Entwicklung der Tsunamiforschung nach der Katastrophe vom 26.12.2004. *Geographische Rundschau,* 61(12), 12-18.

Scheffers, A., Scheffers, S., Kelletat, D. & Browne, T. (2009b). Wave Emplaced Coarse Debris and Megaclasts in Ireland and Scotland: Boulder Transport in a High Energy Littoral Environment. *The Journal of Geology,* 117(5), 553-573.

Schielein, P., Zschau, J., Woith, H. & Schellmann, G. (2007). Tsunamigefährdung im Mittelmeer - Eine Analyse geomorphologischer und historischer Zeugnisse. *Bamberger Geographische Schriften,* 22, 153-199.

Scicchitano, G., Monaco, C. & Tortorici, L. (2007). Large boulder deposits by tsunami waves along the Ionian coast of south-eastern Sicily (Italy). *Marine Geology,* 238(1-4), 75-91.

Soloviev, S.L. (1990). Tsunamigenic Zones in the Mediterranean Sea. *Natural Hazards,* 3, 183-202.

Spiske, M., Böröcz, Z. & Bahlburg, H. (2008). The role of porosity in discriminating between tsunami and hurricane emplacement of boulders – A case study from the Lesser Antilles, southern Caribbean. *Earth and Planetary Science Letters,* 268(3-4), 384-396.

Switzer, A.D. & Jones, B.G. (2008). Large-scale washover sedimentation in a freshwater lagoon from the southeast Australian coast: sea-level change, tsunami or exceptionally large storm? *The Holocene*, 18(5), 787-803.

Switzer, A.D. & Burston, J.M. (2010). Competing mechanisms for boulder deposition on the southeast Australian coast. *Geomorphology,* 114(1-2), 42-54.

U.S. Geological Survey (USGS) (2006). Earth Resources Observation & Science (EROS). Corona satellite images and Aster satellite data. http://edc.usgs.gov.01/2006.

von Seidlitz, W. (1927). Geologische Untersuchung der Inselnatur von Leukas. In: Dörpfeld, W. (ed.), *Alt-Ithaka. Ein Beitrag zur Homer- Frage, 2 Volumes*. München, 352-372.

Vött, A., May, M., Brückner, H. & Brockmüller, S. (2006). Sedimentary Evidence of Late Holocene Tsunami Events near Lefkada Island (NW Greece). *Zeitschrift für Geomorphologie N.F. Suppl. Vol.*, 146, 139-172.

Vött, A., Brückner, H., May, M., Lang, F. & Brockmüller, S. (2007). Late Holocene tsunami imprint at the entrance of the Ambrakian gulf (NW Greece). *Mediterranée,* 108, 43-57.

Vött, A., Brückner, H., May, M., Lang, F., Herd, R. & Brockmüller, S. (2008). Strong tsunami impact on the Bay of Aghios Nikolaos and its environs (NW Greece) during Classical-Hellenistic times. *Quaternary International,* 181(1), 105-122.

Vött, A., Brückner, H., Brockmüller, S., Handl, M., May, S.M., Gaki-Papanastassiou, K., Herd, R., Lang, F., Maroukian, H., Nelle, O. & Papanastassiou, D. (2009a). Traces of Holocene tsunamis across the Sound of Lefkada, NW Greece. *Global and Planetary Change,* 66(1-2), 112-128.

Vött, A., Brückner, H., May, S.M., Sakellariou, D., Nelle, O., Lang, F., Kapsimalis, V., Jahns, S., Herd, R., Handl, M. & Fountoulis, I. (2009b). The Lake Voulkaria (Akarnania, NW Greece) palaeoenvironmental archive - a sediment trap for multiple tsunami impact since the mid-Holocene. *Zeitschrift für Geomorphologie N.F.,* 53(SI 1), 1-37.

Williams, D.M. & Hall, A.M. (2004). Cliff-top megaclast deposits of Ireland, a record of extreme waves in the North Atlantic—storms or tsunamis? *Marine Geology,* 206, 101–117.

Woodroffe, C. (2003). *Coasts – form, process and evolution*. Cambridge, 623 pp.

Chapter VI

Synthesis

6.1 MIDDLE HOLOCENE TO RECENT EVOLUTION OF THE LEFKADA – PREVEZA COASTAL ZONE

A broad suite of geo-scientific investigations were carried out in the coastal zone between Lefkada and Preveza (NW Greece) comprising detailed investigations on (i) the coastal morphology and (sub-) recent coastal morphodynamics (*Chapter 2*), the sedimentary architecture of (ii) the Phoukias sand spit in SE Aktium Headland (*Chapter 3*) and (iii) three washover fan structures in the northern part of the Lefkada Lagoon (*Chapter 4*), and (iv) wave-emplaced block and boulder deposits found in the study area (*Chapter 5*).

Summarizing the results from these investigations (Fig 6-1), four major disturbances are recorded in the Lefkada-Preveza coastal zone since the middle to late Holocene. Evidence for a first disturbance is brought from the northern part of the Phoukias spit, where event layers point to a tsunamigenic inundation and the related formation of ridge structures at ~1000 cal BC. The deposition of the event layer involved the onset of the formation of the Phoukias sand spit in south-western Aktium Headland and a related remarkable erosion of the shoreline in western Aktium Headland, a reorganization of the north-eastern part of the Lefkada barrier beach system, and environmental changes of the Bay of Aghios Nikolaos, though still protected from major wave activity by the Plaka beachrock remains, to a shallow marine environment. Therefore, the inferred event must have been related to a first breakdown of the former Plaka barrier beach. From the southern part of the Phoukias spit, a second disturbance is detected in the stratigraphical record and dated to around or after ~300 cal BC. At least at that time, the Bay of Aghios Nikolaos came under definite marine influence and the breakdown of the Plaka coastline is evident.

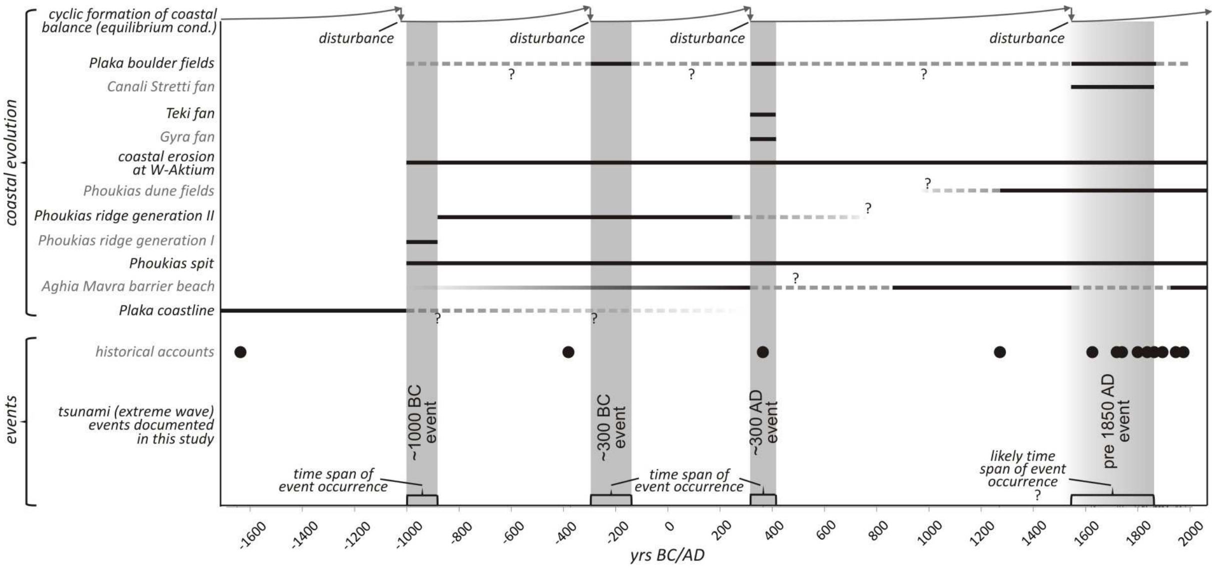

Fig. 6-1: Schematic illustration of the evolution of main coastal features in the Lefkada – Preveza area based on the findings presented in this study. Several landforms and coastal features in the study area are the result of repeated disturbances of the coastal system, triggered by tsunami (extreme wave) impact. Notes: dotted lines – possible or likely period of formation; continuous line – definite period of formation.

The third major disturbing event relates to the two main washover structures in the northern part of the Lefkada Lagoon, representing the most prominent geomorphologic evidence of high-magnitude extreme wave events in the study area. According to their sedimentary composition and their dimension, a tsunamigenic origin is again the most plausible explanation for their formation. The available dating results point to a formation at around or after 300 cal AD. Thus, it seems reliable that coastal morphology in the study area was influenced by the supraregional effects of the 365 AD earthquake off western Crete, which involved tsunamigenic destruction in the entire eastern Mediterranean (e.g. STIROS 2001, STEFANAKIS 2006, PAPADIMITRIOU & KARAKOSTAS 2008). For this event, comparable disturbing effects on the barrier beach system as well as imprints in the geological record of the Phoukias spit must be inferred – in fact, indication for a contemporaneous event-induced disturbance of the stratigraphical sequence was brought from the central part of the Bay of Aghios Nikolaos, but no unchallenged complementary sedimentary and chronological evidence was found in the Phoukias spit sedimentary record. Here, the available results rather point to an earlier major event at ~300 BC which was also inferred by previous findings from the adjacent coastal area (VÖTT et al. 2006, 2008). However, a relation of the two event deposits cannot be excluded, since both event deposits are interpreted to be accompanied by environmental changes and an increased marine influence in the Bay of Aghios Nikolaos. Further investigations, in particular on the local chronology of the sedimentary sequence, are needed to clarify possible analogies and to exclude dating uncertainties, such as reworking.

An at least temporary breakdown of the north-eastern part of the Lefkada barrier beach took place during the younger history of the coastal evolution. It was related to the formation of the younger fan structures in the northern part of the Lefkada Lagoon. The smallest investigated fan structure, the Canali Stretti fan structure, was triggered by breaching of the barrier beach. This most recent major disturbance of the coastal system must have taken place before the middle of the 19th century. Since then, the coastal system is in a state of re-balancing and re-organization, which is manifested in a high morphodynamic activity during the recent past. Whether this disturbing event can be attributed to tsunami or storm impact remains unclear – the extreme wave event origin however is unequivocally manifested. Several younger tsunami events are mentioned in the available tsunami catalogues at 1723, 1820 and 1825 AD (e.g. SOLOVIEV et al. 2000, VÖTT et al. 2006), and it is likely that one of these events contributed to the last major disturbance of the coastal system.

According to the investigations on the block and boulder accumulations in the study area, a contribution of both tsunami and storm events is assumed for their formation. Comparable to numerous studies on block and boulder fields along rocky shorelines, the unequivocal determination of the triggering hydrodynamic process and the number of contributing events remains unclear. However, the documented floating transport of large boulders may point to a significant role of tsunami events in their formation, although the influence of storms of exceptionally high intensity is possible as well. According to the evolution of the coastal system, formation of the encountered block and boulder fields can be restricted to the last 3000, most probably 2300 years. A relation between the dislocation of single blocks and the documented tsunami-related disturbances of the coastal system may be inferred – the dating of transported beachrock slabs can be interpreted to correlate with the major event at ~300 AD and the inferred pre-1850 AD event.

6.2 SIGNIFICANCE OF EVENT DEPOSITS

In the sedimentary record, the encountered event deposits exhibit both similarities and differences. In general, the event deposits were readily identifiable, since they mark significant anomalies within the sedimentary sequence. They are characterized by a number of characteristics commonly used (i) to determine the event induced origin on the one hand, and (ii) to discriminate between storm and tsunami deposits on the other hand.

In a summary view, each of the different investigated sites is characterized by a distinct pattern of event deposits, providing a consistent picture of each site (Fig. 6-2). All encountered event deposits are indicated by several (up to five) subunits, and common sedimentary characteristics are for instance (a) fining up, thinning and fining landward sequences, (b) massive bedding, (c) shell debris layers with a high percentage of angular broken molluscs and (!) articulated bivalves, (d) mixed microfaunal assemblages, as documented for the Gyra and the Teki fan event deposit, and (e) rip-up clasts and/or mixing of the underlying strata within the base of the deposit. However, the appearance of these characteristics is strongly dependant on the pre-event environmental conditions – the occurrence of rip-up clasts for instance was observed in event deposits overlying former (semi)terrestrial surfaces with soil formation, while mixing and incorporation of sediments from the underlying strata was particularly encountered in event units covering lagoonal sediments.

definite ● *probable* ◍ *absent* ○ *no data* -

location of event deposit	*number of subunits*	*sharp lower contact*	*basal erosional unconformity*	*fining upward*	*fining landward*	*thinning landward*	*massive bedding*	*bimodal grain size*	*poor sorting*	*rip-up clasts*	*mud-drapes*	*incorporation of underlying facies*	*shell debris layer*	*allochthonous micro-faunal assemblage*	*microfaunal diversity*	*microfaunal abundance*	*angular mollusc fragments*	*articulated bivalves*	*landform*	*age*	*pre-impact environment*
Gyra fan	**3**	●	◍	○	●	●	●	●	●	○	●	●	●	●	●	●	◍	●	washover fan	~300 AD	lagoonal
Gyra peninsula	**1**	●	●	○	-	-	●	●	●	●	○	○	○	-	-	-	◍	○		~300 AD	former surface
Teki fan	**2-3**	●	◍	◍	●	●	●	●	●	○	○	●	●	●	●	●	◍	◍	washover fan	~300 AD	lagoonal
Canali Stretti fan	**<5**	●	●	●	○	●	●	●	●	○	○	●	○	-	-	-	○	○	scour fan	mediaevel to modern	subaqueous sand (?)
Bay of Agh. Niko.	**1**	●	◍	◍	-	-	○	◍	●	○	○	-	●	-	-	-	◍	◍	-	~300 AD	lagoonal
southern Phou. spit	**1**	●	◍	●	-	-	○	◍	●	○	○	-	●	-	-	-	◍	●	-	post 300 BC (~300 AD?)	lagoonal
central Phou. spit	**2**	●	●	●	◍	●	●	●	●	●	○	◍	●	●	◑*	◑*	●	●	-	post 300 BC	former surface
northern Phou. spit	**2**	●	●	●	◍	●	●	●	●	●	○	◍	●	-	-	-	●	●	ridge	~1000 BC	former surface

*Fig. 6-2: Summary of main characteristics commonly used for the detection of event deposits in fine-grained near-coast geological archives, found for the event deposits at different locations in this study.Notes: * - for the central Phoukias spit area abundance and diversity of ostracods is low in contrast to the foraminiferal assemblage.*

However, plausible conclusions concerning the event process and the provenance of the constituting sediments could be inferred for instance from the succession of sedimentary subunits comprising the Gyra fan. Here, the three different subunits are interpreted to correspond to three major inundation phases during one tsunami event. According to the presented results, sediment transport and related deposition was largest during flooding impulses in the middle part of the tsunami wave train. In a further step, these findings may provide useful input for modeling approaches e.g. of inundation depths and distances, as already shown by FLOTH (2008) and FLOTH et al. (2009) for the study area.

Between the event deposits from different locations considerable differences are documented – if any, only a careful stratigraphic correlation between the different sites can be realized. Apparently, these findings emphasize (i) the univocal relationship of event deposits and their local topographic setting and sedimentary environment, and (ii) the resultant difficulties in the application of significant, generally accepted distinguishing criteria, even in the same study area. In this context, the presented findings agree with several previous studies on extreme wave event deposits. Universally applicable criteria for the differentiation between storm and tsunami do not exist in fine-grained stratigraphies, since the characteristics of each investigated site ultimately determine the specific composition of the event deposit. Thus, besides the detailed analysis of as many sedimentary signatures as possible, a consistent determination of the originating process relies on further, additional information, such as the (palaeo-) geographical context, local geomorphologic characteristics and/or the existence of local modern analogues, which may provide further details on the differences of the different kinds of extreme wave events in the geological record. In this study, the distinct morphology of the washover fan structures represented such additional evidence and, in the case of the Canali Stretti breaching fan, helped to reliably determine the triggering process (see for instance MORTON et al. 2007, SWITZER & JONES 2008, SHIKI et al. 2008, ENGEL et al. in review).

Comparable to the differentiation of event deposits, the physical dating of event deposits exhibits considerable difficulties. ^{14}C-AMS datings of organic material in most cases represent *termini ante*, *ad* or *post quem* for the deposition of event layers, depending on the stratigraphical relation the material was sampled. Even the dating of air-filled, *ex-situ* articulated bivalves, as has been shown in *Chapter 3*, did not reflect depositional ages of the related event deposit. Numerous datings are thus needed to narrow the time of deposition of event layers. In this study, reliable OSL ages helped to establish a local chronology of the Phoukias spit's sedimentary architecture. In combination with ^{14}C-AMS datings, OSL datings of sediment cores provide useful information about the depositional ages of (event-related) marine sediments. However, several restrictions and difficulties remain, which are partly ascribed to methodological problems.

In conclusion palaeo-event and palaeo-tsunami research relies on a number of geo-scientific investigations. Consistent results are in particular expected when combining sedimentological, microfaunal, geochronological and geochemical approaches with comprehensive geomorphological and palaeogeographical studies, geographical observations and actualistic principles.

6.3 BROADER IMPLICATIONS FOR COASTAL EVOLUTIONARY CONCEPTS

During the early (mid- to late Holocene) evolution of the coastal system, long-term gradual coastal processes involved the successive formation of the Lefkada barrier beach system, the evolution of the Lagoon of Lefkada and lagoonal conditions in the Bay of Aghios Nikolaos. These permanently operating processes were episodically affected by few but strong geomorphic crisis of high magnitude, involving distinct disturbances in the coastal system and impulsively initiating major changes in the coastal evolution. For the entire Lefkada barrier beach system, cyclic equilibrium conditions may be inferred when considering the coastal evolution over a longer period of time (middle to late Holocene). Depending on the considered time scale, a state of dynamic equilibrium of steady gradual changes can be inferred for the barrier system over distinct periods of time (e.g. several hundred or thousand years) (e.g. Woodroffe 2003, Bird 2008).

At least four of these disturbances were identified in the fine-grained sedimentary record of the Phoukias spit and the northern Lefkada Lagoon. They are expressed in distinct event deposits found within the investigated sedimentary sequence. These event deposits mark the beginning of changing morphodynamics, allowing linking major impulses in the evolution of the coastal system with the stratigraphical record, and establishing a reliable timeframe for the triggering process of the disturbances. Although the influence of tectonically induced vertical crustal movements is likely in the study area, the event deposits reflect the influence of other episodically occurring impulses.

With regard to the genetic interpretation of these event deposits, manifold lines of evidence was presented (see chapter 6.2) that major tsunami events contributed to repeated disturbances of the Lefkada barrier beach system and its recurring re-organization. More specifically, tsunami events are directly responsible for (i) the breakdown of the Plaka coastline, (ii) the deposition of block and boulder fields, (iii) the formation of ridge structures in the northern part of the Phoukias sand spit, (iv) the evolution of at least two washover generations in the Lefkada Lagoon, and (v) the disturbance and modification of the Lefkada barrier beach system, ultimately leading to severe changes of the coastal configuration. Additionally, these changes have likely invoked indirect and secondary processes involving (vi) the longer-term evolution of the Phoukias sand spit, and (vii) ongoing coastal erosion in western Aktium Headland.

In conclusion, the present coastline in the Lefkada – Preveza area is the result of both long-term, gradual processes mimicking and masking episodically occurring, impulsive coastal changes, acting on different time scales. It is worth noting that many prominent geomorphological structures (landforms) formed within days or even hours during very few high magnitude events, but persisted over a period of several hundred or thousand years. These singularities or crisis in geomorphic systems (Scheidegger 1994, Paris et al. 2009) are thus interpreted to be capable to significantly contribute to coastal evolution in general. In this context, the type and degree of impact of a given high magnitude event on the coastal evolution strongly depends on the character of the affected coastline. For instance, a rapid recovery of numerous coastal areas and beaches was observed after the 2004 Indian Ocean Tsunami in Southeast Asia, whereas for coastal areas characterized by barrier beaches and associated backbarrier lagoons - such as the the Lefkada-Preveza coastal zone - effects must be considered to be stronger and long lasting (Liew et al. 2010) since the reorganization of the coastal configuration requires considerably longer periods.

6.4 PERSPECTIVES

The findings presented in this study are supported by previous findings from the adjacent coastal zone (Vött et al. 2006, 2007, 2008, 2009a, 2009b, May et al. 2007, 2008). In turn, the presented results further and consolidate the previously presented findings. It has been shown that the Lefkada – Preveza coastal zone exhibits a considerable tsunami frequency. Tsunami events, besides the effects of tectonically induced crustal movements and long-term wave-generated sediment transport, turned out to be a major control of coastal change. Consequently, a distinct tsunami risk is apparent also for man and infrastructure. In this context, this study provides valuable basic information for the development of an appropriate hazard assessment. In the Mediterranean and particularly in Greece, public awareness is higher for earthquakes than for tsunami, although the potential of catastrophic tsunami events is evident and may be as high as it is in the Indian Ocean. The up to now neglected though urgent need for intensified focus on the tsunami threat and the installation of tsunami warning systems and warning centers recently was addressed by SYNOLAKIS (2008) in a noteworthy newspaper article.

Apart from possible benefits concerning coastal hazard management and/or hazard assessment, the presented study contributes to the data pool of palaeo-event deposits, which may be of value for future research. Perspectively, further investigations may be considered to improve the data presented in this study. These investigations may comprise

(i) sediment trenches on top of the washover structures and in the northern, ridge-dominated part of the Phoukias sand spit. Although groundwater conditions hamper their realization at many locations, they would provide a closer insight into the sedimentary characteristics and structure of the event deposits.

(ii) additional and deeper corings in the lagoonal parts of the study area, in particular in direct prolongation of the two main washover structures in the northern Lefkada Lagoon and in the central part of the Bay of Aghios Nikolaos. Further event layers can be expected within the sedimentary sequence and may be linked to the findings of VÖTT et al. (2009a, 2009b) from the inner part of the Sound of Lefkada, the Bay of Aghios Nikolaos and the Lake Voulkaria.

(iii) intensified focus on the improvement of the chronological data base. The combined use of OSL and ^{14}C-AMS datings at further locations may provide a more detailed chronological picture of the extreme wave event history in the study area.

(iv) further studies on the evolution of the Plaka boulder fields, such as dating approaches as well as long-term surveys of the boulders' position, the latter providing information about the effects of common wave intensities on block dislocation. Finally, studies on local analogues, such as known (sub) recent storm deposits, may help to further improve the reliability of the presented findings, to enlarge the data base of palaeo-event deposits and to enhance the knowledge about the effects of extreme wave events in the Lefkada – Preveza coastal zone.

Moreover, the presented findings may be incorporated into a supraregional context – in the adjacent coastal zones, the detected events are assumed to have left imprints in geological archives as well. Further investigations on fine-grained near-coast geological archives along the western coasts of Greece, the coasts of northern Africa and eastern Italy are assumed to reveal comparable event layers and significant disturbances of the coastal system which can be linked to the findings presented in this study.

6.5 REFERENCES

Bird, E. (2008). *Coastal Geomorphology – An Introduction*. New York, 411 pp.

Engel, M., Brückner, H., Wennrich, V., Scheffers, A., Kelletat, D., Vött, A., Schäbitz, F., Daut, G., Willershäuser, T. & May, S.M. (in review). The back-barrier record of eastern Bonaire (Netherlands Antilles): new insights into the palaeo-tsunami history of the southern Caribbean.

Floth, U. (2008). *The tsunami hazard between Lefkada and Preveza, NW Greece, based on computer models as well as field and laboratory evidence*. Unpublished diploma thesis, Marburg.

Floth, U., Vött, A., May, S.M., Brückner, H. & Brockmüller, S. (2009): Geo-scientific evidence versus computer models of tsunami landfall in the Lefkada coastal zone (NW Greece). *Marburger Geographische Schriften*, 145, 140-156.

Liew, S.C., Gupta, A., Wong, P.P. & Kwoh, L.K. (2010). Recovery from a large tsunami mapped over time: The Aceh coast, Sumatra. *Geomorphology*, 114(4), 520-529.

May, S.M., Vött, A., Brückner, H. & Brockmüller, S. (2007). Evidence of tsunamigenic impact on Actio headland near Preveza, NW Greece. *Coastline Reports*, 9, 115-125.

May, S.M., Vött, A., Sakellariou, D., Kapsimalis, V., Herd, R. & Brückner, H. (2008). On- and offshore tsunami traces around Actio Headland (NW Greece). *Geophysical Research Abstracts,* 10, EGU2008-A-11034.

Morton, R.A., Gelfenbaum, G. & Jaffe, B.E. (2007). Physical criteria for distinguishing sandy tsunami and storm deposits using modern examples. *Sedimentary Geology,* 200, 184–207.

Papadimitriou, E. & Karakostas, V. (2008). Rupture model of the great AD 365 Crete earthquake in the southwestern part of the Hellenic Arc. *Acta Geophysica*, 56(2), 293-312.

Paris, R., Wassmer, P., Sartohadi, J., Lavigne, F., Barthomeuf, B., Desgages, E., Grancher, D., Baumert, P., Vautier, F., Brunstein, D. & Gomez, C. (2009). Tsunamis as geomorphic crises: Lessons from the December 26, 2004 tsunami in Lhok Nga, West Banda Aceh (Sumatra, Indonesia). *Geomorphology*, 104(1-2), 59-72.

Scheidegger, A.E. (1994). Hazards: singularities in geomorphic systems. *Geomorphology,* 10(1-4):19-25.

Shiki, T., Tsuji, Y., Yamazaki, T. & Minoura, K. (eds.) (2008). *Tsunamiites*. Amsterdam, 432 pp.

Soloviev, S.L., Solovieva, O.N., Go, C.N., Kim, K.S. & Shchetnikov, N.A. (2000). *Tsunamis in the Mediterranean Sea 2000 B.C.-2000 A.D.* Dordrecht.

Stefanakis, M.I. (2006). Natural Catastrophes in the Greek and Roman World: Loss or Gain? Four Cases of Seaquake-Generated Tsunamis. *Mediterranean Archaeology and Archaeometry,* 6*(*1), 61-88.

Stiros, S.C. (2001). The AD 365 Crete earthquake and possible seismic clustering during the fourth to sixth centuries AD in the Eastern Mediterranean: a review of historial and archaeological data. *Journal of Structural geology*, 23, 545-562.

Switzer, A.D. & Jones, B.G. (2008). Large-scale washover sedimentation in a freshwater lagoon from the southeast Australian coast: sea-level change, tsunami or exceptionally large storm? *The Holocene*, 18(5), 787-803.

Synolakis, C. (2008). Europe's Tsunami of Inaction Against Tsunamis. *The Wall Street Journal*, November 5th 2008.

Vött, A., May, M., Brückner, H., & Brockmüller, S. (2006). Sedimentary Evidence of Late Holocene Tsunami Events near Lefkada Island (NW Greece). *Zeitschrift für Geomorphologie N.F., Suppl.-Vol.* 146, 139-172.

Vött, A., Brückner, H., May, M., Lang, F., & Brockmüller, S. (2007). Late Holocene tsunami imprint at the entrance of the Ambrakian gulf (NW Greece). *Mediterranée,* 108, 43-57.

Vött, A., Brückner, H., May, M., Lang, F., Herd, R., & Brockmüller, S. (2008). Strong tsunami impact on the Bay of Aghios Nikolaos and its environs (NW Greece) during Classical-Hellenistic times. *Quaternary International,* 181(1), 105-122.

Vött, A., Brückner, H., Brockmüller, S., Handl, M., May, S.M., Gaki-Papanastassiou, K., Herd, R., Lang, F., Maroukian, H., Nelle, O. & Papanastassiou, D. (2009a). Traces of Holocene tsunamis across the Sound of Lefkada, NW Greece. *Global and Planetary Change,* 66(1-2), 112-128.

Vött, A., Brückner, H., May, S.M., Sakellariou, D., Nelle, O., Lang, F., Kapsimalis, V., Jahns, S., Herd, R., Handl, M. & Fountoulis, I. (2009b). The Lake Voulkaria (Akarnania, NW Greece) palaeoenvironmental archive - a sediment trap for multiple tsunami impact since the mid-Holocene. *Zeitschrift für Geomorphologie N.F.,* 53(SI 1), 1-37.

Woodroffe, C. (2003). *Coasts – form, processes and evolution*. Cambridge, 623 pp.

7 Summary

Research on palaeo-tsunami and palaeo-extreme wave events aims to provide new data about former events and is of remarkable importance in the eastern Mediterranean. In general, coastal geomorphology and fine-grained near-coast geological archives store information about coastal changes over medium to long timescales, as well as short, episodic processes such as palaeo-tsunami events. In the eastern Mediterranean and particularly for the Ionian Sea and the Lefkada – Preveza coastal zone (NW Greece), strong seismic activity and a high tsunamigenic potential are evident. Thus, comprehensive geo-scientific investigations were carried out in the Lefkada – Preveza coastal zone in order to decipher coastal change throughout time, and thereby detect, verify and date the influence of tsunami events on the coastal system and coastal evolution. Herein, particular focus was set on the distinguishability of event deposits in the geological record and the evaluation of event recurrence rates – an issue of major importance in extreme wave event research.

In a first step, detailed analysis of the geomorphological and geomorphodynamic situation in the study area revealed several major disturbances of the coastal system, which mark episodically occurring major impulses of coastal evolution, entailing the recurrent reorganization of coastal balance. In a second step, comprehensive geo-scientific investigations on the main near-coast geological archives provided insight into the palaeogeographical evolution and the palaeo-event history of the Lefkada – Preveza area. In the sedimentary record of the Phoukias sand spit and the washover-dominated northern Lefkada Lagoon, distinct event deposits were identified. These event deposits provide a linkage to the inferred disturbances of the coastal system and allow the dating of the main impulses in coastal evolution. Detailed analyses of the event deposits - comprising sedimentological, microfaunal and geochemical investigations as well as the interpretation of the regional geomorphologic and geographic context - strongly suggest a tsunamigenic origin of the encountered event deposits, proving the significant impact of tsunamis on the coastal system. Moreover, numerous block and boulder fields were mapped along the coastline and equally point to the impact of high energy wave events.

Altogether, four major tsunamigenic disturbances were identified throughout the late Holocene. These disturbances were dated to ~1000 BC, to at around or after 300 BC and, for the main washover structures in the northern Lagoon of Lefkada, to at around or after 300 AD, the latter event most likely triggered by the 365 AD earthquake off western Crete and the related tsunami. During the younger history of coastal evolution a fourth disturbance occurred sometime before 1850 AD. In addition to the detected 365 AD event, the presented findings fit well to previous investigations in adjacent coastal zones.

From a geomorphological and geomorphodynamic point of view, the major tsunami events involved the breakdown of former coastlines (the Plaka), the formation of the Phoukias sand spit and the onset of intense coastal erosion in western Aktium Headland. Moreover, the inferred tsunami events contributed to the formation of block and boulder fields, induced the evolution of ridge structures in the northern part of the Phoukias sand spit and triggered the formation of at least one, probably two washover generations in the northern Lefkada Lagoon. The episodic occurrence of tsunami events was thus responsible for the formation of major geomorphological structures and modifications of the coastal system, which are recurrently masked and mimicked by long term, gradually operating coastal processes. These marked geomorphic changes provide clear evidence that tsunami-induced disturbances exert a major control on the evolution of the coastal system in the study area.

In conclusion, this study presents new geo-scientific evidence of extreme wave event deposits and will thereby expand the regional and global data pool of palaeo-event and particularly palaeo-tsunami deposits. Moreover, it contributes to ongoing research concerned with the detection of extreme wave event deposits in near-coast geological archives, ultimately enabling an improved understanding of type and degree of their impact on the evolution of coastal systems.

8 Zusammenfassung

Die Paläo-Event Forschung befasst sich mit der Erforschung von vergangenen extremen Wellenereignissen. In küstennahen geologischen Archiven werden sowohl stetig wirkende, graduelle Küstenprozesse also auch episodisch auftretende singuläre Ereignisse, wie z.B. Paläo-Tsunamis, gespeichert. Der östliche Mediterranraum und insbesondere das Ionische Meer und das Küstengebiet zwischen Lefkada und Preveza (Nordwestgriechenland) sind durch eine starke seismisch-tektonische Aktivität gekennzeichnet, die ein hohes Risiko für die Entstehung von Tsunami-Ereignissen zur Folge hat.

Vor dem Hintergrund der Hauptziele der Paläo-Event Forschung – der Unterscheidbarkeit von Tsunami und Sturmsedimenten im geologischen Archiv sowie der Berechnung von Wiederkehrwahrscheinlichkeiten solcher Ereignisse – wurden umfassende geowissenschaftliche Untersuchungen im Küstengebiet zwischen Lefkada und Preveza durchgeführt. Dabei war es das wesentliche Ziel, im Laufe der Zeit stattgefundene Küstenveränderungen nachzuvollziehen und mit Hinblick auf Tsunami-Ereignisse und deren Einfluss auf die Küstenentwicklung zu verifizieren, zu datieren und zu interpretieren.

In einem ersten Schritt wurde dafür die lokale Geomorphologie und Geomorphodynamik detailliert untersucht. Die Resultate implizieren wiederholte Störungen und eine darauf folgende Reorganisation des Küstensystems, die episodisch auftretende bedeutende Impulse der Küstenentwicklung markieren. In einem weiteren Schritt wurden umfassende Untersuchungen der bedeutendsten küstennahen Geoarchive vorgenommen, die Rückschlüsse auf die paläogeographische Entwicklung und die Paläo-Event Vergangenheit des Arbeitsgebiets erlauben. Die Ergebnisse der Untersuchungen des Phoukias Sandhakens und der von Washoverstrukturen dominierten Lagune von Lefkada zeigen eindeutige Eventlagen in stratigraphischer Abfolge, die mit den bedeutenden Störungen in der Küstenentwicklung korreliert werden können und deren Datierung ermöglichen. Aufgrund der sedimentologischen, geochemischen und mikrofaunistischen Ergebnisse konnte unter Einbezug des lokalen geomorphologischen und geographischen Kontextes für die meisten der Eventlagen eine tsunamigene Entstehung abgeleitet werden. Darüber hinaus deutet die Existenz von wellenbewegten Großblöcken eindeutig auf den Einfluss von extremen Wellenereignissen hin.

Insgesamt wurden im Rahmen dieser Arbeit vier bedeutende Tsunami-induzierte Störungen des untersuchten Küstensystems identifiziert. Ein erstes Event fand demnach um etwa 1000 v. Chr. statt, ein weiteres um oder kurze Zeit nach 300 v. Chr. Das verheerende Erdbeben 365 n. Chr., das im gesamten Ostmediterranraum für Tsunamis verantwortlich war, beeinflusste höchstwahrscheinlich auch das Küstengebiet um Lefkada und Preveza und führte dort zur Entstehung großflächiger Washoverstrukturen in der Lagune von Lefkada. Überdies wurde eine erhebliche Beeinflussung der Küste in jüngerer Zeit dokumentiert, die vor 1850 n. Chr von einem extremen Wellenereignis induziert worden sein muss.

Aus geomorphodynamischer Sicht lässt sich festhalten, dass die identifizierten Paläo-Tsunamis zur Auflösung einer früheren Küstenlinie (der Plaka) beigetragen haben, sowie die Entstehung des Phoukias Sandhakens und die damit zusammenhängende Küstenerosion im Westen der Aktium Halbinsel induziert haben. Aus geomorphologischer Sicht haben Tsunamis zur

Entstehung von Blockfeldern beigetragen und werden mit der Entstehung von Strandwall-ähnlichen Strukturen sowie mindestens zwei Washovergenerationen in Verbindung gebracht. Episodisch auftretende Tsunami-Ereignisse sind deshalb für die Entwicklung der Küstenmorphologie und Küstenkonfiguration im Bereich Lefkada – Preveza von entscheidender Bedeutung gewesen, die in der Folge immer wieder durch stetige, graduelle Küstenprozesse modifiziert wurden.

Die vorliegende Arbeit präsentiert neue geowissenschaftliche Belege für extreme Wellenereignisse und erweitert damit den Datenpool von Paläo-Event und insbesondere von Paläo-Tsunami Ablagerungen. Die Arbeit leistet einen Beitrag zur Detektierung von extremen Wellenereignissen in küstennahen Geoarchiven und erlaubt Rückschlüsse auf deren Einfluss in der Küstenentwicklung. Letztlich trägt ein damit zusammenhängendes verbessertes Verständnis zur Unterscheidung von Eventlagen im geologischen Archiv und zur Abschätzung von küstennahen Riskien bei.

9 Περίληψη

Στην Ανατολική Μεσόγειο, και ιδιαίτερα στην παράκτια ζώνη Λευκάδας – Πρέβεζας της ΝΔ Ελλάδας, η έντονη σεισμική δραστηριότητα της περιοχής έχει σαν επακόλουθο την παρουσία αυξημένου δυναμικού για τη δημιουργία τσουνάμι. Η έρευνα περιστατικών παλαιο-τσουνάμι και παλαιών ακραίων θαλάσσιων κυμάτων γενικότερα στοχεύει στον εντοπισμό σημαντικών πληροφοριών που σχετίζονται με παρελθόντα περιστατικά τοπικού χαρακτήρα, τα οποία όμως είναι ιδιαίτερα σημαντικά για ολόκληρη την περιοχή της ανατολικής Μεσογείου. Γενικά, η παράκτια μορφολογία και οι λεπτόκοκκοι παράκτιοι γεωλογικοί σχηματισμοί παρέχουν πληροφορίες σχετικά με τις μεταβολές που υφίστανται οι παράλιες περιοχές, για ενδιάμεσες έως μεγάλες χρονικές περιόδους, καθώς επίσης και μικρής διάρκειας γεγονότα (επεισόδια), όπως τα παλαιο-τσουνάμι.

Στην παράκτια ζώνη Λευκάδας – Πρέβεζας, ιζηματογενή αποτυπώματα τσουνάμι σε παράκτιες γεωλογικές αποθέσεις έχουν ήδη καταγραφεί από προγενέστερες μελέτες. Στα πλαίσια αυτής της μελέτης παρελθόντων ακραίων θαλάσσιων κυμάτων, πραγματοποιήθηκε λεπτομερής γεωλογική διερεύνηση της παράκτιας ζώνης Λευκάδας – Πρέβεζας για τη διάκριση των αποθέσεων, που σχηματίστηκαν από τη δράση των παλαιο-τσουνάμι και την εκτίμηση του ρυθμού επανάληψής τους, με στόχο τον προσδιορισμό των παράκτιων μεταβολών με το πέρασμα του χρόνου, καθώς και τη χρονολόγηση και εξακρίβωση της επίδρασης των τσουνάμι στην εξέλιξη του αιγιαλού.

Αρχικά, η εκτενής ανάλυση των γεωμορφολογικών και γεωμορφοδυναμικών χαρακτηριστικών αποκάλυψε την επανειλλημένη διαταραχή του παράκτιου συστήματος, η οποία είχε ως αποτέλεσμα την επαναλαμβανόμενη αναδιάρθρωση της παράκτιας ισορροπίας. Οι διαταραχές αποτυπώνουν τη σποραδικότητα των κύριων παραγόντων αναδιάρθρωσης της παράκτιας ισορροπίας. Στη συνέχεια, η αναλυτική γεωμορφολογική μελέτη των παράκτιων γεωλογικών αρχείων φανέρωσε την παλαιογεωγραφική εξέλιξη και την ιστορία των παλαιο-τσουνάμι στην περιοχή. Στους ιζηματογενής σχηματισμούς (αμμώδεις θίνες) του Φουκιά καθώς και στη βόρεια λιμνοθάλασσα της Λευκάδας προσδιορίσθηκαν ευδιάκριτες αποθέσεις παλαιο-τσουνάμι. Οι αποθέσεις αυτές μπορούν να συσχετισθούν με τις προαναφερθείσες διαταραχές του παράκτιου συστήματος και επιτρέπουν τη χρονολόγηση των κύριων παραγόντων εξέλιξης του αιγιαλού. Η λεπτομερής διερεύνηση των ιζημάτων, των απολιθωμάτων και των γεωχημικών χαρακτηριστικών των αποθέσεων των αποτυπωμένων περιστατικών παρέχουν ενδείξεις για την επίδραση των τσουνάμι στο παράκτιο σύστημα. Επίσης, η παρουσία συνεκτικών παράκτιων ψηφιτοπαγών με κροκάλες μεγάλων διαστάσεων που χαρτογραφήθηκαν κατά μήκος της ακτογραμμής της Πλάκας υποδηλώνει τον αντίκτυπο των επεισοδιακών παλαιο-ακραίων κυμάτων.

Στο πλαίσιο αυτής της μελέτης, προσδιορίσθηκαν τέσσερις κύριες γεωλογικές διαταραχές στη διάρκεια του Ανώτερου Ολόκαινου. Οι διαταραχές αυτές χρονολογήθηκαν κατά προσέγγιση, η πρώτη στο ~1000 π.Χ., η δεύτερη στο ~300 π.Χ., η τρίτη, η οποία σχετίζεται με μηχανισμούς κατάκλυσης στη βόρεια λιμνοθάλασσα της Λευκάδας και τοποθετείται στο ~300 μ.Χ. και η τελευταία, η οποία κατά πάσα πιθανότητα προκλήθηκε από τον ιστορικά καταγεγραμμένο σεισμό του 365 μ.Χ. στη δυτική Κρήτη και το σχετιζόμενο (με το σεισμό αυτό) τσουνάμι που ακολούθησε.

Από γεωμορφολογική και μορφοδυναμική άποψη, τα κύρια γεγονότα τσουνάμι συνέβαλλαν στην αποδόμηση της ακτογραμμής της Πλάκας, στο σχηματισμό των αμμωδών θινών του Φουκιά και στην απαρχή της έντονης διάβρωσης της ακτογραμμής δυτικά της χερσονήσου του Ακτίου. Επίσης, τα προαναφερθέντα περιστατικά συνέβαλλαν στο σχηματισμό παράκτιων συνεκτικών ψηφιτοπαγών με κροκάλες μεγάλων διαστάσεων, στο σχηματισμό υψωμάτων στο βόρειο τμήμα των θινών του Φουκιά και προκάλεσαν τη δημιουργία τουλάχιστον μίας, πιθανότατα και δεύτερης, κατάκλυσης της βόρειας λιμνοθάλασσας της Λευκάδας. Κατά συνέπεια, τα γεγονότα των τσουνάμι είχαν καθοριστική συνεισφορά στην παράκτια εξέλιξη της υπό μελέτη περιοχής. Αυτά τα σποραδικά περιστατικά δημιούργησαν τις κύριες γεωμορφολογικές δομές, οι οποίες συνεχώς συγκαλύπτονται και τροποποιούνται από μακροπρόθεσμες και σταδιακές παράκτιες διεργασίες.

Συνοψίζοντας, αυτή η μελέτη συμβάλλει στην επισήμανση αποθέσεων ακραίων περιστατικών παλαιο-τσουνάμι σε παράκτιους γεωλογικούς σχηματισμούς και στην κατανόηση της επίδρασής τους στην εξέλιξη του αιγιαλού. Επιπροσθέτως, παρέχει περαιτέρω γεωλογικές ενδείξεις για αποθέσεις από περιστατικά ακραίων θαλάσσιων κυμάτων και κατ’ επέκταση εμπλουτίζει την υπάρχουσα βιβλιογραφία σχετικά με τις αποθέσεις παλαιο-τσουνάμι.

Ich versichere, dass ich die von mir vorgelegte Dissertation selbständig angefertigt, die benutzten Quellen und Hilfsmittel vollständig angegeben und die Stellen der Arbeit - einschließlich Tabellen, Karten und Abbildungen -, die anderen Werken im Wortlaut oder dem Sinn nach entnommen sind, in jedem Einzelfall als Entlehnung kenntlich gemacht habe; dass diese Dissertation noch keiner anderen Fakultät oder Universität zur Prüfung vorgelegen hat; dass sie - abgesehen von unten angegebenen Teilpublikationen - noch nicht veröffentlicht worden ist sowie, dass ich eine solche Veröffentlichung vor Abschluss des Promotionsverfahrens nicht vornehmen werde. Die Bestimmungen dieser Promotionsordnung sind mir bekannt. Die von mir vorgelegte Dissertation ist von Univ.-Prof. Dr. A. Vött betreut worden.

____

Simon Matthias May

Teilpublikationen:

May, S. M., Vött, A., Brückner, H. & Brockmüller, S. (2007). Evidence of tsunamigenic impact on Actio headland near Preveza, NW Greece. *Coastline Reports*, 9, 115-125.

Vött, A., May, M., Brückner, H. & Brockmüller, S. (2006). Sedimentary Evidence of Late Holocene Tsunami Events near Lefkada Island (NW Greece). *Zeitschrift für Geomorphologie N.F. Suppl.-Vol.,* 146, 139-172.

Vött, A., Brückner, H., May, M., Lang, F. & Brockmüller, S. (2007b). Late Holocene tsunami imprint at the entrance of the Ambrakian gulf (NW Greece). *Mediterranée,* 108, 43-57.

Vött, A., Brückner, H., May, M., Lang, F., Herd, R. & Brockmüller, S. (2008). Strong tsunami impact on the Bay of Aghios Nikolaos and its environs (NW Greece) during Classical-Hellenistic times. *Quaternary International,* 181(1), 105-122.

Vött, A., Brückner, H., Brockmüller, S., Handl, M., May, S. M., Gaki-Papanastassiou, K., Herd, R., Lang, F., Maroukian, H., Nelle, O. & Papanastassiou, D. (2009a). Traces of Holocene tsunamis across the Sound of Lefkada, NW Greece. *Global and Planetary Change,* 66(1-2), 112-128.